Genes Controlling Zebrafish Development: Roles for Rabs and Glis

Isabel Dantas de Campos

Thesis submitted to the University of London
for the degree of Doctor of Philosophy

National Institute for Medical Research
and University College London

2004

ProQuest LLC
789 East Eisenhower Parkway
P.O. Box 1346
Ann Arbor, MI 48106-1346

Abstract

This thesis is divided in two main sections linked by a common question concerning notochord formation and signalling.

The first section describes a loss-of-function screen of zebrafish Rab proteins using antisense morpholino oligonucleotides (MO). Rab proteins are small GTPases, which constitute the largest subfamily of the Ras superfamily. There are at least 60 human Rab proteins and they are thought to be involved in every step of vesicular traffic within eukaryotic cells. I identified 63 zebrafish *rab* genes, but there are probably more as for fourteen human *RAB* genes the zebrafish counterpart was not identified in this work. The mRNA *in situ* localization of 20 zebrafish *rabs* was assessed. All 20 genes were expressed during embryonic development and 6 showed enhanced expression in certain embryonic structures, such as chordamesoderm and polster (*rab1b, rab2a2* and *rab18*), neurons sub-sets (*rab3c1* and *rab5a1*), or specific brain regions (*rab5c*). MO injections targeting 20 different rab proteins were carried out and 14 resulted in embryos with obvious phenotypic defects. Several of the Rab morpholino-induced phenotypes are analysed and discussed. The phenotypes observed range from defects in very early developmental processes, such as epiboly (Rab5a2), to defects in highly specialized developmental processes, such as melanophore morphology (Rab1b). Knocking down several of these proteins resulted in embryos with defects in structures with high trafficking activity, such as brain, notochord or blood (Rab7b, Rab9a, Rab14a, Rab15).

The second section of the thesis describes efforts to understand the role of Gli3 protein in zebrafish development. Gli proteins are the transcription factors of the Hh signalling pathway and play a variety of roles in processes involving Hh signalling activity such as development of ventral spinal cord and limb. In the zebrafish, mutations in Gli1 and Gli2 proteins are known but no Gli3 homolog had been reported. I cloned the zebrafish *gli3* gene and mapped it to linkage group 24. To analyse the loss-of-function phenotype of zebrafish Gli3 in the ventral neural tube a brief analysis of spinal cord markers was done. Using these spinal cord markers, no obvious mispatterning phenotype was observed in zebrafish embryos injected with a MO targeting *gli3*. Disrupting Gli3 function in zebrafish embryos, however, resulted in a strong early phenotype. At 40% epiboly Nodal signalling is up-regulated and later in development the embryos show convergence-extension defects. Interestingly, the convergence-extension phenotype can be rescued by a short treatment with cyclopamine, a chemical inhibitor of Hh signalling.

Acknowledgements

First and foremost I would like to thank my supervisor, Derek L. Stemple. He has always been enthusiastic about my projects and willing to discuss them at any moment. He taught me a great deal on science but most importantly, he taught me how fun it can be!

I would like to thank James Briscoe, our collaborator in the Hh signalling project, for having great interest on the work, for his constant help and advice and for reading part of this thesis. Despina Stamataki and Vicky Tsoni from his lab were extremely helpful in my debut in the Shh world and in providing all the necessary reagents.

I would like to thank everyone in Derek's lab, past and present members for all the help I got at all times. In particular, I thank Leonor Saúde for teaching me how to take good care of the fish, Mike Parsons for teaching me all the molecular biology I know, Ben Feldman for being so available to discuss every matter and giving me such good advice and Emma Kenyon for helping me with the Rab MO injections. Everyone else: Kevin Thomas, Pedro Coutinho, Richard Gibbons, Rita Sousa-Nunes, Steve Pollard and Wei Wang – you all contributed a great deal to make the lab such a fantastic and fun place to work, thank you!

I would also like to thank Jacky Smith for ensuring all I had to care about whilst at work was science, Liz Hirst for EM sectioning and analysis and Ian Harragan for embryo sectioning.

Finally, I would like to thank all my Family and Friends, in Portugal or spread around the world but always so present at all times.

My work was funded by Programa Gulbenkian de Doutoramento em Biologia e Medicina (PGDBM) and Fundação para a Ciência e a Tecnologia (FCT), Portugal.

Contents

Abbreviations

A/P	antero-posterior
ATP	adenosine 5'-triphosphate
BCIP	X-phosphate/5-Bromo-4-chloro-3-indolyl-phosphate
BHK	Baby hamster kidney
BMP	bone morphogenetic protein
BSA	bovine serum albumin
cAMP	cyclic adenosine 5'-monophosphate
CaP	Caudal Primary
CE	Convergence-extension
CHM	Choroideremia
CiA	Circumferential Ascending
CiD	Circumferential Descending
CNS	central nervous system
CoB	Commissural Bifurcating
CoPA	Commissural Primary Ascending
COPII	Coat Protein II
CoSA	Commissural Secondary Ascending
cR	centiRay
Cys	Cysteine
DEPC	diethyl-pyrocarbonate
DIG	digoxygenin
dNTP	deoxy-nucleotide triphosphate
DoLA	Dorsal Longitudinal Ascending
dUTP	deoxy-uridine triphosphate
EDTA	ethylene-diamine-tetra-acetate
ENU	N-ethyl-N-nitrosourea
ER	Endoplasmic Reticulum
EST	expressed sequence tag
EtOH	ethanol

EVL	enveloping layer
FGF	fibroblast growth factor
GAG	glygosaminoglycan
GAP	GTPase-activating protein
GDI	GDP dissociation inhibitors
GDP	guanidine 5'-diphosphate
GEF	GDP/GTP exchange factor
Gsk	glycogen synthase kinase
GTP	guanidine 5'-triphosphate
HeLa	Henrietta Lacks
Hh-Np	processed N-terminal Hh fragment
Hh-Nu	unprocessed N-terminal Hh fragment
HMM	Hidden Markov model
Hnf3β	hepatic nuclear factor 3β
hpf	Hours post-fertilization
IMAGE	Integrated Molecular Analysis of Genomes and their Expression
kDa	kilo Dalton
L	Leucine
lod	logarithm of odds
MDCK	Madin-Darby canine kidney
MeOH	methanol
MiP	Middle Primary
MN	motor neurons
MO	antisense morpholino oligonucleotide
MVB	multi-vesicular body
N	Asparagine
NBT	4-nitro blue tetrazolium chloride
nt	nucleotides
OD	optical density
ORF	open reading frame
PBS	phosphate buffered saline

PBT	PBS with 0.1% Tween-20
PCR	polymerase chain reaction
PFA	*para*-formaldehyde
PFT	Protein farnesyl transferase
PGGTI	Protein geranylgeranyl transferase-type I
PGGTII	Protein geranylgeranyl transferase-type II (also known as RGGT)
Pi	Inorganic phosphate
PKA	cAMP-regulated kinase
Q	Glutamine
Rab	*ras* genes from rat brain
RACE	rapid amplification of cDNA ends
REP	Rab escort proteins
rER	Rough Endoplasmic Reticulum
RGGT	Rab geranylgeranyl transferase
RND	resistance-nodulation-division
RoP	Rostral Primary
RT	reverse transcriptase
S	Serine
SNARE	soluble N-ethylmaleimide-sensitive factor attachment protein receptors
SSD	sterol sensing domain
TAE	TRIS, acetate, EDTA
TE	TRIS EDTA
TGFß	Transforming Growth Factor ß
TRIS	tris(hydroxymethyl)methylamine
TUNEL	terminal deoxynucleotidyl transferase-mediated dUTP nick end labelling
UTR	untranslated region
UV	ultraviolet
VeLD	Ventral Longitudinal Descending
YSL	Yolk Syncytial Layer

List of figures

List of tables

General Introduction

1 General Introduction

1.1 Rab proteins

Every eukaryotic cell is highly compartmentalised thus requiring transport mechanisms between distinct membrane-bound organelles. This transport is tightly regulated and typically can be subdivided into three main steps: 1) transport vesicle formation and budding from a donor compartment; 2) actin- and tubulin-dependent vesicle transport; 3) and docking and fusion of transport vesicle onto the acceptor compartment.

Rab proteins are the largest subfamily of small GTPases from the Ras GTPase super family and are key regulators of all stages of vesicular transport. The first mammalian *rab* genes were identified in 1987 by two independent groups: Touchot and co-workers screened a rat brain cDNA library to identify members of the *ras* super family and it was then that the term "Rab" was firstly introduced (*ras* genes from rat brain) (Touchot et al., 1987); and Haubruck and colleagues used the yeast YPT1 gene as a probe to screen mouse cells cDNA, thus finding the murine homologue of YPT1, now known as Rab1a (Haubruck et al., 1987).

1.1.1 General characteristics of the Rab GTPase subfamily

Like other GTPases Rab proteins alternate between two different conformations, one bound to GTP and another bound to GDP. There appear to be only two exceptions to this rule, namely Rab24, that appears to be locked in the GTP bound conformation (Erdman et al., 2000), and the Rab40 subfamily, that has a substitution in a site relevant for Mg^{2+} coordination and were thus suggested to be permanently blocked in an inactive state (Pereira-Leal and Seabra, 2000). It is in general believed that the active form of the protein is in its GTP-bound state. That was for the first time shown to be the case for the protein involved in endocytosis Rab5 (Stenmark et al., 1994). In this study, a Rab5 Q79L mutant protein was shown to have very low GTPase activity and was found only on its GTP bound state. Upon expression of this protein in HeLa cells, very large early endocytic structures were observed. In the reverse experiment, a S34N mutant had preferential affinity for GDP and opposite effects to the Q79L mutant, i.e. a very small endocytic profile, when over-expressed in HeLa cells. These results suggested that GTP hydrolysis by Rab5 functions to inactivate the protein and this mechanism is now believed to be generally true for Rab proteins.

The GDP- or GTP-bound forms of Rab proteins adopt different conformations and therefore have different affinities for co-factors. Conversion between these two forms is caused by nucleotide exchange and catalyzed by a GDP/GTP exchange factor (GEF). GTP binding alters the conformation of the Rab protein and interaction with the specific Rab effector is then possible. Shutting down Rab activity is done by GTP hydrolysis, facilitated by a GTPase-activating protein (GAP) and release of an inorganic phosphate (Pi). The GDP-bound form interacts with Rab escort proteins (REP) and GDP dissociation inhibitors (GDI). Rabs must associate with cellular membranes for activity and the REPs play an important role in this process. Membrane attachment is mediated by post-translational regulation of the Rab proteins. This consists in the covalent modification of C-terminal cysteine residues with geranylgeranyl isoprenoids. The enzyme responsible for this modification is a Rab geranylgeranyl transferase (RGGT). Unlike other such enzymes, the RGGT substrate is a 1:1 complex between any given newly synthesized Rab protein and a REP (Anant et al., 1998).

The Rab GTPase cycle is schematized in Figure 1-1.

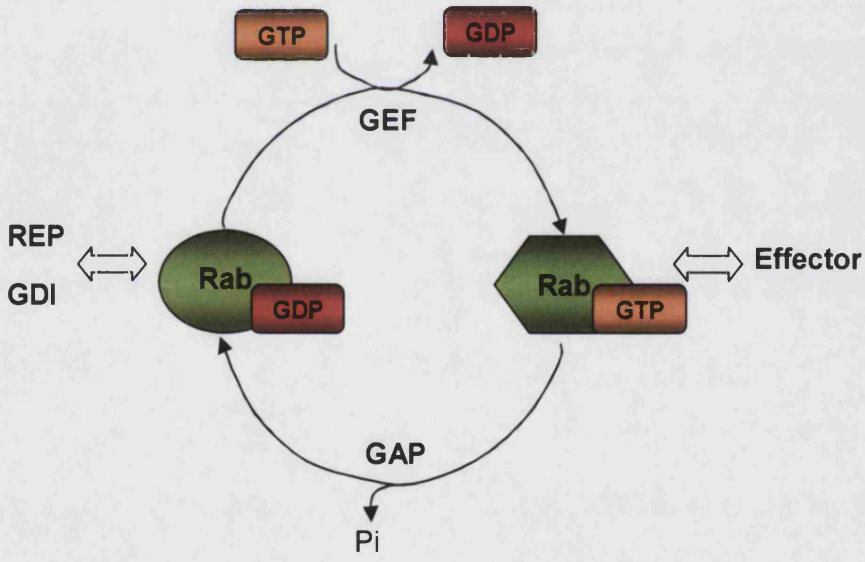

Figure 1-1 The Rab GTPase cycle. Rab proteins can be found in its GDP (inactive) or GTP (active) bound state. Change from the inactive to the active state is accomplished by nucleotide exchange and mediated by GEF proteins. Change from the active to the inactive state is achieved by nucleotide hydrolysis and catalyzed by GAP proteins, with release of a Pi. In their GTP-bound state, Rab proteins interact with their effectors, whereas in their GDP-bound state they interact with GDI proteins and with REPs that will allow their post-translational modification.

1.1.2 Sequence and structure

Rab proteins belong to the super-family of small GTP-binding proteins (or G proteins), which are monomeric G proteins with molecular masses of 20-40 kDa. It is proposed that within this super-family there are five different subfamilies: the Ras, Rho/Rac, Rab, Arf and Ran groups. The degree of amino-acid identity between members of the different subfamilies is approximately 30% (Thoma et al., 2001a). In gross terms, the fold of all these proteins is common consisting of a six-stranded β sheet, comprising five parallel strands and one anti-parallel, surrounded by five α helices.

All small G proteins have consensus amino-acid sequences responsible for interaction with guanine and phosphate/Mg^{2+} and for GTPase activity and these are located in five loops that connect the α helices and β strands. These regions have been referred to as G for guanine (G1-G3) and PM for phosphate/Mg^{2+} (PM1-PM3) (Valencia et al., 1991).

By comparison of the structure of Ha-Ras in the GDP- and GTP-bound conformations, two highly flexible regions surrounding the γ-phosphate of GTP have been established: the switch I region within loop L2 and β_2 (also called effector domain) and the switch II region within loop L4 and helix α_2 (Milburn et al., 1990; Schlichting et al., 1990). More recently, crystallographic analysis of a Rab protein, the yeast Rab Sec4p, in the GDP- and GTP-bound states confirmed that the proteins adopt two different conformations with the major nucleotide-induced differences occurring in the regions denoted switch I and switch II (Stroupe and Brunger, 2000).

High resolution structural information of four Rab GTPases is now available in the literature, namely for the mouse Rab3a bound to a GTP analog (Dumas et al., 1999) and in a complex with its effector Rabphilin-3a (Ostermeier and Brunger, 1999), the *Plasmodium falciparum* Rab6 (Chattopadhyay et al., 2000), *S. cerevisiae* Ypt51p (Esters et al., 2000) and Sec4p (Stroupe and Brunger, 2000). In these three-dimensional studies, the Switch I and II regions were shown to be on the surface of the molecule. Numerous mutagenesis studies have shown that the putative switch regions are crucial for interaction of Rab proteins with regulatory protein partners such as the GEFs or GAPs. Moreover, in the Rab3a/Rabphilin study, these regions were also shown to be an important part of the Rab/Effector interaction (Ostermeier and Brunger, 1999).

Figure 1-2 shows a linear and a three-dimensional representation of a Rab GTPase with the structurally important regions and Table 1-1 lists the amino-acid sequence of such regions.

The GTPase binding regions (regions G and PM) are not useful to distinguish Rabs from other small G proteins. This is due to the fact that they are extremely conserved between all Ras-like proteins and the variations are not typical of one family (Pereira-Leal and Seabra, 2000). However, in an extensive sequence analysis study, Pereira-Leal and Seabra have identified five mammalian Rab specific regions, called RabF motifs, which can be used as diagnostic sequences to define a Rab protein on the basis of its primary structure (Pereira-Leal and Seabra, 2000). Once mapped onto the crystal structure of Rab3a all RabF motifs localize in and around the switch I and II regions, which are known to mediate interaction with effectors and mediators.

The observation that all Rabs are conserved around the switch regions leads to the obvious conclusion that Rab specificity has to lie elsewhere in their sequences. Pereira-Leal and Seabra hypothesized that Rab effectors and regulators would bind RabF regions only to discriminate between active/inactive conformations and elsewhere for specificity. In particular, the binding of general regulators such as REP or GDI would occur via the RabF motifs. In a more recent study, Pereira-Leal et al.. found evidence to support this hypothesis (Pereira-Leal et al., 2003). The study involved the introduction of point mutations in Rab3a as a model Rab and the assessment of its ability to interact with REP. REP:Rab3a binding was affected when residues in motifs RabF1, RabF3 and RabF4 (which include part of the switch I and II regions) were mutated (Pereira-Leal et al., 2003).

Four regions responsible for Rab specificity were proposed and termed RabSF1-RabSF4 (Moore et al., 1995; Pereira-Leal and Seabra, 2000). These regions can be used to define subfamilies of Rab isoforms of which, according to these criteria there would be ten (1, 3-6, 8, 11, 22, 27, 40) (Pereira-Leal and Seabra, 2000). The RabSF motifs lie on two different surfaces of Rab GTPases and the model predicts that they allow specific binding of downstream effector molecules that must recognize a specific Rab or Rab subfamily in addition to detecting the nucleotide binding state.

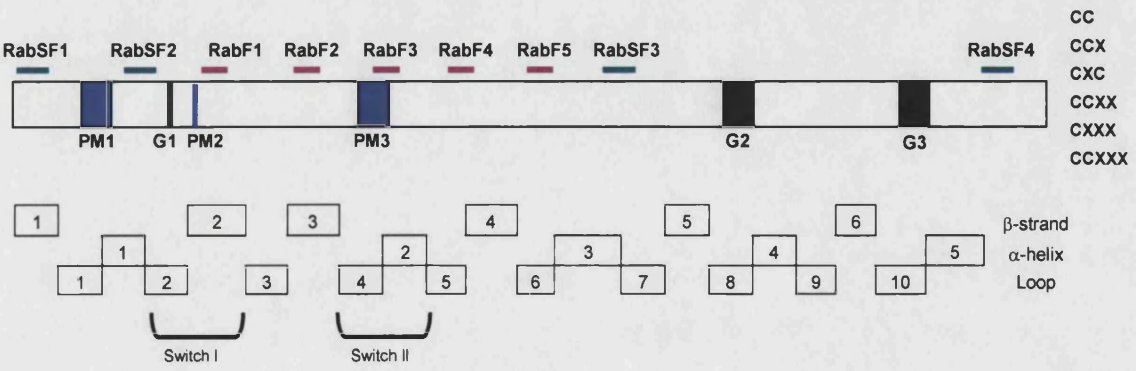

Figure 1-2 The structure of Rab GTPases. The conserved motifs involved in nucleotide binding are indicated in black; the conserved motifs involved in hydrolysis are indicated in blue; Rab family motifs are indicated as pink bars; and Rab subfamily motifs are indicated as green bars. Below the linear representation there is a schematic of the structure with the succession of β strands, loops and α helices. Adapted from (Olkkonen and Stenmark, 1997).

Motif	Sequence
PM1	GXXXGKS/T
PM2	T
PM3	DTAGQE
G1	F
G2	GNKXD
G3	EXSA
RabF1	IGVDF
RabF2	KLQIW
RabF3	RFrsiT
RabF4	YYRGA
RabF5	LVYDIT
RabSF1	ydylFK
RabSF2	SIIIRFtddtFsxxyks
RabSF3	enlknWlkelreyaepndvvimLv
RabSF4	kkareldleasqn

Table 1-1 Amino-acid sequence of Rab motifs. The upper/lower case coding represents outcome of the profile hidden Markov model (HMM), in which upper case characters were found at $p>0.5$. All sequences according to (Pereira-Leal and Seabra, 2000).

1.1.3 Post-translational modification

Despite being hydrophilic proteins, Rabs are localized to the cytosolic face of distinct intracellular membranes. This localization is reversible but seems to be necessary for Rab function (Pereira-Leal et al., 2001). Membrane association is mediated by the covalent attachment, via thioether linkage, of a C20 (geranylgeranyl) isoprenoid group to C-terminal cysteine residues. This reaction is also known by prenylation and it only occurs in the context of a "prenylation motif". The Rab prenylation motifs generally consist of two C-terminal cysteine residues found in one of the following combinations: CC, CCX, CXC, CCXX, CXXX or CCXXX, where X is any amino-acid (see Figure 1-2).

The Rab double-cysteine prenylation motif is useful to confirm that a given small GTPase is a Rab, but its absence should not be use to prove otherwise. In fact, some Rabs present a CXXX box where only one cysteine residue is available for prenylation and some others do not seem to have any cysteine at the C-terminus (Pereira-Leal and Seabra, 2000).

Protein prenylation is a common mechanism for membrane association of cytoplasmic proteins and catalysed by protein prenyl transferases. There are three known prenyl transferases, all heterodimers consisting of an α- and β-subunit. Protein farnesyl transferase (PFT) is responsible for farnesylation of Ras proteins. Protein geranylgeranyl transferase-type I (PGGTI) post-translationally modifies Rho proteins and shares a common α-subunit with PFT. Finally, Rab geranylgeranyl transferases (RGGT or PGGTII) were originally identified as enzymes that modify only Rab proteins (Pereira-Leal et al., 2001).

Unlike other prenyl transferases, RGGT does not recognize its substrate directly. Instead, it recognizes a 1:1 complex of a newly synthesized Rab and a REP thus forming a catalytic ternary complex (Anant et al., 1998). The prenylation reaction is sequential since there is only one lipid binding site in the RGGT. After all the geranylgeranyl groups have been transferred to the Rab protein, binding of an additional lipid group to the RGGT β-subunit destabilizes the complex and the enzyme dissociates from the prenylated Rab:REP complex (Thoma et al., 2001b). REP may then deliver the Rab protein to a cellular membrane where it interacts with its effectors to perform its biological role.

The fact that post-translational prenylation of Rab proteins is an important feature of Rab function is illustrated by the observation that mutations in genes essential for the reaction underlie genetic diseases. Choroideremia (CHM) patients have loss of function mutations in REP1 (Seabra et al., 2002). CHM is an X-linked chorioretinal degeneration that results in complete blindness within two or three decades of the manifestation of the symptoms (van den Hurk et al., 1997). It has been hypothesized that the second human REP protein, REP2, incompletely compensates for REP1 loss in CHM patients thus leaving a sub-set of Rab proteins unprenylated (Cremers et al., 1994). Rab27a has been shown to be selectively un-prenylated in lymphoblasts of CHM patients (Seabra et al., 1995), but there is still wide debate on whether lack of function of this particular Rab could be the cause of the disease (Pereira-Leal et al., 2001). There is a second genetic disorder in which prenylation of Rab proteins is highlighted. Hermansky-Pudlak syndrome (HPS) is caused by mutations in multiple genes involved in the biogenesis and function of melanosomes, platelet dense

granules and lysosomes (Huizing et al., 2000; Swank et al., 1998). One of the several murine models of the disease is the *gunmetal* (*gm*) mutant that has a splice-site mutation in the α-subunit of RGGT (Detter et al., 2000). There is some RGGT activity in the *gm* mutant due to the activation of a cryptic splice-site, but this mouse model suggests that HPS phenotypes may be caused by Rab hypoprenylation (Pereira-Leal et al., 2001).

1.1.4 Rab family evolution

In organisms with nearly completed and published genome sequence the entire family of Rab proteins has been annotated (Bock et al., 2001; Pereira-Leal and Seabra, 2001). The family comprises 29 members in *Caenorhabditis elegans* and *Drosophila melanogaster*, 57 in *Arabidopsis thaliana* and 60 in *Homo sapiens* (59 different *RAB* genes and two alternative splicing isoforms for *RAB6a*). The unicellular organisms *S. cerevisiae* and *S. pombe* have 11 and 7 members of the family, respectively (Bock et al., 2001; Pereira-Leal and Seabra, 2001). Thus, the Rab family of proteins expanded from the unicellular yeast to the multicellular fly and worm. Other family of proteins involved in organizing membrane compartments, such as the coatomer complex or the SNARE families are not expanded. All families analysed in this study, however, have been expanded in humans (Bock et al., 2001).

Both the RabF and the RabSF motifs described for mammalian Rabs are conserved across species (Pereira-Leal and Seabra, 2001). Furthermore, when drawing phylogenetic trees with Rabs from different species, co-segregating Rabs show similar patterns of cellular localization or function. Thus, Rabs across species may be functionally grouped according to their sequence similarity, localization and/or function, and these groups may represent shared ancestry (Pereira-Leal and Seabra, 2001). The next following picture taken from (Zerial and McBride, 2001) summarizes the intracellular localization of Rab proteins in mammalian cells.

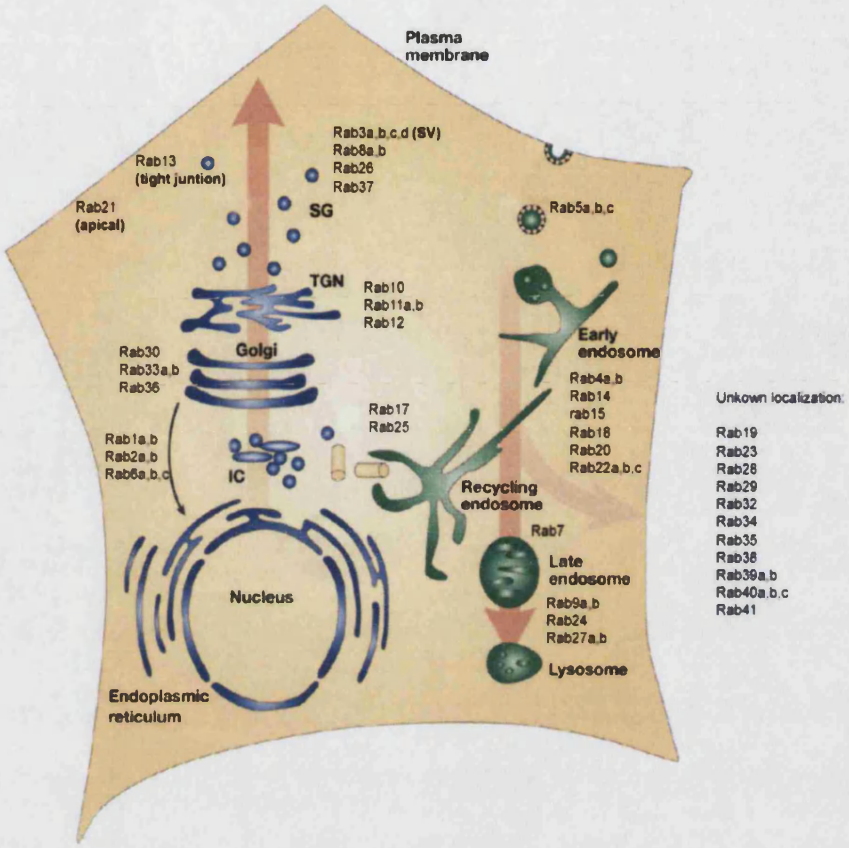

Figure 1-3 Summary of intracellular localization of mammalian Rabs. IC, ER-Golgi intermediate compartment; SG, secretory granules; SV, synaptic vesicle; TGN, *trans*-Golgi network. Taken from (Zerial and McBride, 2001).

1.1.5 Rab function and effectors

The key function of Rab proteins in specific intracellular traffic pathways is the recruitment of effector molecules. The formal definition of an effector molecule for Ras super family members is a factor that binds preferentially to the GTP-bound conformation of the GTPase and will compete for interaction with GAP proteins (Collins and Brennwald, 2000). Unlike Rab proteins themselves, which are extremely related to one another in sequence and structure, Rab effectors are a very heterogeneous group of proteins. Moreover, through two-hybrid studies and affinity chromatography it has been shown that the same Rab protein can interact with more that one effector protein thus multiplying the potential for activity specificity (Simonsen et al., 1998; Stenmark et al., 1995).

1.1.5.1 Rab effectors as tethering factors

Tethering factors are proteins containing extended coiled-coil domains that physically link transport intermediates and acceptor compartments together prior to fusion.

A significant proportion of the known Rab effectors are tethering factors, and binding to such factors has been proposed to be a conserved function of Rab GTPases (Pfeffer, 1999; Waters and Pfeffer, 1999).

1.1.5.1.1 The SNARE hypothesis of vesicle targeting/docking/fusion

SNARE (soluble NSF- N-ethylmaleimide-sensitive factor- attachment protein receptors) proteins mediate fusion of intracellular membranes. The final stage of fusion involves the formation of a bundle of four parallel core SNARE domains. One of these SNARE domains is contributed by the vesicle membrane (v-SNARE) and the remaining three are contributed by the target membrane (t-SNARE) (Chen and Scheller, 2001). This fusion complex is also called trans-SNARE complex and it bridges the two membranes allowing an overcame of the energy barrier to fusion (Chen and Scheller, 2001).

The working hypothesis for SNARE function is that each transport vesicle inherits a unique address marker associated with one or more v-SNAREs (generally related to synaptobrevin /VAMP) from its parental membrane during budding. Each target membrane is identified in part by one or more t-SNAREs (generally related to syntaxin and/or SNAP-25). The v- and t-SNAREs interact with each other resulting in the docking of vesicles with their target membranes (Rothman, 1994; Takai et al., 2001).

Several studies report direct molecular links between Rab effector proteins and components of SNARE complexes.

1.1.5.1.2 Rab1 and its tethering effectors

Rab 1 is involved in the regulation of transport of newly synthesised proteins from the endoplasmic reticulum (ER) to the Golgi apparatus, an initial step in the secretory pathway (Plutner et al., 1990; Tisdale et al., 1992). When an ER-derived coated vesicle targeted to the Golgi (COPII vesicle) is budding, Rab 1 recruits its effector p115 onto the vesicle binding it directly. At the surface of the COPII vesicle, p115 interacts with a set of COPII-associated SNAREs (Allan et al., 2000). This SNARE complex thus promotes targeting to the Golgi apparatus. On the target membrane recognition is ensured by the interaction of Rab1 with another effector, the GM130-Grasp65 complex, a cis-Golgi scaffold tethering complex.

The interaction of Rab1 with the cis-Golgi tethering complex GM130-Grasp65 is independent of p115 and is required for coat protein II vesicle targeting/fusion with the cis-Golgi (Moyer et al., 2001; Weide et al., 2001). Based on this evidence, Moyer and co-workers have proposed a model in which the same Rab interacts with distinct tethering factors at donor and acceptor membranes to program heterotypic membrane fusion events between transport intermediates and their target compartments (Moyer et al., 2001).

1.1.5.1.3 Rab3 and its tethering effectors

Rab3 is the most abundant Rab protein in neurons, where it localizes predominantly to synaptic vesicles. Its expression is up-regulated in endocrine cells where it associates with secretory vesicles. In agreement with its specific pattern of expression, Rab3 has been implicated in a specific trafficking pathway, separate from the constitutive endocytic and exocytic routes, involved in the secretion of hormones and neurotransmitters.

In mammals, there are 4 different isoforms of Rab3 (Rab3a-d) that are all expressed in brain and endocrine tissues although at widely different levels (Schluter et al., 2002). Despite their differential distribution across different tissues, all Rab3 proteins appear to be localized to secretory vesicles, underlying a potential redundancy.

One Rab3a effector is the protein RIM (Rab3-interacting protein), which is also expressed in neurons with a distribution complementary to Rab3a. RIM is localized to pre-synaptic active zones whereas Rab3a is found only on synaptic vesicles (Wang et al., 1997). A *C. elegans* mutant lacking RIM shows that RIM is more than just an effector of Rab3, as the *rim* mutant phenotype is much more severe than the *rab3* phenotype (Koushika et al., 2001; Lloyd and Bellen, 2001). RIM proteins bind to RBPs (RIM binding proteins), which in turn interact with Ca^{2+} channels. It has been proposed that RBPs provide a molecular coupling between the vesicle tethering (RIMs binding Rab3-GTP present on vesicles) and the priming-fusion apparatus (Ca^{2+} channels associated with the SNARE complex) (Hibino et al., 2002).

One additional player in Rab3 mediated exocytosis is granuphilin/Slp-4. This protein binds to Rab3-GTP and to another component of the secretory machinery of pancreatic beta-cells, the SNARE-binding protein Munc-18 (Coppola et al., 2002). Due to granuphilin's ability to interact with Munc-18, a role in secretory vesicle-docking has been proposed for this Rab3 effector (Coppola et al., 2002).

1.1.5.1.4 Rab4 and its tethering factors

Rab4 has been localized to early endosomes and has been implicated in the regulation of membrane receptor recycling (van der Sluijs et al., 1992; van der Sluijs et al., 1991).

In the extra-cellular space a ligand binds its receptor attached to the cell membrane thus producing signal that will be translated intra-cellularly into some sort of event. The way the cell recycles the receptor is by co-internalizing the ligand and receptor in vesicles and targeting these to early endosomes called sorting endosomes. Most ligands then dissociate from their receptors in the mildly acidic internal pH of the early endosome and are usually delivered to degradative late endocytic compartments. The freed receptors are often recycled back to the plasma membrane, either directly through recycling endosomes or by first going to a recycling compartment (Deneka and van der Sluijs, 2002). When cells express a Rab4 dominant negative mutant (Rab4aS22N) a significant reduction in both recycling and degradation of epidermal growth factor (EGF) and low density lipoprotein (LDL) is observed (McCaffrey et al., 2001).

Cells expressing Rab5, Rab4 and Rab11 proteins tagged with green fluorescence protein (GFP) allow the visualization of different Rab domains in the endocytic pathway. Three major populations of endosomes can be distinguished: one that contains primarily Rab5, a second that contains both Rab4 and Rab5, and a third one that contains both Rab4 and Rab11 (Sonnichsen et al., 2000). These three domains correspond to early endosomes, sorting endosomes and recycling endosomes, respectively (Zerial and McBride, 2001). Rab5 cellular domains may mark gateways into the early endosome, whereas the Rab4 and Rab11 domains contain the machinery necessary for sorting and recycling of receptors to the cell surface (Zerial and McBride, 2001).

The first identified molecular link between fusion of early endosomes and receptor recycling was Rabaptin-5. This protein is a tethering effector of Rab5 (Stenmark et al., 1995) shown to have an additional binding site for Rab4 in its GTP-bound form (Vitale et al., 1998). Likewise, Rabenosyn-5 is a bi-functional effector of both Rab5 and Rab4, physically connecting the activities of these sequentially acting GTPases (de Renzis et al., 2002; Deneka and van der Sluijs, 2002). The Rab Coupling Protein (RCP) may constitute the molecular link between the Rab4 and Rab11 domains, as it has been shown to interact specifically with the GTP-bound conformation of Rab4 and belongs to the Rab11-FIP family of interacting targets of Rab11 (Lindsay et al., 2002). Other Rab4 effectors that play a role in tethering of membrane recycling vesicles are

Rabaptin-4 (Nagelkerken et al., 2000), Syntaxin-4 (Li et al., 2001) and Rab-4 interacting protein (Cormont et al., 2001).

1.1.5.1.5 Rab5 and its tethering effectors

In mammals there are 3 isoforms of the Rab5 protein, Rab5a-c. The three proteins co-localize to the plasma membrane and early endosomes and their over-expression leads to changes in the rate of internalisation of endocytic markers and in morphological alterations of the early endosomes (Bucci et al., 1995; Zerial, 1995). Rab5 proteins function in the early endocytic pathway, regulating clathrin-coated-vesicle-mediated transport from the plasma membrane to the early endosomes and homotypic early endosome fusion (Bucci et al., 1992; Gorvel et al., 1991).

Rabaptin-5 is a coiled-coil protein identified as a Rab5 effector in a yeast two-hybrid screen. Although mainly cytosolic a fraction co-localizes with Rab5 to early endosomes and it is recruited to that location by Rab5-GTP (Stenmark et al., 1995). In addition, its over-expression induces the formation of large endosomes in a similar way to Rab5 GTPase-deficient mutant and its immunodepletion strongly inhibits Rab5-dependent early endosome fusion (Stenmark et al., 1995). Apart from binding to Rab5-GTP, Rabaptin-5 also complexes with Rabex-5, a GEF for Rab5 that is essential for endocytic membrane fusion (Horiuchi et al., 1997).

EEA1 (Early Endosome Antigen1) is an evolutionarily conserved protein associated with early endosomes and another effector of Rab5 (Mu et al., 1995; Simonsen et al., 1998). It was shown that this protein is the only factor necessary to confer minimal endosome-fusion activity in an *in vitro* assay (Christoforidis et al., 1999a). Taking this finding into consideration and the fact that EEA1 contains two binding motifs for Rab5 (Simonsen et al., 1998), it is tempting to speculate that EEA1 could bridge two membranes bearing Rab5 together and thus promote fusion of early endosomes (Zerial and McBride, 2001). EEA1 also interacts with phosphatidylinositol-3-OH kinase (PI(3)K), another factor required for fusion between early endosomes. It was previously thought that EEA1 could be the bridge between PI(3)K and Rab5 since it binds to both (Simonsen et al., 1998), but it was later shown that PI(3)K is a Rab 5 effector itself (Christoforidis et al., 1999b).

Rabaptin-5 and EEA1 are part of a large complex required for membrane docking/fusion (McBride et al., 1999). EEA1 is thought to be the core protein in this complex since it replaces the requirement for cytosol in a minimal endosome fusion assay (Christoforidis et al., 1999a) and interacts with Syntaxin 13, a t-SNARE required for endosome fusion transiently incorporated into this large protein complex (McBride

et al., 1999). It should also be noted that EEA1 directly and specifically interacts with syntaxin-6, a SNARE implicated in trans-Golgi network to early endosome trafficking. This suggest that apart from its role in endocytic membrane traffic, EEA1 may participate in trans-Golgi network to endosome traffic as well (Simonsen et al., 1999).

Another link between the Rab5 protein and SNAREs has been found through the identification of yet another effector, Rabenosyn-5 (Christoforidis and Zerial, 2000). Like EEA1, it contains a FYVE finger domain and is recruited in a phosphatidylinositol-3-kinase-dependent fashion to early endosomes. Rabenosyn-5 forms a complex with the syntaxin binding protein hVPS45 thus serving as a molecular link between hVPS45 and the Rab5 GTPase (Christoforidis and Zerial, 2000).

There are probably many Rab5 effectors to be identified. Indeed, 20 such proteins were isolated from bovine brain cytosol using an affinity-chromatography approach with Rab5-GTP as a bait (Christoforidis et al., 1999a).

1.1.5.1.6 The exocyst tethering complex and its relation to Rabs

The exocyst complex was first identified in yeast, but it is now thought to be responsible for targeting secretory vesicles to the appropriate exocytic sites on the plasma membrane of cells across all organisms (Guo et al., 2000). In yeast, it is composed of one copy of 8 different proteins: Sec3p, Sec5p, Sec6p, Sec8p, Sec10p, Sec15p, Exo70p, and Exo84p (Guo et al., 1999a; TerBush et al., 1996; TerBush and Novick, 1995). Most of the components of the yeast exocyst were originally identified as products of genes whose mutations caused accumulation of vesicles destined for plasma membrane (Whyte and Munro, 2002). The complex localizes to small bud tips in yeast, which is the predominant site of exocytosis in this organism (TerBush et al., 1996). This localization seems to be primarily determined by Sec3p. Indeed, this protein may act as a spatial landmark defining sites of exocytosis, since its localization is independent of the secretory pathway function, of the actin and septin cytoskeletons, and of the polarity establishment proteins (Finger et al., 1998). The localization of all the remaining components of the exocyst to the site of exocytosis is dependent on both actin and a functional secreting pathway (Finger et al., 1998; Guo et al., 1999a). One of these components, Sec15p, binds to Sec4p, which is the yeast Rab-GTPase present in secretory vesicles (Guo et al., 1999b). Since Sec15p binds Sec4p in the vesicle and subsequently interacts with the remainder of the exocyst at the site of exocytosis, it is reasonable to conclude that the Rab-GTPase controls the assembly of the whole complex (Guo et al., 1999b).

There is a mammalian equivalent of the exocyst complex formed by the homologues of the same 8 proteins and localized to sites of polarized growth (Hsu et al., 1996; Kee et al., 1997; Matern et al., 2001; Ting et al., 1995). The mammalian exocyst also interacts with small GTPases, but this interaction has been shown for a different component, Sec5 instead of Sec15, and with RalA instead of a Rab protein (Brymora et al., 2001; Moskalenko et al., 2002). It should be noted, however, that the yeast protein Sec4 does not have a putative Rab orthologue in mammals and there are at least two mammalian homologues of Sec15p (Brymora et al., 2001; Pereira-Leal and Seabra, 2001).

In *Drosophila melanogaster*, mutations in the exocyst subunit Sec5 inhibit neurite outgrowth and neuromuscular junction formation but do not impair synaptic vesicle fusion (Murthy et al., 2003). The authors concluded that unlike other yeast exocytosis fly homologues which are required for trafficking for cell growth, membrane protein insertion and neurotransmitter secretion, Sec5 is not involved in transmitter release (Murthy et al., 2003). Likewise, mutations in the fly *sec10* gene showed that Sec10 is required for hormone secretion but not general exocytosis or neurotransmitter release (Andrews et al., 2002).

1.1.5.2 Rab effectors as mobility factors

Long-range vesicle transport depends on the action of protein motors interacting with cytoskeleton. Microtubule motors comprise dyneins and kinesins. Cytoplasmic dyneins move vesicles towards the minus end of microtubules, which converges on the microtubules organizing centre (MTOC), associated with the nucleus. Kinesin family members are generally responsible for movement of vesicles towards the peripheral, actin-rich cortex of the cell. Following or preceding movements on microtubules, vesicles undergo small movements on F-actin, powered by the actin motors of the myosin super family.

1.1.5.2.1 Rab3 and its mobility effectors

Rabphilin-3a is a peripheral membrane protein associated with secretory vesicles and was the first effector to be identified for Rab proteins (Shirataki et al., 1993). The C-terminal part of Rabphilin contains two C_2 domains, which can bind phospholipids (phosphatidylserine and phosphatidylinositol 4,5-bisphosphate) in a Ca^{2+}-dependent manner (Chung et al., 1998; Shirataki et al., 1993). The N-terminal domain of Rabphilin binds specifically to Rab3a and Rab3c and has two conserved Zn^{2+} binding motifs. In the middle of the protein there is a proline rich region substrate for cAMP-

dependent protein kinase and Ca^{2+}/calmodulin-dependent protein kinase II (Collins and Brennwald, 2000). The crystal structure of Rab3a complexed with the N-terminal region of Rabphilin-3a has been solved (Ostermeier and Brunger, 1999). Apart from the expected contact area between the two proteins in the switch regions of Rab3a, this study revealed an additional interface involving a conserved `SGAWFF' motif, and regions of Rab3a called RabCDRs (complementarity determining regions). Ostermeier and Brunger suggested that the interaction with the switch regions, which are sensitive to the nucleotide-binding state, would be a mechanism common to all Rab effectors, whereas the second pocket of contact establishes a specific interaction between each Rab protein and its effectors. Hence, RabCDRs would be major determinants of effector specificity during vesicle trafficking and fusion (Ostermeier and Brunger, 1999). What is the functional relevance of Rabphilin-3a interaction with Rab3a? Analysis of Rab3a mutant mice shows that Rabphilin-3a levels are reduced by 70% despite normal mRNA levels, suggesting degradation of un-complexed Rabphilin-3a *in vivo* (Li et al., 1994). Furthermore, in mutant cells Rabphilin-3a becomes localized to the neuronal cell body in contrast to its normal localization at the synapse (Li et al., 1994). Rab3a is thus required for this specific localization at the synapse, although once recruited, Rabphilin-3a interaction with synaptic vesicles is independent of Rab3a (Shirataki et al., 1994; Stahl et al., 1996). It has been suggested that part of Rabphilin function is to re-organize the synaptic cytoskeleton. In fact, Rabphilin binds to α-actinin, a factor that cross-links actin filaments during Ca^{2+}-dependent exocytosis (Kato et al., 1996). The GTP-bound form of Rab3a competes with α-actinin binding, suggesting that it could act as a timer to prepare synaptic vesicles for docking or fusion before changing its hydrolysis state, thus releasing Rabphilin-3a to re-organize actin filaments.

In addition to its roles in exocytosis, Rabphilin has been suggested to participate in the control of endocytosis (Burns et al., 1998). A possible explanation for this finding may lie on the fact that free Rabphilin-3a can interact with Rabaptin-5, an effector of Rab5 involved in endocytosis (Ohya et al., 1998). Rabphilin-3a may therefore play a dual role in vesicular trafficking at the plasma membrane by participating in the regulation of distinct stages of the exocytic and endocytic pathways.

Noc2 (no C_2 domain) is a soluble cytoplasmic protein expressed predominantly in endocrine tissues and hormone-secreting cell lines and at very low levels in brain (Kotake et al., 1997). It has a high degree of similarity with the N-terminal region of Rabphilin, and it has been shown to bind Rab3a itself (Haynes et al., 2001). The function of Noc2 as a Rab3a effector is not clear. Yeast two hybrid and co-immunoprecipitation experiments show that Noc2 interacts with the LIM domain-

containing protein zyxin, a component of the cytoskeleton (Kotake et al., 1997). Noc2 may therefore be involved in regulated exocytosis in endocrine cells through cytoskeletal interactions.

1.1.5.2.2 Rab4 and its mobility effectors

Rab4 was shown to specifically interact with cytoplasmic dynein light intermediate chain-1 (LIC-1) by yeast two hybrid analysis (Bielli et al., 2001). Cytoplasmic dynein was previously shown to be necessary for the transport of ligand containing vesicles in the late endosome/lysosome direction (Goltz et al., 1992; Oda et al., 1995). Thus, Rab4 is implicated in mediating this motility event.

1.1.5.2.3 Rab5 and its mobility effectors

A role for Rab5 in the regulation of endosome interactions with the microtubule network has been shown (Nielsen et al., 1999). Using GFP-tagged Rab5, Rab5-positive endosomes were visualized moving on microtubules *in vivo* (Nielsen et al., 1999). In *in vitro* studies, Rab5 stimulates the association of purified endosomes with microtubules and increases the frequency with which they move towards the minus end of microtubules (Nielsen et al., 1999). These observations along with the fact that activated Rab5 causes a redistribution of endosomes to the area around the MTOC (Stenmark et al., 1994), led to the proposal that Rab5 interacts with a minus-end-directed kinesin (Nielsen et al., 1999). However, the molecular nature of such an effector is still unknown.

1.1.5.2.4 Rab6 and its mobility effectors

In mammalian cells there are three different isoforms of the Rab6 protein, namely Rab6a, Rab6a' and Rab6b (Darchen and Goud, 2000). The Rab6a isoforms are encoded in the same gene and result from alternative splicing of one of the exons (Echard et al., 2000). Although differing in only three amino-acid residues, these two proteins have different specificity and bind different partners (Echard et al., 2000).

Rab6 has been localized to membranes of the Golgi apparatus, on medial and *trans* cisternae, and to membranes of the *trans*-Golgi network (TGN) (Darchen and Goud, 2000; Goud et al., 1990), using an antibody that does not distinguish between the three isoforms.

GFP-tagged versions of Rab6a were used to unravel this protein's function. Rab6a positive vesicles leave the Golgi and move along microtubules (White et al., 1999).

Using an antibody blocking coatomer function, it was shown that Rab6a is involved in a novel coatomer-independent Golgi to ER retrograde pathway, which requires long-range movement along microtubules (White et al., 1999). The physiological role of the coatomer-independent retrograde pathway regulated by Rab6a remains to be determined. However, it has been hypothesised that such a pathway could allow recycling of lipids to maintain the lipid balance during the secretory process at the level of the Golgi apparatus (Darchen and Goud, 2000).

Consistent with the observation that Rab6a positive organelles move along microtubules, a kinesin-like protein was identified as a direct effector of Rab6a (Echard et al., 1998). The protein was named Rabkinesin-6 and it localizes to the Golgi apparatus where it plays a role in the dynamics of this organelle (Echard et al., 1998), but the precise relationship between Rab6a and Rabkinesin-6 is still unknown. Studies with the human homologue of Rabkinesin-6, RB6K/Rab6-KIFL, suggest a different role for the protein (Hill et al., 2000). Expression of RB6K is regulated during the cell cycle at both the mRNA and protein level and, similar to cyclin B, shows a maximum during M phase (Hill et al., 2000). In human cells, RB6K antibody reveals a weak signal in interphase Golgi but a 10-fold higher signal in prophase nuclei. Importantly, during M phase, the newly synthesized RB6K does not co-localize with Rab6 and accumulates in the spindle mid-zone (Hill et al., 2000). Upon injection of RB6K antibody, cells failed to undergo cytokinesis (Hill et al., 2000).

Two additional effectors of Rab6a are the two mammalian homologues of *Drosophila* Bicaudal-D (BICD1 and BICD2), the dynein-dynactin-binding protein. Dynactin is a multi-subunit complex required for the activity of dynein in several intra-cellular motility processes. Both BICD1 and BICD2 co-localize with Rab6a on the *trans*-Golgi network (TGN) and on cytoplasmic vesicles. In addition, both BICD1 and BICD2 associate with Golgi membranes in a Rab6-dependent manner (Matanis et al., 2002; Short et al., 2002). The recruitment of dynein-dynactin to Rab6a-containing vesicles is made through the BIDC proteins and the interaction between these players seem to control coatomer-independent Golgi-ER transport (Matanis et al., 2002).

1.1.5.2.5 Rab7 and its mobility effectors

Rab7 controls late steps of endocytosis and localizes to late endosomes/lysosomes (Bucci et al., 2000; Zerial, 1995). Using yeast two-hybrid screens, two independent groups identified RILP (Rab7-interacting lysosomal protein) as a Rab7 effector (Cantalupo et al., 2001; Jordens et al., 2001). RILP expression induces the recruitment of functional dynein-dynactin motor complexes to Rab7-containing late endosomes and

lysosomes, which are then transported towards the minus end of microtubules (Jordens et al., 2001). However, no direct interaction between RILP and any of the subunits of the dynein-dynactin motor complex has been observed (Jordens et al., 2001). The most likely explanation for the Rab7/RILP selective recruitment of dynein-dynactin is by modification of the cytosolic membrane of late endosomes and lysosomes in such a way as to allow the complex to form (Jordens et al., 2001).

1.1.5.2.6 Rab11 and its mobility effectors

There is no consensus in the literature as to the number of Rab11 isoforms. Along with Rab11a and Rab11b, the closely related Rab25 is often included in this group (Lapierre et al., 2001; Pereira-Leal and Seabra, 2000). Rab11 proteins are involved in controlling traffic through the recycling endosome. Cells over expressing a Rab11-GDP mutant are inhibited in late recycling endosome function (Ren et al., 1998; Ullrich et al., 1996). In polarized cells, antibodies to Rab11a label an apical pericentriolar endosomal compartment, which is dependent on intact microtubules for its integrity (Casanova et al., 1999). Additional evidence of cytoskeleton involvement comes from localization studies of Rab11 and some of its effectors. Indeed, apart from localizing to the perinuclear region, including Golgi and recycling endosomes, Rab11 is also present along the microtubules oriented towards membrane lamellipodia in an epithelial cell line (Mammoto et al., 1999; Zeng et al., 1999).

Direct evidence of Rab11 interaction with the cytoskeleton is the identification of myosin Vb as Rab11 interacting protein (Lapierre et al., 2001). Myosin Vb co-localizes with Rab11 in plasma membrane recycling systems in both polarized and non-polarized cells in a GTP-dependent fashion (Lapierre et al., 2001). Importantly, expression of a truncated form of myosin Vb lacking the motor domain, retards trafficking through plasma membrane recycling systems (Lapierre et al., 2001).

Rabphilin-11/Rab11BP, Rip11/pp75, and the Rab11-FIP family have also been identified as interacting targets of Rab11 (Hales et al., 2001; Mammoto et al., 1999; Prekeris et al., 2001; Prekeris et al., 2000; Zeng et al., 1999). One of the Rab11-FIP proteins, Rab11-FIP2, was later shown to interact with myosin Vb (Hales et al., 2002). The ternary association of myosin Vb, Rab11-FIP2 and Rab11a suggests the involvement of a multimeric protein complex in vesicle trafficking through plasma membrane recycling systems (Hales et al., 2002).

1.1.5.2.7 Rab27 and its mobility effectors

In mammals there are two Rab27 isoforms, namely Rab27a and Rab27b (Chen et al., 1997). Rab27a is expressed in a large variety of cell and tissue types, excluding brain, but including the eye, lung, spleen, intestine, melanocytes, platelets and pancreas. Rab27b is primarily present in testis but also present in platelets and melanocytes (Chen et al., 1997; Seabra et al., 1995).

Platelet organelles share membrane properties with melanosomes (Nishibori et al., 1993) and Rab27 proteins are expressed in both cell types. Rab27s are thought to be involved in mouse and human disorders characterized by the combination of pigment dilution and a platelet storage pool defect (Chen et al., 1997).

Mammalian melanin is produced by the melanocytes located at the base of the hair bulb and in the basal layer of epidermis. Upon production, melanin is stored in cell organelles called melanosomes that move from the perinuclear Golgi region toward the cell periphery (dendrites) through an interaction with conventional kinesin (Goud, 2002; Wu et al., 1998). At the periphery of the melanocyte, melanosomes detach from microtubules and bind to sub cortical actin bundles before being endocytosed by the adjacent keratinocytes (Goud, 2002).

The genetics of this process in mice has been elucidated by the study of a number of mouse mutations characterised by similar phenotypes that include pigmentation defects. One of these mutations is *dilute*, a gene required for the transfer of melanosomes from the producing melanocyte to the keratinocyte. The *dilute* locus was shown to encode Myosin-Va and in *dilute* melanocytes, although melanosomes travel to dendritic tips, they fail to accumulate there (Mercer et al., 1991; Wu et al., 1998). Another mutation characterized by a similar phenotype and thus likely to encode for a protein involved in the pigment organelle transport pathway is *ashen*. This mutation was positionally cloned and shown to encode for a non-functional version of Rab27a (Wilson et al., 2000). Finally, a third mouse mutation characterized by a lightened coat colour, *leaden*, was identified as a mutation in a 65kDa protein with homology to the Rab3a-binding domain of Rabphilin-3a and is called melanophilin (Matesic et al., 2001). The direct link between Rab27a, Myosin-Va and Rabphilin was then shown by two independent groups (Fukuda et al., 2002; Wu et al., 2002). The N-terminal domain of melanophilin specifically binds Rab27a/b isoforms, and the C-terminal domain directly binds the globular tail of myosin Va (Fukuda et al., 2002). *In vivo*, Rab27a binds to the melanosome first and then recruits melanophilin, in a GTP-dependent fashion, which in turn recruits myosin-Va that holds the whole complex to the actin bundles at the melanocyte dendritic tip (Wu et al., 2002).

Griscelli syndrome (GS) is a rare autosomal recessive disorder associated with partial albinism of hair and skin and immunodeficiency (Seabra et al., 2002).The majority of GS patients have a defect in the *Rab27a* gene, whereas a second form of GS is caused by mutations in the gene *Myosin-Va* (Menasche et al., 2000; Pastural et al., 1997). It is now generally accepted that pigmentation defects in GS patients are due to defects in melanosome transport in a process identical to the one described for the mice models of the disease, *ashen* and *dilute* (Seabra et al., 2002).

1.1.5.2.8 Rab33 and its mobility effectors

In mammals there are two Rab33 isoforms (Rab33a and Rab33b). Whereas Rab33a seems to be expressed only in the brain and immune system, Rab33b is expressed ubiquitously in every mouse tissue (Zheng et al., 1998). Using immunofluorescence studies, Rab33b intra-cellular localization was shown to be in the medial Golgi cisternae (Zheng et al., 1998), where it is thought to regulate the intra-Golgi retrograde transport (Valsdottir et al., 2001).

Using yeast two-hybrid, a novel kinesin-like protein was identified as a binding partner of Rab33b and named Rab33b-BP (Koda et al., 1999). This kinesin-like protein is distinct from Rabkinesin-6 and its interaction with Rab33b only occurs with the GTP-bound form of the GTPase (Koda et al., 1999).

Additional Rab33b effectors were later found. A GST-Rab33b fusion protein stabilised in its GTP form was found to interact by Western blotting or mass spectroscopy with Golgi protein GM130 and rabaptin-5 and rabex-5 (Valsdottir et al., 2001). GM130 had previously been shown to be a Rab1 effector, whereas the two other molecules were thought to function exclusively in the endocytic pathway by interacting with Rab5. These results raise the possibility that Rab proteins have overlapping combinatorial effector sets (Valsdottir et al., 2001).

1.1.6 Rab/cargo interactions

Apart from the conventional role of Rab proteins in intracellular transport, namely tethering, fusion and mobility of vesicles, recent data have uncovered the direct interaction of some Rab proteins with the vesicle cargo (Smythe, 2002).

The first clue as to a possible interaction of Rabs with vesicle cargo was the observation that Rab5-GDI complex is essential for the sequestration of receptors in newly formed clathrin-coated pits of permeabilized cells (McLauchlan et al., 1998). The first step in the formation of the clathrin-coated pits is the recruitment of coat proteins to

the membrane in an ATP-dependent manner. Although lattices are formed under these conditions, these lattices become capable of ligand sequestration only after recruitment of Rab5–GDI and removal of Rab5 inhibits this process (McLauchlan et al., 1998).

TIP47 is a protein that recognizes the cytoplasmic domains of mannose 6-phosphate receptors (MPRs) and is required for its endosome-to-Golgi transport. Interestingly, TIP47 was also shown to directly bind Rab9 in its active conformation and is thus classified as a Rab9 effector (Carroll et al., 2001). Like TIP47 Rab9 is important for shuttling vesicles from endosomes back to the TGN (retrograde transport) (Lombardi et al., 1993; Riederer et al., 1994). Rab9 stimulates the recruitment of TIP47 to endosomes that bear MPRs, and promotes the binding of TIP47 to these receptors (Carroll et al., 2001). Moreover, a functional Rab9 binding site is required for TIP47 stimulation of MPR transport in vivo (Carroll et al., 2001).

While neither of the Rab protein/cargo interactions described above are direct, two other more recent studies have shown that the vesicle cargo can itself be a Rab effector. A direct interaction between Rab5a and the cytoplasmic tail of the angiotensin II Type 1A receptor ($AT_{1A}R$) has been described (Seachrist et al., 2002). This interaction appears to enhance the trafficking of $AT_{1A}R$. Conversely, the data also suggest that $AT_{1A}R$ activation modulates Rab5a activity leading to the homotypic fusion of endocytic vesicles. These observations suggest that vesicular cargo proteins, such as the $AT_{1A}R$, may control their targeting between intracellular compartments by directly regulating the activity of components of the intracellular trafficking machinery such as Rab5a (Seachrist et al., 2002).

The second study implicating a direct interaction between Rab and cargo proteins involves Rab3d and the polymeric IgA receptor (pIgAR) (van IJzendoorn et al., 2002). The dimeric IgA (dIgA) binds to its receptor pIgR at the basolateral surface of epithelial cells and is transcytosed to the apical membrane where it is exocytosed to the surface (Smythe, 2002). In MDCK cells, Rab3b localizes to vesicular structures containing the pIgR and located subjacent to the apical surface (van IJzendoorn et al., 2002). This localization is due to a direct interaction between GTP-bound Rab3b and the cytoplasmic domain of pIgR (van et al., 2002). Binding of dIgA to pIgR at the basolateral surface stimulates subsequent transcytosis to the apical surface and causes a dissociation of pIgR interaction with Rab3b. Over expression of GTP-locked Rab3b inhibits dIgA-stimulated transcytosis (van IJzendoorn et al., 2002). This study further demonstrates that a Rab protein can bind directly to a specific cargo protein and control its trafficking.

1.1.7 Rabs and signalling

In recent years, studies of developmental biology have led to important insights into the cell biology of cell-cell signalling. Trafficking events such as secretion, endocytosis, intracellular transport and targeting to lysosomes regulate various signalling pathways and Rab proteins have been shown to be key players in these events (Vincent, 2003).

Signal transduction usually begins with binding of a ligand to its cell surface receptor. For many receptors, their activation is followed by endocytosis that will be important in the regulation of the signalling pathway.

As an example, epidermal growth factor receptor (EGFR) signalling is linked to EGFR trafficking and involves small GTPases of the Rho and Rab families, respectively (Barbieri et al., 2000; Chen and Wang, 2001; Lanzetti et al., 2000). Signalling and trafficking of this receptor is connected through the protein EPS8 (Lanzetti et al., 2000). EPS8 is a substrate of EGFR and mediates activation of Rac. EPS8 also interacts with RN-tre that is a Rab5 GAP whose activity is regulated by the EGFR. By acting on Rab5, RN-tre regulates both the constitutive and the regulated (for example, EGF-dependent) receptor internalization. The latter activity strictly depends on the interaction of RN-tre with Eps8. Recruitment of RN-tre decreases Rab5 activity, thereby inhibiting receptor internalization and, consequently, prolonging receptor signalling at the plasma membrane (Lanzetti et al., 2000).

The role of Rab4 in integrin recycling is another example of the involvement of Rab GTPases in receptor signalling (Roberts et al., 2001). Integrins are dimeric receptors of a diverse number of extra-cellular matrix components. Vesicular traffic is believed to facilitate cell migration by internalisation of Integrins at the rear of migrating cells and subsequent exocytosis at the leading edge where new contacts with the extra-cellular matrix will form. The formation of integrin-containing focal complexes at the leading edge of the cell is also driven by growth factors such as PDGF. It is unclear, however, whether such cell-signalling pathways coordinate cell motility by regulating the recycling of integrins. When internalised, both $\alpha v\beta 3$ and $\alpha 5\beta 1$ integrins are transported through Rab4-positive early endosomes and arrive at the Rab11-positive perinuclear recycling compartment from where they are recycled to the plasma membrane in a Rab11-dependent manner. Following treatment with PDGF, $\alpha v\beta 3$ integrin, but not $\alpha 5\beta 1$, is rapidly recycled directly to the plasma membrane from the early endosomes via a Rab4-dependent mechanism without the involvement of Rab11 (Roberts et al., 2001). Furthermore, inhibition of this process using dominant negative Rab4 mutants impairs cell adhesion and spreading on $\alpha v\beta 3$ integrin ligands (Roberts et al., 2001).

Morphogens are proteins of particular interest for developmental biologists. A morphogen is a signalling molecule capable of acting directly at a distance to influence the pattern of a developing tissue. One model of morphogen gradient formation in which a signal gradient is established involves planar transcytosis. Experimental evidence in support of this model has come from studies of the TGF-β homolog Decapentaplegic (Dpp) gradient in the *Drosophila* wing imaginal disks (Entchev et al., 2000). The authors studied the effect on Dpp signalling of three established regulators of endocytic transport. Firstly, they observed that Dpp is internalised by Dynamin-dependent endocytosis and fails to move across a Dynamin-defective clone of cells, forming a region of non-responsive but otherwise wild-type cells behind it (Entchev et al., 2000). Secondly, they studied the involvement of the GTPase Rab5, which regulates transport into early endosomes (Bucci et al., 1992). They have shown that impaired DRab5 function results in a reduced Dpp signalling range and DRab5 over expression in the receiving cells leads to an expansion of the Dpp signalling range (Entchev et al., 2000). Finally, these authors studied the involvement of the GTPase Rab7, which targets endocytic cargo from the early to the late endosome and lysosome for degradation (Meresse et al., 1995; Vitelli et al., 1997). Expression of a dominant active version of DRab7 (DRab7Q67L) reduces the range of Dpp signalling, suggesting that Dpp degradation restricts the signalling range (Entchev et al., 2000). Based on these results, the authors propose a model where a Dpp gradient is formed via intracellular trafficking, initiated by receptor-mediated endocytosis of the ligand in receiving cells. The gradient slope would be controlled by endocytic sorting of Dpp toward recycling versus degradation (Entchev et al., 2000).

1.1.7.1 Rab23 and Sonic Hedgehog signalling

The mouse version of Rab23 was reported to have a role of particular interest for developmental biologists as a negative regulator of Sonic Hedgehog (Shh) signalling (Eggenschwiler et al., 2001). There are two mutant alleles of the gene *Open brain* (*Opb*), a spontaneous mutation and an ENU induced mutation (Gunther et al., 1994; Kasarskis et al., 1998). By a map-based approach the mutations were cloned and shown to encode for truncated versions of the mouse Rab23 protein (Eggenschwiler et al., 2001). The *Opb* mutation results in severe defects in the developing neural tube. Homozygous *Opb* embryos exhibit an exencephalic malformation that can be traced back to a failure to initiate neural tube closure at the midbrain-forebrain boundary (Gunther et al., 1994). The spinal cord of *Opb* mutant embryos has severe malformations in both ventral and dorsal regions, namely increased *Shh* and *HNF-3β*

expression ventrally and absent or reduced expression of *Wnt-3a*, *Msx-2* and *Pax-3* dorsally (Gunther et al., 1994). This phenotype is the opposite of the *Shh* mutant phenotype in which ventral neural cell types are lost and dorsal cell types expand into more ventral regions (Chiang et al., 1996), indicating that *Opb* and *Shh* have antagonistic roles in neural patterning.

By generating *Shh;Opb* double mutants, Eggenschwiler and co-workers have shown that *Opb* acts downstream of *Shh* (Eggenschwiler et al., 2001). Ventral neural cell types that are absent in a *Shh* mutant, including the floor plate, are rescued in a *Shh;Opb* double mutant, indicating that *in vivo* Rab23 acts as a Shh negative regulator (Eggenschwiler et al., 2001). The transcription of the Shh receptor *Patched-1* is directly activated by Shh signaling (Goodrich et al., 1996). *Patched-1* transcripts are present in ventral regions of a wild-type spinal cord, absent in *Shh* mutants and expanded to include the entire caudal spinal cord of *Opb* and *Shh;Opb* mutant embryos (Eggenschwiler et al., 2001). These observations indicate that the negative action of Rab23 on Shh signaling is direct (Eggenschwiler et al., 2001).

Rab23 could be acting in the Shh pathway by controlling the secretion of specific signaling components or the transcytosis of the Shh ligand, as appears to be the case for the involvement of Rab proteins in Dpp signaling in the *Drosophila* wing imaginal disk (Entchev et al., 2000). However, chimaera experiments revealed that *opb* is required cell autonomously indicating that this gene product acts intracellularly in the reception or interpretation of Shh signaling (Eggenschwiler and Anderson, 2000). Moreover, the observation that *Shh;Opb* double mutants have a less severe phenotype that the *Shh* mutation alone, indicates that *Opb* bypasses the requirement for *Shh* and makes it unlikely to be involved in Shh secretion or transport (Eggenschwiler et al., 2001).

Alternatively, Rab23 could be involved in the intracellular trafficking of Patched-1 (Ptc1) and/or Smoothened (Smo) through the late endosome-lysosome pathway. The most detailed analysis of the sub-cellular localization of Ptc1 and Smo and how their distribution is affected by Shh ligand, was performed by Incardona and co-workers (Incardona et al., 2002). They show that Ptc1 and Smo co-localize extensively in the absence of ligand and are internalized together after ligand binding, but Smo becomes segregated from Ptc1/Shh complexes destined for lysosomal degradation (Incardona et al., 2002).

Evidence that trafficking might play a role in Shh signaling had been gathered well before the cloning of the *Opb* mutation. Indeed, extensive structural similarity is shared between Ptc proteins (Ptc1 and Ptc2 in vertebrates) and the Niemann-Pick C1 (NPC1)

protein, which includes but is not limited to the sterol-sensing domain (SSD) (Carstea et al., 1997). NPC1 functions in the regulation of intracellular lipid trafficking, namely in the sorting and recycling of cholesterol and glycosphingolipids in the late endosomal/lysosomal system (Blanchette-Mackie, 2000). Another SSD-containing protein has been shown to be involved in trafficking, the protein SREBP (sterol regulatory element-binding protein) cleavage-activating protein or SCAP. SCAP is a key regulator factor in cholesterol metabolism and transport, which acts by chaperoning the transcription factor SREBP between the endoplasmic reticulum and the Golgi apparatus, where it undergoes a cleavage-mediated activation (DeBose-Boyd et al., 1999; Nohturfft et al., 1999). By analogy, Ptc might traffic Smo to an intracellular compartment where it would be targeted for degradation (Ingham and McMahon, 2001). Mutations in the SSD of SCAP cause constitutive translocation of SREBP to the Golgi compartment and similar mutations in NPC1 render the protein incapable of regulating endosomal lipid sorting (Hua et al., 1996; Watari et al., 1999). Consistent with the hypothesis of an analogous trafficking role for Ptc, mutations in its SSD result in loss of its Smo inhibiting activity (Martin et al., 2001; Strutt et al., 2001). However, altering cholesterol levels within the cell has a relatively minor influence on Hh signalling (Incardona et al., 2000a), suggesting that Ptc activity is not modulated by membrane sterol levels, in contrast to the activity of other SSD proteins.

Alternatively, Rab23 could be involved in the formation or stabilization of the Ci (or Gli in vertebrates) cytoplasmic complex. This complex is in close association with the microtubule network through the kinesin-like protein Costal-2 (Robbins et al., 1997; Sisson et al., 1997). Based on the fact that several Rab proteins have been shown to interact directly with molecular motors (Bielli et al., 2001; Echard et al., 1998; Koda et al., 1999), it seems plausible that Rab23 may be providing the link between the Gli cytoplasmic complex and the microtubule network.

1.2 Hh signalling and Gli proteins

Hedgehog proteins are secreted molecules with diverse functions in embryonic development. Depending on the developmental context, these proteins act as mitogens, regulating growth and cell proliferation, or morphogens, acting at a distance from their source in a dose-dependent manner to induce different cell fates in a developing tissue.

The name of the protein stems from the phenotype of the first mutant. In 1980, Nüsslein-Volhard and Wieschaus found, in a screen for mutations that disrupted the *Drosophila* larval body plan, several mutants with a continuous lawn of denticles. This phenotype resembled the spikes of a hedgehog and hence the name of one of the mutations.

It was more than ten years after the identification of *Drosophila* hedgehog (*hh*) mutation that the gene disrupted in the mutant was cloned (Lee et al., 1992; Mohler and Vani, 1992; Tabata et al., 1992; Tashiro et al., 1993). Importantly, the expression of *hh* was not confined to the larval segments responsible for the mutant phenotype, but was also expressed in the wing and leg imaginal discs (Lee et al., 1992). A broader role for Hedgehog signalling in *Drosophila* embryonic development is now well established and there is evidence of it being a key patterning signal in the wing, leg, and eye discs. Moreover, it is also known to be involved in processes such as germ cell migration, and development of optic lamina, gonad, abdomen, gut, and tracheal system (for a review see (Ingham and McMahon, 2001)).

Following the identification of *hh*, vertebrate homologues from fish, chick and mouse were reported (Echelard et al., 1993; Krauss et al., 1993; Riddle et al., 1993). Unlike the fruit fly, which appears to have a single family member, vertebrates have several related *hedgehog* genes. In the mouse there are three such genes: *Desert hedgehog* (*Dhh*), *Indian hedgehog* (*Ihh*), and *Sonic hedgehog* (*Shh*) (Echelard et al., 1993). With the exception of the gut, in which both Ihh and Shh are expressed, the expression patterns of the hedgehog family members do not overlap (Bitgood and McMahon, 1995). These three proteins also seem to have distinct roles: Shh acts to establish cell fate in a number of developing tissues including the limb, somites, neural tube, hair, etc.; Ihh is involved specifically in chondrocyte development; and Dhh plays a key role in germ cell development (for a review see (Ingham and McMahon, 2001)).

In teleosts there appears to have been a further duplication and zebrafish contains two genes equally related to mouse *Shh*, *shh* and *tiggy-winkle hedgehog* (*twhh*), and two

genes equally related to mouse *Ihh*, *echidna hedgehog* (*ehh*) and *qhh* (Currie and Ingham, 1996; Ekker et al., 1995; Ingham and McMahon, 2001).

Although *Dhh* is the vertebrate *hedgehog* gene more closely related to *Drosophila hh* (Ingham and McMahon, 2001), *Shh* has received the most attention. It is expressed in a number of signalling centres in the vertebrate embryo including the notochord, the floor plate and the Zone of Polarizing Activity (ZPA) in the limb bud (Echelard et al., 1993; Krauss et al., 1993; Riddle et al., 1993) and it is on this gene that most work has centred.

1.2.1 The Hh pathway

Genetic studies of fly mutants have provided most information about Hh signalling. Moreover, studies in vertebrate cell culture systems and vertebrate embryos suggest the vertebrate Hedgehog signalling pathway functions in a manner similar to the fly. For the brief description of the Hedgehog pathway that will follow, the *Drosophila* terminology will be used and, when different, the name of the vertebrate homologues will be given.

1.2.1.1 Hh synthesis

Hh proteins are synthesised as a ~40kD precursor that undergoes auto-proteolytic cleavage to generate two predominant protein species (Lee et al., 1994). Both these peptides seem to be secreted but only the smaller (~19kD) N-terminal fragment (Hh-N) is known to be active and able to substitute for full length Shh (Burncrot et al., 1995; Marti et al., 1995; Porter et al., 1995; Roelink et al., 1995). The auto-cleavage is achieved through the nucleophilic attack of a cholesterol molecule resulting in its covalent attachment to the C terminus region of the smaller 19kD peptide (Hh-Np, 'p' for *processed*) (Porter et al., 1996). Hh proteins undergo a further lipid modification consisting of the palmitoylation of a highly conserved NH_2-terminal Cys residue (Pepinsky et al., 1998). The relevance of this lipid modification is not clearly understood and seems to depend on the context in which the Hedgehog protein is acting. Indeed, in *Drosophila* larval cuticle patterning this modification seems to be highly relevant as the cloning of the segment polarity mutation *skinny hedgehog* (ski) revealed. The product of this gene is an acyltransferase required in Hh-producing cells for production of a functional signal (Chamoun et al., 2001; Lee and Treisman, 2001). Hh proteins from *ski* mutant cells are processed and contain carboxyl-terminal cholesterol modification but lack amino-terminal palmitate modification (Chamoun et

al., 2001). In contrast, in vertebrates, both acylated and unmodified forms of the hedgehog protein seem to have equivalent or very similar levels of activity in the ventralization of the neural tube or in the patterning of the mouse limb (Kohtz et al., 2001; Lee et al., 2001).

The lipid modifications described above may play an important role in Hedgehog protein sub cellular localization. In *Drosophila* embryos, Hedgehog associates with lipid rafts, cellular structures known to play a crucial role in intracellular sorting and signal transduction (Ingham, 2001; Rietveld et al., 1999; Tabata and Kornberg, 1994).

1.2.1.2 Hh release

The cholesterol modification of Hh-Np would appear to act as an anchor tethering Hh-Np to membranes. It therefore remained to be explained how Hh-Np is released from the producing cell to act at a distance. A potential answer to this question came with the identification of the *Drosophila* protein Dispatched (Disp) (Burke et al., 1999). Disp is a 12-pass transmembrane protein that has sequence similarity with Patched (Ptc), the Hh receptor. It is required in Hh producing cells and without it, these cells accumulate Hh-Np protein, implying that an active process involving Disp is necessary to overcome the membrane tethering accomplished by the cholesterol modification (Burke et al., 1999).

Vertebrates have two Dispatched proteins (DispA and DispB) but only one seems to be involved in Shh signalling (Caspary et al., 2002; Ma et al., 2002). Cells in which the mDispA protein is absent respond normally to Shh signalling but are incapable of stimulating other cells when expressing Shh (Ma et al., 2002). Apart from presenting homology to the Ptc protein, Disp clearly shows sequence similarity to prokaryotic resistence-nodulation-division (RND) permeases, which are efflux pumps involved in drug or heavy metal resistance that function as proton-driven anti-porters (Tseng et al., 1999). Two out of three residues known to be important for the transport function of RND proteins are present in mDispA, but not in mDispB (Ma et al., 2002). When these residues are mutated, mDispA becomes unable to complement *Drosophila disp* mutations and to release Hh proteins in cultured cell assays (Ma et al., 2002). These results suggest a similar mechanism of action between mDispA and prokaryotic proteins from the RND family.

For Hh to travel between producing and receiving cells, it is likely that it interacts with extra-cellular matrix components. This has been emphasized by the identification of the *Drosophila* protein Tout velou (Ttv) (Bellaiche et al., 1998). Ttv is a putative transmembrane protein necessary for Hh diffusion, the closest vertebrate homolog

being the EXT proteins (Bellaiche et al., 1998). EXT proteins are glygosaminoglycans (GAG) transferases found in the endoplasmic reticulum where they help to regulate the synthesis and display of cell surface heparin sulphate GAGs (McCormick et al., 1998). It has thus been hypothesised that *ttv* activity is necessary for the synthesis of a GAG that specifically interacts with Hh at the cell surface to facilitate its movement between cells (Ingham, 1998). Indeed, there is recent evidence to support this model. In *Drosophila* embryonic ectoderm, cholesterol modified Hh assembles intercellularly into large punctate structures in a Disp dependent manner (Gallet et al., 2003). These structures seem to be sorted to the apical surface of the ectoderm cell and then move towards a receiving cell in a Ttv dependent manner (Gallet et al., 2003).

In addition, it was shown that Shh-N binds to Vitronectin (VN), an extra-cellular matrix protein expressed in the notochord and ventral neural tube, where its expression is induced by Shh-N (Martinez-Morales et al., 1997; Pons and Marti, 2000). Both Shh-N and VN can promote motor neuron differentiation in neural tube explants (Martinez-Morales et al., 1997). When added in combination, these proteins seem to synergize and increase the extent of motor neuron differentiation in cultures of dissociated neuroepithelial cells (Pons and Marti, 2000).

More recently, it has also been suggested that Hh movement is compromised in *trol* mutants (Park et al., 2003). Trol is the *Drosophila* homolog of perlecan, an extra-cellular matrix component, and co-immunoprecipitation studies are consistent with a direct interaction between Hh and this protein (Park et al., 2003).

1.2.1.3 Hh reception

The receptor of the Hh protein is a multi-transmembrane domain protein encoded by the *patched* (*ptc*) gene (Ingham et al., 1991). In *Drosophila* there is a single *ptc* gene, but in vertebrates there are two, *Ptc1* and *Ptc2* (Motoyama et al., 1998b). A direct physical interaction between Hh and Ptc has been demonstrated *in vitro* and implied from *in vivo* data (Briscoe et al., 2001; Marigo et al., 1996a; Stone et al., 1996).

Genetic studies indicate that *Ptc* activity suppresses Hh target gene expression leading to the suggestion that Hh acts by antagonizing Ptc activity (Ingham et al., 1991). Intriguingly, the worm *C. elegans* which does not have any obvious Hh homolog, contains at least two *ptc* homologues (Kuwabara et al., 2000).

Apart from Disp, the closest eukaryotic relative of Ptc is the Niemann-Pick C1 (NPC1) protein (Carstea et al., 1997; Loftus et al., 1997). NPC1 is a gene mutated in patients of Niemann-Pick type C disease, an autosomal recessive disorder characterized by lysosomal accumulation of cholesterol (Carstea et al., 1997; Loftus et al., 1997). All

three proteins have multi transmembrane domains (TM) (Ptc and Disp have 12 and NPC1 13 to 16) and the homology between them is in the TM encompassing the sterol sensing domain (SSD) of NPC1 (Burke et al., 1999; Carstea et al., 1997; Loftus et al., 1997). SSD domains are also found in two proteins involved in cholesterol metabolism: sterol regulatory element binding protein (SREBP) cleavage-activating protein (SCAP) and 3-hydroxy-3-methyl-glutaryl coenzyme A (HMG-CoA) reductase (Carstea et al., 1997; Loftus et al., 1997). HMG-CoA reductase catalyses the production of mevalonate, a key intermediate in the synthesis of sterols and non-sterol isoprenoid metabolites important for many cellular functions. The SSD of HMG-CoA reductase appears to be important for sensing sterol levels because a truncated form is degraded in response to intracellular sterol levels (Gil et al., 1985). HMG-CoA is additionally regulated at the transcriptional level by SREBP. SREBP is a membrane bound transcription factor, activated by cleavage and released from the membrane by the sterol-responsive protein, SCAP. A single amino-acid change in the SSD of SCAP renders it insensitive to intracellular cholesterol levels (Hua et al., 1996). Importantly, this amino-acid is conserved in SSD containing proteins (Loftus et al., 1997).

Why would proteins like Ptc and Disp contain SSDs, so far only know to be relevant in cellular cholesterol control? The SSD of Ptc appears to be important, as a mutation that renders this domain unresponsive to cholesterol also results in Hh signalling misregulation (Martin et al., 2001; Strutt et al., 2001). One attractive model is that these proteins interact with the cholesterol moiety of the processed form of Hh through their SSDs (Ingham and McMahon, 2001). Consistent with this, when a modified version of Hh proteins, truncated but without the cholesterol molecule covalently bound (Hh-Nu or Shh-Nu, 'u' for *unmodified*), is expressed in embryos, Hh signalling is compromised (Lewis et al., 2001; Porter et al., 1996).

Apart from homology with NPC1, and as previously mentioned for Disp, Ptc also has homology with prokaryotic RND permeases (Ingham and McMahon, 2001). Additionally, the two residues important for RND transport activity and mDispA function are also conserved in Ptc (Ingham and McMahon, 2001). This raises the striking possibility that Ptc may also function as a permease.

Not only does Ptc seem to be involved in Hh signal transduction, it also seems to have a role in restricting Hh movement. The receptor is a transcriptional target of Hh and evidence suggests that increasing Ptc expression acts to sequester Hh creating a barrier to its further transport (Chen and Struhl, 1996).

A second transmembrane protein, Smoothened (Smo), is essential for the transduction of Hh signalling in both *Drosophila* and vertebrates (Alcedo et al., 1996; Chen et al.,

2001; van den Heuvel and Ingham, 1996; Zhang et al., 2001). Smo belongs to the superfamily of G-protein-coupled receptors and is most closely related to the Frizzled family of Wnt receptors (Stone et al., 1996).

The first model put forward for the Hh receptor complex was based on the direct interactions between Hh and Ptc, and between Ptc and Smo (Murone et al., 1999; Stone et al., 1996). It postulated that Ptc exerted a physical and direct inhibitory action upon Smo that would only be released when Hh was bound to Ptc, through, for instance, an induced change of conformation. However, more recent experimental data suggest an alternative possibility. When Hh is added to culture cell lines, Ptc is removed from the cell membrane whereas Smo accumulates there in a highly phosphorylated form (Denef et al., 2000). In this view, Ptc inhibits Smo only when in the same compartment and ligand induces segregation of the transmembrane proteins (Incardona et al., 2002). Accordingly, Incardona et al.. showed that Ptc1 and Smo co-localize extensively in the absence of ligand (Incardona et al., 2002). After treatment with Shh, the authors saw that Ptc1 and Smo are internalised together, but become segregated in the late endocytic pathway (Incardona et al., 2002).

The Incardona et al. model implies that Ptc1 must have close proximity to Smo in order to inhibit it, but co-immunoprecipitation studies ruled out a direct interaction between both proteins (Incardona et al., 2002). Co-immunoprecipitation had previously been shown in cell lines but levels of expression were very high and the Ptc1/Smo complex was estimated to represent only 30% of the total amount of each protein (Incardona et al., 2002; Stone et al., 1996).

In vertebrates, it has been shown that apart from binding to its receptor Ptc1, Hedgehog proteins bind another protein, Hedgehog-interacting protein-1 (Hip1). Hip1 is a membrane glycoprotein expressed in cells adjacent to Hedgehog producing cells and with no *Drosophila* counterpart (Chuang and McMahon, 1999). Like *Ptc1*, *Hip1* is a general transcriptional target of vertebrate Hedgehog signalling and its activity seems to be the attenuation of the pathway, probably by sequestering Hedgehog proteins (Chuang and McMahon, 1999).

1.2.1.4 Hh signal transduction

The biochemical activity of the Smo protein, not only at the level of its interaction with Ptc, but also downstream of Smo itself, is unclear. However, the major target of Smo is known to be the transcription factor encoded by the *Drosophila* segment polarity gene *cubitus interruptus* (*ci*), homologous to the vertebrate *Gli* genes (Forbes et al., 1993; Murone et al., 1999; Orenic et al., 1990). Ci is a bifunctional transcription factor that

controls expression of Hh target genes by both activation and repression and the regulation of the balance between activating and repressing forms appears to be the key event in Hh signalling (Ingham and McMahon, 2001). This explains the disparity between mild phenotypes caused by mutations in *ci* compared to the severe phenotype of *hh* mutants. Complete removal of Ci results in loss of both the repressor and activating isoforms, thus corresponding to a *hh* partial gain-of-function phenotype, rather than to a *hh* mutant phenotype (Methot and Basler, 2001).

In the absence of Hh signalling, Ci protein is present in the cytoplasm as part of a multi-component protein complex. Three members of this complex, Costal (Cos2), Fused (Fu) and Ci bind each other directly (Stegman et al., 2000). Through Cos2, a kinesin-related protein, this complex is bound with high affinity to microtubules. In cells exposed to Hh, binding is reversed (Robbins et al., 1997; Sisson et al., 1997; Stegman et al., 2000; Wang et al., 2000b).

The cytoplasmic complex is involved in the proteolytic processing of Ci. The 155kDa full length Ci protein is cleaved to form a 75kDa transcriptional repressor. The proteolytic cleavage removes the transcriptional activating domain of the protein but retains its zinc-finger DNA binding domain and a N-terminal repression domain (Aza-Blanc et al., 1997). The proteolysis requires the presence of Cos2, Protein Kinase A (PKA), Casein Kinase 1 (CK1), Shaggy (Sgg) (*Drosophila* Glycogen Synthase Kinase 3, GSK3) and the F-box/WD40 repeat protein Slimb (supernumerary limbs) (Chen et al., 1998; Jia et al., 2002; Jiang and Struhl, 1998; Methot and Basler, 2000; Price and Kalderon, 2002).

The role of Cos2 in Ci proteolysis is not clear, but the fact that it binds microtubules in a Hh sensitive manner (Robbins et al., 1997) suggests that Ci cleavage depends on microtubule attachment (Ingham and McMahon, 2001). If this were the case, Hh-induced dissociation of the complex from the microtubules would suffice to prevent Ci cleavage. For Ci cleavage to occur, there is first direct phosphorylation of a cluster of sites by PKA, that act to prime subsequent phosphorylation of additional sites, this time by Sgg/GSK3 and CK1 (Jia et al., 2002; Price and Kalderon, 2002). After Ci phosphorylation, Slimb seems to act to further promote the protein for processing. In *slimb* mutant cells Ci accumulates in its uncleaved form and there is ectopic activation of Hh target genes (Jiang and Struhl, 1998).

Slimb is related to budding yeast Cdc4p and vertebrate βTRCP, involved in targeting proteins for degradation by the ubiquitin/proteosome pathway (Jiang and Struhl, 1998; Maniatis, 1999). By analogy, Slimb could act to target phosphorylated Ci, or other components of the Hh pathway, for ubiquitin/proteosome-mediated proteolysis

(Maniatis, 1999). Consistent with this, the proteosome has been shown to be required for Ci processing (Chen et al., 1999).

Additionally, a recently identified *Drosophila* protein, Debra, associates with both Ci155 and Slimb causing polyubiquitination of Ci (Dai et al., 2003). Debra appears to induce lysosomal degradation of Ci155 rather than promoting its degradation by the ubiquitin/proteosome pathway (Dai et al., 2003). It has been shown that ubiquitination serves as a signal for the sorting of proteins into the multi-vesicular body (MVB) pathway that leads to lysosomal degradation (reviewed in (Hicke, 2001)) and Debra localizes with the MVB (Dai et al., 2003). The model proposed by Dai et al. suggests that, in the absence of Debra, Slimb induces the proteolytic processing of Ci155 to Ci75 via the proteosome, whereas when Debra is present it co-operates with Slimb to induce the full ubiquitination of Ci155 that targets it for lysosomal degradation via MVBs (Chen et al., 1999; Dai et al., 2003).

The cleavage of Ci is inhibited by Hh signalling and results in the generation of a full-length activating protein (Ci155). Stimulation of cells by Hh releases the Fu/Cos2/Ci trimeric complex from microtubules and induces the phosphorylation of both Fu and Cos2 components (Robbins et al., 1997).

Once the complex is 'free' in the cytoplasm it is bound by another protein involved in Hh signalling at the level of Ci regulation, Suppressor of fused (Su(fu)) (Pham et al., 1995; Stegman et al., 2000). The role of this protein in Hh signalling is not clear but it probably represents an extra level of control in Ci activity. Flies lacking this gene are completely viable and fertile but the absence of Su(fu) in a *fu* mutant background fully suppresses the embryonic and adult phenotypes of *fused* (Preat, 1992). It has been proposed that Su(fu) could act to retain Ci in the cytoplasm (Methot and Basler, 2000). Su(fu) may modulate full-length Ci activity either preventing it from entering the nucleus or even by entering the nucleus bound to it and attenuating its transcriptional activity (Kogerman et al., 1999). In this view, the dissociation of Ci from Su(fu) would be necessary to elicit maximal response of cells to Hh signaling. This dissociation appears to be mediated by the activity of Fu (Alves et al., 1998; Ohlmeyer and Kalderon, 1998). Fu is a serine-threonine kinase and it thus seem plausible that phosphorylation of Su(fu) is necessary for its dissociation from Ci (Ingham and McMahon, 2001).

Apart from a putative role in Ci cytoplasmic retention, recent data using the mammalian counterpart of the protein, mSu(Fu), has raised the possibility that Su(Fu) constitutes a transcriptional co-repressor. mSu(Fu) was shown to interact with SAP18 that in turn is part of a transcriptional repressor complex, the mSin3 and histone deacetylase

complex (Cheng and Bishop, 2002). mSu(fu) was shown to repress transcription by recruiting the SAP18-mSin3 complex to promoters containing the Gli-binding element (Cheng and Bishop, 2002).

Once inside the nucleus, Ci155 binds to consensus sites in Hh target genes promoters activating their transcription (Kinzler and Vogelstein, 1990; Sasaki et al., 1997). Gene transcriptional activation by Ci may be dependent on additional factors, such as CREB-binding protein (CBP) since a CBP binding site was found in Ci155 (Akimaru et al., 1997).

1.2.2 Hh and trafficking

Although the control of Ci processing by Hh signalling and Smo activation is a critical event, how these processes are connected remains unclear. Several lines of evidence support the idea that membrane trafficking plays a critical role in modulating Hedgehog signalling activity. In particular, the mechanism by which Ptc controls Smo signalling seems to involve vesicular transport. In Hh-responding cells, both in *Drosophila* embryos and imaginal discs, Ptc and Hh co-localized to intracellular vesicles identified as endosomes, suggesting a receptor-mediated internalisation of the signalling molecule (Burke et al., 1999; Tabata and Kornberg, 1994). This is supported by evidence from vertebrate cells and *Drosophila* wing discs cells (Incardona et al., 2000b; Martin et al., 2001). In both *Drosophila* and mammalian cells, the internalisation of the receptor is dynamin-dependent and thus mediated by clathrin-coated pits (Capdevila et al., 1994; Incardona et al., 2000b). Once internalised both proteins seem to be targeted to the lysosome, at least in neurons (Mastronardi et al., 2000).

In a mammalian cell line Ptc1 and Smo co-localize extensively prior to Shh exposure and undergo co-transport into the endosomal system after ligand binding (Incardona et al., 2002). Segregation of Smo from Ptc1/Shh complexes occurs in the late endocytic pathway, and while Ptc1/Shh complexes are destined for degradation, Smo is recycled to the plasma membrane (Incardona et al., 2002). The authors suggest this stabilization of Smo at the plasma membrane releases it from inhibition and enables it to signal (Incardona et al., 2002).

A recent study using explants of *Drosophila* salivary gland cells supports the hypothesis that cellular locations of Smo and Ptc are regulated by Hh (Zhu et al., 2003). The authors overcame the problem of the reduced size of cells of both fly embryos and imaginal discs by using the much bigger salivary gland fly cells, which they show to be responsive to Hh signalling (Zhu et al., 2003). Although it was not possible to monitor simultaneously the movements of Ptc and Smo proteins in these

cells, they were reported to be strikingly different (Zhu et al., 2003). Without added Hh protein, Smo is mainly located in a network of intracellular structures with a surface to intracellular protein ratio of 2:9. Upon addition of Hh, Smo relocated to the cell surface resulting in a surface to intracellular ratio of 7:3. In contrast, in unstimulated cells, Ptc accumulated at higher levels throughout the cell membrane, a network of intracellular structures and perinuclear regions. Upon addition of Hh there was a dramatic movement of Ptc that was no longer detected in the plasma membrane and instead accumulated in perinuclear regions (Zhu et al., 2003). Although Zhu et al. and Incardona et al. studies are not in direct contradiction, the extent of co-localization and association between Ptc and Smo proteins needs to be clarified (Denef et al., 2000; Incardona et al., 2002; Johnson et al., 2000; Zhu et al., 2003). However, both studies agree that Ptc (or Ptc1) and Smo are segregated intracellularly by the addition of the ligand (Incardona et al., 2002; Zhu et al., 2003).

These studies of Ptc and Smo proteins suggest that the mechanism by which Ptc controls Smo signalling involves vesicular trafficking. In addition, it seems that the means by which Smo signal is transduced to the Ci complex also involves intracellular movement (Ruel et al., 2003). A link between Smo and the Cos2/Fu/Ci cytoplasmic complex has recently been uncovered (Ruel et al., 2003). Independent of Hh stimulation, Smo directly associates with the C-terminal region of Cos2. In the model emerging from these studies, Smo is directly associated with Cos2/Fu/Ci complex, both in a vesicular cytoplasmic pool and in the plasma membrane. However, Hh stimulation decreases the cytoplasmic pool, probably by increasing transport of the vesicles to the plasma membrane. All three proteins are phosphorylated at the plasma membrane but with different outcomes: phosphorylation of Smo correlates with its increased stability, while phosphorylation of Cos2 and Fu appears to destabilize the proteins. Inhibition of Cos2 allows Ci dissociation from the complex, leading to its activation and translocation to the nucleus (Ruel et al., 2003).

Another important observation that adds to the importance of trafficking in Hh signalling is the extensive structural similarity shared by Ptc, Disp and NPC1 proteins (Carstea et al., 1997; Loftus et al., 1997). NPC1 functions in the sorting and recycling of cholesterol and glycosphingolipids in the late endosomal/lysosomal system and it localizes extensively with Ptc1 in transfected cells. Furthermore, compounds that block cholesterol transport are weak Shh antagonists (Incardona et al., 2000a). These results may suggest that function of these proteins involve a common vesicular transport pathway (Blanchette-Mackie, 2000; Incardona et al., 2000a).

Involvement of vesicular transport in Hedgehog signalling received further support from a completely different direction. As previously mentioned and described in the introduction to Rab proteins in the first part of this thesis, the mouse *open-brain* mutant phenotype was shown to be due to a defect in the *Rab23* gene (Eggenschwiler et al., 2001). RAB23 is a member of the Rab family of small GTP-activated proteins associated with many dynamic aspects of membrane trafficking and was genetically shown to be required for negative regulation of Shh signalling in the vertebrate neural tube (Eggenschwiler and Anderson, 2000; Eggenschwiler et al., 2001).

1.2.3 Shh as a morphogen in the neural tube

In vertebrates, Shh is expressed along the entire length of the notochord, a mesodermal rod that underlies the ventral neural tube, and floor plate, a specialized population of cells at the ventral midline of the neural tube (Echelard et al., 1993; Krauss et al., 1993). Both structures are known to be important for the specification of different cell identities in the neural tube, and Shh was more recently shown to be a long-range morphogen responsible for ventral neural tube patterning (Briscoe and Ericson, 2001; Placzek, 1995).

Several studies have shown that Shh protein secreted by the notochord and the floor plate controls specification of ventral cell types in the neural tube (Chiang et al., 1996; Ericson et al., 1996; Marti et al., 1995; Roelink et al., 1995). *In vitro*, distinct classes of ventral neurons can be generated in response to distinct Shh concentrations (Ericson et al., 1997). Moreover, the concentration of Shh required for induction of ventral neuronal subtypes *in vitro* corresponds to their position of generation *in vivo* (Ericson et al., 1997).

How do different Shh protein concentrations induce different ventral neuronal subtypes? The answer to this question lies in part on Shh regulation of homeodomain proteins expression in ventral neural tube progenitors (Briscoe et al., 2000; Briscoe et al., 1999; Ericson et al., 1996; Ericson et al., 1997; Goulding et al., 1993b; Pierani et al., 1999).

Briscoe et al. propose a model in which dose-dependent activation or repression of homeodomain proteins is a key response to Shh signalling (Briscoe et al., 2000). According to this model, homeodomain transcription factors expressed in the neural tube can be subdivided into two types based on their mode of regulation by Shh. Class I proteins are repressed by Shh signalling (Pax7, Irx3, Dbx1, Dbx2 and Pax6), whereas Class II proteins are induced by Shh signalling (Nkx6.1 and Nkx2.2). The differential expression of these homeodomain proteins by neural progenitors allows their

classification into five distinct domains (Briscoe and Ericson, 2001; Briscoe et al., 2000). From ventral to dorsal: progenitors of v3 neurons (p3) express Nkx6.1 and Nkx2.2; progenitors of motor neurons (pMN) express Nkx6.1 and Pax6; progenitors of v2 neurons (p2) express Nkx6.1, Irx3, and Pax6; progenitors of v1 neurons (p1) express Dbx2, Irx3 and Pax6; and progenitors of v0 neurons (p0) express Dbx1, Dbx2, Irx3, and Pax6 (Briscoe and Ericson, 2001). The defined and sharp boundaries of Class I and Class II protein expression domains observed *in vivo* are achieved by cross-repression between pairs of Class I and Class II proteins that occupy adjacent progenitor domains (Briscoe et al., 2000). This led to the suggestion that cross-repressive interactions serve not only to refine boundaries, establishing discrete patterns of gene expression, but also to consolidate progenitor domain identity once the initial period of graded Shh signalling fades (due to, for instance, neural tube growth) (Briscoe and Ericson, 2001).

After evidence that different concentrations of Shh induce different neuronal subtypes *in vitro* had been provided (Ericson et al., 1997), evidence that Shh works as a morphogen *in vivo*, directly patterning the ventral neural tube, emerged from a number of studies (Briscoe et al., 2001; Wijgerde et al., 2002).

Making use of a mutant form of Shh receptor Ptc1 to produce cells that are not responsive to Shh, it was possible to show that this protein acts directly to specify different neuronal progenitor identities in the spinal cord (Briscoe et al., 2001). The mutant form of Ptc1 ($Ptc1^{\Delta loop2}$) retains the ability to inactivate Smo but lacks the extra-cellular region where Shh binds, thus being unresponsive to its presence (Briscoe et al., 2001). Once electroporated into the chick neural tube, the authors observed cell autonomous repression of Shh target genes induced at different levels of the protein *in vitro* and at different distances from the source *in vivo* (Briscoe et al., 2001). Using a different approach, Wijgerde et al. reached the same conclusion (Wijgerde et al., 2002). In this study, the authors took advantage of the fact that all Hh signalling is transduced through the transmembrane protein Smo to make chimeras with *Smo* null mutant neural progenitor cells in the ventral spinal cord progenitor population (Wijgerde et al., 2002). They were able to confirm that direct Hh signalling is essential for the specification of all ventral spinal cord progenitor populations (Wijgerde et al., 2002).

1.2.4 Gli's and Hh signalling

The dual repressor and activator function of Ci means loss of function mutants of Ci in *Drosophila* have a distinct phenotype from *hh* mutants: *hh* mutants lose expression of all Hh target genes, whereas loss of Ci leads to loss of some Hh target genes and de-

repression of others (Methot and Basler, 2001). In contrast to flies, vertebrates have three Ci-related proteins named Gli1, Gli2 and Gli3 (after glioblastoma) that are all involved in mediating Hh signalling. The presence of three *gli* genes causes even more difficulties in phenotype analysis since apart from the, at least theoretical, dual role of each vertebrate Gli protein, total or partial redundancy is also a possibility.

The expression of vertebrate *Gli* genes is consistent with them acting as the transcription factors of Hh signalling and they are expressed in the neural tube of mice, chick, *Xenopus* and zebrafish embryos (Hynes et al., 1997; Karlstrom et al., 1999; Karlstrom et al., 2003; Lee et al., 1997; Marigo et al., 1996b; Ruiz i Altaba, 1998; Sasaki et al., 1997).

The function of *gli* genes has been analysed by both loss of function and gain of function approaches using both model organisms and cultured cells, and mutant studies in mouse and zebrafish. The conclusions drawn from individual studies aren't always clearly translatable between vertebrate systems, which may reflect species specificities of Gli proteins or shortcomings of the methodology employed.

1.2.4.1 Gain of function approaches to study vertebrate Gli function

Conservation of Gli proteins function in transducing Hh signalling in vertebrates was first demonstrated in misexpression studies in mouse and *Xenopus* (Hynes et al., 1997; Lee et al., 1997). When ectopically expressed in dorsal regions of the brains of transgenic mice, Gli1 lead to the activation of ventral neural tube markers and suppression of dorsal neural tube markers (Hynes et al., 1997). Similarly, over-expressing Gli1, but not Gli3, in *Xenopus* embryos results in ectopic differentiation of floor plate cells and ventral neurons within the neural tube (Lee et al., 1997). These studies further showed that Shh signalling activates Gli1 transcription, something that does not seem to occur with Ci and in the fly (Hynes et al., 1997; Lee et al., 1997). Furthermore, this function of Gli1 seems to be achieved through its activating form since a fusion of Gli1 and VP16 transactivating domain still induced ectopic floor-plate cells in frog embryos (Lee et al., 1997).

In contrast to Gli1, Gli2 and Gli3 seem to function both as transcriptional activators and repressors, as revealed by cell culture studies of wild-type and mutant forms of the proteins (Dai et al., 1999; Sasaki et al., 1999; Shin et al., 1999). Sasaki et al., developed a cell-culture assay that measures Gli-transcriptional activity through the use of a reporter gene driving luciferase inserted downstream of 8 copies of Gli binding sites from the *HNF3β* specific floor plate promoter (Sasaki et al., 1997). Using this assay, wild type mouse Gli1 and Gli2 act as transcriptional activators, while human

GLI3 behaves as a mild repressor (Sasaki et al., 1999). For Gli2, truncation of the activation domain in the C-terminal half results in a protein with repressor activity, while removal of the repression domain at the N terminus converts it into a strong activator (Sasaki et al., 1999). GLI3, but not Gli1, also seems to have a repressor domain in its N-terminus, since deletion of a N-terminal fragment of the protein converts it from a weak repressor into an activator (Sasaki et al., 1999). To test the *in vivo* relevance of this finding, N-terminal truncated Gli2 was expressed in transgenic mouse embryos where it was able to activate a Shh target gene, *hnf3β* (Sasaki et al., 1999). The authors hypothesize that when the Shh signal derived from the notochord is received by the neural plate, the widely expressed Gli2 and Gli3 proteins are presumably converted to their activator forms in the ventral cells, leading to activation of transcription of their target genes, including Gli1 (Sasaki et al., 1999).

Using the same cell culture assay, Karlstrom et al. found that wild-type zebrafish Gli1 protein acted as an activator, in a similar, albeit weaker, manner to mouse Gli1 (Karlstrom et al., 2003). In contrast, wild-type zebrafish Gli2 seems to act as a weak repressor and is able to partially block transcriptional activation by Gli1 or Shh (Karlstrom et al., 2003).

To make a more direct comparison of vertebrate Glis and the *Drosophila* Ci protein, two independent groups expressed vertebrate proteins in the fly wing and monitored their activities, with or without Hh (Aza-Blanc et al., 2000; von Mering and Basler, 1999). In this heterologous system they showed that frog Gli1 and Gli2, and human GLI1, in their full length versions have activator functions, whilst GLI3 is cleaved to act as a repressor, all dependent on Hh (Aza-Blanc et al., 2000; von Mering and Basler, 1999). Similar to GLI3, Gli2 can also be found in a truncated form that acts as a repressor, however, evidence that this process is regulated by Hh signalling is lacking. Gli1 was only detected in its full-length version (Aza-Blanc et al., 2000).

1.2.4.2 Genetic approaches to study vertebrate Gli function

1.2.4.2.1 Mouse Gli knock-outs

Despite the apparently important role uncovered for Gli1 in Hh signal transduction through cell culture and mis- or over-expression studies, functional disruption of *Gli1* in mice does not result in developmental defects (Bai et al., 2002; Matise et al., 1998; Park et al., 2000). Mice homozygous for a Gli1 mutation lacking the DNA binding domain are viable and appear normal (Park et al., 2000). This result suggests that Gli1 does not act as primary or sole transducer of Shh signalling in development

(Koebernick and Pieler, 2002). The observation that Gli1 expression itself is dependent on Hh signalling, at least in the limbs and CNS, further supports this conclusion (Bai et al., 2002; Dai et al., 1999; Hynes et al., 1997; Lee et al., 1997).

In contrast to mice lacking Gli1, mice mutant for Gli2 have a developmental phenotype with several tissues being affected, including the neural tube, lung, foregut and skeleton (Ding et al., 1998; Mo et al., 1997; Motoyama et al., 1998a). In the neural tube, there is lack of floor plate and the adjacent cell type, ventral interneuron 3 neurons (v3) (Ding et al., 1998; Jacob and Briscoe, 2003). However, motor neurons are generated and their domain expands ventrally (Ding et al., 1998). These results imply that mouse Gli2 is required to mediate high level Shh signalling in the mouse ventral neural tube (Ding et al., 1998).

Extra-toes^{J} (*Xt*^{J}) is a spontaneous semi-dominant mouse mutant with defects in limb development that is almost completely penetrant in heterozygotes (Hui and Joyner, 1993). This mouse is a model of Greig cephalopolysyndactyly syndrome (GCPS), an autosomal dominant disorder affecting limb and craniofacial development in humans (Hui and Joyner, 1993). Both in human patients with GCPS and in the *extra-toes*^{J} mouse the gene *Gli3* is affected and the *Xt*^{J} alleles results in a Gli3 protein truncated from its first zinc finger domain (Hui and Joyner, 1993). Mice lacking Gli3 have severe forebrain defects and alterations in the patterning of the neural tube (Persson et al., 2002; Theil et al., 1999). In the absence of Gli3 there is a dorsal shift in the identity of intermediate progenitor domains at the expense of more dorsal progenitors (Persson et al., 2002) and ectopic activation of *Shh* expression (Ruiz i Altaba, 1998). The analysis of the limb phenotype of the *Xt* mutant suggested that Gli3 acts as a repressor of Hh targets and of *Shh* itself (Masuya et al., 1997; Masuya et al., 1995; Wang et al., 2000a). The requirement for Gli3 repressor activity in the neural tube was demonstrated with mice homozygous for a target mutation in *Gli3* that results in a premature termination of translation, *Gli3*$^{\Delta 699}$. The Gli3 protein encoded by these mice is similar to that generated by proteolytically processing Gli3 to the repressor isoform (Dai et al., 1999). Unlike *Xt*^{J}/*Xt*^{J} mice, the neural tube of *Gli3*$^{\Delta 699}$/ *Gli3*$^{\Delta 699}$ seems to be correctly patterned (Bose et al., 2002; Persson et al., 2002). It should be noted, however, that for correct patterning of the limbs, the unprocessed form of Gli3 must also play a role, since *Gli3*$^{\Delta 699}$/ *Gli3*$^{\Delta 699}$ mice still present polydactyly (Bose et al., 2002). In vitro studies have revealed such a putative activating activity of human GLI3 in acting as a mediator of Shh signalling in the activation of the target genes Gli1 and Ptch1 (Dai et al., 1999; Shin et al., 1999).

Although mice homozygous for a Gli1 mutation are viable and appear normal, $Gli1^{-/-}$; $Gli2^{-/+}$ double mutants have a severe phenotype with multiple defects, including a variable loss of ventral spinal cord cells (Park et al., 2000). Additionally, Gli1/Gli2 double homozygous mutants have more extreme CNS and lung defects than $Gli1^{-/-}$; $Gli2^{-/+}$ but less extreme than $Shh^{-/-}$ mutants (Park et al., 2000). These results imply that Gli1 is dispensable for embryonic development probably due to compensation by Gli2. On the other hand, $Gli1^{-/-}$;$Gli3^{-/+}$ double mutants do not present an obvious phenotype, indicating that, unlike Gli1 and Gli2, Gli1 and Gli3 do not have extensive overlapping activities (Park et al., 2000).

Gli2 also seems to have overlapping functions with Gli3, namely in the foregut and lung (Motoyama et al., 1998a). In fact, a reduction of 50% in the gene dosage of Gli3 in a $Gli2^{-/-}$ background resulted in an increase of the Gli2 homozygous phenotype in these tissues, whereas mice lacking both Gli2 and Gli3 function did not form esophagus, trachea or lung at all (Motoyama et al., 1998a).

Mice mutant for *Shh* show early embryonic defects in the establishment and maintenance of midline structures, such as the notochord and the floor plate, that later result in the absence of ventral cell types in the neural tube (Chiang et al., 1996). As mentioned previously, in the Xt^{J} mutant there are minor defects in the neural tube patterning (Persson et al., 2002). Although Gli3 had already been implicated in Shh repression (Masuya et al., 1997; Masuya et al., 1995; Wang et al., 2000a), the most compelling evidence of the antagonistic interaction between these proteins is the phenotype of the Shh/Gli3 double mutant in the CNS (Litingtung and Chiang, 2000; Persson et al., 2002; Rallu et al., 2002). In this double mutant, some of ventral cell types that are missing in Shh single mutants are restored, notably V2 neurons and motor neurons (Litingtung and Chiang, 2000; Persson et al., 2002). These two cell types are present in each of the Gli mutants, raising the possibility that Gli activity is not necessary for their development (Persson et al., 2002). However, upon forced expression of a dominant repressor version of Gli in the chick neural tube none of the ventral neuronal subtypes are specified (Persson et al., 2002). This result indicates that Gli activity is required for patterning the entire ventral neural tube and raises the possibility that the retention of MNs in each of the single mutants is probably due to partial redundancy between the Gli proteins (Persson et al., 2002).

Consistent with the hypothesis that Smo is necessary for all Hh signalling, loss of Smo and Gli3 leads to a similar rescue of the neural tube mis-patterning phenotype of Smo mutants (Wijgerde et al., 2002). Together, these analyses indicate that in the complete absence of Shh signalling considerable ventral neural tube patterning remains

(Litingtung and Chiang, 2000; Persson et al., 2002; Wijgerde et al., 2002). These results suggest that ventral patterning can proceed via a mechanism either parallel to or independent of graded Shh signalling (Litingtung and Chiang, 2000; Persson et al., 2002; Wijgerde et al., 2002). Over-expression of a dominant repressor Gli indicates that blocking all Gli function severely disrupts dorsal-ventral patterning of the neural tube (Persson et al., 2002). Bearing in mind these two central observations, Persson *at al* hypothesise that Gli proteins may act as common mediators of spinal cord dorsal-ventral patterning, integrating Shh signals and other sources of positional information (Jacob and Briscoe, 2003; Persson et al., 2002).

1.2.4.2.2 Zebrafish Gli mutants

In contrast to the mouse, Gli1 loss-of-function in zebrafish embryos has a strong developmental phenotype (Karlstrom et al., 1996; Karlstrom et al., 2003). *Detour (dtr)* mutants were originally isolated because of errors in retinal axon guidance and their body curvature (Brand et al., 1996; Karlstrom et al., 1996). Recently, *dtr* mutations were proposed to be complete or partial loss-of-function alleles of the zebrafish *gli1* gene (Karlstrom et al., 2003). Consistent with this, the injection of anti-sense morpholino oligonucleotides targeting the initiation of translation of the *gli1* gene phenocopied *dtr* spinal cord and forebrain defects (Karlstrom et al., 2003). Apart from the defects originally identified, *detour* mutants lack lateral floor plate and have reduced expression of *ptc1*, the Hh receptor and a direct target of the pathway (Karlstrom et al., 2003; Odenthal et al., 2000). Moreover, the expression of *nkx2.2*, a Hh-induced marker for ventral neurectoderm, is absent in the spinal cord and some regions of the ventral forebrain and midbrain (Karlstrom et al., 2003). In contrast, expression of *pax6*, that has been shown to be negatively regulated by Shh in zebrafish, is expanded (Karlstrom et al., 2003; Macdonald et al., 1995). The data presented by Karlstrom et al. indicate that zebrafish Gli1 is necessary for ventral CNS patterning, but it is not required for all Hh signalling in the embryo, as somites, fins and dorsal aorta development seem to occur normally (Karlstrom et al., 2003). Another interesting difference between mouse and zebrafish *gli1* genes is that not all expression of the latter is dependent in Hh signalling as in embryos completely devoid of Smoothened activity there is still weak *gli1* expression, while no *Gli1* expression has been detected in mouse *Smo* embryos (Bai et al., 2002; Karlstrom et al., 2003).

There is another identified zebrafish *gli* mutant, *you-too* in which the gene affected is *gli2* (Karlstrom et al., 1999). *You-too* mutants lack an optical chiasm and a horizontal myoseptum in the somites, have reduced expression of Hh target genes such as

nkx2.2 and *ptc1*, and expanded expression of *pax6* (Karlstrom et al., 1999; Karlstrom et al., 1996; Karlstrom et al., 2003). However, the fact that all *you-too* alleles encode truncated proteins and that *yot*$^{-/+}$ embryos show a weak dominant muscle phenotype (van Eeden et al., 1996), led Karlstrom et al. to purpose that *you/gli2* alleles encode repressors of Hh signalling (Karlstrom et al., 2003). The authors present two main pieces of evidence to support this hypothesis. First, in the cell culture system developed by Sasaki et al. and described previously, co-transfection of the C-terminal *you/gli2* truncations with *gli1* abolishes Gli1-mediated transcriptional activation (Karlstrom et al., 2003). Second and more importantly, the *you* phenotype seems to be rescued rather than phenocopied by morpholino oligonucleotides designed to disrupt *gli2* translation (Karlstrom et al., 2003). The fact that *you-/+; dtr-/+* embryos display a phenotype indicative of reduced Hh signalling and the hypothesis of the dominant repressor truncated Gli2, lead the authors to suggest that the *you* phenotype is the result of Hh signalling interference, in part by antagonizing Gli1 (Karlstrom et al., 2003).

Materials and Methods

2 Materials and Methods

2.1 Bioinformatics and genomics

All manipulations of DNA sequences were performed with Sequencher, DNAStrider and DNASTAR software. Protein alignments were performed with the Clustal method in MegAlign (DNASTAR), MacVector, or using the software available at the "Human Genome Sequencing Centre - Baylor College of Medicine" website at http://searchlauncher.bcm.tmc.edu/multi-align/multi-align.html.

2.1.1 Identification of zebrafish orthologues of mouse or human proteins

Zebrafish ESTs corresponding to orthologues of mouse or human genes were sought by name in the nucleotide databases and by probing the zebrafish EST database with a given mouse or human protein using the tblastn algorithm at http://www.ncbi.nlm.gov/BLAST/. Sequences found were clustered using Sequencher software. When available (from the Integrated Molecular Analysis of Genomes and their Expression, IMAGE or Resource Centre/Primary Database, RZPD) ESTs were ordered to obtain DNA templates for riboprobe synthesis.

When no corresponding EST was found, the zebrafish genomic database was searched at http://www.ensembl.org/Danio_rerio/ssahaview. Genomic supercontigs sequences containing exons of the required gene were used to predict the gene sequence with the help of the software available at http://www.softberry.com/berry.phtml?topic=gfind.

In some cases, no genomic supercontigs were found and the sequences of genomic trace files were sought by probing the Ensemble Trace Server with the mouse or human protein using the SSAHA algorithm, at http://trace.ensembl.org/.

In all cases, cluster consensus sequences were used to probe the protein databases using the blastx algorithm, at http://www.ncbi.nlm.gov/BLAST/, to confirm their coding for the desired protein.

2.1.2 Oligonucleotide design

2.1.2.1 Primers

Primers for sequencing or performing rapid amplification of cDNA ends (RACE) were designed using the program Primer3 (Whitehead Web Page) at http://www-genome.wi.mit.edu/cgi-bin/primer/primer3_www.cgi, from regions where reliable DNA sequence was available. The parameters used for designing primers with the program Primer3 are shown in Table 2-1.

		Minimum	Optimum	Maximum
Sequencing	Length	18 nt	20 nt	27 nt
	Tm	57 °C	60 °C	63 °C
	G/C content	20%	50%	80%
RACE or long range PCR	Length	23 nt	25 nt	27 nt
	Tm	70 °C	72 °C	75 °C
	G/C content	50%	60%	70%

Table 2-1 Parameters used in Primer3 for primer design.

2.1.2.2 Antisense morpholino oligonucleotides (MOs)

To disrupt mRNA translation, MOs were designed to target the region around the first codon. In general, the translation start site of zebrafish genes was identified by alignment of orthologues protein sequences belonging to several species and by looking in the cDNA for a Kozak consensus sequence in the identified region. Sequence encompassing the target was sent to Gene Tools LLC, which designed the MO to be purchased. All MOs were 25-mers of approximately 50% G/C content, with less than 36% G content and no more than two consecutive Gs, and forming no more than 4 contiguous internal base pairing. The MOs designed for this work are listed in Table 2-2.

Targeted gene	MO sequence (5'-3')
gli3 control	CATCGCAAGTGGGGATTGCTCACAG
gli3 MO1	CATGGCAACTGGGCATTCCTCAGAG
gli3 MO2	AACTGGTCTGGAATTGGGGTTCCAT
rab10	GCAGATCATAGGTCTTCTTCGCCAT
rab13	AAGTCGTACTTCTTTGCCATTGTTC
rab14a	ATATGGTGCGGTCGTCATTTTGGCT
rab15	CATGGTGTCTTATGGTCAACAATTA
rab1a1	TAAGTAGTCATATTCAGGGTTCATG
rab1b	ATAAATAGTCATATTCGGGATTCAT
rab23	CCACCTCCATGTCCTCCTCCAGCAT
rab27a	GGTAATCATAGTCCCCATCGGACAT
rab2a2	GCCAACCGCACCTGCCCG
rab32a	ACTCCGACACGGACCCGCCTGCCAT
rab34	GGCAGTACACTCATAATGATGCTTC
rab35a	AGAGGTGATCGTAGTCGCGGGCCAT
rab3c1	CAAACATCTTCCCGTATAACTCCAT
rab3c2	CCGACGCCATCTTATCCGGCTCTTC
rab5a1	GACAGTTGTCAATCACCCCGTCTTC
rab5a2	TCGTTGCTCCACCTCTTCCTGCCAT
rab5b	CCTGCCTGTCCCACGGGTACTCATG
rab5c	CGCTGGTCCACCTCGCCCCGCCATG
rab7b	TTCTTACGAGAAGCCATCCTTGAGG
rab9a	TCAGGAGAGATGATTTAGATGACAT
silberblick/wnt11	GAAAGTTCCTGTATTCTGTCATGTC
Standard control	CCTCTTACCTCAGTTACATTTATA

Table 2-2 MOs used in this thesis.

2.2 Embryo manipulation

2.2.1 Embryo collection

Zebrafish (*Danio rerio*) female and male pairs were placed in tanks together in the evening preceding the desired collection day. Eggs are usually laid and fertilised the following morning shortly after the lights are turned on. Embryos were collected in Embryo Water (red sea salt 0.06g/l, methylene blue 2mg/l) shortly after having been laid. Embryos were raised from the day of collection up to 3 days at 28°C in Embryo Water or, when de-chorionated, in 0.3 – 1x Danieau's solution (58 mM NaCl, 0.7 mM KCl, 0.4 mM $MgSO_4$, 0.6 mM $Ca(NO_3)_2$, 5 mM HEPES (pH 7.6)). Embryos were staged according to the morphological criteria provided in (Kimmel et al., 1995). Zebrafish embryos collected for staining procedures were fixed at least overnight in 4% PFA in phosphate buffered saline (PBS: 137mM NaCl, 2.7mM KCl, 4.3mM $Na_2HPO_4.7H_2O$, 1.4mM KH_2PO_4) at 4 C. 24 hpf or older embryos were de-chorionated prior to fixation (so that their trunk and tail would be straight) whereas embryos younger than 24 hpf were de-chorionated after fixation and before dehydration. Following fixation, embryos were dehydrated in increasing concentrations of MeOH in PBS. Dehydrated embryos were stored in 100% methanol at -20 °C until used.

2.2.2 Whole-mount *in situ* hybridisation

Zebrafish embryos were re-hydrated in decreasing concentrations of MeOH in PBT (0.1% Tween 20 in PBS). Whole-mount in situ hybridisation of zebrafish embryos was performed with a simplified form of the protocol described in (Thisse and Thisse, 1998). Embryos were re-fixed in 4% PFA in PBT for 20 min at room temperature and then washed 5 times in PBT, 5 min each. Embryos older than 24 hpf were digested with 10μg/ml proteinase K for 15 min and washed twice in PBT. Embryos were then transferred to hybridisation buffer (Hyb; 50% formamide, 5x SSC (0.75 M NaCl, 75 mM $Na_3citrate.2H_2O$ (pH 7.0)), 500 μg/ml type VI torula yeast RNA, 50μg/ml heparin, 0.1% Tween-20, 9 mM citric acid (pH 6.0-6.5)) for 2-5 hours at 68° C. The Hyb was then replaced with Hyb containing 1μg/ml of digoxigenin (DIG)-labelled riboprobe and the embryos were incubated at 68°C overnight. The first washes of the following day were done at the hybridisation temperature with preheated solutions: 50% Hyb / 2xSSC; 100% 2x SSC for 15 min; and two washes with 0.2x SSC for 30 min each. Next, two washes were performed at room temperature: 50% 0.2x SSC / PBT; and 100% PBT for 10 min each. The embryos were blocked in 2mg/ml BSA, 2 % heat-inactivated goat or sheep serum in PBT for several hours, after which they were incubated with

alkaline-phosphatase-conjugated anti-DIG Fab fragments diluted 1:2500 in blocking solution at 4° C, overnight. The following day embryos were washed with PBT at least 8 times, for 15 min each. The embryos were then rinsed 3 times for 5 min each in NTMT buffer (0.1 M tris(hydroxymethyl)methylamine (TRIS)-HCl pH 9.5; 50mM $MgCl_2$; 0.1 M NaCl; 0.1% Tween 20). Detection was performed using NBT / BCIP (112.5 µl of 100mg/ml NBT in 100% dimethyl-formamide and 175 µl of 100mg/ml BCIP in 70% of dimethyl-formamide, in 50 ml of NTMT). After stopping the reaction with 2mM EDTA in PBS (pH 5.5), embryos were re-fixed in 4% PFA in PBS for 20 minutes at room temperature. Stained zebrafish embryos younger than 24 hpf were dehydrated in increasing concentrations of MeOH in PBT and two final washes in 100% MeOH. These were then cleared in a fresh 2:1 mixture of benzyl-benzoate:benzyl alcohol (BBA) and mounted in a 10:1 mixture of Canada Balsam:methyl-salicylate. As soon as embryos were in BBA their exposure to light was kept to a minimum to avoid the yolk turning red. Embryos 24 hpf or older were placed straight into 80% Glycerol in PBT, which was both the clearing and mounting solution. The yolk cell of these older embryos was removed also in 80% Glycerol before photographing. These embryos were stored in 80% glycerol at 4° C.

2.2.3 Embryo sectioning

After having been subject to whole-mount in situ hybridisation, embryos were put in 100% ethanol through a series of increasing concentrations (70%, 80%, 90%, and 4 times in 100% ethanol, 10 minutes each wash). They were then washed in ethanol:xylene (1:1) and twice in 100% xylene (10 minutes each wash). Finally, they were transferred to molten fibrowax at 60°C, with at least 3 changes of wax every 20 minutes. Embryos were blocked out in fibrowax for cutting of 14µm thick sections.

2.2.4 Whole-mount fluorescent immunocytochemistry

Fixed embryos were washed in PBT and blocked in 5% goat serum (GS) in PBT for two hours or longer, at room temperature. Embryos were then incubated in 2% GS/PBT containing primary antibody, overnight at 4 °C. For the work described in this thesis only one primary antibody was used, anti-catenin β produced in rabbit (C2260, Sigma, 1:500). Following primary incubation, embryos were washed extensively in PBT at room temperature before overnight incubation in 2% GS/PBT containing secondary Cy3-conjugated antibody (Jackson ImmunoResearch Laboratories; 1:400 dilution), at 4 °C. 4',6-diamidino-2-phenyindole (DAPI) counter-stain was added

(0.2μg/ml) and incubation continued for 1 hour at room temperature. Embryos were washed thoroughly in PBT, stored and mounted in 70% citifluor/PBS (Citifluor) to reduce fluorescence fading.

2.2.5 Whole-mount terminal deoxynucleotidyl transferase-mediated dUTP nick end labelling (TUNEL) staining

Zebrafish embryos were re-hydrated, washed and, for embryos older than 24 hpf, digested with proteinase K followed by post-fixation with 4% PFA in PBS, as for whole-mount in situ hybridisation. Embryos older than 24 hpf were then subject to endogenous alkaline phosphatase inactivation, by incubation with pre-chilled (-20 °C) EtOH:glacial acetic acid (2:1) for 10 min at -20 °C. Specialised reagents subsequently used were those of Apoptag kit (Oncor Inc.). All embryos were incubated in 75 μl Equilibration Buffer for 1 h at room temperature and then incubated in at least 50 μl working strength TdT enzyme (prepared fresh by mixing Reaction Buffer:TdT enzyme 2:1 + 0.3% TritonX-100) overnight at 37 °C. The following day, the reaction was stopped by washing embryos in working strength Stop/Wash Buffer (Stop/Wash Buffer:water 1:17) for 3 h at 37 °C. Blocking was performed by incubation in 2 mg/ml BSA, 5% goat serum in PBT for at least 1 h at room temperature, after which embryos were incubated with alkaline-phosphatase-conjugated anti-DIG Fab fragments diluted 1:2500 in blocking solution at 4 C, overnight. Subsequent washes and detection were performed as for whole-mount in situ hybridisation.

2.2.6 Zebrafish embryo injections

Injection needles were prepared by pulling filament-containing borosilicate glass capillaries (Word Precision Instruments, 1B100F-4, outside diameter 1.0mm, inside diameter 0.75mm) with a vertical pipette puller (David Kopf Instruments), cutting the edge with a razor blade, and calibrating under the microscope with a millimetre ruler. Injection system consisted of a needle holder (Word Precision Instruments), carried by a 3-axis micromanipulator (Narishige), connected to nitrogen-filled tubing commanded by a control panel (World Precision Instruments) and triggered by a foot pedal. Zebrafish embryos were injected at the 1 – 4-cell stages with 1.4 nl of the desired solution. Embryos were aligned on the side of a glass slide in a glass Petri dish, with just enough Embryo Water to ensure their hydration.

2.2.7 Cyclopamine treatment

Cyclopamine (Toronto Research Chemicals Inc., New York, Ontario, Canada) was dissolved at 10mM in 100% EtOH and stored at -20°C. Embryos were incubated in 25µM cyclopamine in 0.3x Danieau's solution, from shield stage until fixation, without chorion removal. In negative control experiments, the same quantity of 100% EtOH was added to the 0.3x Danieau's solution.

2.2.8 Embryo photographing

High-power images from both live and fixed embryos were obtained using a Zeiss Axiophot microscope fitted with either a Kodak DCS420 digital camera, or a Jenoptik Jena system that used Openlab 3.1.2 software. Living zebrafish embryos were photographed in 3% methylcellulose (Sigma). Embryos subject to fluorescent immunocytochemistry were initially visualised in a Leica FLUO-TM dissection microscope to assess the quality of the staining. Subsequently the samples were imaged on a Biorad radiance 2100 confocal microscope with a radiance 2100 software. Images were treated with AdobePhotoshop.

2.2.9 Electron microscopy

Whole zebrafish embryos were dechorionated manually and fixed overnight with 2% glutaraldehyde, 2% paraformaldehyde in 0.1M sodium cacodylate buffer (pH 7.2) (SCB). The following day, embryos were washed for 10 min in SCB and post-fixed for 1h in 1% osmium tetroxide in SCB. They were washed again with SCB and stained *en bloc* with 1% aqueous uranyl acetate for 1h. The samples were then dehydrated through a graded ethanol series, followed by 2 changes of propylene oxide over 20 min and embedded in Epon resin (Agar Scientific). 50 nm ultra thin sections were cut and mounted on pioloform coated slot grids and stained with 1% aqueous uranyl acetate for 15 min, followed by Reynold's lead citrate for 7 min. Sections were visualised in a Jeol 1200 EX electron microscope.

2.3 Molecular biology

2.3.1 Small scale preparation of DNA

The Qiagen Spin miniprep kit (Quiagen) was used for all small-scale plasmid preparations, according to the manufacturer's protocol.

2.3.2 Nucleic acid quantification by spectrophotometry

Nucleic acid quantification was performed by spectrophotometry at λ = 260 nm, where an optic density (OD) unit corresponds to 50μg/ml of double-stranded DNA or to 40μg/ml single-stranded RNA. The ratio between the readings at λ= 260 nm and λ= 280 nm provided an estimate of the purity of the nucleic acid preparation (pure preparations of DNA should have OD_{260}/OD_{280} ratio of 1.8).

MOs solutions were diluted 1/1000 in 0.1 N HCl and quantified by spectrophotometry at λ = 265 nm. MO concentration corresponds to the ratio between the OD and their molar extinction coefficient (ε), multiplied by their molecular weight (MW). Manufacturers provide ε and MW values for each MO synthesised.

2.3.3 Agarose gel electrophoresis

Nucleic acid size determination and/or separation were performed by agarose gel electrophoresis. Gels were prepared by dissolving agarose in 1x TAE (20 mM TRIS acetate, 1 mM $Na_2EDTA.2H_2O$ (pH 8.5)) to a final concentration of 0.8 – 2% (w/v), depending on the expected size of the DNA fragments, and 0.4% ethidium bromide. Nucleic acid samples were mixed with 6x gel loading buffer (6x TAE, 50% v/v glycerol, 0.25% w/v bromophenol blue) and, in the case of RNA, with RNase inhibitor. Electrophoresis was performed at 5 – 20 V/cm gel length until appropriate resolution was achieved. Ethidium bromide-stained nucleic acid was visualised using ultraviolet light ($\lambda \approx$ 302 nm) and fragment size was estimated by comparison with the 1 kb ladder molecular weight markers (Gibco BRL) run in at least one of the gel lanes.

2.3.4 Gel extraction of DNA

For the extraction of DNA from agarose gels the QIAquick Gel Extraction Kit (Qiagen) was used according to manufacturer's protocol.

2.3.5 Phenol/chloroform extraction of nucleic acids

To remove proteins from nucleic acid solutions, one volume of a 25:24:1 mixture of phenol:chloroform:isoamyl-alcohol (v:v:v) was added to the nucleic acid solution and mixed for 1 minute. After a 5 min centrifugation, the upper (aqueous) layer was transferred into a new micro centrifuge tube and extracted again with one volume of chloroform:isoamyl-alcohol (24:1, v:v).

2.3.6 Ethanol precipitation of nucleic acids

EtOH precipitation of nucleic acids was carried out by adding 1/10 volume of 3 M sodium acetate (NaOAc) (pH 5.2) and 2.5 volumes of cold 100% EtOH to the nucleic acid solution. This mixture was left at -20°C or -80°C (depending on how much concern salt precipitation is for subsequent procedures) for approximately 20 min. Centrifugation was carried out at 20,000 x g for 5–20 min, the DNA pellet was washed in 70% EtOH and spun again at the same speed for 5 min. After EtOH removal nucleic acid was left to air-dry at room temperature for approximately 10 min and re-suspended in TE (1 mM EDTA, 10 mM TRIS.HCl (pH 8.0)) or distilled water.

2.3.7 Restriction digestion of DNA

Restriction enzyme digests were performed at the recommended temperature for approximately 2h using commercially supplied restriction enzymes and buffers (Boehringer Mannheim, Promega, New England Biolabs). The enzyme component of the reaction never comprised more than 10% of the reaction volume. For multiple enzymatic digests, the most compatible buffer for all the enzymes used was chosen as long as all the enzymes were predicted to digest at least 75% of the DNA in those conditions; when enzymes required incompatible buffers, one digest was done at a time and the DNA was either phenol/chloroform extracted and precipitated or gel extracted between digests.

2.3.8 TOPO cloning

The cloning of PCR products was performed using the TOPO TA Cloning® kit (Invitrogen). The cloning reaction was performed according to the following conditions: 4µl fresh PCR product or 4µl of gel purified product, 1µl of 1.2M NaCl solution and

0.5μl pCR®-TOPO® vector. These were mixed gently and incubated for 5 min at room temperature.

2.3.9 Transformation of chemically competent bacteria

Transformation of the ligated vector was performed using chemically competent TOP10 cells (Invitrogen) and according to the manufacturer's protocol.

2.3.10 Automatic sequencing of plasmid DNA

DNA sequencing was performed using the ABI PRISM Big Dye Terminator Cycle Sequencing Ready Reaction kit, according to the manufacturer's instructions, in an ABI 377 automatic sequencer.

2.3.11 Total RNA purification

Embryos used for RNA purification were either fresh or quick-frozen for 10-15 min in dry-ice and stored at -80 °C. TRIzol reagent (GibcoBRL) was used for total RNA purification, essentially according to manufacturer's instructions. 750 μl TRIzol Reagent was added to approximately 100 μl of embryos triturated thoroughly by passing them through increasingly smaller diameter needles.

2.3.12 Messenger RNA purification from total RNA

Poly-T-coated Dynabeads (Dynal) were used to purify messenger RNA from total RNA, according to manufacturer's instructions.

2.3.13 RT-PCR

First strand cDNA was synthesised from total RNA template using random hexamer primers or a poly-T primer and superscript reverse transcriptase (GibcoBRL). To this end 20μl aqueous reactions were prepared, containing 1μg of RNA, 1μl of 0.1mg/ml primer, 4μl 5x RTase buffer, 1μl 20mM dithiothritol (DTT), 0.5μl RNase inhibitor, 2μl 5mM dNTP mix and 0.25μl RT. A negative control devoid of RT was also prepared. Reactions were allowed to proceed at 42 °C for 30 min, after which cDNAs were used as templates for PCRs with specific primers. Primers used to amplify genes or gene fragments used in this thesis are listed in Table 2-3.

Gene/Gene fragment	Forward primer	Reverse primer
nkx6.1	TTTTGAAAGGACGACGCTCT	TTGCAGGATCCAAAACACTG
nkx6.2	ATCTGCAGAATTCGCCCTTA	GAGAGTGTGTCGGCTGAATTT
pax3	CACAACTCCTGACGTGGAAA	CTGGCAGAGCTTCCAGTCTC
rab23	TTCATCCCAGCACATCCATA	TCTGTGTGGCCAGAAGAGG
ΔNp63α	GATGGCACAAAGAGCAGTGA	TCAGCCTGGACAAGTCCTCT

Table 2-3- Primers used for RT-PCR.

2.3.14 Long-range PCR

To amplify cDNA fragments longer than 1.5kb long range PCR was performed using the eLongase kit (GibcoBRL), following manufacturer's guidelines. The primers used to perform long-range PCRs are listed in Table 2-4.

Gene/Gene fragment	Forward primer	Reverse primer
gli3	AGTTGCCATGGAACCCCAATTCCAG	GGTGGGGGAGTTCACAAACTATTGGATG
gli3 fragment 1	ATCAGTGAGAAGGCTGTGGCCTCCA	CCGATTCTGGTGTTTGGCTCGGTCT
gli3 fragment 2	TGGTCCTGAAGCCCATGTCACCAAA	GGGTGGTGAGGAGGGAGCTCATGTC

Table 2-4 Primers used for long long-range PCR.

2.3.15 Rapid amplification of cDNA ends (RACE)

RACE was performed using the GeneRacer cDNA amplification kit (Invitrogen). mRNA was isolated from total RNA purified from pooled zebrafish embryos of the following stages: sphere, 50% epiboly, 11-13 somite, 40 hpf and 4 days. The synthesis of the cDNA modified with the Generacer 5' and 3' adaptors was done according to the manufacturer's protocol and using either random primers or poly-T primer in the reverse transcription reaction. All RACE reactions were performed by nested PCR. The GeneRacer 5' primer (CGACTGGAGCACGAGGACACTGA) or the GeneRacer 3' primer (GCTGTCAACGATACGCTACGTAACG), when performing 5' or 3' RACE reactions, respectively, and a gene-specific primer (GSP 1) designed using Primer3 software (see above), were used in a first round of PCR, for 15 cycles. The product of

this round of PCR was diluted 1/40 and 5 μl of this dilution were used as template for the second round of PCR. In the latter, the GeneRacer 5' nested primer (GGACACTGACATGGACTGAAGGAGTA) or the GeneRacer 3' nested primer (CGCTACGTAACGGCATGACAGTG), when performing 5' or 3' reactions, respectively, and a second nested gene-specific primer (GSP 2) were used for 25 cycles. The GSP primers used for 5' or 3' RACE are indicated in Table 2-5 and Table 2-6, respectively. Touchdown PCR program was used in all cases with the extension time varying according to the size of the expected product (2min per kb).

Gene	GSP1(5'-3')	GSP2 (5'-3')
gli3	ATAGGGCAGGGTGTGGTCTGCCAAG	TGCGCACTAATGGTGTTTCGCCTCT
nkx6.1	GGGCTCTTTCAGGGCCGGCTAAATA	AAAACGTCGGTCGCGTGTGTTTCCT
nkx6.2	TCCGTTGATCCTGGGGAAACCAGAG	GCTGTCCTGCAGTGGTGATGGGTCT
rab18	AAAATGACACCCTGGGCCCCTCTGT	GAAGTCCACACCGATGGTTGCTGCT
rab23	CGCCGATGGTCTTCTTGTGGTCCTT	GCTCCGTTTAGCACCACCACCACCT
rab28	TCTTCACTGTCCGCATGTGCTCCA	ATGGCCGGCTGTACGTCTGACTCCT
rab2a1	TTCTCTGGCAAAGGCCTCTCCTTCC	GACTCCTGTCCAGCCGTATCCCAGA
rab3c1	TTAGGATGAAGCCCATGGCCCCTCT	CGCCCAGTCCTGTACAGCAGCAAAA
rab6c2	CGTTCGGACGTCATCGATCCATTTG	AGCAACCGTCGAGTCCCGGATGTAG

Table 2-5 Primers used for 5' RACE.

Gene	GSP1(5'-3')	GSP2 (5'-3')
gli3	AGTTGCCATGGAACCCCAATTCCAG	ATCAGTGAGAAGGCTGTGGCCTCCA
nkx6.1	GCTGAAATGGCCTCGGCGAAGAAAA	CGGAAAATGAAGACGACGACGACGA
nkx6.2	TCGCACTGGAGAAAACCTTCGAGCA	GTCCGGAGAGAGCCAGACTCGCCTA
rab23	GCCATCAAGGTGGTGGTGGTGCTAA	GTGGGCAAGTCCAGCATGATCCAGA

Table 2-6 Primers used for 3' RACE.

2.3.16 Riboprobe synthesis

For the synthesis of riboprobes, template (plasmid) DNA was linearised for 2 h. In all cases, digoxigenin (DIG)-labelled uracil triphosphate (UTP) (Boehringer Mannheim) was incorporated during RNA transcription, following manufacturer's instructions. After synthesis, riboprobes were treated with 20 U DNase I (Boehringer Mannheim) at 37 °C for 15 min to remove DNA template and were purified by size-exclusion chromatography through a DEPC water column (Clontech Chroma Spin-100). All riboprobes were electrophoresed on a 1% agarose gel to check size and integrity prior to use. Riboprobes were added to Hyb shortly after synthesis and were stored at -20 °C. Table 2-7 has a list of all cDNAs used as templates for anti-sense RNA probes used in this work, as well as the respective origin.

cDNA	Linearization	RNA polymerase	Origin
bik	Pst I	T7	(Vogel and Gerster, 1999)
cyc	Hind III	T7	(Rebagliati et al., 1998)
dbx1a	Sal I	SP6	fc15c04
dct	Eco RI	T7	(Kelsh et al., 2000)
dlx3	Eco RI	T7	(Akimenko et al., 1994)
evx1	Sal I	SP6	MPMGp609L2014Q
fgf8	Xba I	T7	(Fürthauer et al., 1997)
fli1	Xba I	T3	(Thompson et al., 1998)
gata2	Xba I	T7	(Detrich et al., 1995)
hnf3β	Sac I	T3	(Strähle et al., 1993)
iro1	Eco RI	SP6	MPMGp637C0711Q
iro3	Sal I	SP6	MPMGp609G0341Q
isl1	Xba I	T3	(Inoue et al., 1994)
nkx2.2	BamH I	T7	(Barth and Wilson, 1995)
nkx6.1	Not I	SP6	RT-PCR, this thesis
nkx6.2	Not I	SP6	RT-PCR, this thesis
ntl	Xho I	T7	(Schulte-Merker et al., 1994)
pax2.1	BamH I	T7	(Krauss et al., 1991a)

pax3	Not I	SP6	RT-PCR, this thesis
pax6a	BamH I	T7	(Puschel et al., 1992)
ptc1	BamH I	T3	(Concordet et al., 1996)
rab10	Sal I	SP6	fe05f12
rab11a1	Sal I	SP6	fc54g10
rab11b2	Sal I	SP6	fj14c03
rab14a	BamH I	T7	fa95h12
rab18	Sal I	SP6	fd09c04
rab19a	Sal I	SP6	fb57a08
rab1a1	Sal I	SP6	fc83b07
rab1b	Sal I	SP6	fe48e04
rab20	BamH I	T7	fb01f02
rab23	Not I	SP6	RT-PCR, this thesis
rab28	Sal I	SP6	fe49e06
rab2a2	Sal I	SP6	fr65d08
rab34	Sal I	SP6	fo87a09
rab3c1	Sal I	SP6	fc17c05
rab3c2	EcoR I	SP6	fj46d08
rab5a1	Sal I	SP6	fc19e05
rab5b	Sal I	SP6	fj89a11
rab5c	Sal I	SP6	fl57z22
rab6a1	Sal I	SP6	fb43c01
rab7b	Sal I	SP6	fc16a12
shh	Hind III	T7	(Krauss et al., 1993)
sqt	Hind III	T7	(Feldman et al., 1998)
ΔNp63α	Not I	SP6	RT-PCR, this thesis

Table 2-7 Templates used to prepare riboprobes used in this work.

2.3.17 Capped RNA synthesis

5µg of DNA template was digested with the appropriate restriction enzyme and extracted with phenol/chlorophorm and precipitate with EtOH. The *in vitro* capped RNA

synthesis reaction consisted in adding 5µg of linearised template DNA re-suspended in 10µl with 5µl 5x transcription buffer, 5µl 0.1mM DTT, 5µl 5mM CAP analogue (m^7G(5´)ppp(5´)G, New England Biolab), 5µl 1mM GTP, 5µl 10mM UTP, 5µl 10mM ATP, 5µl 10mM CTP, 2µl RNase inhibitor and 3µl of the corresponding RNA polymerase. The reaction was allowed to proceed for 20min at 37°C before 4µl of 10mM GTP were added. The reaction proceeded for 2 more hours at 37°C after which 3µl of DNase were added and allowed to act for 20min at 37°C. The RNA was purified by size-exclusion chromatography through a DEPC water column (Clontech Chroma Spin-100) and quantified in a spectrophotometer. For the work described in this thesis only *shh* RNA was synthesized. The template was linearised with BamH I and transcribed with SP6 (Krauss et al., 1993).

2.3.18 MO column-purification

Concern about MO purity led to the standard procedure of MO column-purification using Micro-spin G-25 diethyl-pyrocarbonate (DEPC) water columns (Amersham Pharmacia). Columns were pre-spun at 4,000 rpm for 2 min in a bench top centrifuge. 300 nmole MO were dissolved in 60 µl DEPC water and 50 µl of these were loaded onto a column and spun at 4,000 rpm for 2min in a bench centrifuge. The first eluate is the most concentrated and was subsequently diluted in MO Buffer (1:4 25mg/ml phenol red : 5mM HEPES (pH 7.2), 200 mM KCl) to the desired concentration for injection into zebrafish. A second eluate was also recovered from the columns by adding 50µl of DEPC water and spinning at 4,000 rpm for 2 min in a bench centrifuge.

2.3.19 Radiation hybrid panel mapping

96 PCR reactions were performed using the LN54 panel (Hukriede et al., 1999). The total volume of the reactions was 10µl, including 2µl 5x PCR buffer, 0.1µl of Taq polymerase and 1µl of each primer at 10µM, water and the panel samples. The PCR program used was: 94°C, 3min; 30x (92°C, 30sec; 60°C, 30sec; 72°C, 23sec); 72°C, 30sec. The primers used for *gli3* mapping were (5'-3'):CTCAAGTGCTGATTGCTCCA and GGGATCTGAACCTCACTCCA. Analysis of the results and calculation of linkage and LOD scores was carried out at http://mgchd1.nichd.nih.gov:8000/zfrh/beta.cgi.

Loss of function screen of zebrafish Rab proteins

3 Loss of function screen of zebrafish Rab proteins

In this chapter I describe the identification of 63 different zebrafish *rab* genes. *In situ* hybridisation analysis for 20 zebrafish *rab* genes was carried out. Six out of these twenty *rab* genes showed enhanced mRNA expression in a specific site of the embryo at a specific stage of development and only those are described in this chapter. Subsequently, injection of 20 different morpholinos targeting different zebrafish *rab* genes was performed. Injection of 14 of these morpholinos results in embryos with obvious developmental defects, which I describe here.

3.1 Cloning of zebrafish *rab* genes

The sequence of zebrafish *rab* genes, orthologous to human genes was obtained by a combination of different methods. Firstly, corresponding zebrafish ESTs were searched by both name and sequence and their sequences assembled using the Sequencher software. When the EST clone did not comprise the whole gene sequence, 3' or 5' RACE was performed to obtain the full cDNA sequence. Finally, when no ESTs corresponding to a particular *rab* gene was found, the zebrafish genomic database was searched. In some cases, the sequence of a supercontig corresponding to the genomic locus was available and used to predict the *rab* gene sequence. In other cases, no supercontig sequence was found and genomic trace files of the respective gene were used to design both 3' and 5' RACE primers thus allowing the cloning of its full cDNA. A list of the zebrafish Rab gene sequences which were obtained by RACE and the corresponding primers used can be found in the Materials and Methods section of this thesis.

The cloning of zebrafish *rab* genes is an on-going project, not self-contained in the scope of this thesis. As of May 2003, 63 different zebrafish *rab* genes had been identified. The whole gene sequence had been obtained or predicted for 37 *rab* genes, but for the remaining 26 genes the sequence was incomplete. Priority was given to the 5' region of the gene that would allow the design of morpholino oligonucleotides, and the missing sequence was typically in the middle (when a single sequencing reaction from each plasmid end did not result in sequence overlap) or 3' end region of the gene.

A table listing the identified zebrafish *rab* genes and their closest human orthologue and corresponding sequence accession numbers is presented in the appendix section of this thesis.

In some cases, more than one zebrafish sequence for the same orthologue isoform was found, thus I have named each sequence with the orthologue name and adding the number "1" or "2". If the particular gene had only one isoform in human but several isoforms were found in zebrafish, the nomenclature used was adding the letters "a", "b", etc., after the name (that was the case for *rab7*, *rab14*, *rab19*, *rab32* and *rab35*).

3.2 Expression pattern of zebrafish Rab mRNA

The mRNA *in situ* localization of 20 zebrafish *rabs* was assessed at different stages of embryonic development. With the exception of the probe for *rab23*, the probes used in the *in situ* protocol were obtained using EST clones for the corresponding gene as template. For *rab23*, the probe was transcribed from a plasmid containing the complete coding region of the gene, amplified from cDNA from zebrafish embryos at different stages of development and using the primers listed in 'Materials and Methods' section. The list of probes with the EST clone name, restriction enzyme that linearised the plasmid and the RNA polymerase used in the reaction can be found in the 'Materials and Methods' section of this thesis.

All the zebrafish *rab* genes analysed are expressed during embryonic development. In general, they appear to be expressed in a ubiquitous manner, but at least for 6 of these genes, there was clear up-regulation of the expression in some parts of the embryo at a certain stage of development, as described below.

3.2.1 *rab1b* expression pattern during zebrafish development

The *rab1b* mRNA is expressed maternally at low levels as seen by a uniform low signal at 2-4 cell stage embryos in an *in situ* hybridisation assay (data not shown). At shield stage, zygotic transcription maintains a uniform and low level distribution of *rab1b* mRNA throughout the entire blastoderm (data not shown). By the end of epiboly, up-regulation of *rab1b* expression starts being observed in the most axial tissues (panel A, Figure 3-1). When the embryo has approximately 5 somites, this up-regulation is evident not only in the chordamesoderm but also in the polster (panels B and C, Figure 3-1). At 24 hpf there is accumulation of transcript in the eye, in cell adjacent to the neural tube, presumably neural crest, and in the blood (panels D-H, Figure 3-1).

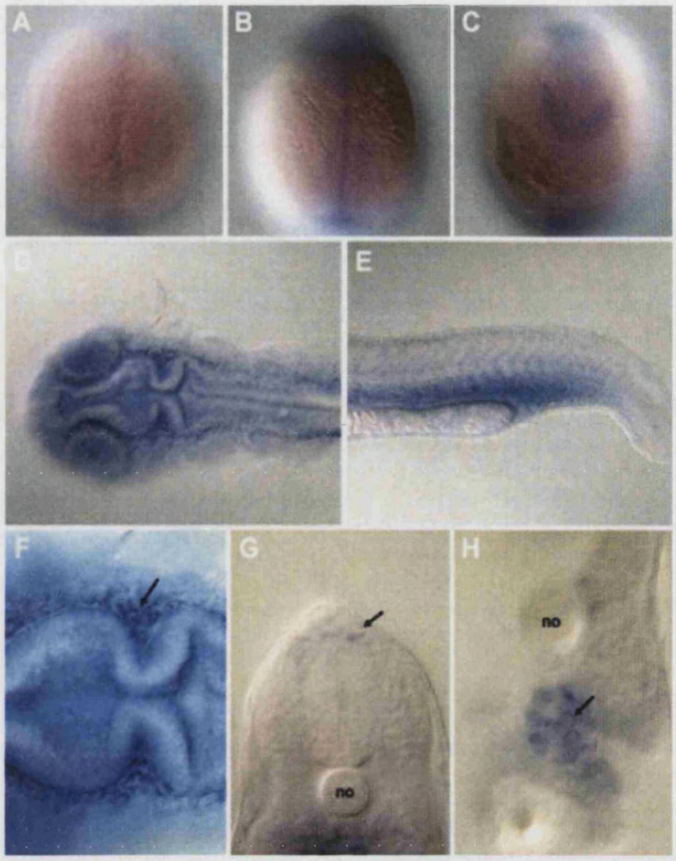

Figure 3-1 Expression pattern of *rab1b*. (A)-at 90% epiboly there is up-regulation in the most axial tissue (dorsal view, anterior up); (B,C)-at 5 somites up-regulation in chordamesoderm can be seen as well as in the polster (dorsal views); (D-H)-at 24 hpf *rab1b* expression is up-regulated in the blood and in cells adjacent to the neural tube, presumably neural crest. (D,F) are dorsal views of the anterior region, (F) is a high magnification of (D); (E) is a side view of the tail region; (G,H) are manual sections at the level of the end of yolk extension. In (G) arrow points to putative neural crest cells and in (H) arrow points to blood cells. no-notochord.

3.2.2 *rab2a2* expression pattern during zebrafish development

The *rab2a2* mRNA is weakly expressed maternally (data not shown), immediately after the onset of zygotic transcription and at shield stage (panels A, B, Figure 3-2). At 90% epiboly there is up-regulation in the chordamesoderm, which can be better appreciated at 5 somites (panel C, D, Figure 3-2). Later in development, the expression in the chordamesoderm persists only in the most posterior part of the embryo and there is a new site of gene up-regulation in a patch of cells, in the otic placode region (panels E, F, Figure 3-2). At 24 hpf the gene transcript is again present more homogeneously throughout the whole embryo, but the otic vesicles are outlined (panels G and H, Figure 3-2). At this stage, a new patch of cells up-regulating the gene can be seen posteriorly to the otic vesicle and presumably corresponding to cranial ganglia.

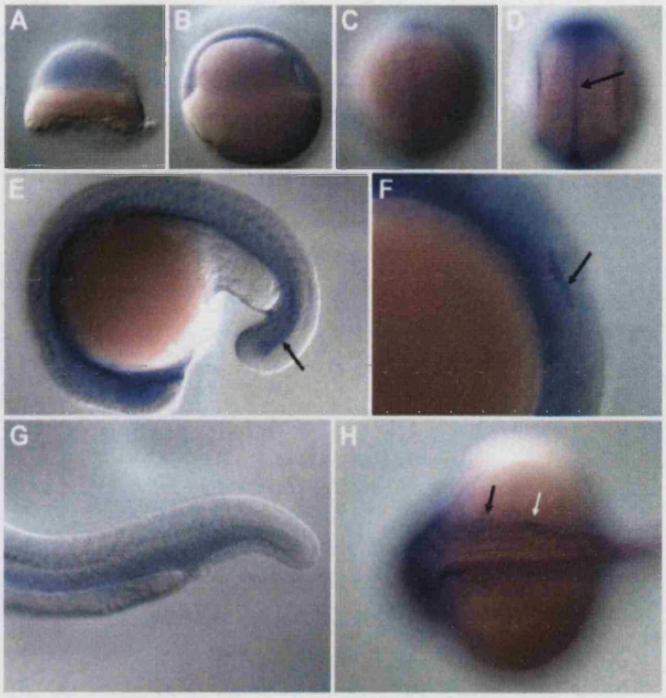

Figure 3-2 Expression pattern of *rab2a2*. (A)-embryo at 1000-cells showing expression throughout the whole blastoderm, that is maintained at shield stage (B). (C)-at 90% epiboly up-regulation in axial tissue can be seen but is even more evident in the chordamesoderm at 5 somites (D, see arrow). (E, F)-embryo at 18 somites stage with persistent up-regulation in posterior regions of chordamesoderm (arrow in E) and in a patch of cells at the level of the otic vesicle (arrow in F). (G, H)- 24 hpf embryo with ubiquitous expression but up-regulation outlining the otic vesicles (black arrow) and in a patch of cell more posteriorly (white arrow). (A, B, E, F, and G) are side views with animal up (A), dorsal to the right (B), and posterior to the right (E, F, and G). (C, D, H) are dorsal views with anterior up (C, D) or anterior left (H). (F) is a higher magnification of (E).

3.2.3 *rab3c1* expression pattern during zebrafish development

rab3c1 is expressed at low levels throughout the whole embryo before the onset of neuronal differentiation (data not shown). At 24 hpf, the expression of this gene is restricted to a sub-set of cells, presumably differentiated neurons (Figure 3-3). In the forebrain region, two bilateral patches of expression can be seen ventrally, probably corresponding to the postoptic area (panel A, Figure 3-3). Still in the forebrain but dorsally, there are two additional bilateral patches, presumably in the telencephalon and more posteriorly there is a central patch of expression probably corresponding to the epiphysis region (panels B and C, respectively, Figure 3-3). In the ventral midbrain there is bilateral expression in what could be the region where the medial longitudinal fasciculus forms (posterior in panel A, Figure 3-3). In the hindbrain there is bilateral

expression on a central patch of cells in each rhombomere, corresponding to the region that reticulospinal neurons occupy (panels D, E Figure 3-3). At the level of the midbrain/hindbrain boundary there are two sets of bilateral patches of cells expressing *rab3c1* outside the neural tube (panels D, E Figure 3-3). These cells could correspond to the anterior lateral line ganglia, further axially (panel D Figure 3-3), and to the trigeminal ganglia more adaxially (panel E Figure 3-3). In the trunk region, there are *rab3c1* positive cells throughout the dorsal half of the embryo (panel F, Figure 3-3). In a manual cross section at the level of the end of the yolk extension, it can be seen that the positive cells are all located inside the neural tube and with their cell bodies near its pial surface (panel G Figure 3-3).

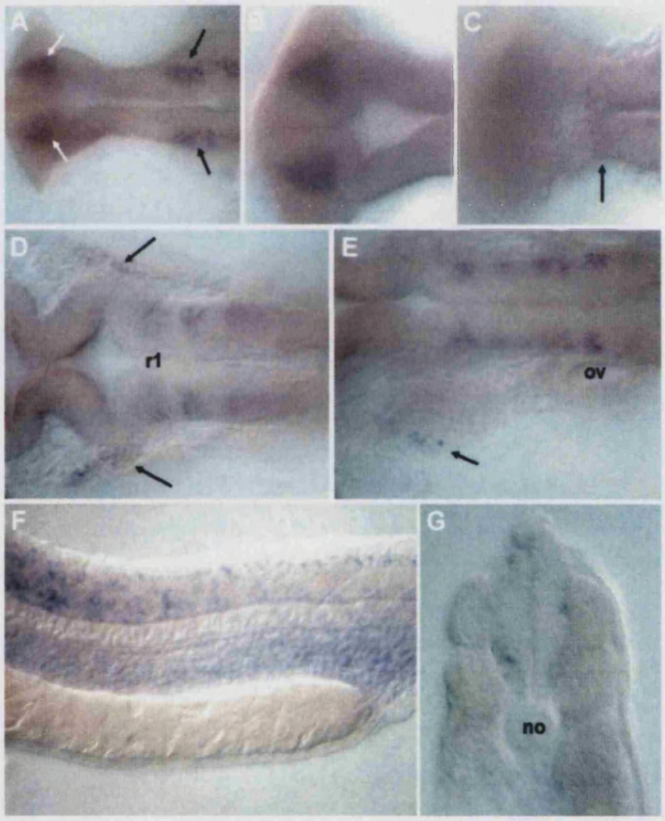

Figure 3-3 Expression pattern of *rab3c1* at 24hpf. (A)-forebrain and midbrain region with focus on the ventral part of the neural tube showing expression in two bilateral patches of cells ventral to the telencephalon (white arrows) and to the midbrain (black arrows). (B, C)-forebrain region with dorsal focus showing two patches of bilateral telencephalic cells (B) and another patch of cells, more posteriorly located in the epiphysis region (arrow in C). (D, E)- hindbrain region with focus on the ventral part of the neural tube revealing positive cells in the middle of each rhombomere and two sets of bilateral patches adjacent to the neural tube (arrows in D mark cells immediately adjacent to the neural tube and in E arrow marks the patch located more adaxially). (F) side view of trunk region, anterior to the left, showing positive cells scattered in the dorsal half of the embryo. (G) manual section at the level of the end of the yolk extension

revealing that positive cells in the trunk are all located in the outer region of the neural tube. (A-E) are dorsal views, anterior to the left and the eyes were manually removed for simplification. no-notochord; ov-otic vesicle; r1-rhombomere 1.

3.2.4 *rab5a1* expression pattern during zebrafish development

Expression of *rab5a1* is very similar, if not identical, to *rab3c1*. At early stages of development, low-level uniform expression is seen throughout all tissues (data not shown). However, at 24hpf of development, *rab5a1* is up regulated in a sub-set of cells that seem to be all of neuronal origin. Like *rab3c1* there is expression in the ventral most anterior part of the neural tube, the forebrain and midbrain (see panel A Figure 3-4). In the same region but dorsally there is expression in a bilateral patch of telencephalic cells and another more posterior patch around the region of the epiphysis (see panels B, C Figure 3-4). More posteriorly, there are cells in the middle of each rhombomere expressing the gene, presumably reticulospinal neurons (panel D Figure 3-4). Adjacent to the neural tube, there are bilateral patches of expression at the level of the midbrain/hindbrain boundary and at the level of the last rhombomere (see panels E and F Figure 3-4). These expressing cells outside the neural tube could be anterior and posterior lateral line, judging by their position along the anterior/posterior axis of the embryo. In the trunk and tail region of the embryo, there are cells expressing *rab5a1* and they all seem to occupy outer positions in the neural tube, as seen in cross-sections (panels I and J Figure 3-4).

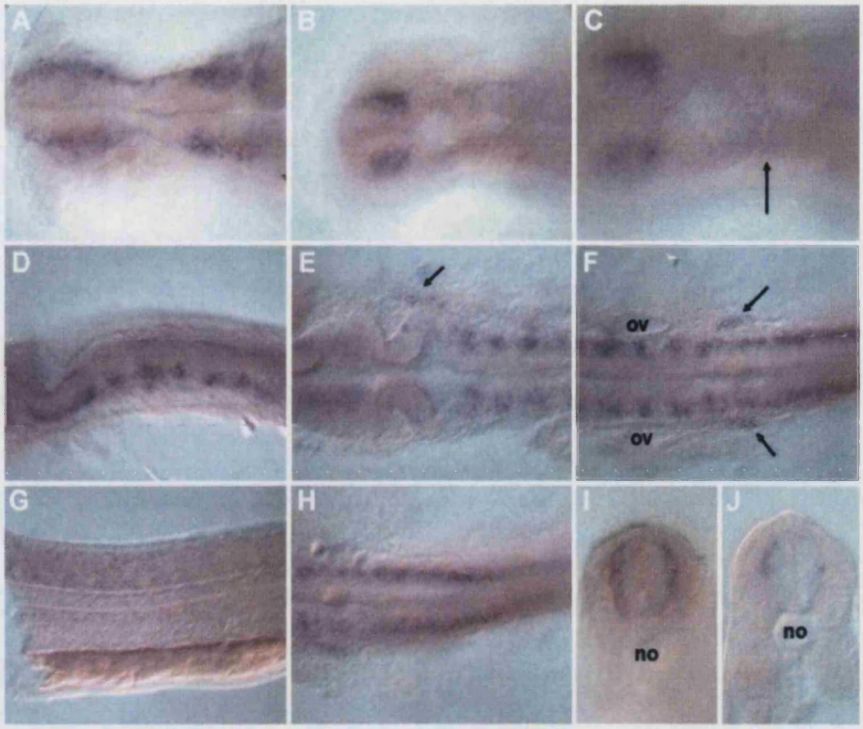

Figure 3-4 Expression pattern of *rab5a1* at 24hpf. (A)-forebrain and midbrain region with focus on the ventral part of the neural tube. (B, C)-forebrain region with dorsal focus showing two patches of bilateral telencephalic cells (B) and another patch of cells, more posteriorly located in the epiphysis region (arrow in C). (D-F)-hindbrain region showing expression on the central region of each rhombomere (D) and in cells outside the neural tube at the level of the midbrain/hindbrain boundary (arrow in E) and at the level of the end of the hindbrain (arrows in F), presumably corresponding to anterior and posterior lateral line, respectively. (G, H) trunk region showing positive cells scattered in the dorsal half of the embryo. (I,J) manual sections at the level of the end of the yolk extension revealing that positive cells in the trunk are all located in the outer region of the neural tube. (A-C, E-F, H) are dorsal views, anterior to the left and the eyes were manually removed for simplification. (D, G) are side views, anterior to the left. no-notochord; ov-otic vesicle.

3.2.5 *rab5c* expression pattern during zebrafish development

The *rab5c* gene is expressed at high levels maternally (see panel A, Figure 3-5). High levels of *rab5c* expression continue after the on-set of zygotic transcription throughout the whole blastoderm (panel B, Figure 3-5). At shield stage, however, *rab5c* is down-regulated (panel C Figure 3-5). At the 5 somite stage, expression is up-regulated, weakly in every cell and strongly in a stripe of cells that lie around the hindbrain region, possibly in a single rhombomere (arrows in panels D,E Figure 3-5). By 18 somites, up-regulation in the hindbrain region is no longer evident but there seems to be up-regulation of *rab5c* in the whole ventral region of the embryo, particularly at the level of the trunk and tail in the forming blood and/or gut regions (panel F, Figure 3-5). The

presence of high levels of transcript in this region is evident in a 24hpf embryo as well (panels G, H Figure 3-5).

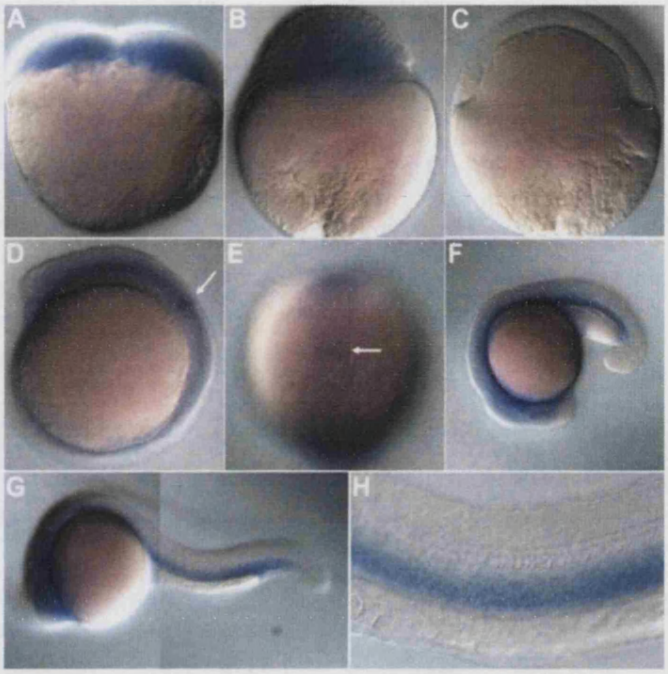

Figure 3-5 Expression pattern of *rab5c*. (A)- two-cell stage embryo expressing maternal *rab5c* transcript. (B)- in a 1000-cell embryo expression is still high throughout the whole embryo. (C)- at shield stage the gene is down-regulated in the whole blastoderm. (D, E)- at 5 somites there is low expression in the whole embryo but a stripe of cells in the hindbrain region is expressing the gene at higher levels. (F)- 18-somites stage embryo revealing weak expression throughout the whole embryo, but higher in the head region and ventral portion of the trunk and tail. (G, H)- 24hpf embryo showing clear up-regulation of the transcript in the head region and in the forming blood and/or gut region of the embryo. (A-C) are side views, animal pole up and dorsal side to the right in (C). (D, F-H) are side views, anterior to the left and (H) is a close-up of (G). (E) is a dorsal view, anterior up.

3.2.6 *rab18* expression pattern during zebrafish development

Similar to *rab5c, rab18* is expressed maternally very strongly and when zygotic transcription begins the transcript is present at high levels throughout the embryo (panel A, B Figure 3-6). However, at shield stage there is pronounced down-regulation in all tissues (panel C Figure 3-6). When the embryo is at 5-somite stage, there seems to be transcript in all cells but some regions with higher signal can be clearly distinguished: anteriorly in the forming hatching gland region or polster, two bilateral patches at the level of the hindbrain region, probably corresponding to the otic

placodes, in the chordamesoderm and in some adaxial cells (panels D-F, Figure 3-6). At 24 hpf, there is weak expression of *rab18* but the outline of the otic vesicles can still be clearly seen (panel G, Figure 3-6). At this stage there is strong expression in a bilateral patch of cells, adjacent to the neural tube at the level of the beginning of the spinal cord (panel H, Figure 3-6).

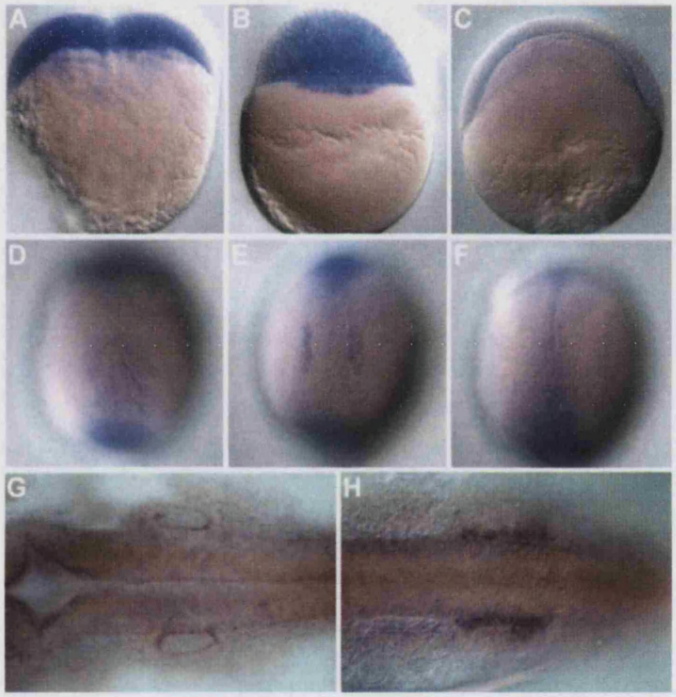

Figure 3-6 Expression pattern of *rab18*. (A)- two-cell stage embryo expressing maternal *rab18* transcript. (B)- in a 1000-cell embryo expression is very high throughout the whole embryo. (C)- at shield stage the gene is down-regulated in the whole blastoderm. (D-E)- at 5 somites there is low expression in the whole embryo and up-regulation in the hatching gland (D), otic vesicles (E) and axial tissues such as the notochord and some more adaxial cells (F). (G, H)- 24hpf embryo showing clear up-regulation of the transcript outlining the otic vesicles (G) and in a bilateral patch of cells, posterior to the otic vesicles and adjacent to the neural tube (H). (A-C) are side views, animal pole up and dorsal side to the right in (C). (D-F) are dorsal views, anterior up. (G, H) are dorsal views, anterior to the left.

3.3 Rab morphant phenotypes

Morpholinos targeting the 5' region of the gene comprising the first codon were designed by GeneTools for 20 zebrafish *rab* genes (see Materials and Methods). All the MOs were injected at the 1-4 cell stage of zebrafish embryos as described in the Materials and Methods section of the thesis. A developmental phenotype was evidently observed upon injection of 14 different MOs targeting 14 different zebrafish *rab* genes.

3.3.1 *rab1a1* morphant phenotype

Morpholino oligonucleotide targeting the region of initiation of translation of *rab1a1* (see MO sequence in the Material and Methods section) were injected into 1-4 cell stage embryos, at three doses, 9, 4 and 2ng. At 24hpf only embryos injected with the highest amount showed a phenotype (see Figure 3-7). These embryos had a smaller head and otic vesicles (compare panels C and D with A and B in Figure 3-7). The head region presents an opaque colour typical of dying cells. At 72hpf differences between embryos injected with *rab1a1* and with control MOs were more obvious: the *rab1a1* morphants were smaller in size, had a curled body and hadn't hatched from the chorions. The shape of the head was also clearly altered, namely with a much reduced forebrain (compare panel F with E in Figure 3-7).

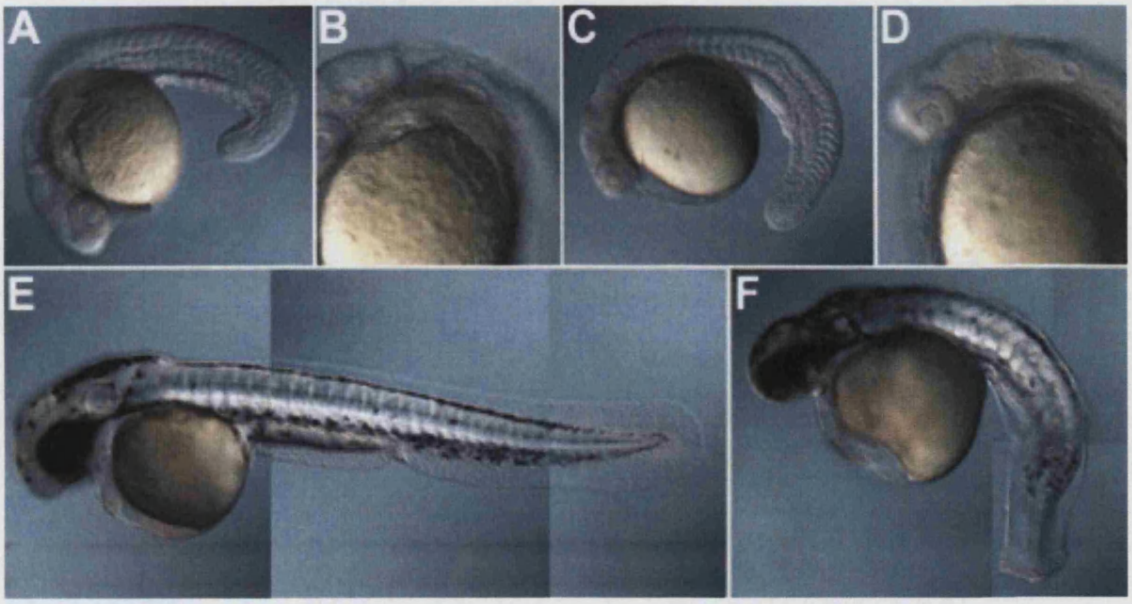

Figure 3-7 Phenotype of the *rab1a1* morphant at 24hpf and 72hpf. (A, B and E)- embryos injected with 10ng of control MO. (C, D and F)- embryos injected with 9ng of *rab1a1* MO have several developmental defects, namely reduced heads and otic vesicles (C,D) and abnormal

body shape, smaller in length than control MO injected embryos (F compare with E). (A-D) are embryos at 24hpf and (E-F) are embryos at 72hpf.

3.3.2 *rab1b* morphant phenotype

At 48hpf embryos injected with 9ng of rab1b MO were indistinguishable from embryos injected with control embryos, with one exception: melanophores in *rab1b* morphants seemed to be fewer in number and smaller in size than in control embryos (panels D-F compared to A-C in Figure 3-8).

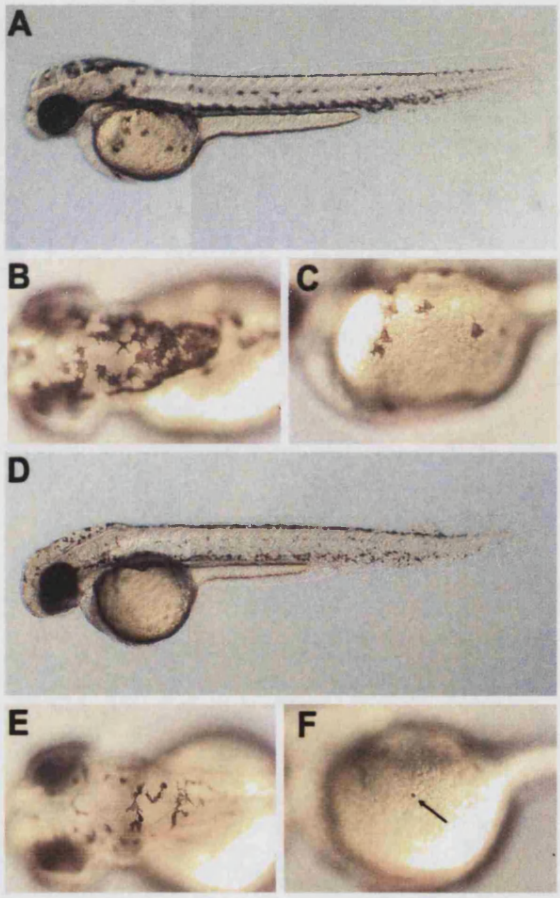

Figure 3-8 Phenotype of the *rab1b* morphant at 48hpf. (A-C)- embryos injected with 10ng of control morpholino. (D-F)- embryos injected with 9ng of *rab1b* MO appear to have fewer and differently shaped melanophores. (C, F) are higher magnifications and (B, E) are dorsal views of the head region of the embryos depicted in (A, D), respectively. Arrow in (F) points to a single melanophore present on the photographed side of the yolk cell.

At 48hpf *rab1b* morphants appear to have fewer melanophores than control embryos. It seemed relevant, therefore, to check whether the melanophore precursors were

formed normally in these embryos. Melanophores are melanin producing cells and are neural crest derived (Eisen and Weston, 1993). Before the on-set of melanin production, melanophore precursors, called melanoblasts, can be visualized through a mRNA *in situ* staining for an enzyme involved in melanin synthesis, *dopachrome tautomerase* (*dct*) (Kelsh et al., 2000). In 24hpf *rab1b* morphants the number of melanoblasts is comparable to a control embryo, as seen by *in situ* analysis of *dct* mRNA depicted in Figure 3-9.

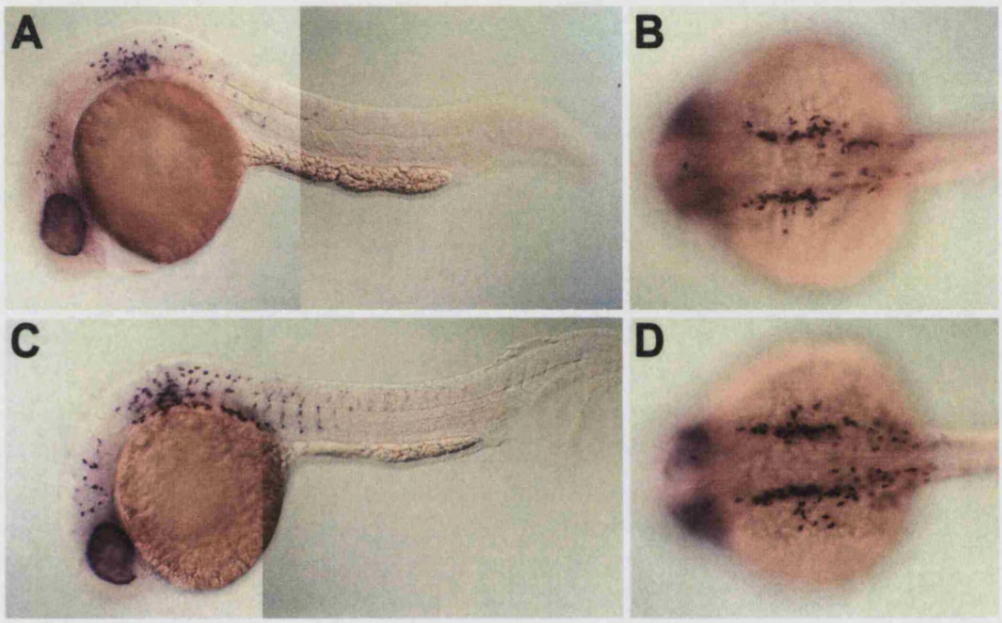

Figure 3-9 Expression pattern of *dct* in *rab1b* morphant embryos at 24hpf. (A, B)- Embryos injected with 10ng of control MO. (C, D)- embryos injected with 9ng of *rab1b* MO have *dct* positive cells in comparable numbers to control embryos. (A, C) are side views and (B, D) are dorsal views. In all panels anterior is to the left.

Melanophores are formed in normal numbers in *rab1b morphants*. Therefore, the apparent reduced number of melanophores in these embryos at 48hpf could be due to increase apoptosis in this specific cell type. To test this hypothesis, a TUNEL assay was performed. At approximately 30hpf, apoptotic cells are scattered throughout control embryos, but more predominantly in the neural tube region. In an embryo injected with *rab1b* MO, there is no difference in the levels of apoptotic cells, apart from a slight increase in the end of the tail (see panel E Figure 3-10) and, possibly, in the

region around the otic vesicle (see panel F Figure 3-10), where many melanoblasts accumulate.

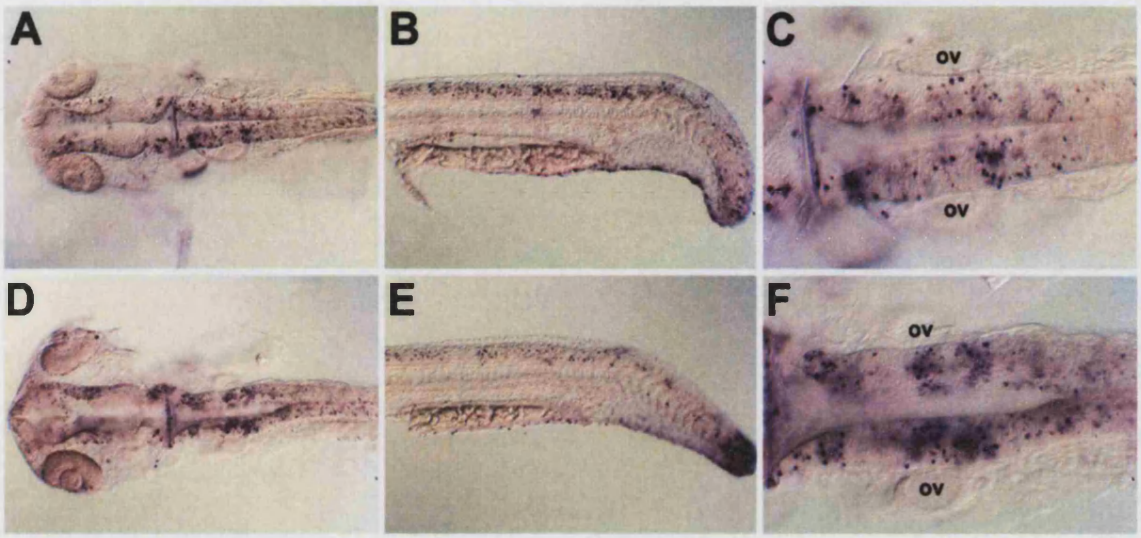

Figure 3-10 TUNEL positive cells in a 30hpf *rab1b* morphant embryo. (A-C)- embryo injected with 10ng of control MO showing apoptotic cells scattered throughout the whole embryo but predominantly in the neural tube region. (D-F)- embryo injected with 9ng of *rab1b* MO showing higher levels of apoptotic cells mainly in the end of the tail (E) and in the otic vesicle (ov) region (F). (C, F) are close ups of dorsal views of head region depicted in (A, D), respectively. (B, E) are side views of trunk/tail region. In all panels anterior is to the left.

3.3.3 *rab2a2* morphant phenotype

At 24hpf an embryo injected with 8ng of *rab2a2* MO shows several defects in comparison with an embryo at the same stage injected with control MO. Firstly, the brain is smaller particularly in the midbrain region. This might be due to increase cell death in this region, as indicated by greyness typical of dying cells in this region of a *rab2a2* morphant (see panel C Figure 3-11). Secondly, the yolk extension is much thinner than that of a control embryo (see panel D Figure 3-11). The third obvious developmental defect in these embryos is the shape of the somites as seen clearly by the change from a chevron shape in control embryos to a u-shape in *rab2a2* morphants (panels B, D Figure 3-11).

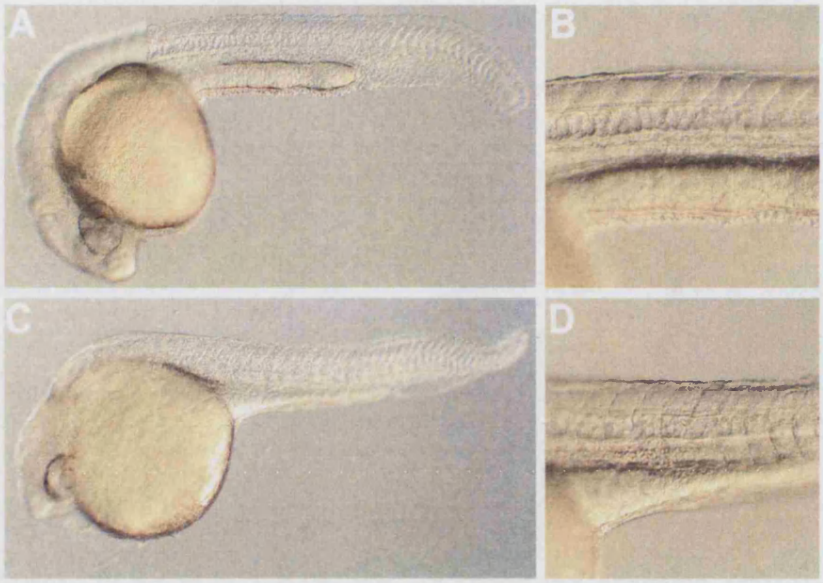

Figure 3-11 Phenotype of the *rab2a2* morphant at 24hpf. (A, B)- embryo injected with 10ng of control MO. (C, D)- embryo injected with 8ng of *rab2a2* MO showing brain defects, a thinner yolk extension and u-shaped somites. (B, D) are close ups of the trunk region of the embryos depicted in (A, C), respectively. In all panels anterior is to the left.

When embryos injected with *rab2a2* MO are left to develop until 72hpf it becomes obvious that they are much shorter than control embryos of the same age (Figure 3-12). Moreover, the brain defects are also more obvious at this developmental stage and a clear depression in the zone of the midbrain can be observed (panel B Figure 3-11).

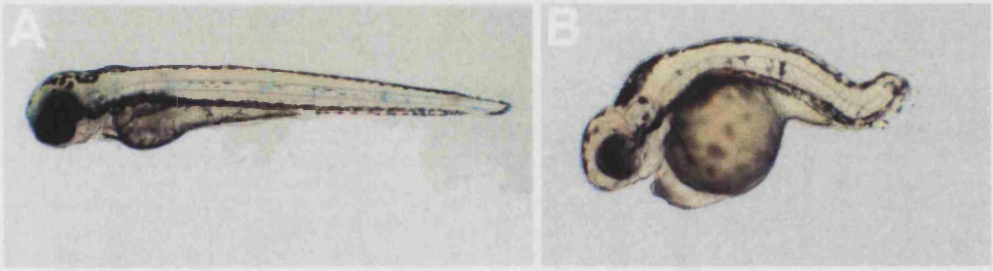

Figure 3-12 Phenotype of the *rab2a2* morphant at 72hpf. (A)- embryo injected with 10ng of control MO. (B)- embryo injected with 8ng of *rab2a2* MO showing a depression in the midbrain region and a much shorter body axis.

3.3.4 *rab3c2* morphant phenotype

Injection of 6ng of *rab3c2* MO into zebrafish embryos results in a multiplicity of developmental defects. At 24hpf the most obvious phenotype is in the somites that are thinner and u-shaped (Figure 3-13). Probably related to the somite defect, a *rab3c2* morphant is considerably shorter than a control embryo at the same stage (Figure 3-13). Another cause for a shortened body axis is notochord failure to differentiate, which occurs in these embryos.

Figure 3-13 Phenotype of the *rab3c2* morphant at 24hpf. (A) embryo injected with 10ng of control morpholino and (B) embryo injected with 6ng of *rab3c2* MO presenting thinner and u-shape somites.

3.3.5 *rab5a2* morphant phenotype

Knocking down *rab5a2* using the morpholino technology leads to a dramatic and early phenotype. The first difference between the embryonic development of a zebrafish embryo injected with 3ng of *rab5a2* when compared to that of a control embryo is obvious at shield stage. When control embryos have a well defined embryonic shield (panels A, C Figure 3-14) *rab5a2* MO injected embryos are at 50% epiboly but have no obvious dorsal thickening of the blastoderm (panels B, D Figure 3-14). Epiboly movement seems to progress very slowly in these morphants and when control embryos have reached around 80% epiboly, embryos in which *rab5a2* was knocked down are still roughly at 50% epiboly (panels E,F Figure 3-14). A considerable proportion of *rab5a2* morphants continue epiboly until 80%, but by then control embryos are already at 7-somite stage (panels G, H Figure 3-14). A few hours later they are all dead.

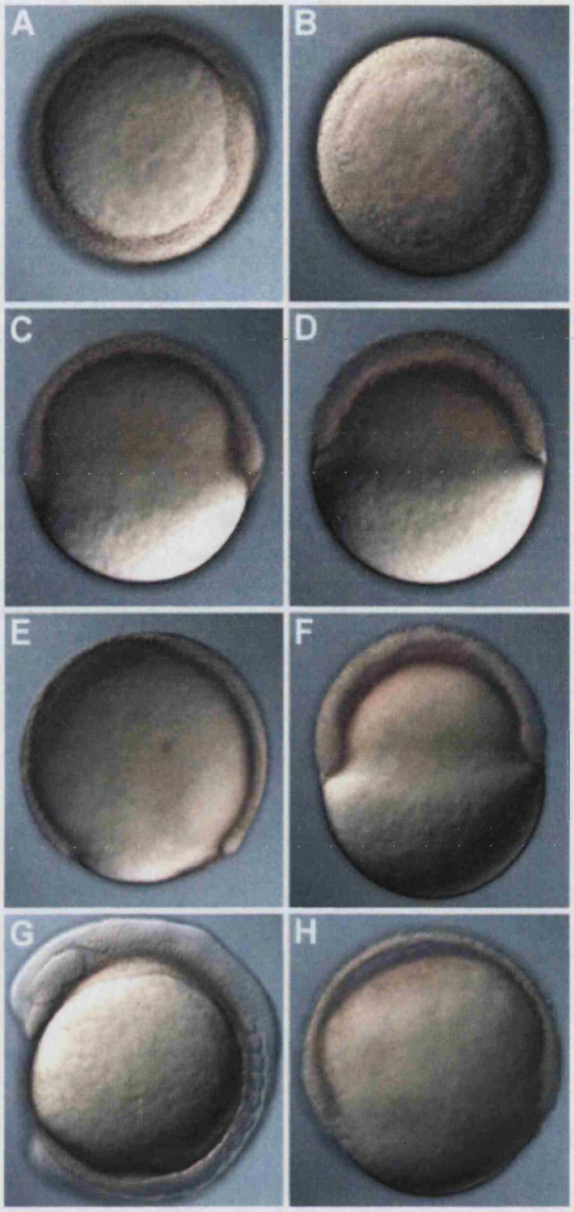

Figure 3-14 Early phenotype of the *rab5a2* morphant. (A, C, E, G)- embryos injected with 3ng of control MO at shield (A, C), 80% epiboly (E) and 7-somite stages (G). (B, D, F, H)- embryos injected with 3ng of *rab5a2* MO photograph at the same time as control embryos on the corresponding left panel. When control embryos are at shield stage, *rab5a2* morphants are at 50% epiboly but with no obvious dorsal thickening (A-D). When control embryos are at 80% epiboly *rab5a2* morphants are still at 50% (E, F). Some *rab5a2* morphants reached 80% epiboly, but, by then, control embryos are already at 7-somite stage (G, H). (A, B) are animal views, dorsal to the right in (A). (C-H) are side views with dorsal to the right.

To study the pace of epiboly in *rab5a2* morphants, 12 control MO injected embryos and *rab5a2* MO injected embryos were closely monitored approximately every hour after the start of the epiboly movement. The results are plotted in Figure 3-15. From the beginning *rab5a2* morphants progress more slowly through epiboly than control

embryos. Whereas control embryos have an approximately constant rate of epiboly, as seen by the minor changes in the slope of the lines that pass through the experimental points, *rab5a2* morphants seem to undergo epiboly at an increasingly slower rate. Within five hours control embryos have completed the movement, but *rab5a2* morphants are at approximately 60% epiboly. Eventually, these embryos will reach 80%-epiboly, but only 9 hours after the onset of the movement, when control embryos have reached the 7-somite stage.

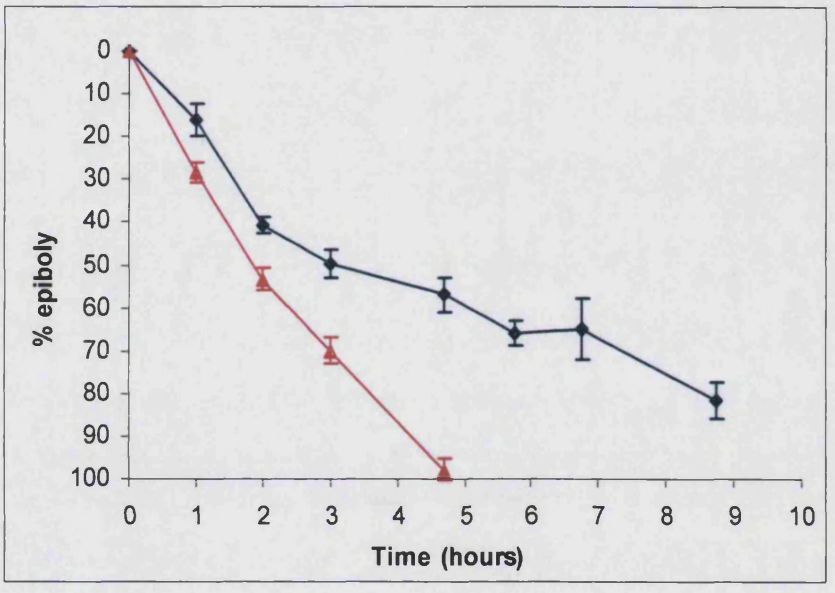

Figure 3-15 Progression of epiboly in *rab5a2* morphant embryos (blue, squares) and in control embryos (red, triangles). Control embryos take approximately 5 hours to epibolise and do it at a constant rate. Embryos injected with *rab5a2* MO epibolise much slower right from the beginning and even slower as epiboly carries on. Experimental embryos eventually reach 80% of epiboly but only 9 hours later, when control embryos are at 7-somite stage. (n=12).

Although epiboly is severely slowed down in *rab5a2* morphants it is formally possible that other aspects of developmental timing are normal. To assess ingression of axial tissue, an *in situ* hybridisation for the gene *no tail* (*ntl,* also known as *brachyury*) was performed. Control embryos at 70% epiboly express *ntl* all around the margin and in involuting mesendoderm tissue in the dorsal side of the embryo (panels A, C Figure 3-16). In contrast, *rab5a2* morphants reach only 40-50% epiboly during the same period, express *ntl* only at the margin of the blastoderm and do not have any involuted *ntl*-positive axial mesendoderm (panel B, D Figure 3-16).

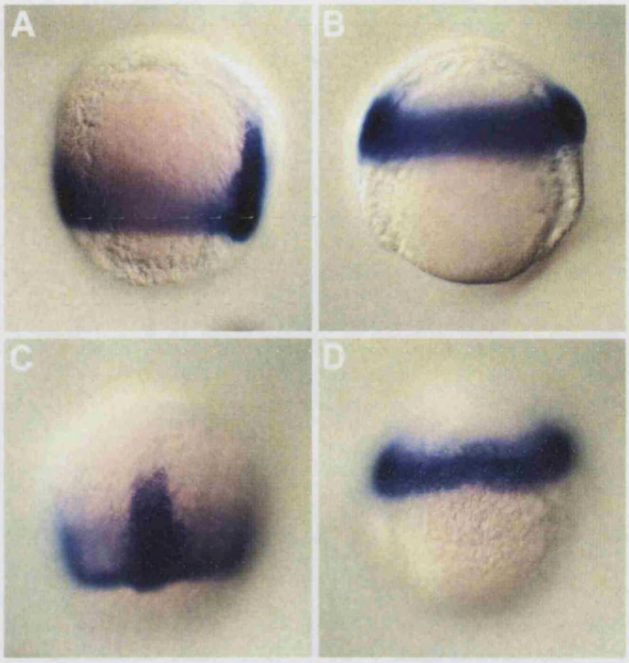

Figure 3-16 Expression pattern of *brachyury* in a *rab5a2* morphant embryo at "70% epiboly". (A, C) an embryo injected with 3ng of control MO at 70% epiboly expresses the gene *brachyury* around the margin and in involuting mesendoderm. (B, D) An embryo injected with 3ng of *rab5a2* MO only reached around 40-50% epiboly and expresses *brachyury* around the margin, but there is no involuting axial mesendoderm as seen by this marker. (A, B) are side views with dorsal to the right; (B, D) are dorsal views; in all panels animal is up.

There were epiboly mutants identified in previous large scale mutagenesis screens (Kane et al., 1996; Solnica-Krezel et al., 1996). In these mutants there is an arrest of epiboly of the deep blastoderm cells, but not yolk syncytial layer or the enveloping layer cells (Kane et al., 1996). In contrast, *rab5a2* morphant epibolic movement of all tissues is strongly delayed, but in a synchronous manner (data not shown). Only embryos that survive until late stages of epiboly show any loss of registration with the enveloping layer preceding the deep embryonic layer (Figure 3-17).

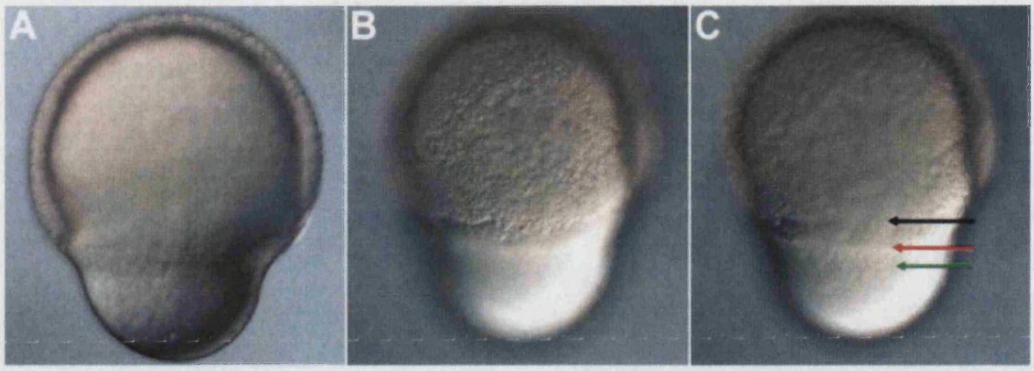

Figure 3-17 Epiboly of cells of the blastoderm (black arrow), enveloping layer (red arrow) and yolk syncytial layer (green arrow) in a 70% epiboly *rab5a2* morphant. (A,B,C) are three different focal planes of the same embryo injected with 3ng of *rab5a2* MO, in a side view, dorsal to the right and animal up. It was only in a few cases and only at later stages of epiboly that an occasional lack of synchronicity was spotted in cells of the blastoderm, enveloping layer and yolk syncytial layer of *rab5a2* morphants.

The mammalian version of Rab5a has been shown to function as a regulatory factor in the early endocytic pathway, stimulating membrane fusion in endocytosis (Bucci et al., 1992; Gorvel et al., 1991; Stenmark et al., 1994). In BHK cells, over-expression of a mutant form of the protein incapable of binding to GTP leads to the accumulation of a large number of very small vesicles at the periphery of the cell (Bucci et al., 1992; Stenmark et al., 1994). Over-expression of a constitutively active form of the protein, defective in GTP hydrolysis, leads to appearance of unusually large early endocytic structures (Stenmark et al., 1994). To check on the cell morphology of *rab5a2* morphant cells EM microscopy was performed (Figure 3-18). Surprisingly, putative depletion of rab5a2 protein has a cellular phenotype comparable to over-expression of the constitutively active mammalian counterpart and not to the over-expression of the dominant negative form. As it can be seen in Figure 3-18, *rab5a2* morphant cells accumulate huge smooth membrane profiles that were never found in control MO injected embryo cells. In many cases, these large vesicles were found to have an irregular shape, which would be expected from dynamic structures. Finally, *rab5a2* morphant cells also appear to have an increase number of large secondary lysosomes containing membranous contents.

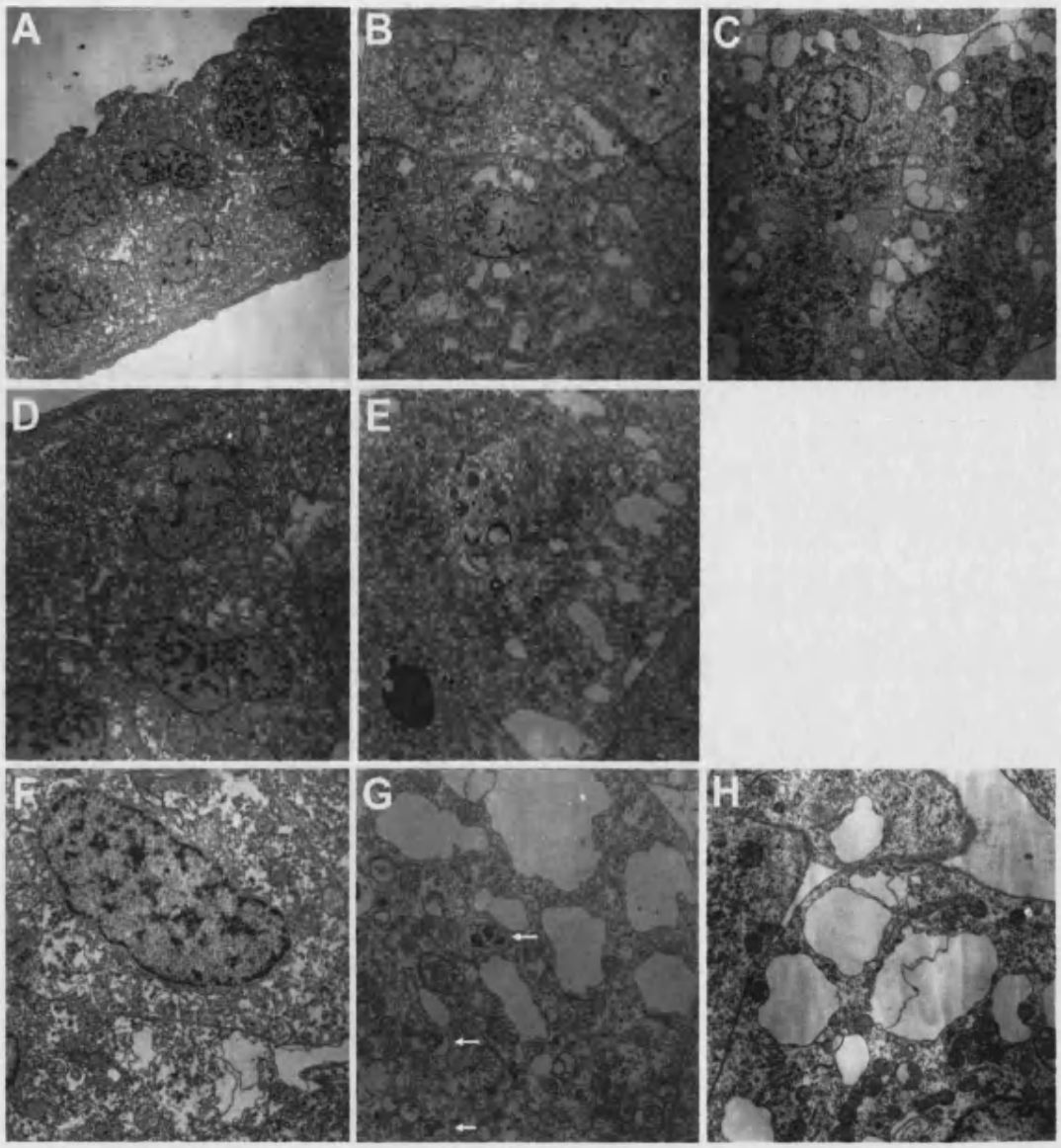

Figure 3-18 Electron microscopy of *rab5a2* morphant cells. All panels shown transverse sections of the leading edge of the enveloping layer. (A,D,F) are cells from a control morpholino injected embryo (3ng) and fixed at 80% epiboly; (B,E,G) cells from embryo 1 injected with 3ng *rab5a2* MO fixed when control embryos were at 80% epiboly, but when it had only completed 40% epiboly; (C,H) are cells from embryo 2 treated in the same way as embryo 1. *rab5a2* morphant cells show huge smooth membrane profiles with highly irregular shapes (B,C,E,G,H) and many large secondary lysosomes with membranous contents (white arrows in G). (A-C) are at 5,000x; (D, E) are at 10,000x; and (F-H) are at 18,750x.

3.3.6 *rab5b* morphant phenotype

In contrast to the early phenotype of embryos injected with *rab5a2* MO, loss of rab5b function produces a much later phenotype. At 24hpf *rab5b* morphants have very thin and u-shaped somites and brain defects, namely a reduced forebrain and cell death as indicated by the lack of transparency of cells in this region (see Figure 3-19). In

addition, notochord cells fail to fully differentiate which results in a shorter embryonic axis.

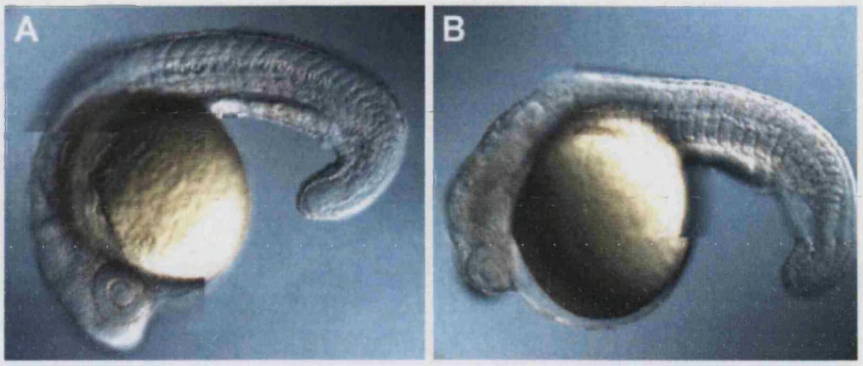

Figure 3-19 Phenotype of the *rab5b* morphant at 24hpf. (A) embryo injected with 10ng of control morpholino and (B) embryo injected with 8ng of *rab5b* MO presenting thinner and u-shape somites, forebrain defects and cell death in the brain.

3.3.7 rab5c morphant phenotype

Injection of a *rab5c* morpholino in zebrafish embryos results in a phenotype very similar to the *rab5b* morphant. At 24hpf, an embryo injected with 6ng of *rab5c* morpholino has an axis much shorter than that of a control morpholino injected embryo (see Figure 3-20). In addition, these fishes have u-shaped somites and the head region is poorly developed (Figure 3-20).

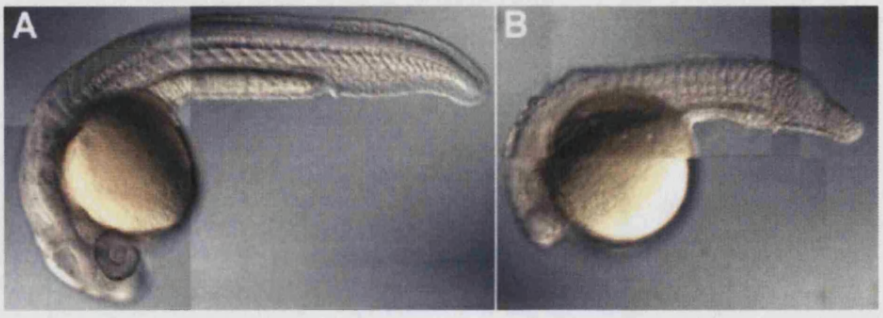

Figure 3-20 Phenotype of the *rab5c* morphant at 24hpf. (A) embryo injected with 5ng of control morpholino and (B) embryo injected with 6ng of *rab5c* MO. *rab5c* morphants have a shorter embryonic axis and their head is poorly developed.

On the second day of development, *rab5c* morphants survive but the notochord fails to differentiate properly (compare panels D' with D in Figure 3-21). Moreover, muscle formation is disrupted and muscle fibres misaligned, as seen under polarized light (compare panels C' and C Figure 3-21).

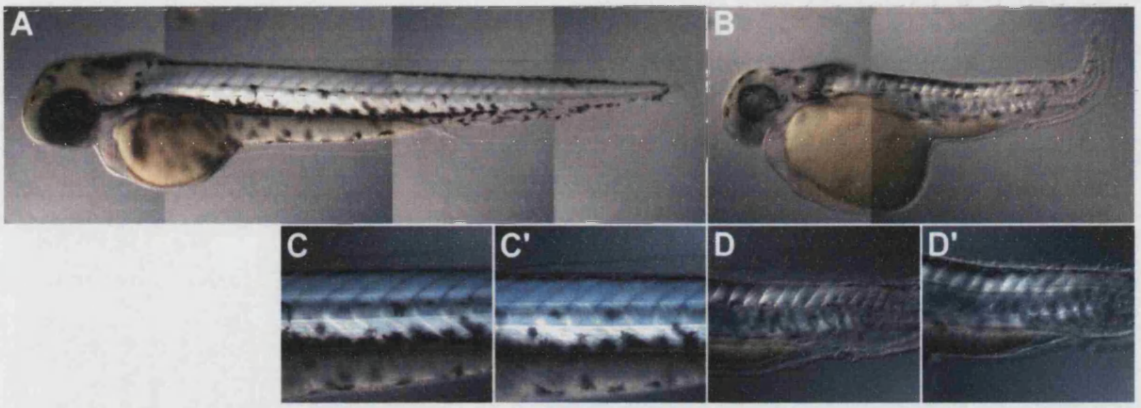

Figure 3-21 Phenotype of the *rab5c* morphant at 48hpf. (A, C, C') embryo injected with 5ng control morpholino. (B, D, D') embryo injected with 6ng *rab5c* morpholino. At 48hpf zebrafish *rab5c* morphants have a clear shorter axis, the notochord is abnormally vacuolated (D') and muscle fibres are not aligned in a longitudinal way (D). (C, C') and (D, D') are close ups of the trunk region of the embryos depicted in (A) and (B), respectively.

3.3.8 *rab7b* morphant phenotype

For Rab7b an embryonic phenotype is seen only at high amounts of MO. An embryo injected with 16ng of *rab7b* MO shows at 24hpf defects in the eye, in particular, and the brain, in general (see Figure 3-22). In the trunk, defects in the somites and a thinner yolk extension can also be observed (see Figure 3-22).

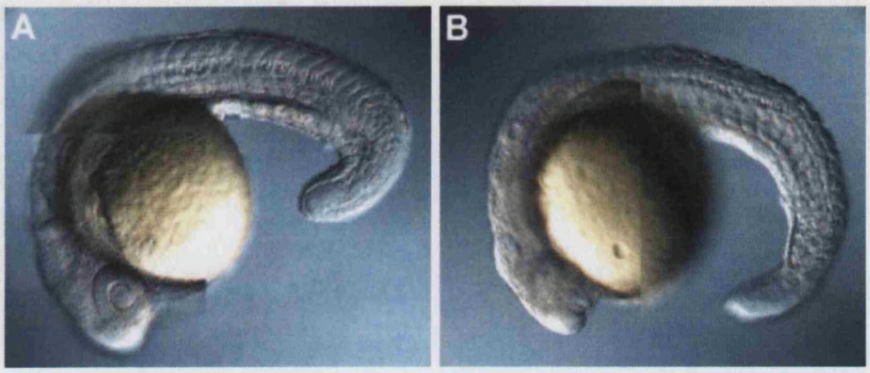

Figure 3-22 Phenotype of the *rab7b* morphant at 24hpf. (A) embryo injected with 10ng of control morpholino and (B) embryo injected with 16ng of *rab7b* MO. *rab7b* morphants have defects in the eye, brain, oddly shaped somites and a thinner yolk extension than control embryos.

3.3.9 *rab9a* morphant phenotype

Injection of 6ng of *rab9a* MO at 1-4 cell embryos leads to a strong developmental phenotype. At tail bud stage, morphant embryos have an oval morphology (data not shown). At 24hpf, defects in *rab9a* morphants are diverse: dying cells are evident in the brain; the trunk and tail have a blistering appearance; and the yolk extension is abnormally thin (panels C, D Figure 3-23). By day two, these defects are more obvious and the embryos have a constriction in the brain at the level of the midbrain/hindbrain boundary and an oddly shaped trunk and tail with an undifferentiated notochord (panel F Figure 3-23). In addition, *rab9a* morphants have a rough epidermis and almost complete lack of pigmentation (panel F Figure 3-23).

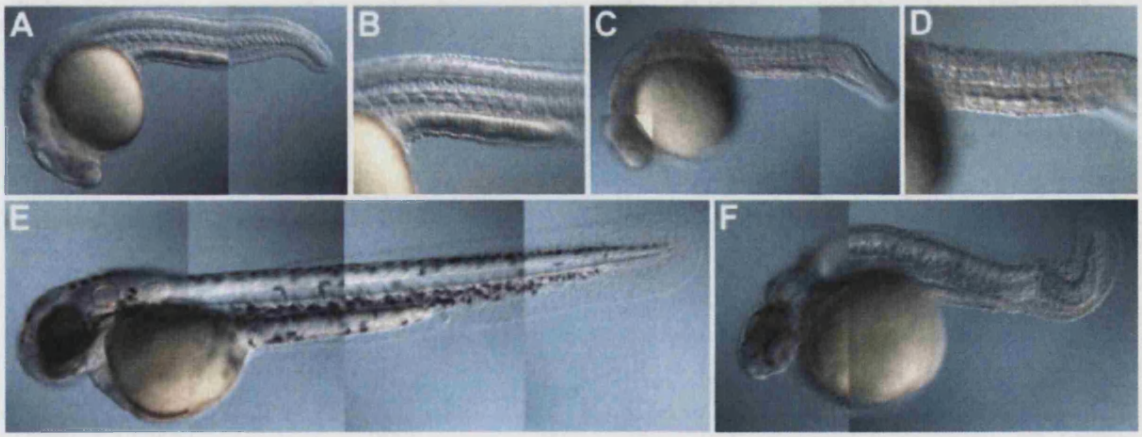

Figure 3-23 Phenotype of the *rab9a* morphant at 24hpf and 48hpf. (A, B, E) embryos injected with 5ng control MO; (C, D, F) embryos injected with 6ng of *rab9a* MO. (A-D) are 24hpf embryos and (E, F) are 48hpf embryos. At 24hpf *rab9a* have a wide range of defects including cell death in the brain region, a thinner yolk extension and blistering in the epidermis (C, D). One day later, *rab9a* morphants have an obvious constriction in the midbrain/hindbrain region, a very malformed trunk and tail and almost complete absence of pigmentation (F). (B, D) are close ups of (A, C), respectively.

3.3.10 *rab13* morphant phenotype

Polarized epithelial cells have morphologically and functionally distinct apical and basolateral surfaces separated by tight junctions. The protein Rab13 has been shown to localize to tight junctions of a variety of epithelial cells (Sheth et al., 2000; Zahraoui et al., 1994), whereas in cells devoid of these structures was found associated with vesicles dispersed throughout the cytoplasm (Zahraoui et al., 1994). Furthermore, over-expression of a constitutively active form of Rab13 in MDCK cells disrupts the tight junction fence diffusion barrier revealing that this protein plays an important role in tight junction structure and function (Marzesco et al., 2002).

The most striking phenotype of an embryo injected with 6ng of *rab13* MO is an epidermis defect consistent with the above observations (Figure 3-24). In a 48hpf *rab13* morphant the epidermis is blistered (panel B Figure 3-24). This phenotype is most obvious in the caudal fin, which has a very rough border when compared to that of a control embryo (panel D Figure 3-24).

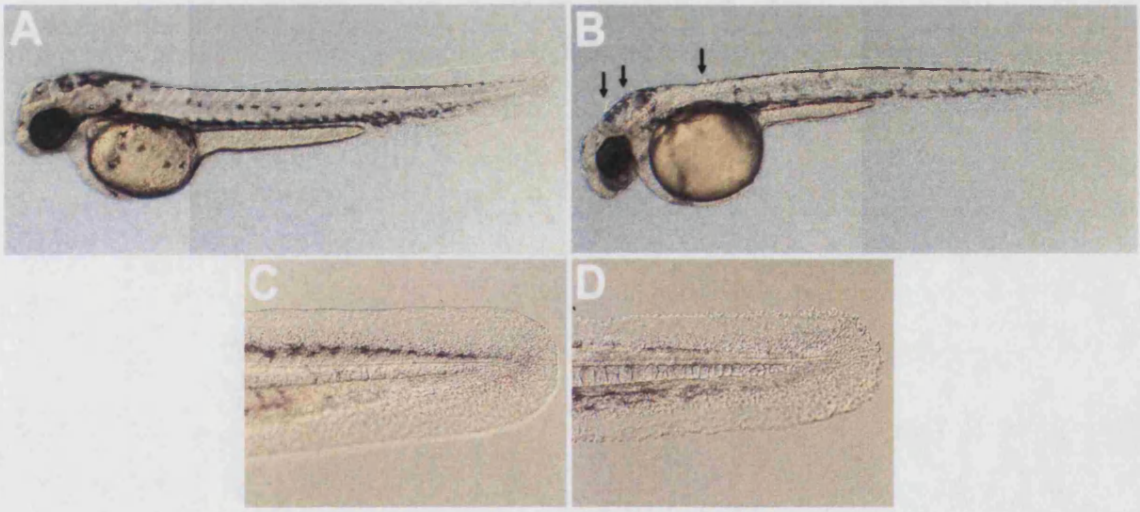

Figure 3-24 Phenotype of the *rab13* morphant at 48hpf. (A, C) embryo injected with 5ng of control MO. (B,D) embryo injected with 6ng of *rab13* MO showing blisters in the epidermis (black arrows in B) and a loss of the regular outline of the caudal fin (D). (C, D) are close ups of the caudal fins of the embryos depicted in (A, B), respectively.

3.3.11 *rab14a* morphant phenotype

Loss of Rab14a function results in abnormal embryonic development evident at 24hpf. An embryo injected with as little as 2.5ng of *rab14a* MO shows brain defects, somite defects and a very thin yolk extension (panels B, D Figure 3-25).

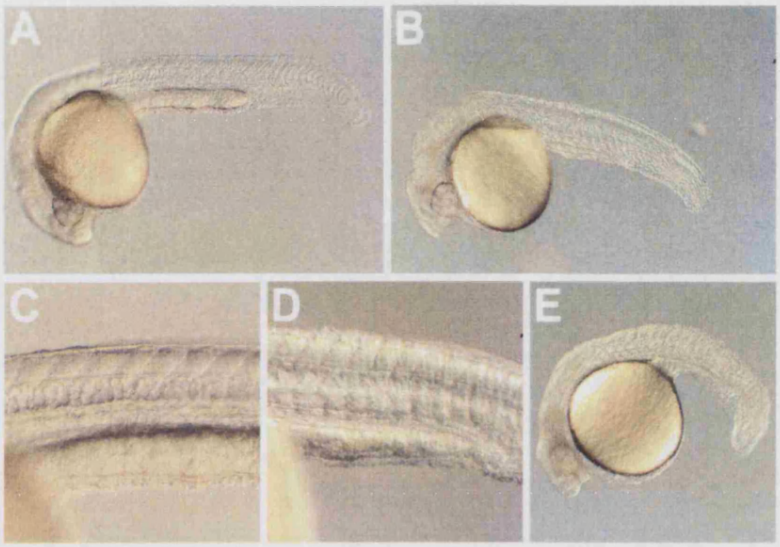

Figure 3-25 Phenotype of the *rab14a* morphant at 24hpf. (A, C) embryo injected with 5ng of control morpholino. (B, D) an embryo injected with 2.5ng of *rab14a* MO showing brain and somite defects and a thinner yolk extension. (E) embryo injected with 5ng of *rab14a* where the brain and somite defects are more pronounced. (C, D) are close ups of (A, B), respectively.

If the morpholino amount injected is increased to 5ng these phenotypes are more dramatic (panel E Figure 3-25) and by 48 hpf *rab14a* morphants have a very shortened embryonic axis and brain defects, including swollen ventricles (Figure 3-26).

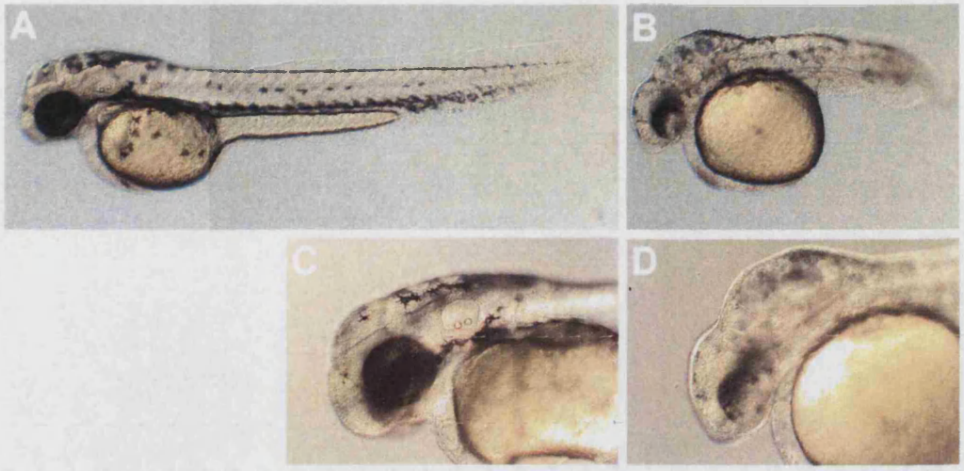

Figure 3-26 Phenotype of the *rab14a* morphant at 48hpf. (A, C) embryo injected with 5ng of control MO. (B, D) an embryo injected with 5ng of *rab14a* morpholino has a very short anterior/posterior axis and brain malformations, namely a swollen in the midbrain region. (C, D) are close ups of (A, B), respectively.

Brain ventricle swelling, somite defects and the thinner yolk extension are phenotypes indicative of a circulation defect. To assay the state of blood vessel formation in *rab14a* morphant embryos, I examined *fli1* expression. This gene is an early marker for vasculogenesis and is expressed in intermediate cell mass cells located where the major blood vessels of the trunk develop, namely the dorsal aorta and the caudal vein (Thompson et al., 1998). More dorsally it is also expressed in cells that will form the inter-somitic arteries and veins (Thompson et al., 1998). In *rab14a* morphants, there are intermediate cell mass cells that express *fli1* but more dorsal *fli1* positive cells are never observed, indicating that inter-somitic blood vessels are absent (Figure 3-27).

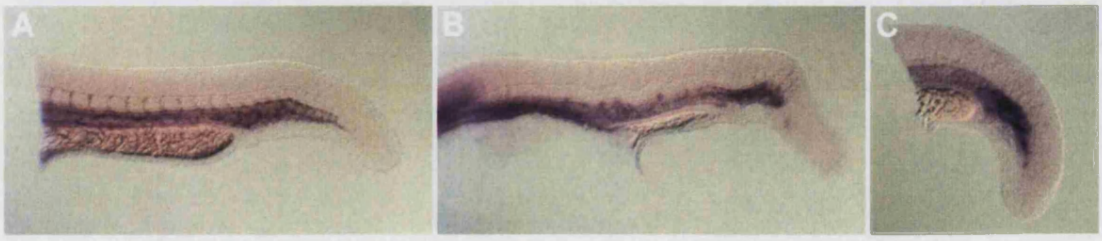

Figure 3-27 Expression pattern of *fli1* in a *rab14a* morphant embryo at 24hpf. Trunk and tail portions of embryos injected with 5ng of control MO (A), 2.5ng of *rab14a* MO (B) and 5ng of *rab14a* MO (C). In *rab14a* morphant embryos there are no *fli1* positive cells between the somites where the inter-somitic vessels should form.

3.3.12 *rab15* morphant phenotype

To knock down the rab15 protein, 6ng of *rab15* MO were injected in 1-4 cell stage zebrafish embryos. The most obvious phenotype of the embryos thus obtained is a reduction of the brain size (Figure 3-28). In addition, they also have an abnormal body shape, probably as a result of a poorly differentiated notochord.

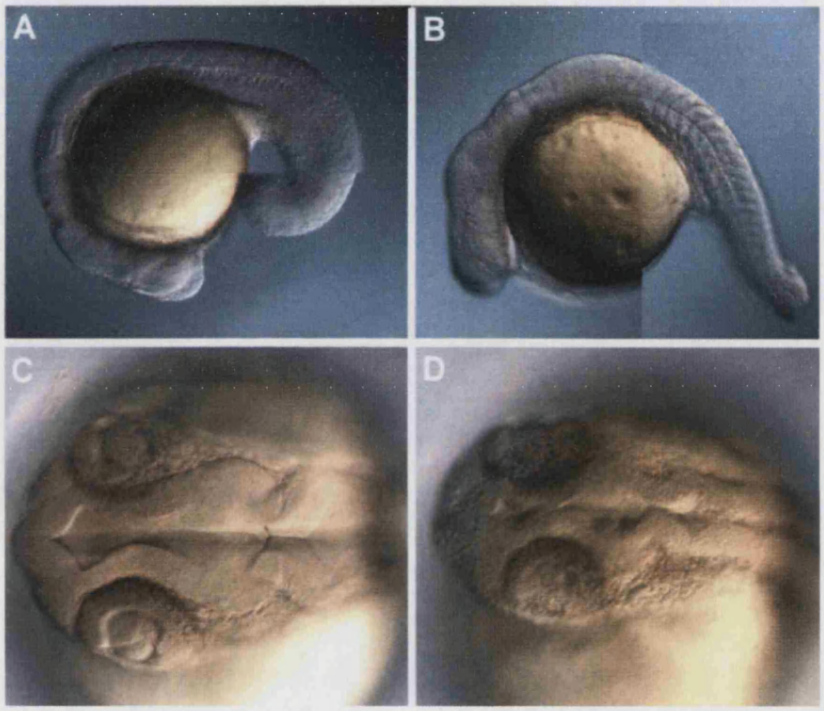

Figure 3-28 Phenotype of *rab15* morphant at 24hpf. (A, C) embryo injected with 5ng of control MO. (B, D) embryo injected with 6ng of *rab15* morpholino. The brain of the experimental embryos is much smaller than that of control embryos. (C, D) are dorsal views of the head region of the embryos depicted in (A, B), respectively.

3.3.13 *rab23* morphant phenotype

The study of the loss-of-function phenotype of the protein rab23 in zebrafish was of particular interest to us. The mouse version of this protein is known to be a negative regulator of the Shh pathway (Eggenschwiler et al., 2001).

Injection of a small quantity of *rab23* MO results in a very strong developmental phenotype that leads to embryo death at segmentation stages (Figure 3-29).

When 3.5ng of morpholino is injected the embryos fail to form somites (panels B, D Figure 3-29). They progress through involution stages normally (data not shown), but when control embryos are at 3 somites, no morphological somite boundary is apparent on *rab23* MO injected embryos (panel D Figure 3-29). Convergence and extension movements appear to be impaired in these fish as chordamesoderm is much wider than in control embryos (panel D Figure 3-29). Finally, cells detaching from the blastoderm and possibly dying can be seen (panel B Figure 3-29) and the whole embryo will die after a few hours.

If only 1ng of *rab23* morpholino is injected, embryos survive until later developmental stages (panels F, H Figure 3-29). When control embryos are at 18-somites, these experimental embryos have roughly the same number of somites but irregularly shaped (panels F, H Figure 3-29). Moreover, these embryos do not extend normally judging from the complete lack of yolk extension (panel F Figure 3-29).

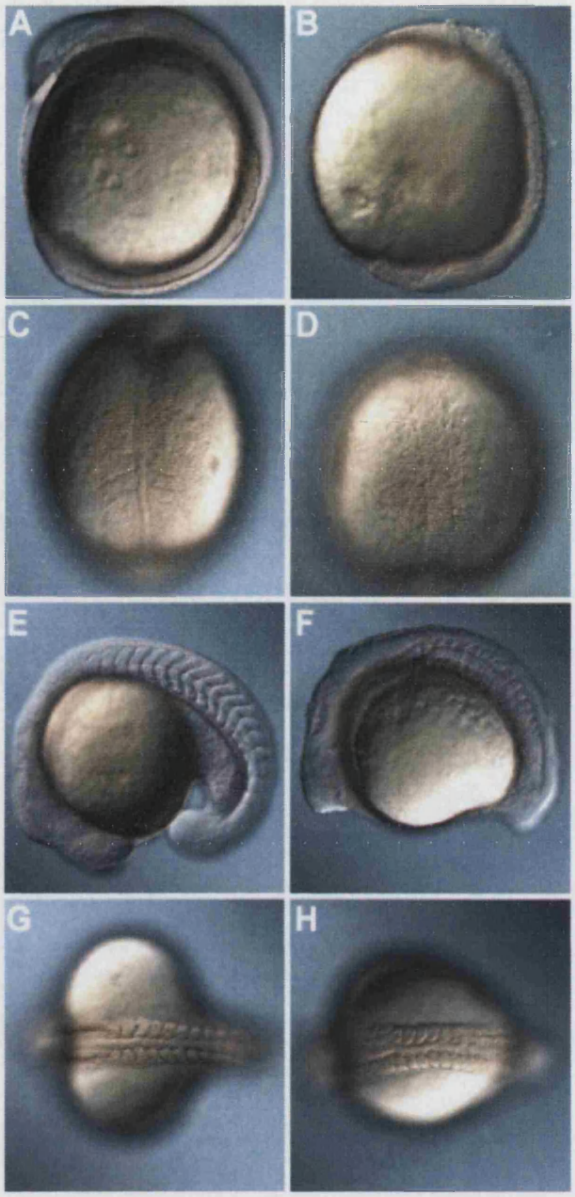

Figure 3-29 Phenotype of the *rab23* morphant. (A, C, E, G) embryo injected with 5ng of control MO at 3-somites (A, C) and 18-somites (E, G) stages. (B, D) embryo injected with 3.5ng of *rab23* morpholino, supposedly at 3-somite stage, but with no distinguishable structures apart from a wider chordamesoderm (D). (F, H) embryo injected with 1ng of *rab23* morpholino at 18-somites stage showing malformed somites and a shorter embryonic axis. (A, B) side views, dorsal to the right; (C, D) dorsal views animal up; (E, F) side views anterior to the left; and (G, H) dorsal views anterior to the left.

Knocking down rab23 protein using morpholino oligonucleotides gives a much stronger phenotype than the one reported for the mouse mutation *open-brain*, deficient in the mouse version of Rab23 (Eggenschwiler and Anderson, 2000; Eggenschwiler et al., 2001; Gunther et al., 1994). To analyse the function of Rab23 and compare it with that of the mouse, I analysed several molecular markers on *rab23* morphants. If, like in the

mice, rab23 were a negative regulator of Shh signalling, the loss of function phenotype would be expected to be comparable to the phenotype of an embryo over-expressing Shh. I therefore analysed the expression of several genes on control MO injected embryos, *rab23* morphants and embryos injected at 1-cell stage with 100pg of *shh* RNA (Figure 3-30).

All the markers analysed are expressed in different regions of a 24hpf zebrafish spinal cord. As *rab23* morphants do not survive to 24 hpf, all embryos were fixed when controls were at 3-somite stage.

The *nkx* genes are known to be direct targets of Shh signalling (Briscoe et al., 2000; Briscoe et al., 1999). Consistently, the expression of these genes is up-regulated in embryos over-expressing Shh (panels B, E, H Figure 3-30). However, the expression of *nkx2.2* is absent in *rab23* morphants, *nkx6.1* is down-regulated despite the field of expression being more diffuse, and the expression of *nkx6.2* is also down-regulated, over a slightly larger field (panels C,F,I Figure 3-30). Therefore, there is no evidence supporting the hypothesis that rab23 is a negative regulator of the Shh signalling pathway in zebrafish.

Given that rab23 does not have an equivalent developmental role to the corresponding mouse protein, an obvious concern is whether the protein that we are disrupting is indeed the closest homologue to the mouse Rab23. Figure 3-31 shows an alignment between the human, mouse and zebrafish rab23 proteins. The rab23 is 83.1% identical to both the mouse and human proteins and is therefore expected to be the closest zebrafish homologue. Among all the Rabs identified in this study, the next closest homologue to mouse Rab23 is Rab35a, only 34% identical.

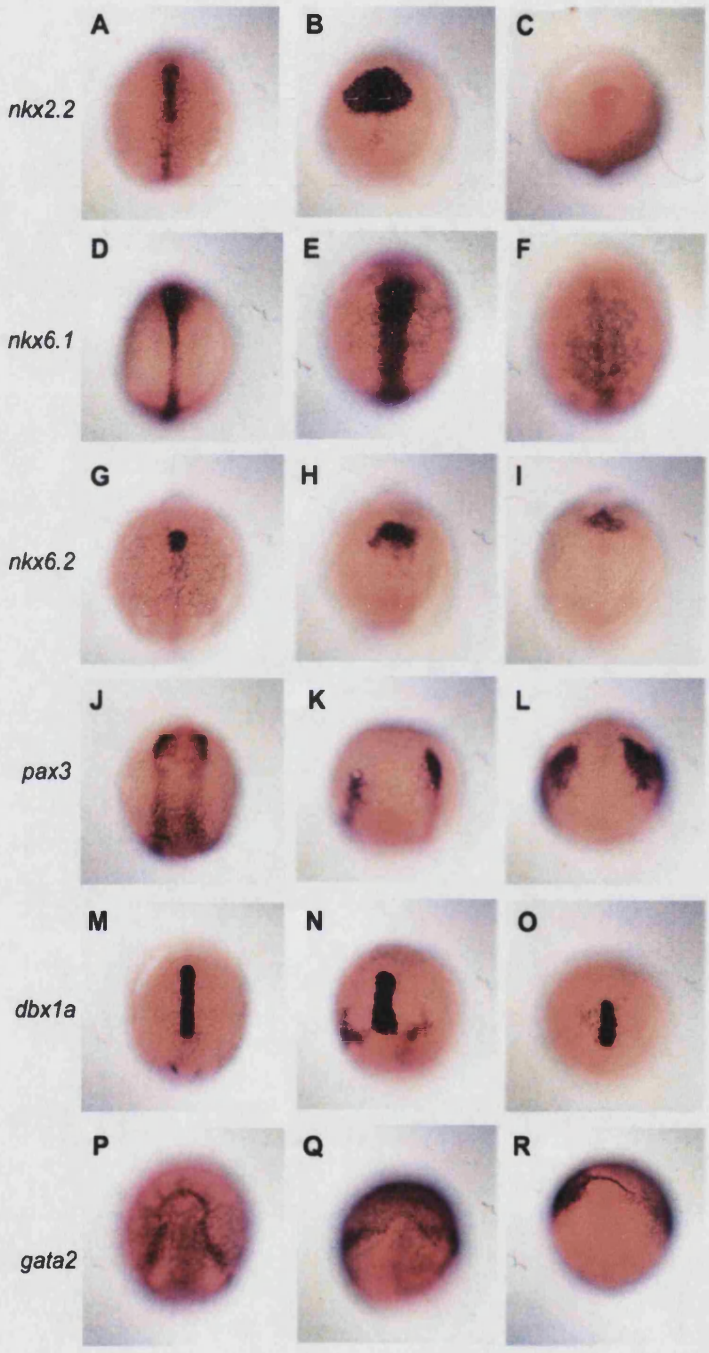

Figure 3-30 Marker analysis in Shh over-expressing embryos and *rab23* morphant at 3 somites. (A,D,G,J,M,P) are embryos injected with 5ng of control MO; (B,E,H,K,N,Q) are embryos injected with 100pg of *Shh* RNA; (C,F,I,L,O,R) are embryos injected with 3,5pg of *rab23* MO. All embryos in dorsal view over the head region, anterior up.

Figure 3-31 ClustalW protein alignment between the human, mouse and zebrafish Rab23 proteins. Identical amino-acids are shaded in black and similar amino-acids are shaded in grey.

3.3.14 *rab35a* morphant phenotype

Injection of 6ng of *rab35a* morpholino in 1-4 cell stage zebrafish embryos resulted in a very strong developmental phenotype (Figure 3-32). When control embryos are at 3-somite stage, *rab35a* MO injected embryos have no distinguishable somite boundary (panel B Figure 3-32). Moreover, they have a pronounced oval shape with a thicker chordamesoderm, reminiscent of dorsalised embryos (Mullins et al., 1996) (panel D Figure 3-32). *rab35a* morphants form somites but these are always abnormal in shape (panels F, H Figure 3-32).

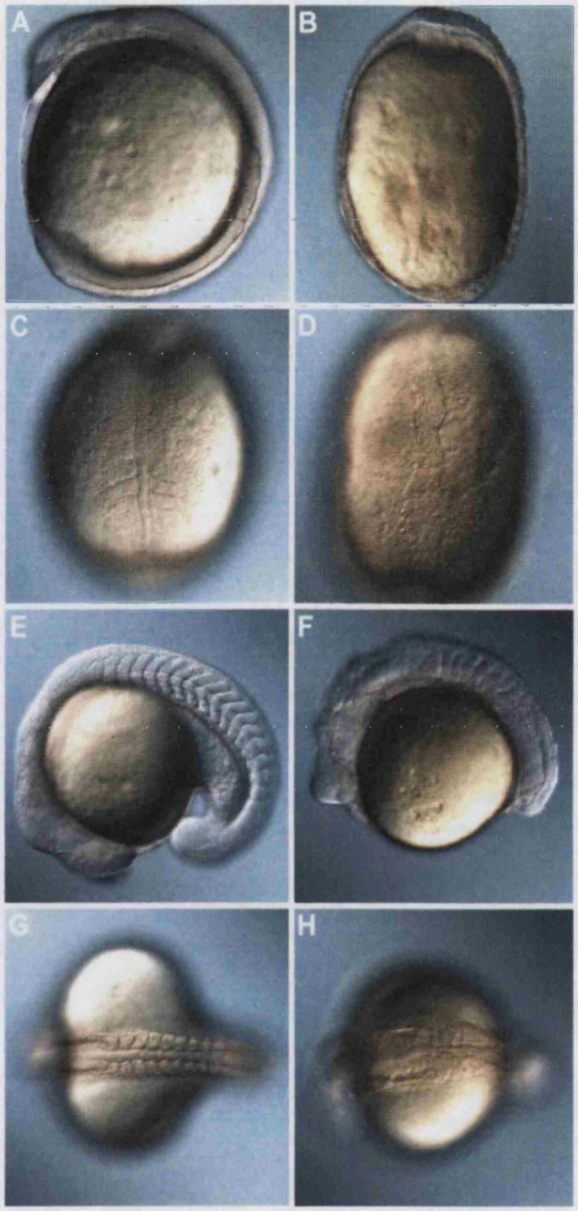

Figure 3-32 Phenotype of the rab35a morphant. (A, C, E, G) embryo injected with 5ng of control MO at 3-somites (A, C) and 18-somites (E, G) stages. (B, D, F, H) embryo injected with 6ng of rab35a morpholino photographed at the same time as the corresponding control. When control embryos are at 3-somite stage, experimental morphants have no distinguishable somite boundaries formed (B). At this stage, rab35a morphants have a very pronounced oval shape with no other recognizable structure apart from a thicker chordamesoderm (D). At later stages, rab35a morphants form very abnormal somites and have a shorter body axis (F, H). (A, B) side views, dorsal to the right; (C, D) dorsal views animal up; (E, F) side views anterior to the left; and (G, H) dorsal views anterior to the left.

3.4 Discussion

The first Rab protein was identified almost two decades ago and there is now a considerable body of evidence linking the function of different Rabs with all steps of vesicular transport. Some Rabs have been shown to interact with vesicle cargo indicating that they may be involved in vesicle formation (Carroll et al., 2001). Several Rabs were shown to interact with protein motors or the microtubule and actin cytoskeleton, thus indicating a role in vesicle motility (Bielli et al., 2001; Echard et al., 1998; Koda et al., 1999; Lapierre et al., 2001). In addition, a large quantity of Rab effectors are tethering factors, that is, proteins that form extended structures to bridge adjacent membranes, implicating Rab function in vesicle docking (Allan et al., 2000; Christoforidis et al., 1999a). Finally, there is same evidence that Rab proteins are also involved in membrane fusion, specifically through interactions with the SNARE complex (Coppola et al., 2002; McBride et al., 1999).

Rab5, probably due to the fact that is one of the most well studied Rab proteins, is known to interact with effectors that are involved in several vesicular transport steps. On the other hand, there are 11 members of the Rab family in *S. cerevisiae* and 60 in humans (Bock et al., 2001; Pereira-Leal and Seabra, 2001). If one single Rab protein seems to be able to do a multitude of different tasks, why would their number be so widely expanded through evolution from the unicellular eukaryote to humans? Undoubtedly, part of the explanation for this question has to lie in an increase of specificity of higher organisms' Rab proteins, as a response to specialised cell function or distinct developmental requirements. As an example, mouse Rab23 has been implicated in negatively regulating Shh signalling during embryonic development (Eggenschwiler et al., 2001).

The reason I chose to study Rab protein function was two-fold. Firstly, previous work in the Stemple lab identified an important specific role for the coatomer complex in notochord development. The coatomer complex is involved in transport of protein machinery from the Golgi to the Endoplasmic Reticulum (ER). Although this work established a role for vesicular trafficking in notochord development, the coatomer complex is a general factor and is essential for all eukaryotic cells. By contrast, Rab proteins are candidate mediators of specific membrane trafficking events and it is conceivable that a specific Rab or Rabs are dedicated to vesicular trafficking during notochord development. My second reason for studying Rabs stems from the Eggenschwiler et al. study that established mouse Rab23 as a negative regulator of Shh signalling (Eggenschwiler et al., 2001). Shh is a morphogen important for several developmental processes, but in the midline is produced by notochord and floor plate

where it acts to pattern the neural tube and somites. Neural tube patterning and the pathway's transcription factors (Gli proteins) function during zebrafish development was part of the work developed during my research.

3.4.1 Zebrafish *rab* genes

As a first step, I identified zebrafish Rab genes homologous to mouse and/or human Rabs. As previously mentioned, the Rab family in humans is thought to consist of 60 members. As of May 2003 I identified 63 zebrafish *rab* genes. I was expecting to find more *rab* genes in zebrafish than there were in humans, since the teleost genome has apparently undergone partial or complete genome duplication. It should be said that 63 is far from being the final number of zebrafish *rab* genes judging from the fact that for fourteen human *RAB* genes the zebrafish counterpart has not yet been identified (*RABs 2b, 3d, 4b, 6c, 8a, 9b, 17, 22c, 24, 29, 39a, 40a, 40b* and *41*). For eleven human *RAB* genes two different homologous zebrafish genes were identified (*RABs 1a, 2a, 3c, 5a, 6a, 6b, 7, 11a, 11b, 19* and *32*). Finally, for the human gene *RAB14*, I found four zebrafish sequences differing among themselves but equally related to *RAB14*, and for *RAB35* and *RAB39b*, three zebrafish counterparts were found for each (see Appendix).

3.4.2 Some *rab* genes have shared expression patterns

It had been previously reported that some Rab proteins were specifically expressed in certain cell types or tissues, or had a developmentally regulated pattern of expression (Murphy and Zerial, 1995). Specifically, Rab3a is expressed in neurons and exocrine cells, Rab3d in adipocytes, Rab15 and 23 are predominantly expressed in the brain, Rab17 in epithelial cells, Rab20 in the midgut, Rab18 in the developing kidney (Murphy and Zerial, 1995), Rab27 in melanosomes and T-cells (Stinchcombe et al., 2001; Wilson et al., 2000) and multiple *RAB* transcripts (*RAB1A, RAB4A, RAB5B, RAB7, RAB8, RAB10, RAB12A, RAB13, RAB18, RAB21* and *RAB22*) were found to be expressed in human skeletal muscle (Bao et al., 1998).

At the intracellular level, the localization of these proteins has been mostly investigated in cultured cells where they have been found associated with different cellular compartments of the exocytic and endocytic pathways. For example, Rab18 and Rab20 although present in both non-polarized and polarized cells, are highly localized in the apical side of kidney epithelial cells (Lutcke et al., 1994) and Rab13 is localized

to tight junctions of epithelial mouse cells (Sheth et al., 2000). For reviews on Rab intracellular localization see (Seabra et al., 2002; Zerial and McBride, 2001).

In this study, the mRNA *in situ* localization of 20 zebrafish *rabs* was assessed at different stages of embryonic development. All 20 seemed to be expressed during embryonic development and for 6 of these there is clear up-regulation of the expression in some parts of the embryo and at certain stages.

3.4.2.1 Zebrafish *rabs* expressed in chordamesoderm

Three zebrafish *rab* genes are clearly up-regulated in the chordamesoderm tissue, *rab1b*, *rab2a2* and *rab18* (see Figure 3-1, Figure 3-2 and Figure 3-6). In human cells, RAB1B and RAB2A localize to the ER-Golgi intermediate compartment (Seabra et al., 2002). It is thought that RAB1B is involved in ER to Golgi and intra-Golgi transport whereas RAB2A is thought to be involved in Golgi to ER retrograde transport (Seabra et al., 2002).

The chordamesoderm differentiates from the posterior axial mesendoderm and is fated to become notochord. The notochord is common to members of the phylum Chordata and is a rod-like structure that serves as a major skeletal element of the embryo and as a source of signals required to pattern the surrounding tissues. It is formed of only one cell-type containing a large central vacuole and surrounded by a peri-notochordal basement membrane (BM) that serves to restrain the swelling cells. Notochord cells must have high protein trafficking activity since they have both to inflate a large vacuole and to secrete components of the BM that surround the notochord. Furthermore, the gene shown to be disrupted in zebrafish *sneezy* mutants is *coatomer subunit α (copa)*. This gene codes for a subunit of the coatomer complex that, together with the small GTPase ARF1, constitutes the protein coat of COPI vesicles, an essential component of the early secretory pathway (Coutinho, 2001). It is therefore not surprising to find *rab* transcripts up-regulated in chordamesodermal cells, since these proteins seem to be key components of the trafficking machinery.

Another site of up-regulation of *rab1b* expression in a 5-somite stage embryo is the polster (panel C, Figure 3-1). This structure is also a derivative of axial mesendoderm and gives rise to the hatching gland. Hatching gland cells have secretory activity involving high levels of protein trafficking and it is tempting to hypothesise Rab1b to play a role in this process.

In a 24hpf embryo *rab1b* is expressed in putative neural crest and blood cells (panels D-H, Figure 3-1). The expression in neural crest cells matches the phenotype of *rab1b* morphant fish (Figure 3-8). These morphants have an obvious phenotype in the melanophores, which are neural-crest derived cells. In a superficial observation, it seems that the number of melanophores in *rab1b* morphants is reduced. However, expression of *dct,* an enzyme involved in melanin synthesis and a good marker of melanoblasts, reveals no apparent difference in the number of these melanophores precursors (Figure 3-9). Moreover, a TUNEL assay did not reveal a significant increase in cell death in *rab1b* morphants that could account for the apparent smaller numbers of melanophores (Figure 3-10).

A plausible explanation for the *rab1b* melanophore phenotype could have to do with a change in melanophore morphology rather than a change in its numbers. On closer inspection, it seems that either the shape of the melanophores or the distribution of melanin within them is disrupted. It could be that Rab1b plays a role in ensuring the even spreading of the melanin containing organelles, the melanosomes, and that in its absence, melanosomes would be localized to the same cellular location. Such a role in melanosome transport was uncovered for the mouse protein Rab27a (Fukuda et al., 2002; Wu et al., 2002). This protein is present at the surface of melanosomes and is responsible for holding these organelles onto actin bundles at the dendritic tips of melanocytes, by specifically binding melanophilin that in turn binds myosin Va (Fukuda et al., 2002; Wu et al., 2002). It could be that Rab1b has in the zebrafish an equivalent function to mouse Rab27a, namely establishing a connection between the melanosomes and actin. To achieve uniform distribution of pigment granules in fish melanophores an actin-based motility system has to be in place (Rodionov et al., 1998). In fish melanophores treated with latrunculin A, an inhibitor of actin polymerization, melanin granules show virtually no motion and when stimulated to disperse, through addition of caffeine, the granules move towards the cell periphery but are never found evenly dispersed (Rodionov et al., 1998). To test this hypothesis, it would be important to first know whether the cell shape of *rab1b* morphant melanophores is equivalent to control melanophores and if so, what would happen when morphant melanophores were exposed to a pigment granule dispersing agent such as caffeine.

Apart from expression in chordamesodermal cells, *rab2a2* has other sites of up-regulation in the zebrafish embryo (Figure 3-2). In particular, in 18-somite stage embryos there is a clear bilateral patch of cells expressing *rab2a2* at high levels at the

level of the hindbrain (panels E, F, Figure 3-2), which probably correspond to cranial ganglia. After performing this *in situ* hybridisation assay, I found that in the "Zebrafish Information Network" (ZFin, http://zfin.org/cgi-bin/webdriver?MIval=aa-ZDB_home.apg) there is an entry for a zebrafish *rab2* (clone cb75) gene with information on its expression pattern. I confirmed that this sequence corresponds to what I call on this thesis *rab2a2*. This probe was probably of better quality and apart from expression in the chordamesoderm it clearly reveals expression in the polster, cranial ganglia and different regions of the brain.

The phenotype of *rab2a2* morphant was very superficially analysed, but two of the obvious defects in these morphants are a reduced brain, especially in the midbrain region, and a short embryonic axis (Figure 3-11 and Figure 3-12). Both these phenotypes correlate well with *rab2a2* sites of higher expression, namely the brain and chordamesoderm.

Another chordamesoderm Rab, *rab18* is also expressed at higher levels in the polster and in two bilateral patches of cells at the level of the hindbrain of a 5-somite stage embryo (see Figure 3-6). It is not clear what these cells correspond to but judging from their position they could be otic placode. In a 24hpf embryo the otic vesicles have slightly higher expression but more posteriorly there are cells on either side of the beginning of the spinal cord expressing the gene at high levels. These cells are roughly positioned around the 3rd somite and could correspond to the migrating posterior lateral line primordium (24hpf stage corresponds approximately to the prim-3 stage, i.e., the stage at which the migrating posterior line primordium is positioned at the level of the 3rd somite). It would be interesting to knock down Rab18 protein through morpholino injection and analyse the resulting phenotype, particularly the development of the posterior lateral line primordium.

While I did not examine the localization of the *rab13* transcript, it has been published on ZFin (clone cb764). These data indicate that *rab13* is expressed in the chordamesoderm and later in the notochord. Moreover, there is expression in axial vasculature, at basal levels in the brain and in the pectoral fin of a 48hpf embryo. At the intracellular level, Rab13 has been shown to localize to tight junctions in a variety of epithelial cells (Sheth et al., 2000; Zahraoui et al., 1994). Additionally, over-expression of a constitutively active form of Rab13 disrupts tight junction function and structure (Marzesco et al., 2002). The phenotype I observe upon injection of *rab13* morpholino is in accordance with the protein localization in epithelial cells. In particular, the

epidermis of the morphant embryos appears loose and blisters are observed (see Figure 3-24). None of the sites of high transcript expression seem to be affected in the morphant fish, which could be indicative of partial redundancy from other Rab proteins.

3.4.2.2 zebrafish *rabs* expressed in differentiated neurons

In 24hpf zebrafish embryos *rab3c1* and *rab5a1* have an almost identical expression pattern that appears to be restricted to differentiated neurons in the brain, spinal cord and ganglia (Figure 3-3 and Figure 3-4). In mammalian cells both proteins were shown to be localized to synaptic vesicles in neurons (Seabra et al., 2002). The localization of these proteins is probably conserved in zebrafish embryos judging from the fact that the transcripts are present in differentiated neurons, where synaptic activity is expected to occur.

The fact that both transcripts have such a similar pattern of expression raises the hypothesis of functional redundancy between Rab3c1 and Rab5a1 proteins. This hypothesis is further reinforced judging from the fact that injection of neither morpholino oligonucleotide results in an observable phenotype. Co-injection of both morpholinos and inspection of synaptic activity is an obvious experiment to do to understand the function of these proteins in zebrafish neuronal development.

3.4.3 Unrelated zebrafish *rabs* at the sequence level share loss of function phenotypes

Injection of morpholinos targeting Rab1a1, Rab7b, Rab9a, Rab14a and Rab15 resulted in embryos developing with shared phenotypic defects (see Figure 3-7, Figure 3-22, Figure 3-23, Figure 3-24, Figure 3-26, Figure 3-28), despite the fact they share less than 40% identity at the sequence level. All these morphants have defects in the brain where cells appear to be dying. More posteriorly, the somites are abnormally shaped and the yolk extension is very thin. Injection of *rab9a* morpholino resulted in the strongest phenotype and, apart from the mentioned defects, the embryos have a very rough epidermis and completely lack pigmented cells (see Figure 3-23).

Somite defects and a thinner yolk extension may be related to a circulation defect. The formation of inter-somitic vessels was assayed in *rab14a* morphant embryos. Although having intermediate cell mass *fli1* expression, vessels between the somites in the trunk and tail fail to form (see Figure 3-27). The expression pattern of *rab14a* (cb731) is published on ZFin. According to this information, *rab14a* is expressed in the chordamesoderm and in various structures of neuronal origin, such as the trigeminal

placode and ganglia, various regions in the brain and a sub-set of spinal cord neurons. Phenotypes in these specific regions should be analysed in greater depth.

3.4.4 Related zebrafish *rabs* at the sequence level have different loss of function phenotypes

There is a zebrafish gene that I named *rab3c2*, which is 60% identical to *rab3c1* and 74% identical to *RAB3C*. Similarly, there is a second zebrafish *rab5a*, *rab5a2*, 93.5% identical to *rab5a1* and 91% identical to *RAB5A* (see Figure 3-33 and Figure 3-34).

Figure 3-33 ClustalW protein alignment between the human RAB3C and two zebrafish Rab3c proteins. Identical amino-acids are shaded in black and similar amino-acids are shaded in grey.

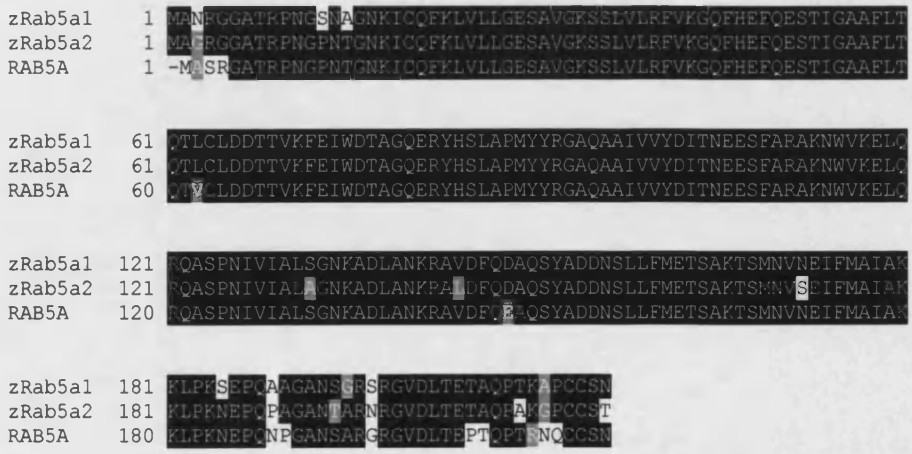

Figure 3-34 ClustalW protein alignment between the human RAB5A and two zebrafish Rab5a proteins. Identical amino-acids are shaded in black and similar amino-acids are shaded in grey.

Although both Rab3c's and Rab5a's appear very similar at the sequence level, they probably have quite different developmental roles in the embryo. Whereas the *rab3c1* morphant has no obvious developmental defects, *rab3c2* morphant embryos have a very severe phenotype (see Figure 3-13), showing, in particular, a poorly developed notochord and u-shape somites. Likewise, *rab5a2* morphants have a very strong phenotype and never develop beyond gastrulation stages (see Figure 3-14), contrasting to the lack of obvious phenotype resulting from injection of *rab5a1* morpholino.

It is remarkable that Rab5a1 and Rab5a2 that share 93.5% identity at the sequence level, have such divergent developmental roles. An obvious concern when analysing these results is whether the morpholinos designed to knock-down these proteins functions were specific. However, inspection of the 5' targets of morpholino oligonucleotides does not reveal any significant sequence homology (see Figure 3-35).

>rab5a1

TCAGCCAGTACTGGGACAGCTCTCGGCGTGTGTGTGAGCACTCAAGAAGACGGGGTGATTGAC

AACTGTC**ATG**GCCAATAGGGGAGGAGCAACACGCCCCAACGGGTCCAACGCGGGCAATAAGA

TCTGCCAGTTTAAACTGGTCTTGCTAGGAGAGTCAGCGGTGGGGAAGTCCAGCCTCGTTCT

>rab5a2

CGAACGCAAAAGGGGAAGTTGGGAGGAACCTAGAGGAAGATCTGGTAGTGACCGTCTTGACTT

CAGTACAGGAGATTGGGGTTTTGGGTC**ATG**GCAGGAAGAGGTGGAGCAACGAGACCTAACGG

GCCGAACACCGGCAACAAAATCTGTCAGTTCAAATTAGTGCTGCTGGGAGAGTCTGCTGTG

Figure 3-35 The 5'region of rab5a1 and rab5a2. The region where morpholino oligonucleotides were designed does not appear to have significant homology. Starting codon is in bold and in a bigger font size. Region of morpholino oligonucleotide hybridization is shaded in red.

Rab5 proteins are probably the most well studied Rab proteins and appear to play an important role in the early endocytic pathway (Zerial and McBride, 2001). In particular, they regulate clathrin-coated endocytosis and early endosome fusion (Bucci et al., 1992; Stenmark et al., 1994). Judging from the fact that injecting a small amount of *rab5a2* morpholino results in a severe developmental phenotype, evident from early epiboly stages, I hypothesise that Rab5a2 must play an important role in a basic cellular function, such as endocytosis.

Epiboly corresponds to the enveloping of the yolk cell by the blastoderm and is the first zebrafish morphogenetic movement. It can be considered as the first real morphological challenge to the forming embryo and it will inevitably go wrong if some fundamental protein, with insufficient maternal stores, fails to be synthesised. In the Tübingen large scale mutagenesis screen some epiboly mutants were isolated. However, Rab5a2 is unlikely to be any of these since it shows an epiboly delay but not a complete arrest as seen in the mutants (Kane et al., 1996). In addition, in all epiboly mutants there is an arrest in the epiboly movement of the deep cells of the blastoderm but not the yolk syncytial layer or enveloping layer (Kane et al., 1996). In contrast, *rab5a2* morphants have the movement of all tissues strongly delayed in an almost synchronous manner (see Figure 3-17).

To check whether the endocytic profile of *rab5a2* morphant cells was altered, EM was performed (see Figure 3-18). In BHK cells, over-expression of a Rab5a mutant form incapable of binding GTP leads to the accumulation of a large number of very small vesicles at the cell periphery, whereas over-expression of a constitutively active form results in unusually large early endocytic structures (Bucci et al., 1992; Stenmark et al., 1994). Electron microscopy revealed *rab5a2* morphant cells surprisingly comparable to cells over-expressing the constitutively active mammalian counterpart and not the dominant negative form (see Figure 3-18). In fact, *rab5a2* morphant cells accumulate huge smooth membrane profiles that in many cases have an irregular shape, which would be expected from dynamic structures (see Figure 3-18). Another feature of *rab5a2* morphants is an increase number of large secondary lysosomes containing membranous contents (see Figure 3-18).

Two additional zebrafish Rab5s sharing more than 80% identity were identified in this study. Unlike *rab5a2* morphant embryos, both *rab5b* and *rab5c* morphants survive beyond epiboly stages (see Figure 3-19, Figure 3-20 and Figure 3-21). In both cases, the embryos have a shortened axis and u-shape somites, in addition to brain abnormalities. The first two defects are linked as when the notochord fails to

differentiate, the somites are u-shaped and the embryonic axis does not extend. In the case of *rab5c* morphants, the brain phenotype requires a more detailed analysis, in particular in the hindbrain region, as there are higher levels of expression of the transcript in a rhombomere at the 5-somite stage (see Figure 3-5).

The *rab23* morphant phenotype is very severe, even at very low doses of morpholino oligonucleotide (see Figure 3-29). There is a mouse mutant for this gene, *open brain*, which has a constitutive Shh signalling phenotype (Eggenschwiler and Anderson, 2000; Eggenschwiler et al., 2001; Gunther et al., 1994). On the basis of this phenotype and the fact that the Rab23 mutation suppresses the Shh phenotype, mouse Rab23 was postulated to be a negative regulator of Shh signalling (Eggenschwiler et al., 2001). I analysed several Shh downstream targets in *rab23* morphant fish and the results were very different from what would be expected if Rab23 were a negative regulator of Shh signalling in the zebrafish (see Figure 3-30). Instead of up-regulation of genes such as *nkx2.2*, *nkx6.1*, or *nkx6.2*, as seen in embryos over-expressing Shh, these transcripts were either absent (*nkx2.2*) or down-regulated (*nkx6.1* and *nkx6.2*, see Figure 3-30). The Rab23 protein is 83% identical to both the human and mouse versions and would be expected to be the closest homologue. However, as mentioned above, Rab5a proteins that are 93.5% identical appear to have distinct functions in zebrafish development. On the other hand, Rab3c1 and Rab5a1 which only share 31% identity have almost identical expression patterns and similar embryonic functions. These observations lead to the idea that functional Rab homologues across species do not necessarily have to be the obvious homologue at sequence level. It is conceivable that small differences/similarities in few residues will suffice to enable or prevent the interaction of the Rab protein with a specific effector.

The last morphant phenotype shown in the result section of this chapter refers to Rab35a loss of function. This phenotype is very similar to the one observed for Rab23 loss of function (see Figure 3-32). The embryos are oval shaped and have a wide chordamesoderm at early segmentation stages and somites form in a very abnormal fashion. Interestingly, out of the 63 *rab* genes identified in this study Rab35a is mostly identical to Rab23 at the sequence level, sharing 32.4% identity.

Table 3-1 sums up expression patterns and loss of function phenotypes observed in this study.

Rab protein	mRNA expression pattern	M O phenotype
Rab1b	Chordamesoderm; polster; neural crest; blood	Abnormal melanophores
Rab2a2	Chordamesoderm; polster; cranial ganglia; brain*	Small brain; short embryonic axis
Rab18	Chordamesoderm; polster; otic placode (?); lateral line primordium (?)	-
Rab13	Chordamesoderm and notochord; axial vasculature; brain; pectoral fin*	Loose epidermis; blisters
Rab14a	Chordamesoderm; trigeminal placode and ganglia; brain; spinal cord neurons*	Brains defects and cell death; abnormal somites; thin yolk extension; lack of inter-somitic vessels
Rab1a1	Ubiquitous	Brain defects and cell death; short embryonic axis; abnormal somites; small otic vesicles; do not hatch
Rab7b	Ubiquitous	Brain defects and cell death; abnormal somites; thin yolk extension
Rab15	-	Brain defects and cell death; abnormal somites; thin yolk extension
Rab9a	-	Brain defects and cell death; abnormal somites; thin yolk extension; rough epidermis; lack of pigmentation

* Published in ZFin (http://zfin.org/cgi-bin/webdriver?MIval=aa-ZDB_home.apg)

Rab protein	mRNA expression pattern	M O phenotype
Rab3c2	Ubiquitous	Undifferentiated notochord; u-shaped somites
Rab5b	Ubiquitous	Undifferentiated notochord; short embryonic axis; u-shaped somites; brain abnormalities
Rab5c	Maternal; up-regulated in a rhombomere at 5-somite stage; ventral region at 24 hpf	Undifferentiated notochord; short embryonic axis; u-shaped somites; brain abnormalities
Rab3c1	Differentiated neurons	No phenotype observed
Rab5a1	Differentiated neurons	No phenotype observed
Rab5a2	-	Developmental arrest at epiboly; cells with big smooth membrane profiles and large secondary lysosomes
Rab23	Ubiquitous	(very severe) Oval shape at beginning of segmentation; wide chordamesoderm; abnormal somites
Rab35a	-	(very severe) Oval shape at beginning of segmentation; wide chordamesoderm; abnormal somites

Table 3-1 Summary table of mRNA expression patterns and loss of function phenotypes of some zebrafish Rabs identified in this thesis.

Loss of function of six zebrafish Rabs did not result in any obvious developmental defect (Rab3c1, Rab5a1, Rab10, Rab27a, Rab32a and Rab34). Rab3c1 and Rab5a1 might play redundant roles in zebrafish development, judging from the fact that they have overlapping mRNA expression patterns and co-injection of both morpholinos should be performed. Rab10 might also be redundant to other Rabs and interestingly, it shares over 46% identity with nine other Rab proteins identified in this study (46% with Rab12, 48% with Rab2a2, 15 and 35a, 48% with Rab1a1, 1a2 and 1b, 50% with Rab35b and 60% with Rab13). As for the remaining proteins whose loss of function did not result in an embryonic phenotype, Rab32a and Rab35b, a possible explanation, apart from the redundancy concern, could be their absence during embryonic development. Indeed, the sequence for both genes is found in the database as ESTs derived from adult cDNA libraries and their embryonic expression should be assessed.

Several Rab proteins have been shown to be involved in different stages of intracellular vesicular transport. As such, some would predict that depleting a forming embryo of such proteins could lead to a very strong phenotype due to disruption of a basic cellular function. On the other hand, Rab proteins are part of a large protein family and could therefore be functionally redundant, thus masking individual loss-of-function phenotypes. Both these predictions seem to be incorrect to a certain extent. In fact, I injected 20 morpholinos targeting 20 different zebrafish Rab proteins and 14 of those lead to a clear developmental phenotype, some with defects in very specific processes.

Role of Gli3 in zebrafish development

4 Role of Gli3 in zebrafish development

In this chapter I describe the cloning of *gli3* and study its role in zebrafish development. As Gli3 in other species is known to have a role in ventral spinal cord patterning, this chapter begins with the identification of zebrafish spinal cord markers. Analysis of *gli3* morphants, however, shows that spinal cord patterning is not grossly disrupted. Unexpectedly, loss of Gli3 function in zebrafish results in a strong early developmental phenotype, which I describe here.

4.1 Zebrafish spinal cord

4.1.1 Morphology of the zebrafish spinal cord

The spinal cord of a 1-day-old zebrafish embryo consists of neuroepithelium cells, floor plate cells and approximately 18 neurons per hemisegment (i.e., each side of a spinal cord portion a somite width) (Bernhardt et al., 1990).

The floor plate is located in the ventral midline of the cord. It is approximately three cells wide and extends along the entire length of the spinal cord. The cells that form the floor plate are not thought to be neuronal, thus extend no processes, and differ from the other neuroepithelial cells in shape (Kuwada and Bernhardt, 1990).

Immediately dorsal to the floor plate motor neurons are positioned. Each hemisegment contains three primary and a larger number (up to 20) of secondary motor neurons (Kuwada and Bernhardt, 1990). Primary motor neurons have much larger cell bodies than secondary and they have been named according to the specific location of their cell bodies in the spinal cord: caudal primary (CaP), middle primary (MiP) and rostral primary (RoP) (Eisen et al., 1986). In addition, about half of the spinal hemisegments contain a fourth primary motor neuron, VaP, that later dies (Eisen, 1992). In contrast, CaPs, MiPs and RoPs, persist through adulthood, innervate fast muscles, and are involved in the startle response and fast swimming (Lewis and Eisen, 2003).

The most dorsal neurons in the spinal cord are the mechano-sensory Rohon-Beard (RB) neurons. In a 24hpf zebrafish spinal cord there are 2-3 RB neurons per hemisegment characterized by their large somata and ascending and descending ipsilateral, longitudinal axons (Bernhardt et al., 1990). The ascending axon can be more than 20 somites long and terminates in the hindbrain (Bernhardt et al., 1990).

Between the ventrally located motor neurons and the dorsal RB neurons lie the embryonic interneurons. Seven different classes of interneurons have been identified and named according to morphological characteristics, such as the position of their cell bodies and direction of projected axons (Bernhardt et al., 1990).

Longitudinal interneurons have axons that run longitudinally from their cell bodies. Immediately ventral to RB cells lies the dorsal longitudinal ascending interneuron (DoLA). There are relatively few DoLA neurons in the embryo, with many segments containing none, and they probably all die before larval stages (Kuwada et al., 1990). Slightly dorsal to motor neurons, lie the ventral longitudinal descending interneurons (VeLD). There are 1-2 VeLD interneurons per hemisegment and they have a tendency to be positioned halfway between consecutive CaP motor neurons (Bernhardt et al., 1990).

Commissural interneurons have axons that run ventrally before crossing the midline to run longitudinally on the contra-lateral side. Commissural interneurons can be further subdivided into primary or secondary interneurons. There is no more than one commissural primary ascending interneuron (CoPA) per spinal hemisegment. CoPA neurons are the largest interneurons and are located in the dorsal half of the cord, ventral to RB and DoLA neurons (Bernhardt et al., 1990). Commissural secondary ascending interneurons (CoSA) occupy positions just ventral to the level of CoPA cells. They are smaller and more numerous (up to five per somite) than CoPA (Bernhardt et al., 1990). There is a third type of commissural interneuron (CoB) that forms slightly later, is positioned dorso-laterally and has an axon that crosses the ventral midline and bifurcates to send ascending and descending axons (Bernhardt et al., 1990).

Finally, circumferential interneurons have axons that run ventrally but turn longitudinally, ipsilaterally to their cell bodies. Circumferential descending interneurons (CiD) are situated just ventral to CoSA cells and there are up to three per spinal hemisegment (Bernhardt et al., 1990). Circumferential ascending interneurons (CiA) have a circumferential axon that runs ipsilaterally but ends up joining the dorsal lateral fasciculus (DLF) after running ventrally first (Bernhardt et al., 1990).

In Figure 4-1 a schematic of the zebrafish developing spinal cord and relative position of cord neurons is represented.

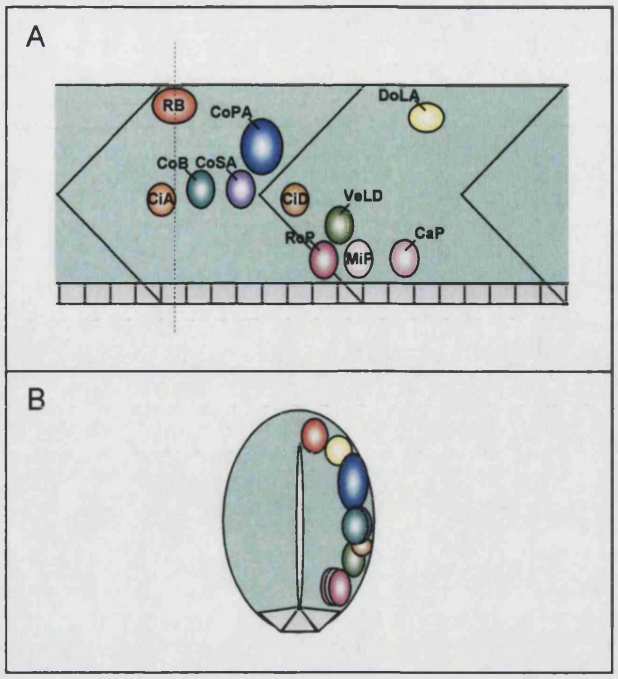

Figure 4-1 A schematic summarizing neuronal classes in the spinal cord of developing zebrafish. (A) side view, anterior to the left. Segment borders are indicated by diagonal lines. Floor plate cells are in grey. RB – Rohon-Beard neurons; CoPA – commissural primary ascending interneuron; CoSA – commissural secondary descending interneuron; CoB – commissural bifurcating interneuron; DoLA – dorsal longitudinal ascending interneuron; VeLD – ventral longitudinal descending neuron; CiA – circumferential ascending interneuron; CiD – circumferential descending interneuron; RoP – rostral primary motor neuron; MiP – middle primary motor neuron; CaP – caudal primary motor neuron. Secondary motor neurons aren't represented. (B) anterior view of a cross section of (A) at the level of the dashed line. Adapted from (Bernhardt et al., 1990).

Panel B in Figure 4-1 represents a virtual stack of sections through the whole trunk region represented in panel A of the same picture. To know how many cells can be found in one single focal plane of a zebrafish spinal cord transverse section, I performed whole-mount antibody staining with anti β-catenin antibody that marks cell membranes (see Figure 4-2).

Through analysis of pictures representing one single focal plane I confirmed that the spinal cord of a 24hpf zebrafish embryo has three cells at the ventral most tip that constitute the embryo floor plate. The middle cell has a triangular shape and is surrounded by two more cells that are lateral floor plate. At the most dorsal region of the neural tube there is another triangular shaped cell. The structure formed by these cells across the anterior/posterior axis of the embryo is the roof plate. Across the ventral/dorsal axis of the neural tube and excluding both floor plate and roof plate cells,

there are approximately 10-15 cells in a 24hpf embryo. From the neural tube lumen to either axial side of the tube there are approximately 3 cells, as seen in the cross sections of the whole mount anti β-catenin stained embryos depicted in Figure 4-2.

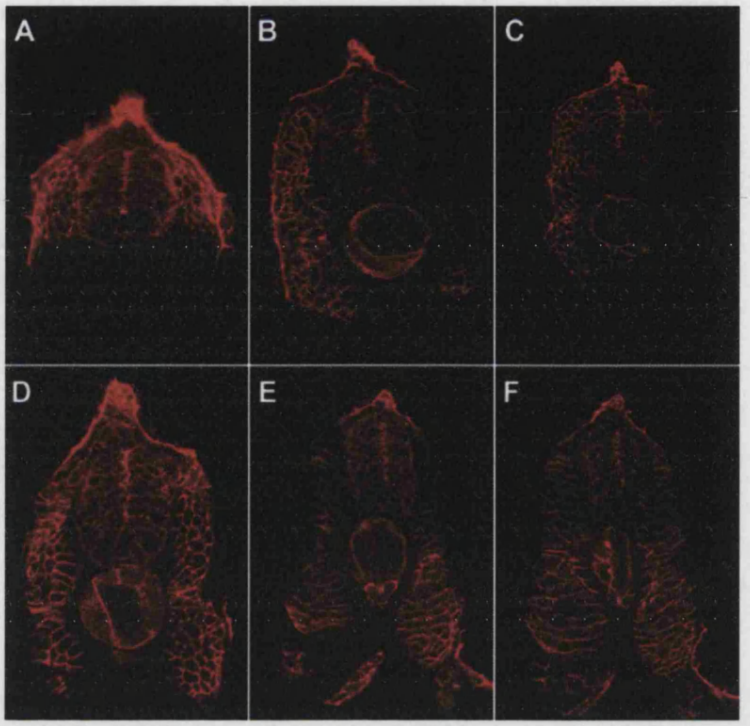

Figure 4-2 Cross sections of the trunk region of 24hpf embryos stained with anti β-catenin antibody. At this stage, the neural tube of a zebrafish embryo has three floor plate cells in the ventral extremity, a roof plate cell in the dorsal extremity, 10-15 cells across the ventral/dorsal axis (excluding floor and roof plates) and approximately three cells on either side of the lumen.

4.1.2 Cloning zebrafish genes expressed in the spinal cord

To know if zebrafish spinal cord development happens as in the chick and mouse I looked at the spinal cord expression pattern of several genes. Most spinal cord markers analysed had previously been cloned by other groups or EST clones were available and ordered (see 'Materials and Methods'). However, zebrafish *nkx6.1* and *nkx6.2* sequences weren't present in available databases and had to be cloned.

4.1.2.1 Cloning *nkx6.1* and *nkx6.2*

By BLASTing the mouse and/or human sequences for *nkx6.1* and *nkx6.2* against the zebrafish genomic database, trace files containing putative fragments of the fish homologues were identified. The sequence contained in the trace files was used to

design primers to perform 5' and 3' RACE nested reactions (see 'Materials and Methods'). In Figure 4-3 an alignment of the predicted zebrafish Nkx6.1 protein and the mouse and human homologues is depicted. In Figure 4-4 an alignment of the predicted zebrafish Nkx6.2 protein and mouse and human homologues is depicted.

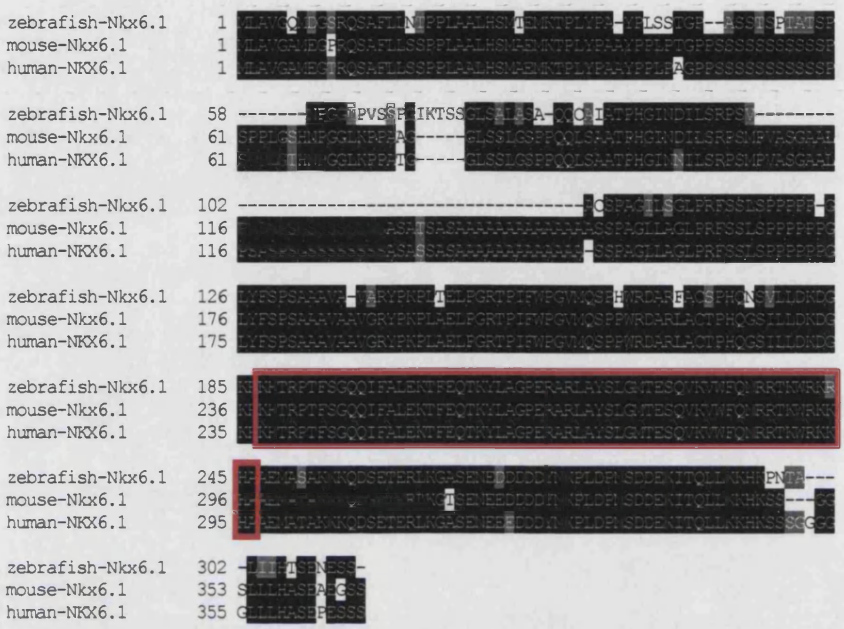

Figure 4-3 Protein alignment between the predicted zebrafish, mouse and human Nkx6.1 proteins. Identical amino acids are shaded in black and similar amino acids are shaded in grey. The homeodomain is boxed in red.

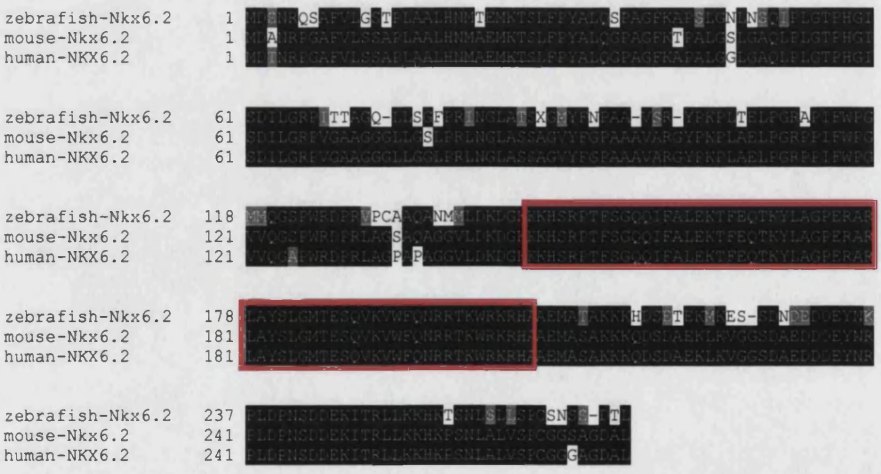

Figure 4-4 Protein alignment between the predicted zebrafish, mouse and human Nkx6.2 proteins. Identical amino acids are shaded in black and similar amino acids are shaded in grey. The homeodomain is boxed in red.

4.1.3 Expression pattern of zebrafish spinal cord markers

To identify markers of different regions of the zebrafish developing spinal cord, I performed *in situ* hybridisations of candidate genes in 24hpf embryos. I examined expression patterns of these genes in sections made at different anterior/posterior levels of the developing spinal cord.

4.1.3.1 Markers of the zebrafish ventral neural tube

Across vertebrate species, Shh is expressed in the notochord and the floor plate of developing embryos. In 24 hpf zebrafish embryos, the notochord expression of *shh* is down-regulated but it remains in the medial floor plate (Krauss et al., 1993; Strähle et al., 1993) (Figure 4-5, panels A-C). The gene *hnf3β* is another vertebrate floor plate marker, and in zebrafish is expressed by both medial and lateral floor plate (Schauerte et al., 1998; Strähle et al., 1996) (Figure 4-5, panels D-F). The Nkx proteins, Nkx2.2, Nkx6.1 and Nkx6.2 are all part of the Class II homeodomain proteins directly induced by Shh. In zebrafish, the gene *nkx2.2* is expressed in neural tube cells adjacent to the floor plate (Barth and Wilson, 1995) (Figure 4-5, panels G-I) in a fashion that closely resembles what is seen in mouse or chick spinal cords. In addition, *nkx2.2* expression pattern appears to be spatially regulated by Shh (Barth and Wilson, 1995). Both *nkx6.1* and *nkx6.2* are also expressed in cells adjacent to the floor plate but in these cases the domain of expression extends more dorsally (Figure 4-5, panels J-O). The expression pattern of these two proteins differs between the mouse and chick. In both systems, Nkx6.1 is expressed in the region of the three most ventral neuronal progenitors (p3, pMN and p2), but Nkx6.2 is expressed in the immediately dorsal progenitor domain (p1) in the mouse, whereas in the chick besides the p1 region, it overlaps with the Nkx6.1 domain down to the floor plate (Briscoe et al., 2000; Vallstedt et al., 2001).

In Figure 4-5 the neural tube expression of these 5 genes is shown through sections at the level of the otic vesicle (Figure 4-5, panels A, D, G, J and M), beginning of the notochord (Figure 4-5, panels B, E, H, K and N) and trunk region of zebrafish embryos (Figure 4-5, panels C, F, I, L and O).

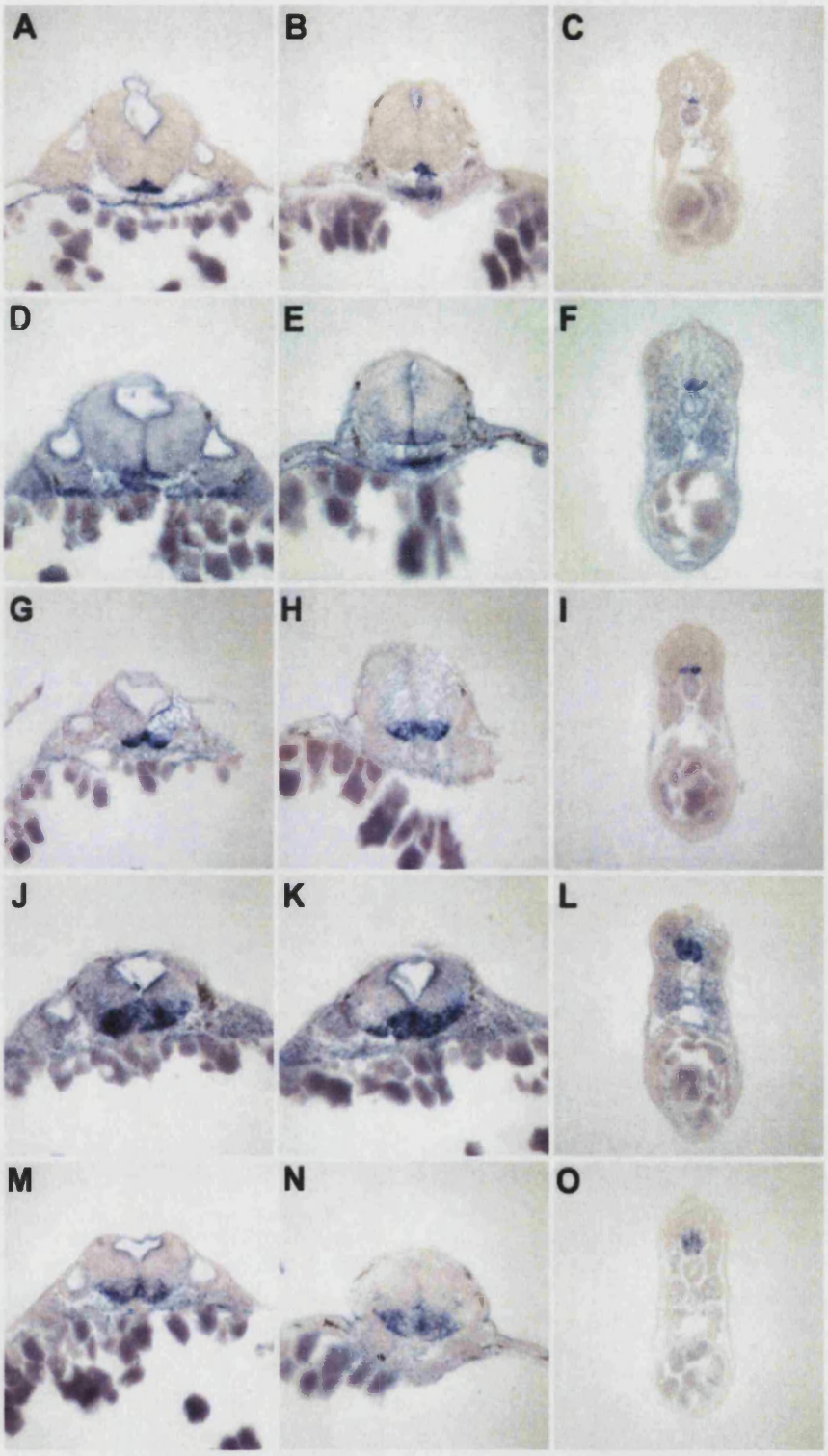

Figure 4-5 Markers of the zebrafish ventral neural tube at 24hpf. (A, D, G, J, M) are sections at the level of the otic vesicle; (B, E, H, K, N) are sections at the level of the beginning of the notochord; and (C, F, I, L, O) are sections in the trunk region, approximately at the middle of the yolk extension. (A-C) *shh* expression is seen the floor plate along the entire anterior/posterior extension of the zebrafish neural tube. (D-F) *hnf3β* expression is similar to *shh*, marking the floor plate of the embryo. (G-I) *nkx2.2* expression can be seen in ventral neural tube cells adjacent to the floor plate. (J-L) *nkx6.1* expression and (M-O) *nkx6.2* expression is very similar occupying a broader ventral neural tube territory than *nkx2.2* expressing cells.

4.1.3.2 Markers of zebrafish spinal cord neurons

In the spinal cord of a 15hpf zebrafish embryo, *pax2.1* is expressed in an average of two single cells on the lateral surface of each hemisegment (Krauss et al., 1991a). Later in development, the timing and pattern of axonal outgrowth of these neurons suggest they are the commissural secondary ascending (CoSA) interneurons (Mikkola et al., 1992) (see panel A-C, Figure 4-6).

The proteins Dbx1 and Dbx2 are expressed in an intermediate region along the rostrocaudal axis of the spinal cord of both mouse and chick (Pierani et al., 1999). The domain of expression of Dbx2 extends both more dorsally and ventrally than that of Dbx1 (Pierani et al., 1999). In zebrafish embryos, the gene *dbx1a* is expressed in a horizontal stripe located at medial regions of the neural tube along its entire length (Fjose et al., 1994) (Figure 4-6, panels D-E). This region comprises both progenitors and the corresponding differentiated neurons. In contrast to zebrafish, the expression of Dbx1 and Dbx2 in both chick and mouse is extinguished in differentiated neurons (Pierani et al., 1999). In chick and mouse spinal cords, Evx proteins are expressed in a sub-set of interneurons called v0 interneurons (Burrill et al., 1997). These neurons differentiate from a subset of progenitors that express both Dbx1 and Dbx2 (Pierani et al., 1999). In zebrafish, *evx1* is expressed in two different sub-types of interneurons in the spinal cord (Thaeron et al., 2000) (Figure 4-6, panels D-F). The most dorsal bilateral patch of *evx1*$^+$ (clearly seen in panel G, Figure 4-6) cells is probably primary interneurons (Thaeron et al., 2000). The *evx1*$^+$ interneurons located more ventrally are probably secondary interneurons since most co-express *pax2.1* (Thaeron et al., 2000). In more posterior regions of the spinal cord only one continuous row of *evx*$^+$ interneurons can be seen along the anterior/posterior axis on either side of the spinal cord (Thaeron et al., 2000) (Figure 4-6, panel I). It is possible that *evx1*$^+$ neurons are a subset of the cells that express *dbx1a*.

Newly generated v2 mouse interneurons express GATA2 (Zhou et al., 2000). In zebrafish, the gene *gata2* is expressed in unidentified individual interneurons of the spinal cord of a 24hpf zebrafish embryo that appear to be positioned dorsal to *isl1*$^+$ motor neurons (Detrich et al., 1995) (Figure 4-6, panels J-L).

In both chick and mouse, Isl1 is expressed by post-mitotic motor neurons. Cells expressing *isl1* in the zebrafish spinal cord include, dorsally, the Rohon-Beard neurons and, ventro-medially, primary motor neurons (Inoue et al., 1994; Korzh et al., 1993). There are four different types of primary motor neurons: RoPs, MiPs, and CaPs are present in each spinal hemi-segment of the embryo, and VaPs are present in about

half the hemi-segments of the embryo and die later in development (Lewis and Eisen, 2003). All these four types of primary motor neurons express *isl1* but at mid-somitogenesis stages CaPs and VaPs down regulate the expression of this gene (Appel et al., 1995; Tokumoto et al., 1995). In addition, more sparsely distributed along the anterior/posterior spinal cord, typically one or two *isl1*$^{+}$ cells per several segments are observed that may correspond to the interneuron dorsal longitudinal ascending neuron (DoLA) (Inoue et al., 1994).

The neural tube expression of *pax2.1*, *dbx1a*, *evx1*, *gata2* and *isl1* is shown through sections at the level of the otic vesicle (Figure 4-6, panels A, D, G, J and M), beginning of the notochord (Figure 4-6, panels B, E, H, K and N) and trunk region of zebrafish embryos (Figure 4-6, panels C, F, I, L and O).

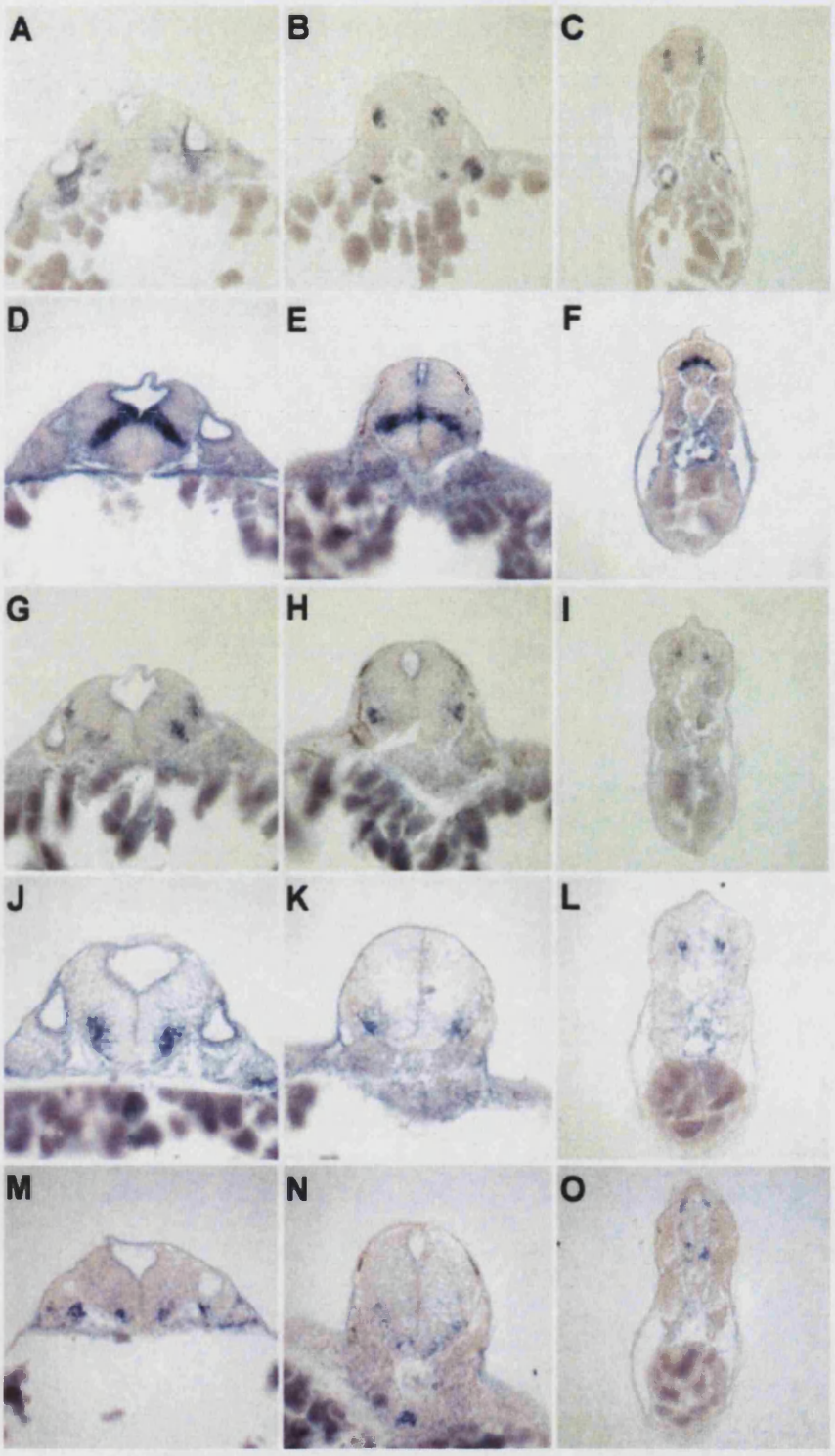

Figure 4-6 Markers of zebrafish neural tube neurons at 24hpf. (A, D, G, J, M) are sections at the level of the otic vesicle; (B, E, H, K, N) are sections at the level of the beginning of the notochord; and (C, F, I, L, O) are sections in the trunk region, approximately at the middle of the yolk extension. (A-C) *pax2.1* marks CoSA interneurons in the spinal cord of the zebrafish embryo. (D-F) *dbx1a* expression marks a sub-set of interneurons, located laterally, and their progenitors, located more medially next to the tube lumen. The expression of *evx1* is thought to mark primary interneurons dorsally and secondary interneurons more ventrally (dorsal and ventral patches of expression, respectively, on G and H); more posteriorly, only one continuous row of evx^{+} interneurons can be seen along the anterior/posterior axis on either side of the

spinal cord (I). (J-L) *gata2* expression marks a subset of interneurons in the spinal cord of the zebrafish embryo. (M-O) *isl1* expression marks Rohon-Beard neurons dorsally (dorsal patches of expression on O) and motor neurons ventrally (expression in M, N and ventral *isl1*$^{+}$ cells in O).

4.1.3.3 Other markers of the zebrafish spinal cord

In mice, Pax6 expression in the neural tube is confined to mitotically active cells in the ventricular zone, but excluded from the most ventral and most dorsal progenitors population (Ericson et al., 1997; Walther and Gruss, 1991). This protein is considered a Class I homeodomain protein and it represses the expression of the Class II protein Nkx2.2, thus establishing the boundary of the ventral progenitor cell population v3 (Ericson et al., 1997). The zebrafish *pax6a* is expressed along the complete anterior/posterior neural tube of a 24hpf zebrafish embryo (Krauss et al., 1991b; Puschel et al., 1992). The transcripts are detected within a ventral longitudinal column that probably includes the basal and intermediate plates but excludes the most ventral region (Krauss et al., 1991b; Puschel et al., 1992) (panels A-C, Figure 4-7). The expression is clearly higher in the lumen and the lateral regions close to the tube wall, which might reflect the role of *pax6a* in neuronal maturation and/or differentiation (Krauss et al., 1991b) (panel C, Figure 4-7). Iro3 is another Class I protein repressed by Shh (Briscoe et al., 2000). This protein is expressed in intermediate regions of the mouse neural tube and its ventral limit defines the p2/pMN boundary by cross inhibition with Olig2 expressed in the pMN domain (Briscoe et al., 2000; Kessaris et al., 2001; Novitch et al., 2001). Similarly, the zebrafish spinal cord expression of *iro3* comprises the dorsal intermediate and ventral parts of the neural tube, where interneurons and motor neurons form (Tan et al., 1999) (panels D-F, Figure 4-7). Another zebrafish *iroquois* gene, *iro1*, is expressed in two layers positioned at different levels of the dorsal/ventral axis of the hindbrain (Wang et al., 2001) (panels G and H, Figure 4-7). In more posterior regions of the spinal cord of a 24hpf embryo, only one layer is discernible but expression in the lateral floor plate cells is also seen (Wang et al., 2001) (panel I, Figure 4-7). In chick and mouse spinal cords, Pax3 and Pax7 expression domains are restricted to the dorsal most region (Ericson et al., 1997; Goulding et al., 1993a; Goulding et al., 1993b). The zebrafish *pax3* gene is also expressed in the spinal cord along all its anterior/posterior length and in most of the dorsal portion. However, transcripts do not seem to be present at a detectable level in the dorsal most part of the neural tube (Seo et al., 1998) (panels J-L, Figure 4-7).

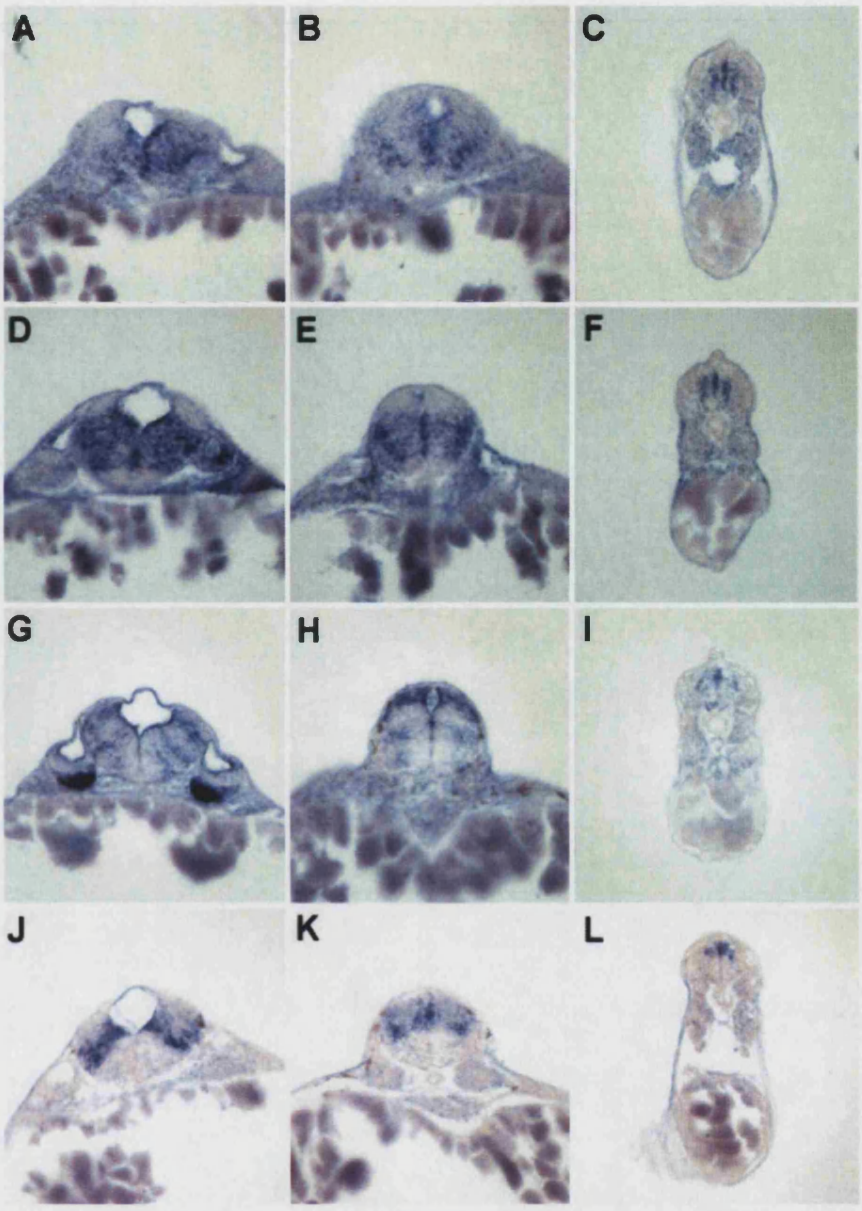

Figure 4-7 Markers of middle and dorsal regions of the zebrafish neural tube at 24hpf. (A, D, G, J) are sections at the level of the otic vesicle; (B, E, H, K) are sections at the level of the beginning of the notochord; and (C, F, I, L) are sections in the trunk region, approximately at the middle of the yolk extension. (A-C) *pax6a* expression is detected in the basal and intermediate plates of the spinal cord and excluded from the floor plate. (D-F) *iro3* expression can be seen in dorsal intermediate and ventral parts of the neural tube. (G-I) *iro1* expression can be seen in two stripes positioned in different dorsal/ventral levels of the hindbrain (G, H), and at a single layer in more posterior regions of the spinal cord in addition to expression in the lateral floor plate (I). (J-L) *pax3* expression in the spinal cord is detected in the dorsal region comprising most of the alar plate, but absent from the dorsal most cells.

4.2 Gli3 in zebrafish development

Shh produced in the notochord and floor plate provides a gradient of hedgehog signalling in the ventral neural tube. Dorsal-ventral cell fate decisions in the neural tube are controlled by sets of transcription factors activated or repressed by signals emanating from the dorsal and ventral sources in the neural tube. The activity of these transcription factors results in the generation of different neuronal subtypes. Although the process has been fairly well studied in the mouse and chick neural tube, little has been described for the zebrafish neural tube.

As mentioned in the introduction to this section, in mice double mutants for Shh and one of its transcription factors, Gli3, there is a surprising rescue of the Shh phenotype. The analysis of this phenotype suggests that ventral patterning of the neural tube can proceed via a mechanism either parallel to or independent of graded Shh signalling in which Gli3 may play an important role. Motivated by the quest for such an alternative patterning mechanism and more specifically by the understanding of Gli3 function during zebrafish development, I cloned the zebrafish *gli3* and analysed its loss of function phenotype using morpholino oligonucleotides.

4.2.1 Cloning zebrafish *gli3*

A search of the Genbank database revealed two zebrafish ESTs with sequence homology with Gli3: fc85b05 and fc71b03. These ESTs were ordered but after sequencing the ends it was clear that they were *gli2* and had been incorrectly named in the database.

The approach taken to clone *gli3* was to search for gli3 exons sequence within the zebrafish genome sequencing project sequence repository. By BLASTing the mouse and human sequences for Gli3 against the zebrafish genomic database, trace files containing putative exons of the fish homologue were identified. The sequence contained in the trace files was used to design primers to perform 5' and 3' RACE nested reactions (see 'Materials and Methods'). In this way it was possible to obtain a 5' fragment of *gli3* that was used to design morpholino oligonucleotides. However, 3' RACE reactions with primers designed in this region never allowed the amplification of the whole transcript, which is approximately 5 kb long in both mouse and human.

With the continuation of the zebrafish genome project, supercontig (contigs of linked trace files) genomic sequence became available in the databases. BLASTing of the

mouse and human Gli3 proteins gave homology with 3 different supercontigs. Two of these supercontigs contained exons of the middle portion of Gli3 and yet were different. This raised the possibility that there might be two zebrafish *gli3* genes. We now know, however, that there is only one zebrafish Gli3 gene. The third supercontig contained exons from the 3' end of the protein. Using the 5' cloned fragment and sequence information from the supercontigs, primers to amplify the two halves of the gene were designed. Only the primers designed to one of the middle exon supercontigs resulted in the amplification of a *gli3* fragment. We could then show that the second supercontig encodes a zinc-finger protein with no homology to Gli proteins outside the zinc-finger domain. In the end, a *gli3* full-length clone was obtained by amplification using Long Range PCR. In Figure 4-8 is an alignment of the human, mouse, chicken and zebrafish Gli3 proteins. Importantly, all the residues putatively phosphorylated prior to cleavage are conserved in all four sequences (Lefers and Holmgren, 2002; Price and Kalderon, 2002). In Figure 4-9 an alignment between all zebrafish Gli proteins is shown. Gli3 is approximately 30% identical to Gli1 and 40% identical to Gli2. It is interesting to note that only two putative phosphorylation sites are missing in the Gli1 protein, raising the hypothesis that zebrafish Gli1 may undergo cleavage, in contrast to the mouse protein. Finally, in Figure 4-10 a phylogenetic tree of all the vertebrate Gli proteins, and the *Drosophila* Ci protein for comparison, is depicted.

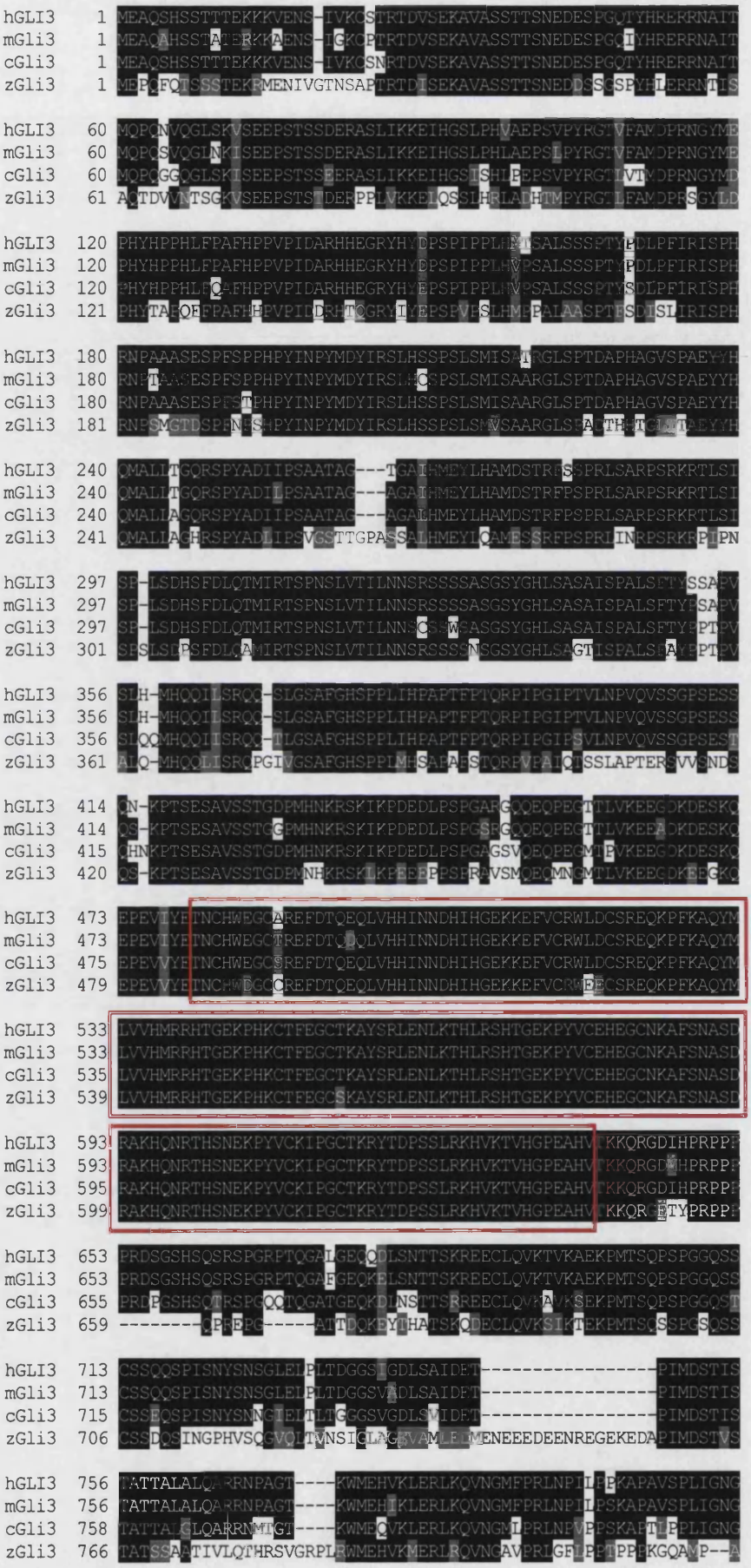
hGLI3
mGli3
cGli3
zGli3

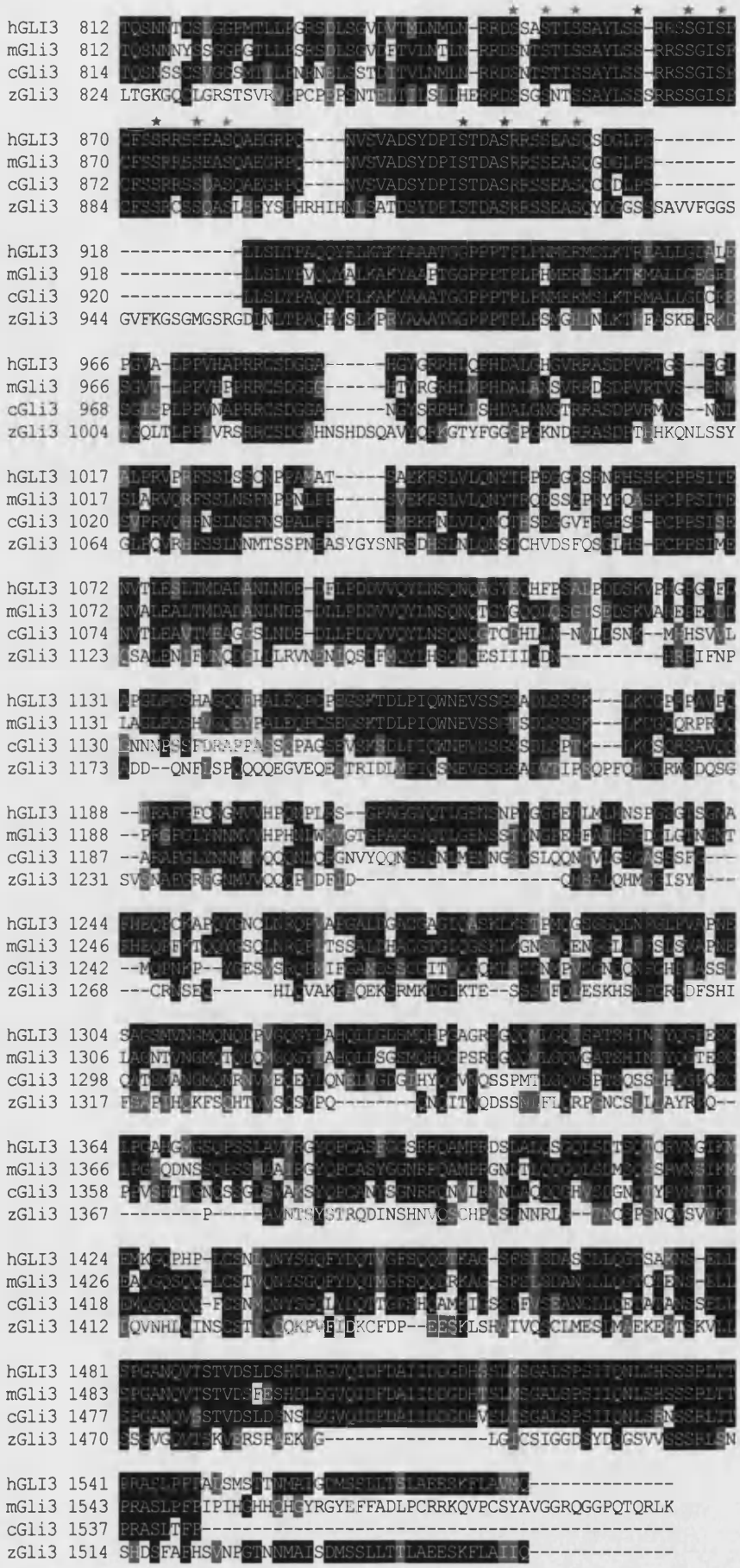

Figure 4-8 ClustalW protein alignment between the human, mouse, chicken and zebrafish proteins. Identical amino acids are shaded in black and similar amino acids are shaded in grey. . The zebrafish sequence is approximately 50% identical to any of the other three. The zinc-finger domain region is boxed in red. All the residues putatively phosphorylated prior to cleavage are conserved in all four sequences. ★ - PKA conserved phosphorylation sites; ★ - Sgg/GSK3 conserved phosphorylation sites; ★ - CK1 conserved phosphorylation sites. All phosphorylation sites according to (Lefers and Holmgren, 2002).

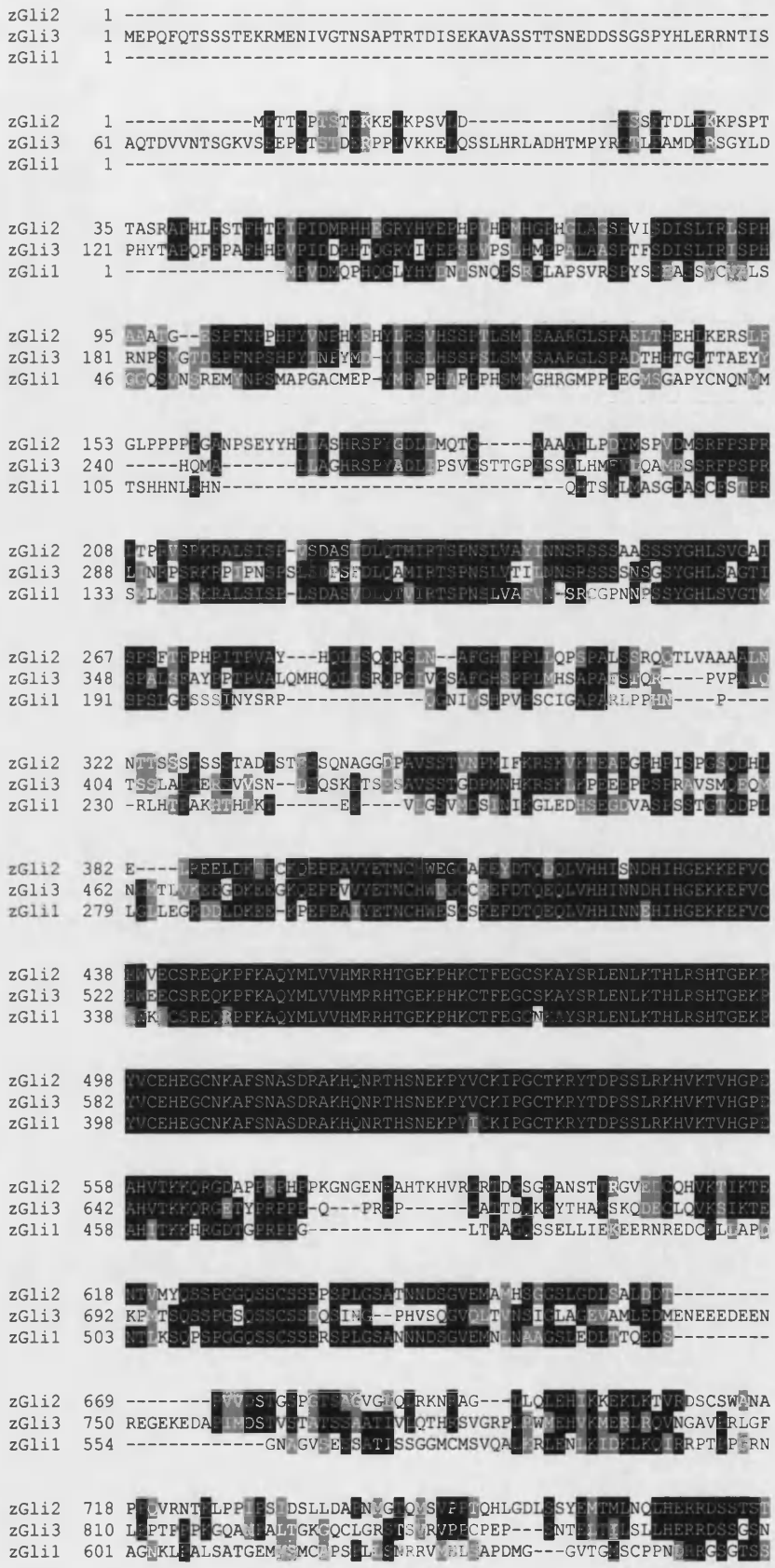

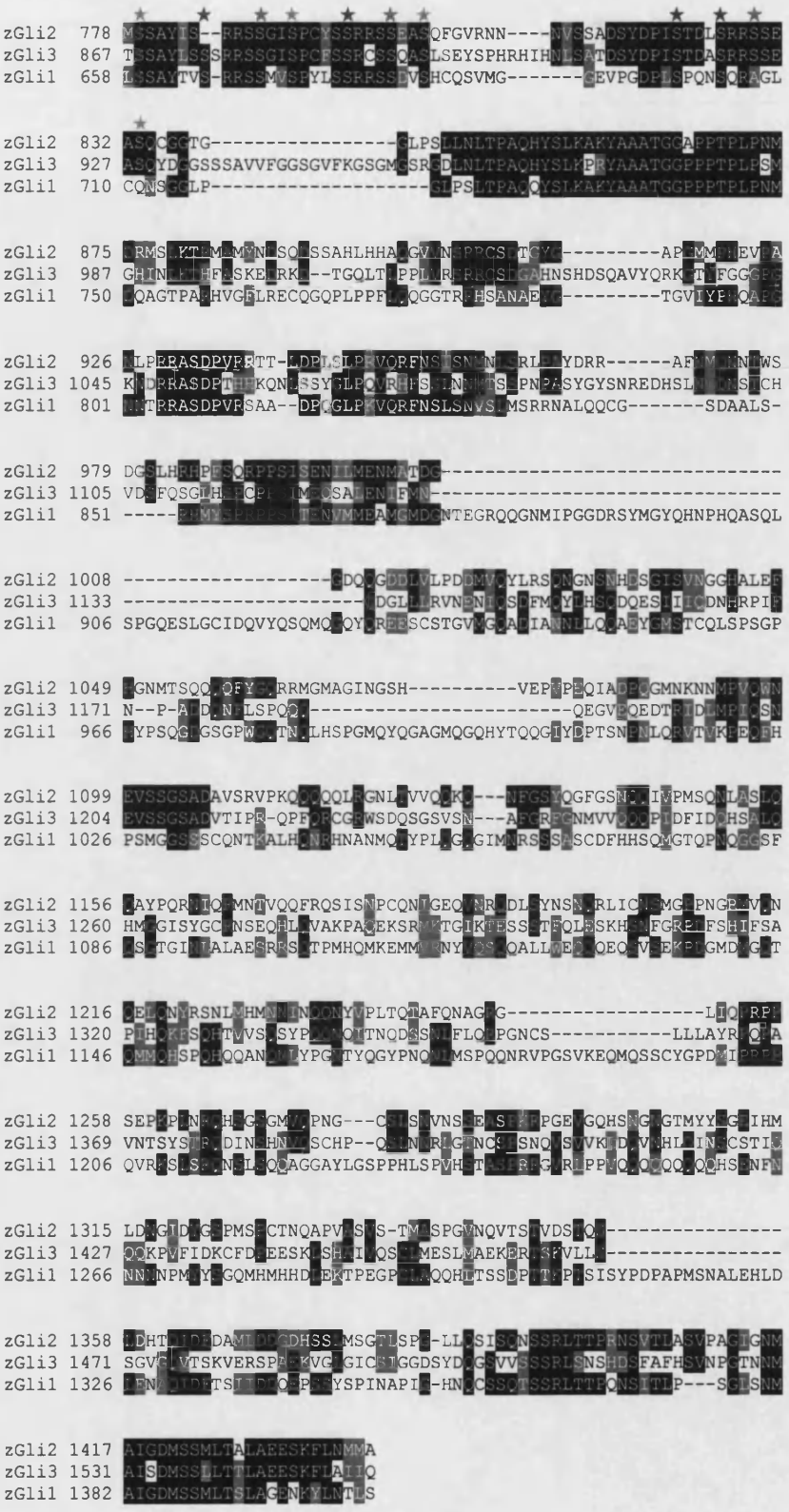

Figure 4-9 ClustalW protein alignment between the zebrafish Gli proteins. Identical amino acids are shaded in black and similar amino acids are shaded in grey. Gli3 is approximately 30% identical to Gli1 and 40% identical to Gli2. ★ - PKA conserved phosphorylation sites; ★ - Sgg/GSK3 conserved phosphorylation sites; ★ - CK1 conserved phosphorylation sites. All phosphorylation sites according to (Lefers and Holmgren, 2002)

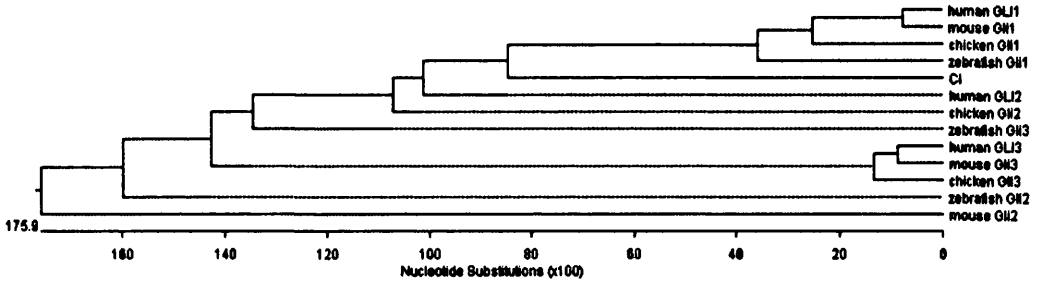

Figure 4-10 Phylogenetic tree of vertebrate Gli proteins.

4.2.2 Mapping zebrafish *gli3*

Radiation hybrid panels are a collection of hybrid cell lines that contain random genomic fragments from the species of interest. The construction of the panel involves the fusion of tissue culture cells of one species to cells of a target species. Prior to fusion, tissue culture cells of the target species are irradiated to fragment genomic DNA. The DNA from hybrid clonal cell lines is extracted and then tested by PCR for retention of chromosomal fragments. Statistical comparison of the set of positive samples with that of other mapped markers identifies the position of the locus under analysis.

Using a zebrafish RH panel, *gli3* was mapped to linkage group 24, 4.40 cR from the marker fb72b09, with a lod score of 18.7.

4.2.3 *gli3* mRNA expression pattern

Following the cloning of the zebrafish *gli3* gene, I studied the expression of the mRNA to further elucidate its role during embryogenesis.

Three different probes were used in the *in situ* hybridisation experiment, namely a probe generated from each half of the gene and a probe generated from the full-length

cDNA. The results in all three experiments were the same and are illustrated in Figure 4-11.

A low level of maternal transcripts is detected at 8-cells stage (panel A, Figure 4-11). At the on-set of zygotic transcription, 1000-cells, expression of *gli3* is very strong in all cells of the blastoderm (panel B, Figure 4-11). High levels of ubiquitous expression are maintained at shield stage (panel C, Figure 4-11) but at 5-somites stage, although still fairly ubiquitous, expression levels seem to be lower (Panels D-F, Figure 4-11). At the 5-somite stage transcripts are present throughout the whole embryo but concentrated in the brain and axial tissue, probably corresponding to the forming spinal cord. From 5-somite onward until the 24hpf stage transcripts are present ubiquitously and at low levels in the developing embryo (data not shown).

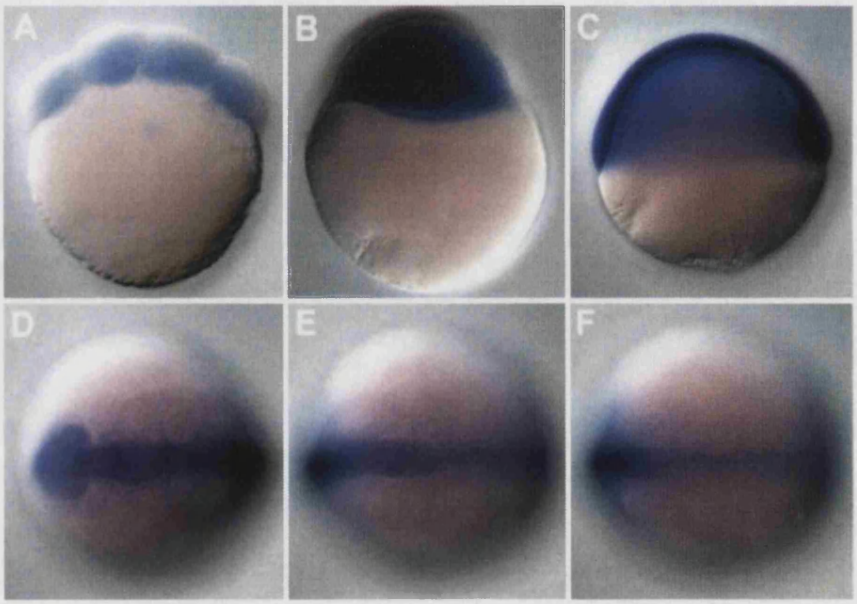

Figure 4-11 Expression of *gli3* during early zebrafish development. (A) low levels of expression at the 8-cell stage reveal the presence of maternal transcripts. (B) at the on-set of zygotic expression level of expression is high and homogeneous throughout the whole embryo. (C) at shield stage expression is still high and ubiquitous, but at 5-somites stage (D-F) levels appear lower and concentrated in the brain region (D) and in axial tissue that may correspond to the developing spinal cord (E, F). (A-C) are side views, animal is up and dorsal to the right in C. (D-F) are dorsal views, anterior to the left, representing the same embryo that was rotated anti-clockwise from D to F.

4.2.4 Gli3 loss-of-function phenotype

To understand the function of Gli3 in zebrafish embryonic development, I used a loss-of-function approach employing anti-sense morpholino oligonucleotides. Two different morpholino oligonucleotides (MO1 and MO2) targeting the region of the start codon of *gli3* were designed, along with a third morpholino that was similar to MO1 but had 5 mis-pairs and was used as a control (see Figure 4-12).

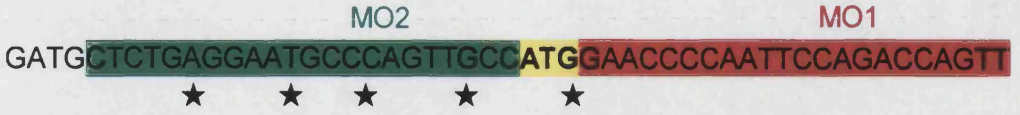

Figure 4-12 Morpholino oligonucleotides designed to knock down Gli3 function in zebrafish development. MO1 and MO2 only overlap in the starting codon (ATG, shaded in yellow). Black stars indicate bases mismatches in the control morpholino. MO1 is shaded in green and MO2 is shaded in red.

Injection of 5ng of either MO1 or MO2 resulted in a strong phenotype at 24hpf (see Figure 4-13). The brains of the morphant fish are smaller and the midbrain region is strongly affected (compare panels B and C with control injected embryo in panel A, Figure 4-13). In addition, the somite morphology is altered, possessing a u-shape instead of the usual chevron shape (Figure 4-13). Finally, abnormalities in the trunk region extend to the tail of the embryo, which is curled and distinctively different from the tail of a control embryo (Figure 4-13).

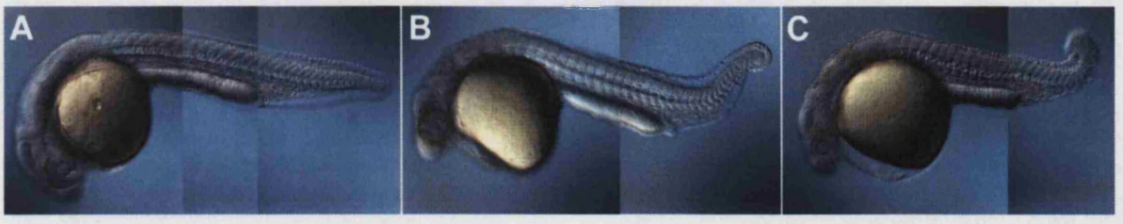

Figure 4-13 Phenotype of the *gli3* morphant at 24hpf. (A) embryo injected with 5ng of control morpholino. (B) embryo injected with 5ng of MO1. (C) embryo injected with 5ng of MO2. Embryos injected with both MO1 and MO2 have midbrain defects, u-shaped somites and curled tails (B, C).

4.2.4.1 Spinal cord phenotype

I expected Hh signalling to be compromised in *gli3* morphants. The *gli3* morphants have u-shape somites at 24hpf, like the so-called u-type mutants, which are often the result of mutations in Hh signalling pathway components.

To test whether Shh signalling is affected in *gli3* morphants, I assayed expression of *shh* and two direct downstream targets of the pathway, *ptc1 and nkx2.2* (Figure 4-14). None of the three expression patterns is substantially altered in *gli3* morphants. The expression of *shh* extends along the entire floor plate and pre-chordal plate of morphant embryos but expression in the zona limitans intrathalamica (ZLI) is disrupted (panels A, A', B, B', Figure 4-14). In addition, expression in the notochord is only partially down regulated at 24hpf, which might be due to a general delay in embryonic development or indirect consequence of abnormal notochord development (panel B, Figure 4-14). Expression of *ptc1* is in general unaffected in *gli3* morphants (panels C, D, Figure 4-14). The somite expression is less regular than in control embryos, probably as a consequence of the abnormal somite shape. Finally, expression of *nkx2.2* is unaltered in *gli3* morphants (panels E and F, Figure 4-14).

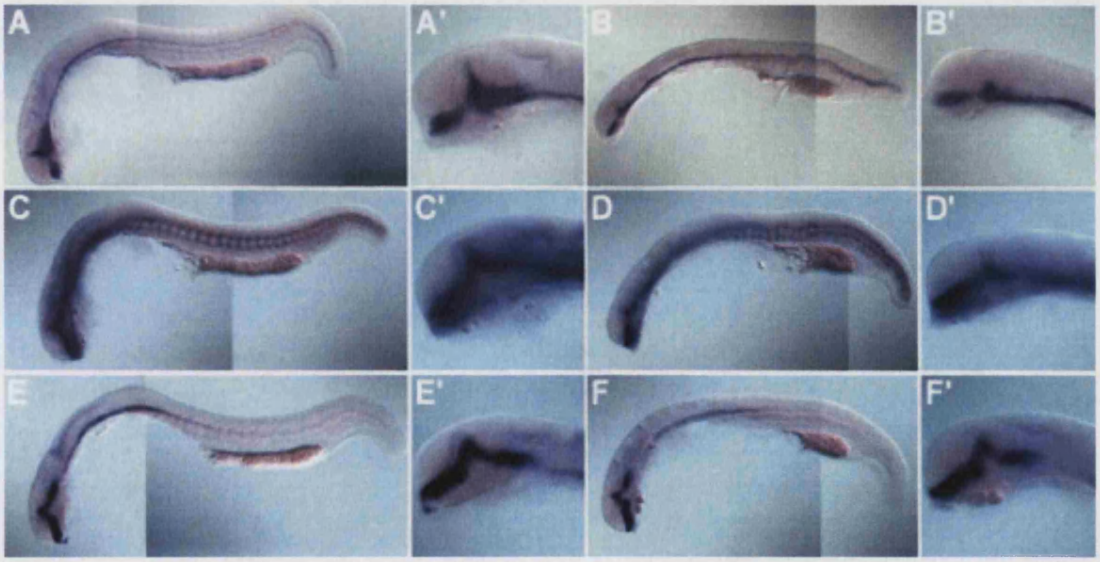

Figure 4-14 Shh signalling seems unaffected in 24hpf *gli3* morphant embryos, as revealed by *shh* (A,B), *ptc1* (C,D) and *nkx2.2* (E,F) expression patterns. (A, C, E) embryos injected with 5ng of control morpholino. (B, D, F) embryos injected with 5ng of *gli3* morpholino (MO1). All three markers seem unaltered in the morphant embryos with the exception of *shh* expression in the ZLI that is absent (B'). (A', B', C', D', E', F') are close ups of the head region of (A, B, C, D, E, F).

In mouse Gli3 mutants neural tube patterning is affected (Persson et al., 2002; Theil et al., 1999). To test whether loss of *gli3* results in spinal cord patterning defects in zebrafish, I examined the expression pattern of several spinal cord markers (Figure 4-15).

In broad terms, expression of all spinal cord markers analysed is unaffected in *gli3* morphant fish. The only conspicuous exception is motor neurons *isl1* expression (panels A, and B, Figure 4-15). It appears that a subset of *isl1*$^{+}$ motor neurons is absent from the spinal cord of experimental embryos that, instead of the almost continuous row of *isl1*$^{+}$ cells, have patches of *isl1*$^{+}$ cells roughly at the distance of 1 somite apart (compare panels A and B, Figure 4-15). *pax3, dbx1a, nkx2.2* and *nkx6.1* expression pattern in the spinal cord of experimental embryos seems roughly comparable to that of control embryos (panels C-J, Figure 4-15).

Figure 4-15 Expression pattern of spinal cord zebrafish markers at 24hpf reveals grossly unaltered patterning of this region of *gli3* morphants. (A, C, E, G, I) are embryos injected with 5ng of control MO. (B, D, F, H, J) are embryos injected with 5ng of *gli3* morpholino (MO1). (A,B) *isl1* expression reveals less *isl1*$^{+}$ motor neurons in experimental embryos. (C,D) *pax3* (E,F) *dbx1a*, (G,H) *nkx2.2* and (I,J) *nkx6.1* expression seems unaltered in the spinal cord of *gli3* morphant embryos. In (A-F) only the tails of the embryos are shown and (G-J) are manual sections at the level of the end of the yolk extension, approximately 1-2 somites width.

4.2.4.2 Early phenotype

Although the spinal cord of *gli3* morphants appears to be patterned correctly at 24hpf (Figure 4-15), these embryos have obvious phenotypic defects (see Figure 4-13). To understand the embryonic defects of *gli3* morphants, I focused on earlier developmental stages.

4.2.4.2.1 Five somite stage

When control embryos are at approximately the 5-somite stage, embryos injected with *gli3* morpholino show severe developmental defects (Figure 4-16). Some of the obvious defects include a shorter anterior/posterior axis (notice distances between arrow heads in Figure 4-16), loose cells detaching from the embryo proper and thinner and wider somites.

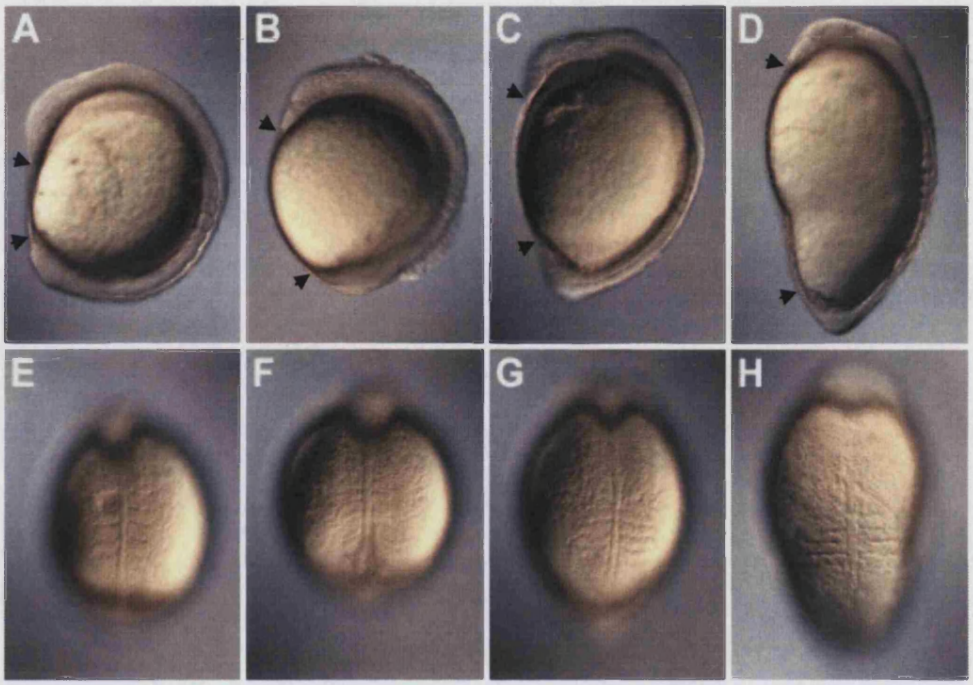

Figure 4-16 Phenotype of the *gli3* morphant at 5-somites. (A, E) embryo injected with 5ng of control morpholino. (B, F) embryo injected with 5ng of MO1. (C, D, G, and H) embryos injected with 5ng of MO2 may have different severities in the defects, ranging from the embryo depicted in (C, G) to the embryo depicted in (D, H). The morphant embryos do not extend as much as control embryos (notice distances between black arrow heads), have cells detaching from the embryo and the somite blocks are wider and thinner.

To understand the developmental defects of *gli3* morphants at 5-somites, I performed *in situ* hybridisation experiments with probes for the genes *isl1, dbx1a, nkx6.1, pax2.1,* and *pax3* (Figure 4-17). Though all these genes are expressed, the appearance of their expression patterns reflects severe changes in *gli3* morphant embryo morphology.

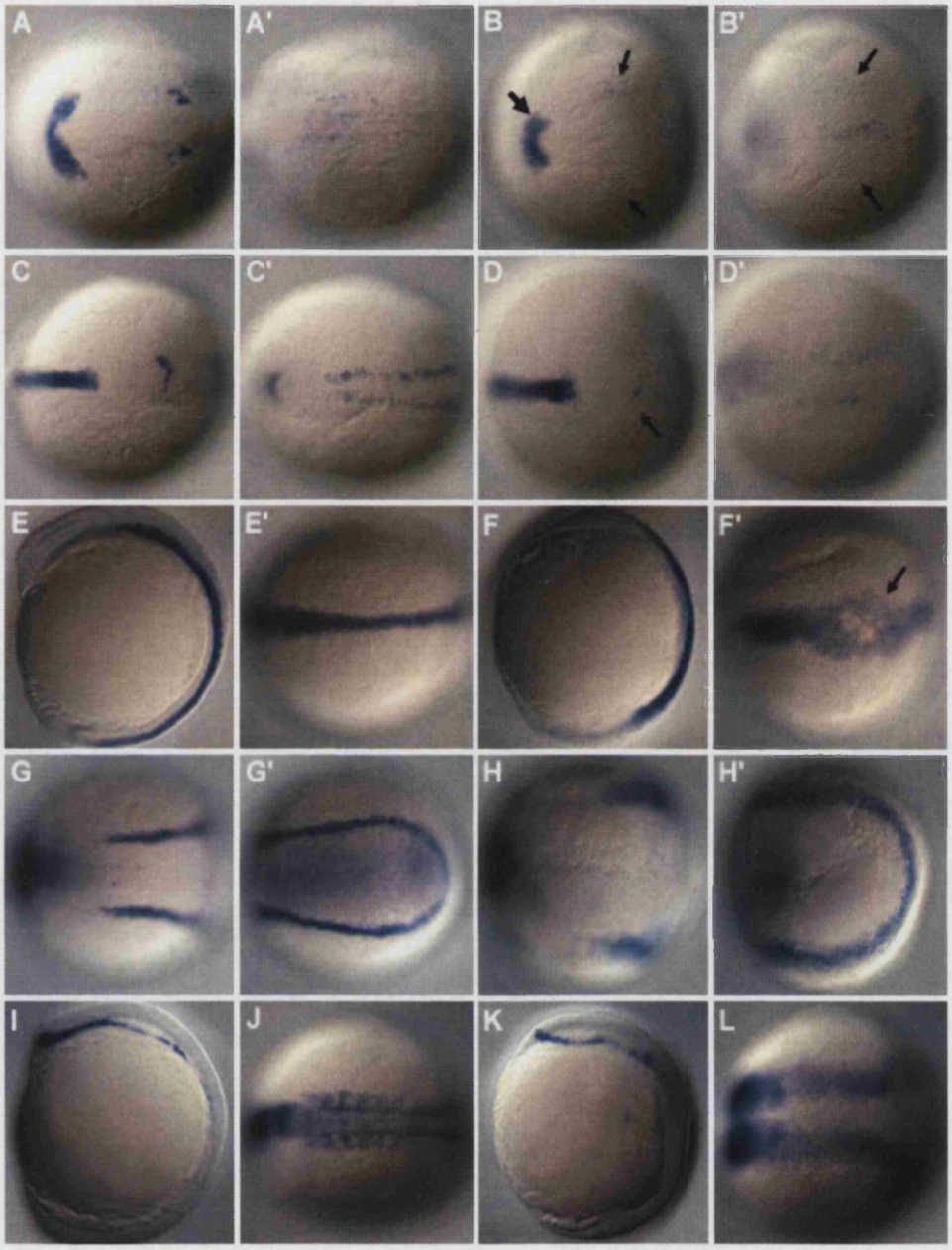

Figure 4-17 Marker analysis of the *gli3* morphant phenotype. (A, C, E, G, I, J) are embryos injected with 5ng of control morpholino. (B, D, F, H, K, L) are embryos injected with 5ng of *gli3* MO1. (I, F, I, K) are lateral views and all the other panels are dorsal views with anterior to the left. (A', B', C', D', G', H') are more posterior views of (A, B, C, D, G, and H) and (E', F') are dorsal views of (E, F). (A-B') *isl1* expression in the polster of morphant embryos is reduced in size (thick arrow in B), expression in the trigeminal ganglia is fainter (thin arrows in B) and Rohon-Beard neurons expression is pushed laterally (arrows in B'). (C-D') *dbx1a* expression in the rhombomeres of the morphant fish is reduced in size (arrow in D) and expression in the interneurons is pushed laterally (D', compare with C'). (E-F') *nkx6.1* expression is wider in the morphants and in some cases gaps in the stripe of expressing cells can be observed (arrow in F'). (G-H') *pax2.1* expression in the pronephric mesoderm of morphant fish is pushed laterally. (I, K) *nkx2.2* expression is unaltered in experimental embryos. (J, L) *pax3* expression in the two stripes of neural tissue is pushed laterally in morphant embryos and somitic expression is absent.

During gastrulation, the movements of convergence and extension (CE) are responsible for proper embryo elongation. These processes consist of medio-lateral cell intercalation movements as well as directed cell migration towards the dorsal midline and result in the medio-lateral convergence and antero-posterior extension of the body axis (for a review see (Keller, 2002)). From my marker analyses the neural plate is apparently wider in *gli3* morphant embryos, as neural plate expression of the markers is observed in a much more lateral position than in control embryos (Figure 4-17). In addition, the body axis of these morphants is shorter (Figure 4-16). One explanation for this phenotype could be altered convergence extension movements.

To understand whether CE is affected in *gli3* morphants, I injected *gli3* morpholino in a CE compromised embryo and assessed whether the resulting phenotype was enhanced.

Silberblick/Wnt11 activity is required for cells to undergo correct CE movements during gastrulation in zebrafish (Heisenberg et al., 2000). One of the main functions of Wnt11 (and Wnt5a) is to polarize cells along their medio-lateral axis in mesodermal tissues undergoing CE movements in a process similar to the planar polarization of cells in many *Drosophila* epithelia, commonly termed *planar cell polarity* (PCP) (Tada et al., 2002). In *silberblick* mutants the prechordal plate is more elongated and the notochord is shorter and wider than in wild-type embryos (Heisenberg and Nüsslein-Volhard, 1997). As injection of morpholino oligonucleotides targeting Silberblick/Wnt11 phenocopies the mutation (Lele et al., 2001), in my experiment I co-injected *gli3* and *silberblick* morpholinos and assessed whether the CE phenotype was enhanced. I then examined the expression of *dlx3* at the anterior edge of the neural plate and the expression of *ΔNp63α* marking the edge of the neural plate (Bakkers et al., 2002; Heisenberg and Nüsslein-Volhard, 1997) (see Figure 4-18). The expression of these two markers reveals that the neural plate is broader, both anteriorly (panels E-H, Figure 4-18) and at the level of the somites (panels A-D, Figure 4-18), in *silberblick* and *gli3* morphants (panels B, C, F, G, Figure 4-18) and this phenotype is dramatically enhanced in embryos injected with both morpholinos (panels D, H, Figure 4-18).

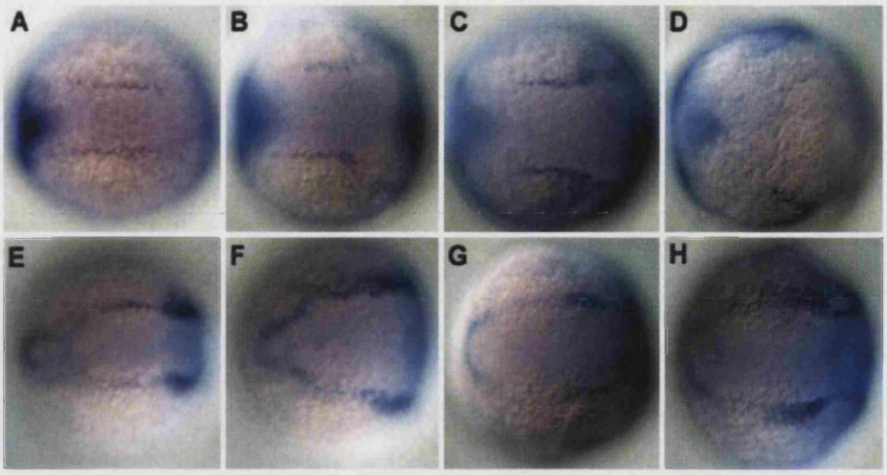

Figure 4-18 Co-injection of *silberblick/wnt11* and *gli3* morpholinos enhances the convergence /extension phenotype of *silberblick/wnt11*. All the embryos are at 3 somites stage. (A, B, C, D) is *ΔNp63α* expression, dorsal views at the level of the somites, anterior to the left. (E, F, G, and H) is *dlx3* expression, dorsal views at the level of the forming head, anterior to the left. (A, E) embryo injected with 5ng control MO. (B, F) embryos injected with 5ng *gli3* MO1 have broader anterior (F) and medial (B) neural plate. (C, G) embryos injected with 4ng *silberblick/wnt11* MO have broader anterior (G) and medial (C) neural plate. (D, H) embryos injected with 5ng *gli3* MO1 and 4ng *silberblick/wnt11* MO have a very broad anterior (H) and medial (D) neural plate.

4.2.4.2.2 At 40% epiboly

By 5-somite stage, *gli3* morphants have such an obvious and severe phenotype (Figure 4-16) that I decided to look at an earlier stage of development. I performed a marker analysis at 40% epiboly, since at this stage experimental and control embryos are still undistinguishable but major signalling pathways that control germ layer formation are already operating. Expression pattern of *cyclops, squint, bhikhary, fgf8* and *flh* was analysed (Figure 4-19). The expression of all these genes is up-regulated in *gli3* morphants. The increase in expression could be explained by either an increase in nodal signalling or an increase in nodal responsiveness, since *bhikhary, fgf8* and *flh* are all induced by nodal signalling and *cyclops* and *squint* are zebrafish nodal genes (Erter et al., 1998; Feldman et al., 1998; Griffin et al., 1995; Gritsman et al., 2000; Sampath et al., 1998; Vogel and Gerster, 1999).

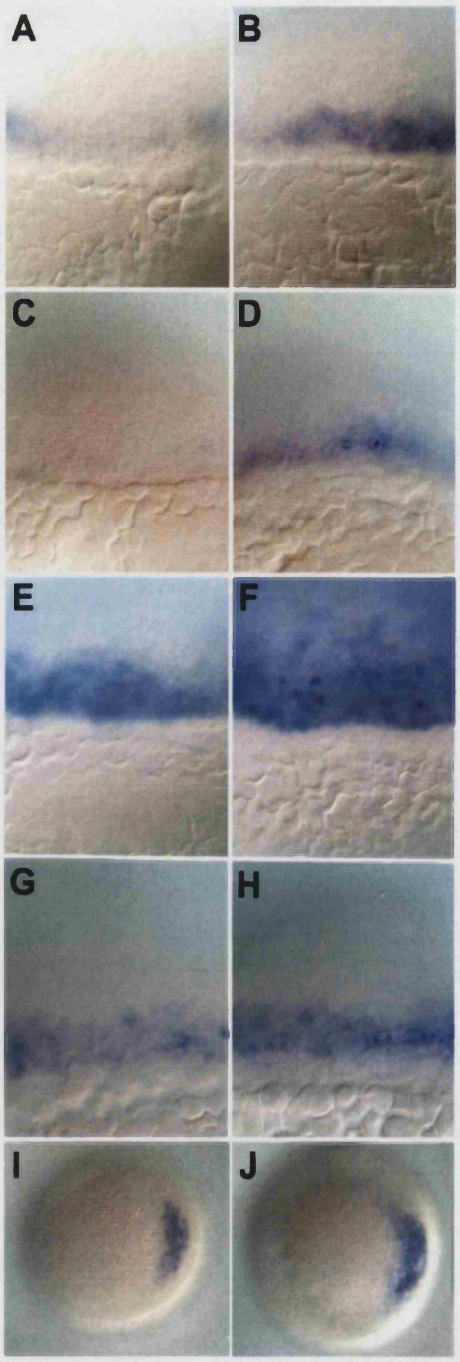

Figure 4-19 Nodal and nodal-responsive genes are up-regulated in 40% epiboly *gli3* morphants. (A, C, E, G, I) are embryos injected with 5ng control MO. (B, D, F, H, J) are embryos injected with 5ng *gli3* MO1. The expression of *cyc* (A, B), *sqt* (C, D), *bik* (E, F), *fgf8* (G, H) and *flh* (I, J) is up-regulated in *gli3* morphants. In (A, B, C, D, E, F, G, and H) the lateral margin of the embryo was photographed. (I, J) are top views, dorsal to the right.

4.2.4.3 Cyclopamine treatment

Although I did not detect any Hh signalling alteration in *gli3* morphants (Figure 4-14 and Figure 4-15) I was still interested in analysing what would happen to a zebrafish

embryo developing in the absence of both Hh signalling and Gli3. In mice double mutants for Shh and Gli3 there is a rescue of the Shh phenotype (Litingtung and Chiang, 2000; Persson et al., 2002; Rallu et al., 2002). It was thus interesting to determine whether the same kind of rescue would happen in the zebrafish. However, contrary to the mouse, zebrafish has three *hedgehog* genes expressed in axial tissues that may all be involved in spinal cord patterning. Zebrafish *shh* is expressed in the notochord and floor plate, whereas *twhh* is expressed exclusively in the floor plate and *ehh* exclusively in the notochord during early development (Currie and Ingham, 1996; Ekker et al., 1995; Krauss et al., 1993). Despite the fact that there are three *hedgehog* genes expressed in axial tissues of the zebrafish embryo, there seems to be only one *smoothened* gene (Varga et al., 2001). It is believed that all hedgehog signalling is transduced through the Smoothened protein, so disrupting Smoothened activity would be equivalent to disrupting all Hedgehog signalling.

To knock down Smoothened activity in zebrafish, I used the alkaloid cyclopamine. Cyclopamine is a steroidal alkaloid isolated from a plant, *Veratrum californicum*, capable of inducing cyclopia and other birth defects in sheep that graze in fields were the plant is present. It was shown that the potent teratogenic activity of cyclopamine was due to an inhibition of Shh signalling (Cooper et al., 1998; Incardona et al., 1998). The inhibitory effect of cyclopamine on Hh signalling is mediated through direct binding to the Smoothened protein (Chen et al., 2002).

4.2.4.3.1 Cyclopamine works as a Shh inhibitor

To confirm that cyclopamine works as a Hh signalling inhibitor in zebrafish (Neumann et al., 1999), I treated embryos with the reagent and assessed the expression of two direct targets of Hh signalling, *nkx2.2* and *ptc1*. As a positive control, I injected embryos with *shh* RNA and expected a dramatic up-regulation of both genes. To optimise the cyclopamine treatment, the embryos were incubated in two different concentrations of the reagent, 25µM and 100µM, either from the 1-cell stage until fixation, or just from shield stage until fixation, with or without the chorions. The results obtained in all conditions were undistinguishable as seen by expression of *ptc1* and *nkx2.2* (data not shown) and for all the following experiments the embryos were incubated in 25µM cyclopamine solution, from shield stage until fixation, without chorion removal.

In embryos treated with cyclopamine and fixed at 5-somite stage, *nkx2.2* expression was undetectable and *ptc1* expression is de-localized (panels B, E, Figure 4-20). In contrast, in embryos injected with *shh* RNA the situation was completely reversed and

nkx2.2 expression was dramatically up-regulated in the pre-chordal plate region, whereas *ptc1* expression was very high throughout the whole embryo and localized to adaxial cells (panels C, F, Figure 4-20).

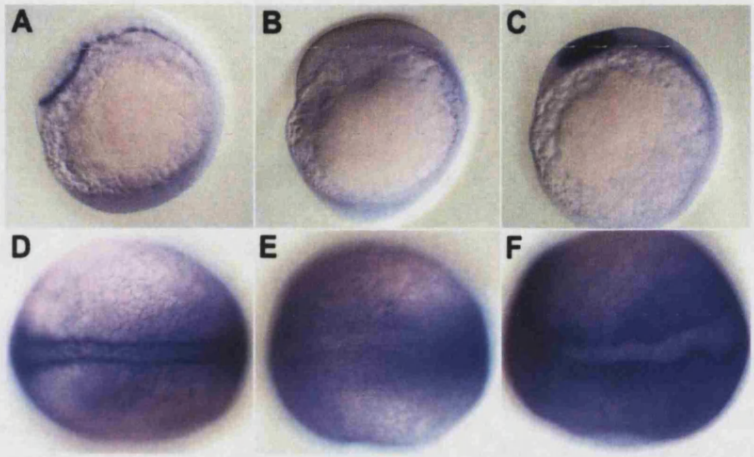

Figure 4-20 *nkx2.2* and *ptc1* expression in 5-somite embryos treated with cyclopamine. (A-C) *nkx2.2* expression in a control embryo (A), an embryo incubated in the presence of cyclopamine (B), and an embryo injected with 100pg *shh* RNA and incubated in 0.25% EtOH (C). (D-F) *ptc1* expression in a control embryo (D), an embryo incubated in the presence of cyclopamine (E), and an embryo injected with 100pg *shh* RNA and incubated in 0.25% EtOH (F). *nkx2.2* expression is absent from cyclopamine treated embryos (B) and up-regulated in Shh over-expressing embryos (C). *ptc1* is de-localize from adaxial cells of a cyclopamine-treated embryo (E) and up-regulated in Shh over-expressing embryos (F). Control embryos were injected with 1.4nl of phenol red solution and incubated in 0.25% EtOH. (A-C) are lateral views, dorsal to the right; (D-F) are dorsal views, anterior to the left.

In embryos treated with cyclopamine from shield stage to 24hpf the situation is very similar (Figure 4-21). Expression of *nkx2.2* is undetectable everywhere except in a small patch of cells in the ventral brain and *ptc1* expression in only detectable at background levels (panel B and E, Figure 4-21).

Figure 4-21 *nkx2.2* and *ptc1* expression in 24hpf embryos treated with cyclopamine. (A-C) *nkx2.2* expression in a control embryo (A), an embryo incubated in the presence of cyclopamine (B), and an embryo injected with 100pg *shh* RNA and incubated in 0.25% EtOH (C). (D-F) *ptc1* expression in a control embryo (D), an embryo incubated in the presence of cyclopamine (E), and an embryo injected with 100pg *shh* RNA and incubated in 0.25% EtOH (F). *nkx2.2* expression is only detectable in a patch of ventral brain cells in cyclopamine treated embryos (B) and up-regulated in Shh over-expressing embryos (C). *ptc1* is only present at background levels in a cyclopamine-treated embryo (E) and up-regulated in Shh over-expressing embryos (F). Control embryos were injected with 1.4nl of phenol red solution and incubated in 0.25% EtOH.

4.2.4.3.2 Cyclopamine rescues gli3 *morphant phenotype*

Having confirmed that cyclopamine inhibits Hh signalling in zebrafish embryos, I examined the phenotype of embryos both injected with *gli3* morpholino and incubated in cyclopamine. To my surprise, the *gli3* morphant phenotype was rescued by the cyclopamine treatment (Figure 4-22). I found 86% (n=37) of the embryos injected with *gli3* morpholino had a very severe phenotype (panels D and J, Figure 4-22). When the embryos were treated in cyclopamine following morpholino injection, only 28% (n=36) had a severe phenotype (panels F and L, Figure 4-22) whereas the remaining had a very mild phenotype (panels E and K, Figure 4-22). The rescue of the *gli3* phenotype by cyclopamine treatment was confirmed by marker analysis (Figure 4-23). Importantly, although the overall appearance of *gli3* morphants treated with cyclopamine was rescued, *nkx2.2* expression is still absent as in embryos treated with cyclopamine alone (panel R, Figure 4-23).

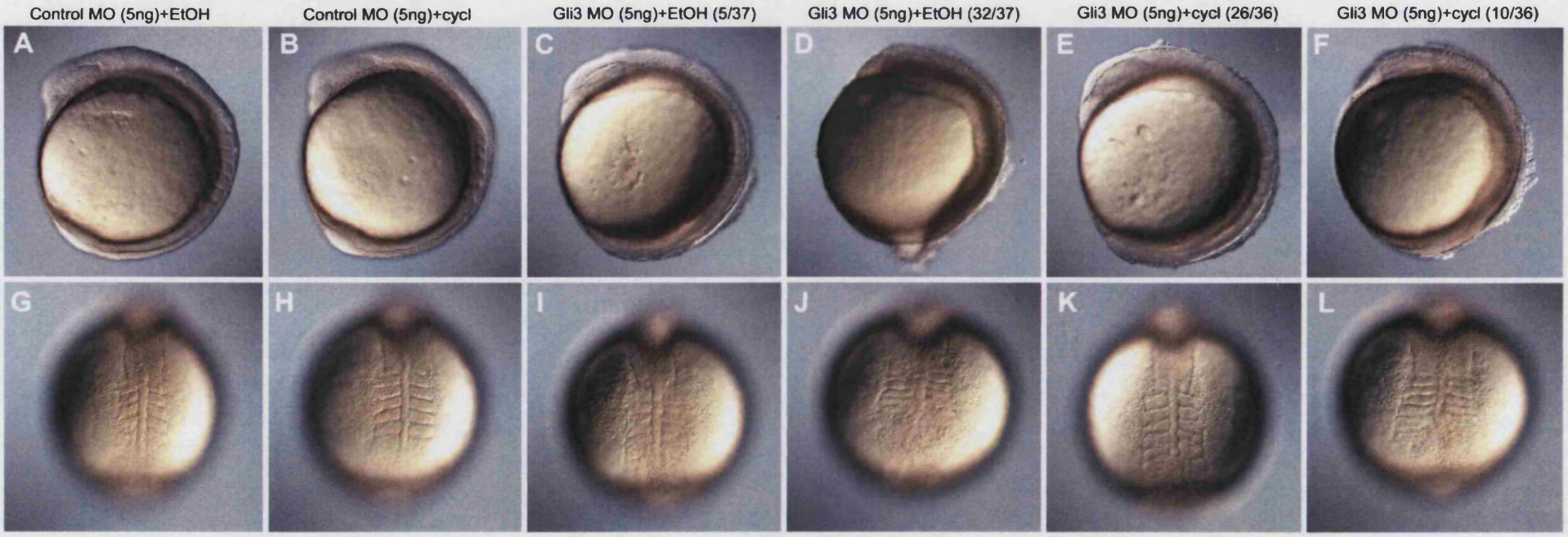

Figure 4-22 Cyclopamine treatment rescues the *gli3* morphant phenotype at 5-somites. Upper panels are side views with dorsal to the side and lower panels are dorsal views with anterior up. (A, G) embryo injected with control morpholino and incubated in 0.25% EtOH. (B, H) embryo injected with control morpholino and incubated in 25μM cyclopamine solution. (C, I) 14% (n=37) of the embryos injected with 5ng of *gli3* MO1 and incubated in 0.25% EtOH had a mild phenotype. (D, J) 86% (n=37) of the embryos injected with 5ng of *gli3* MO1 and incubated in 0.25% EtOH had a severe phenotype. (E, K) 72% (n=36) of the embryos injected with 5ng of *gli3* MO1 and incubated in 25μM of cyclopamine had a mild phenotype. (F, L) 14% (n=36) of the embryos injected with 5ng of *gli3* MO1 and incubated in 25μM of cyclopamine had a severe phenotype.

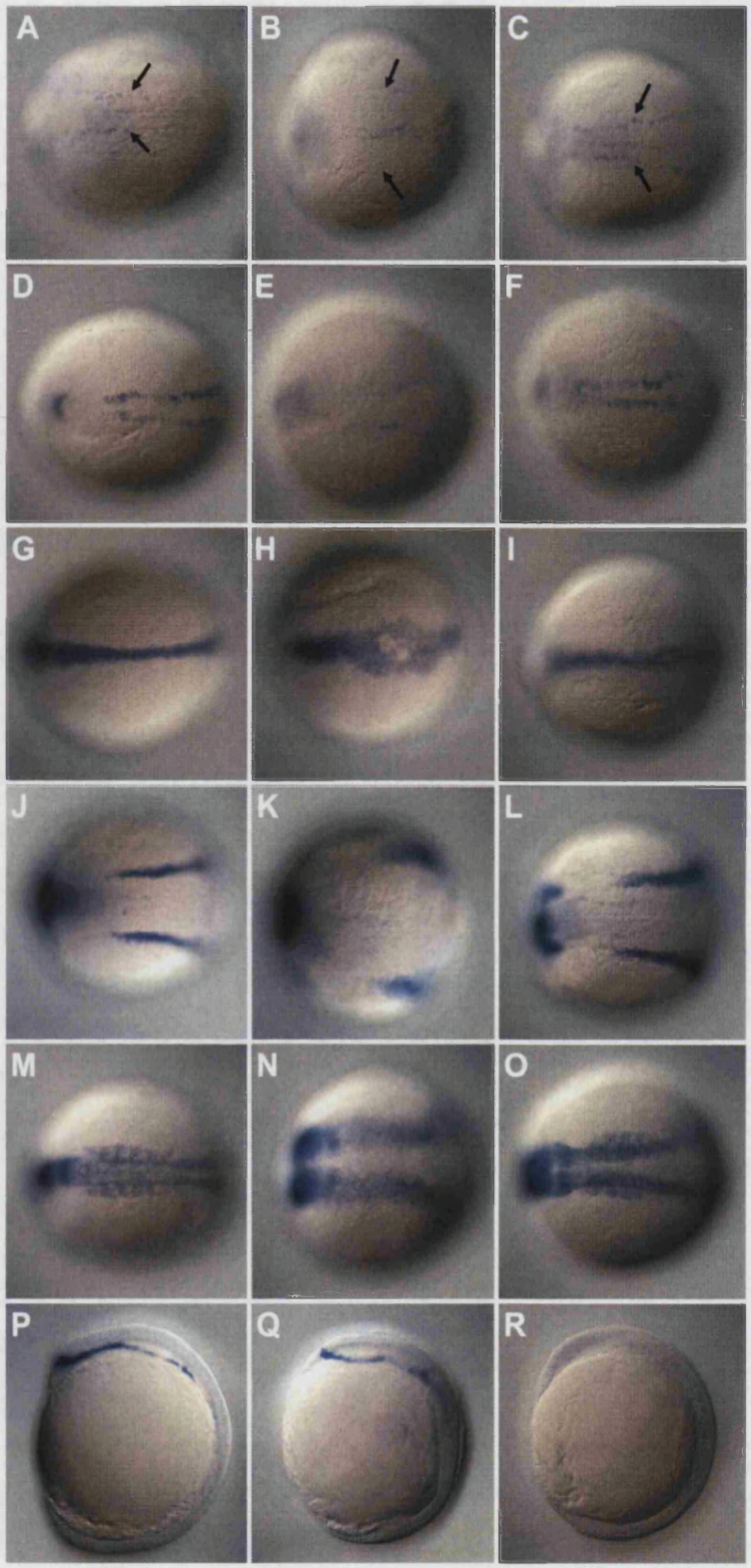

Figure 4-23 Marker analysis on cyclopamine rescued *gli3* morphant fish. (A, D, G, J, M, P) embryos injected with control morpholino and incubated in 0.25% EtOH. (B, E, H, K, N, Q) embryos injected with 5ng of *gli3* MO1 and incubated in 0.25% EtOH. (C, F, I, L, O, R) embryos injected with 5ng of *gli3* MO1 and incubated in 25µM of cyclopamine. (A, B, C) *isl1* expression reveals that position of Rohon-Beard neurons is rescued in *gli3* morphant fish treated with cyclopamine (notice black arrows). (D, E, and F) *dbx1a* expression shows a rescue in the positioning of interneurons in *gli3* morphant fish treated with cyclopamine. (G, H, I) midline

expression of *nkx6.1* is less disrupted in *gli3* morphant embryos treated with cyclopamine. (J, K, and L) pronephros expression of *pax2.1* in *gli3* morphant fish is less lateral than in *gli3* morphants alone. (M, N, and O) neural expression of *pax3* is less lateral in *gli3* morphants treated in cyclopamine than in *gli3* morphants alone. (P, Q, R) expression of *nkx2.2* shows that although the overall appearance of *gli3* morphants treated with cyclopamine is less severe there is total loss of the marker as would be expected in embryos treated with cyclopamine.

4.3 Discussion

The zebrafish spinal cord has a relatively simple organization and therefore provides an excellent system for studying neuronal specification and differentiation in vertebrates. At early stages (18-24hpf), the zebrafish cord contains approximately 18 postmitotic neurons per hemisegment (Kuwada and Bernhardt, 1990) (see Figure 4-1). These neurons were identified through visualization with Nomarski optics, microelectrode filling with horseradish peroxidase (HRP) or lipophilic dyes and through labelling with monoclonal antibodies to general neuronal antigens (Kuwada and Bernhardt, 1990). However, very little is known about the protein code expressed by zebrafish neuronal progenitors that drives their differentiation into specific postmitotic neurons.

Because of the apparent simplicity of the zebrafish neural tube, and the possibility of easily disrupting expression of specific genes with antisense morpholino oligonucleotides, I originally intended to study zebrafish dorsal-ventral spinal cord patterning. In particular, I was interested to test whether a signalling pathway parallel to Hh signalling was operating in zebrafish, as had been shown in mouse Shh/Gli3 double mutants (Litingtung and Chiang, 2000; Persson et al., 2002; Wijgerde et al., 2002).

Other signalling pathways have been previously implicated in ventral neural tube specification. Additional evidence for their existence stems from the observation that mice mutant for Shh still form V0 and V1 interneurons, despite the fact that Shh is sufficient for their induction *in vitro* (Pierani et al., 1999). Moreover, the source of signals that participate in the induction of these cell types is mainly pre-somitic and/or somitic mesoderm (Pierani et al., 1999). Retinoids are expressed at high levels in these regions and are able to induce these cell types in explant assays (Pierani et al., 1999). More recently, two different groups showed that retinoic acid (RA) and FGF pathways have opposing actions in ventral neural tube patterning (Diez del Corral et al., 2003; Novitch et al., 2003). The activator functions of retinoid receptors are required to pattern the expression of homeodomain and basic-helix-loop transcription factors in the ventral neural tube, and FGFs suppress progenitor homeodomain protein expression (Novitch et al., 2003). FGF is a general suppressor of differentiation and has to be attenuated by RA to allow neural differentiation in the ventral neural tube (Diez del Corral et al., 2003). Importantly, exposure of progenitors to retinoids and

FGFs is sufficient to induce motor neuron differentiation in a Shh-independent manner (Novitch et al., 2003).

Another candidate pathway to play a role in ventral neural tube patterning is the Bone Morphogenetic Protein (BMP) signalling pathway. BMP-family members are known to be key mediators in the specification of dorsal neural tube cell-types (Lee et al., 2000; Liem et al., 1997; Liem et al., 1995; Nguyen et al., 2000). It is therefore possible that they also play a role in specifying ventral neural tube cells. Indeed, there is some evidence suggesting this is the case. Zebrafish embryos mutant for BMP-family members have expanded ventral interneuron populations, consistent with the hypothesis of a BMP-dependent positional information gradient extending to the most ventral regions of the neural tube (Barth et al., 1999; Nguyen et al., 2000). In addition, in an *in vitro* assay, BMP signalling counteracts Shh signalling eliciting a ventral-to-dorsal switch of neuronal fates (Liem et al., 2000). Conversely, the addition of BMP-antagonists sensitises neural cells to Shh signalling (Liem et al., 2000). Finally, the application of an exogenous source of Shh is not capable of mimicking the ability of the notochord to induce floor plate. However, when Shh is applied together with a BMP-antagonist, also expressed in the notochord, the floor plate induction activity of the notochord is reproduced (Patten and Placzek, 2002). BMP sources, which must be inhibited for floor plate induction, are thought to be the surface ectoderm and the dorsal-most neuroepithelium, thus implying a long-range action of these signalling molecules (Patten and Placzek, 2002). Furthermore, oligodendrocytes originate in a restricted region of the neuroepithelium and this localization depends on both an inductive influence of Shh and a specific repression of BMPs (Mekki-Dauriac et al., 2002; Tekki-Kessaris et al., 2001). Taken together, these data indicate that dorso-ventral position and/or specification of some neural cell-types in the spinal cord depends on a tightly regulated balance between Shh and BMP activities. These two signalling pathways seem to intersect and BMPs could be acting to limit the ventralizing activity of Shh. Could the intersection of these pathways occur via a common mediator? Could this mediator be Gli3 or some of the other Gli proteins? Indeed, there seems to be some evidence supporting this possibility.

A genetic interaction between Gli3 and BMP4 was uncovered through the analysis of the trans-heterozygote phenotype. BMP4 heterozygotes present several abnormalities including pre-axial polydactyly (Dunn et al., 1997). The penetrance and expressivity of this phenotype is highly enhanced in the BMP4/Gli3 trans-heterozygote (Dunn et al., 1997). In cell culture assays, it was shown that carboxy-terminally truncated Gli3

proteins associate with Smads, the intracellular transducers of TGFβ family signals, including BMPs (Liu et al., 1998). Full-length Gli1, Gli2 or Gli3 proteins did not interact with Smad proteins in this assay. In contrast, C-terminal truncated Gli3, but not Gli1, associated with Smad1, -2, -3 and -4 and this interaction was stronger with the two latter (Liu et al., 1998). A promoter analysis of the human BMP-4 and BMP-7 proteins revealed that they were stimulated upon the co-transfection of GLI1 or GLI3 proteins (Kawai and Sugiura, 2001). These data are in agreement with the observation that the Hh transcription factor in flies, Ci, is a regulator of the transcription of *decapentaplegic* (*dpp*), a BMP-family member in *Drosophila* (Aza-Blanc and Kornberg, 1999). In addition, in the vertebrate limb, Shh is necessary to initiate and sustain *bmp2b* expression (Drossopoulou et al., 2000).

To identify spinal cord patterning defects in zebrafish embryos, it would first be necessary to establish markers of different neuronal subsets in this system. The strategy that I adopted was to test several candidate genes for their specific expression pattern in the spinal cord of the 24hpf zebrafish embryo. Two of these genes, *nkx6.1* and *nkx6.2* were cloned *de novo* whereas the remaining had either been previously cloned by other groups or existed as EST clones that were ordered and used to make *in situ* hybridisation probes.

The expression of Shh and Hnf3ß in the floor plate is seen across vertebrate species. In a 24hpf zebrafish embryo, *shh* is down-regulated in the notochord but persists in the floor plate (Krauss et al., 1993) (see Figure 4-5, panels A-C). In the same way, *hnf3ß* is expressed in the floor plate of a 24hpf zebrafish embryo, though, unlike *shh* it is not confined to the most ventral cell, but is expressed in both medial and lateral floor plate (Strähle et al., 1996) (see Figure 4-5, panels D-F). The *shh* floor plate expressing cell is surrounded on either side by cells expressing *nkx2.2*, which is a direct target of Shh signalling (Barth and Wilson, 1995) (see Figure 4-5, panels G-I). The main difference between the *hnf3ß* and *nkx2.2* domains of expression is that *nkx2.2* is not expressed in medial floor plate (see Figure 4-5, panels G-I). Nkx2.2, as well as other Nkx proteins, is a Class II protein based on its expression being induced by Shh. The other two Class II factors analysed, *nkx6.1* and *nkx6.2*, are also expressed in cells adjacent to Shh-expressing cells, but in broader domains. In chick and mouse, Nkx6.1 is expressed in the region of the most ventral neural progenitors, p3, pMN and p2, and this appears to be maintained in the zebrafish (Briscoe et al., 2000; Vallstedt et al., 2001) (Figure 4-5, panels J-L). The expression of Nkx6.2, however, differs between mouse and chick. In chick, Nkx6.2 is expressed in a broader domain than Nkx6.1 that

comprises the p1 region, whereas in the mouse it is expressed in the p1 region only (Briscoe et al., 2000; Vallstedt et al., 2001). In the zebrafish, *nkx6.2* expression overlaps with that of *nkx6.1* but it is not clear from the results presented here whether both domains absolutely coincide (Figure 4-5, panels J-O).

The dorsal limit of Nkx2.2 expression coincides with the ventral limit of Pax6 expression in both chick and mouse spinal cords. The sharp expression boundary is achieved by cross-repression between both proteins and defines the border between the p3 progenitor domain and the MN domain (Briscoe et al., 2000). In zebrafish, expression of *pax6a* can be detected in most of the spinal cord of a 24hpf zebrafish embryo, excluding the most ventral and dorsal regions (see Figure 4-7, panels A-C). The ventral limit of expression of *pax6a* is likely to coincide with the dorsal limit of *nkx2.2* expression, as seen in other vertebrates, but double *in situ* hybridisation analysis has to be performed to address this hypothesis.

The dorsal limit of the motor neuron progenitor domain is defined by cross-repression interactions between another set of Class I/Class II proteins, Iro3/Olig2 (Kessaris et al., 2001; Novitch et al., 2001). The zebrafish gene *iro3* is also expressed in the spinal cord and its ventral limit appears to be dorsal to the motor neurons region, consistent with maintenance of the pMN/p2 border in this system (Figure 4-7, panels D-F).

Further dorsally, the p2/p1 border in mouse and chick is defined by interactions between Nkx6.1 and Dbx2 (Briscoe et al., 2000). The zebrafish *nkx6.1* has a domain of expression consistent with the maintenance of this border (Figure 4-5, panels J-L), but in my hands *dbx2* expression appeared to be ubiquitous in a 24 hpf zebrafish embryo (data not shown). The zebrafish *dbx2* gene (also known as *hlx3*), although related to murine *dbx2*, is apparently too divergent to be orthologous (Seo et al., 1999). In contrast, there are two zebrafish genes approximately 60% identical to mouse *dbx1* (Seo et al., 1999). One of these transcripts, *dbx1a*, is expressed in individual neurons in the zebrafish spinal cord that could be the same neurons also expressing *evx1* (Figure 4-6, panels D-I). By analogy to other vertebrate systems, these neurons might be the zebrafish equivalent to v0 interneurons, but double *in situ* hybridisation analysis of *dbx1a* and *evx1* should be performed to resolve this. In zebrafish *dbx1a* is expressed in both progenitors and neurons, whereas Dbx1 and Dbx2 expression in chick and mouse is extinguished in differentiated neurons (Pierani et al., 1999).

Apart from *evx1,* another three of the analysed genes are expressed in a subset of differentiated neurons. Rohon-Beard neurons dorsally and primary motor neurons ventrally express *isl1* (Inoue et al., 1994; Korzh et al., 1993) (see Figure 4-6, panels M-O). Expression of *gata2* is seen in unidentified individual ventral interneurons (Detrich

et al., 1995) that, by analogy to other organisms, may correspond to v2 interneurons (see Figure 4-6, panels J-L). Finally, *pax2.1* is expressed in CoSA interneurons (Mikkola et al., 1992) that appear dorsal to *dbx1a* expressing cells and thus may correspond to a dorsal interneuron (Figure 4-6, panels A-C).

The expression patterns of class I and class II homeodomain proteins and their relationship to classes of neurons in mouse and chick are schematized in Figure 4-24. For comparison, a similar scheme is showing the zebrafish spinal cord.

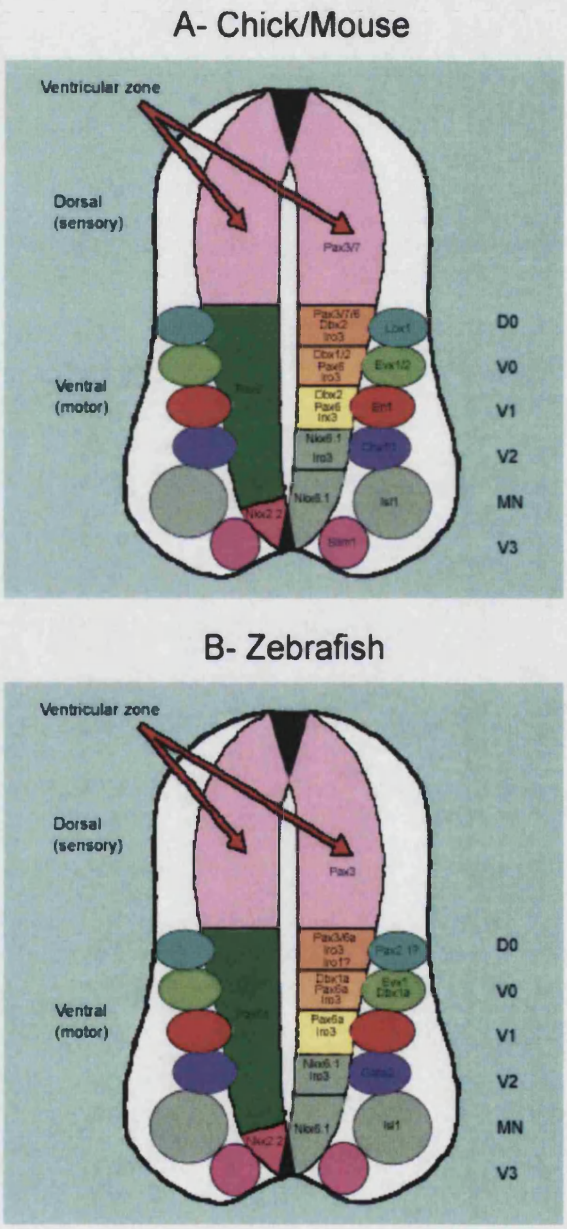

Figure 4-24 Expression pattern of class I and class II homeodomain proteins and their relationship to classes of neurons in mouse and chick (A) and in zebrafish (B). Information in panel B is in part presented in this thesis or inferred by analogy with the mouse and chick situations. Adapted from (Goulding and Lamar, 2000).

To study the role of zebrafish Gli3 in spinal cord patterning in particular and in zebrafish embryonic development in general, I first cloned *gli3* and mapped it to linkage group 24. When compared to the other zebrafish Gli proteins, Gli3 shares approximately 30% identity with Gli2 and approximately 40% identity with Gli1. When vertebrate Gli proteins are expressed in *Drosophila* only Gli2 and Gli3 are processed and can be found in both a cleaved repressor form and a full-length activator form (Aza-Blanc et al., 2000). Consistent with this observation 6 out of the 13 serines that are believed to be phosphorylated prior to cleavage are absent from the mouse Gli1 sequence. In contrast, in the zebrafish Gli1 sequence only 2 of these serines are missing (see Figure 4-9). This raises the possibility that zebrafish Gli1 may have dual activator/repressor functions.

Following the cloning of the zebrafish *gli3* gene, I studied its expression pattern during development. The signal observed in 8-cell stage embryos reveals that there is a considerable maternal contribution at the mRNA level (see Figure 4-11, panel A). At the time of the on-set of zygotic expression, *gli3* transcripts can be observed at high levels in the whole embryo (see Figure 4-11, panel B). These high levels are maintained at shield stage but by 5-somites expression seems to be weaker and more concentrated in the head and axial tissue, presumably the neural tube (see Figure 4-11, panels C-F). By 24hr *gli3* mRNA levels are low but ubiquitously expressed.

The expression pattern of *gli3* observed is quite different from that reported in other organisms. In frogs, *gli3* is not maternal but is first detected at early gastrula stages, a time when *Shh* transcripts are still undetectable (Lee et al., 1997). At mid-blastula stages it is expressed in neural plate folds and posterior mesoderm (Lee et al., 1997). At neurula stages it is absent from the midline but present around it with highest levels laterally (Lee et al., 1997). Finally, in the spinal cord *gli3* is restricted to the dorsal ventricular zone although it is not present in the roof plate (Lee et al., 1997). Similarly, in mice, the expression of *Gli3* is seen in the neural plate and later in the spinal cord confined to the dorsal ventricular zone (Hynes et al., 1997; Lee et al., 1997).

The expression pattern of *gli3* is distinct from the other zebrafish *gli* genes. Both *gli1/detour* and *gli2/you-too* transcripts are first detected at 80% epiboly in the anterior neural plate and pre-somitic mesoderm (Karlstrom et al., 1999; Karlstrom et al., 2003). Later in development *gli1/detour* is expressed ventrally in the spinal cord, but excluded from the floor plate (Karlstrom et al., 2003), whereas *gli2/you-too* is expressed in more dorsal regions of the neural tube (Karlstrom et al., 1999).

Disruption of zebrafish Gli3 by MO injection leads to a variety of defects obvious by 24hpf (see Figure 4-13). The brain of these morphants is smaller than control embryos, specifically in the midbrain region. In addition, these embryos have u-shaped somites and curly tails.

To check whether Shh signalling was affected in *gli3* morphants I analysed the expression pattern of *shh* and two direct targets, *ptc1* and *nkx2.2*. There is no obvious difference in the expression of these markers in experimental embryos (see Figure 4-14). This is in contrast with what is reported for the zebrafish *gli* mutants *detour* and *you-too*. In *yot* fish, the rostral *nkx2.2* expression in the anterior pituitary is absent and *ptc1* expression is reduced throughout the brain and absent in the post-optic area (Karlstrom et al., 1999). Likewise, *nkx2.2* is absent in the spinal cord and some regions of the ventral forebrain and midbrain and reduced in the anterior pituitary anlage of *dtr* embryos (Karlstrom et al., 2003).

As spinal cord patterning is affected in the mouse Gli3 mutant I wanted to know whether a similar defect occurs in zebrafish *gli3* morphant. The expression of *nkx2.2, nkx6.1, dbx1a* and *pax3* in these embryos is similar to that of control embryos (see Figure 4-15). The only patterning defect detected is a reduction in *isl*$^{+}$ motor neurons. Instead of an almost continuous row of *isl*$^{+}$ motor neurons, only a subset are present, spaced roughly 1 somite apart. One possibility is that these cells are primary motor neurons and that secondary motor neuron generation might be prevented in the absence of Gli3.

Despite the fact that *gli3* morphants display normal expression of Shh targets and a reasonably normally patterned spinal cord, it is clear that other embryonic processes are affected. Before the embryos have a fully developed spinal cord they show gross phenotypic abnormalities. By the 5-somite stage, embryos injected with *gli3* morpholino are severely shortened, whereas control embryos at the same stage have normal length body axis (see Figure 4-16). Moreover, somites of *gli3* morphants are thinner and wider than somites of control embryos (see Figure 4-16).

In general, while none of the markers tested at the 5-somite stage are quantitatively different in gli3 morphants, their pattern is strikingly distinct from control embryos (see Figure 4-17). In particular, *isl1*$^{+}$ Rohon-Beard neurons and *dbx1a*$^{+}$ interneurons are much further from the midline than corresponding neurons in control embryos. Midline expression of *nkx6.1* is broader and holes in the expression domain can be observed. Pronephric mesoderm is displaced laterally as seen by expression of *pax2.1*. Finally,

the neural expression of *pax3* is also displaced to the sides of the embryo (see Figure 4-17). The fact that expression of these markers is displaced laterally in *gli3* morphants is consistent with a defect in convergence-extension. The medio-lateral intercalation of cells at the midline results in a lenghtening of the axis. As a result of the disruption of this process, the embryos are shorter and have wider neural plates, in a way that resembles the *gli3* morphant phenotype.

The polarized movements of cells undergoing CE are controlled by homologues of genes that control the polarity of epithelial cells in *Drosophila* (for a review see (Keller, 2002)). In *Xenopus* and zebrafish Silberblick/Wnt11 and Pipetail/Wnt5a are two of the ligands of the PCP pathway necessary for normal convergence-extension (Heisenberg et al., 2000; Moon et al., 1993; Rauch et al., 1997; Tada and Smith, 2000). Since injection of MO targeting Silberblick/Wnt11 phenocopies the mutation (Lele et al., 2001), I made use of *silberblick* morphants as a sensitised background to test the role of Gli3 in CE. Co-injection of *gli3* and *silberblick* morpholinos results in embryos with more dramatic defects than either morphant alone (see Figure 4-18). These results raise the possibility that Gli3 may be part of a signalling pathway important for CE and parallel to the PCP.

At 40% epiboly *gli3* morphants are still undistinguishable from control embryos but major signalling pathways that control germ layer formation are already operating. My marker analysis shows that both nodal genes and nodal-responsive genes are up-regulated following injection of morpholino targeting *gli3* (see Figure 4-19).

Nodal proteins, like BMPs, are part of the TGFβ family of secreted proteins. There are three nodal-related proteins in zebrafish but attention has been mainly focused on *cyclops (cyc)* and *squint (sqt)* (Long et al., 2003). Like BMP signalling, Nodal signalling has been implicated in ventral neural tube cell fate specification. Zebrafish nodal mutants have revealed the importance of this signalling pathway in the specification of axial structures, in particular the floor plate. Medial floor plate is absent from zebrafish *cyc*, *sqt*, and *one-eyed-pinhead* (*oep*) mutants (Feldman et al., 1998; Hatta et al., 1991; Odenthal et al., 2000; Strähle et al., 1997). The *oep* gene encodes an EGF-CFC protein that acts as an extra-cellular co-factor for Nodal signalling (Gritsman et al., 1999).

The fact that nodal mutants lack medial floor plate suggests an interaction between the Hh and the Nodal signalling pathways in this process. In both *cyc* and *oep* mutants the medial floor plate defect is corrected on the second day of development suggesting compensatory pathways (Odenthal et al., 2000; Strähle et al., 1997). Moreover,

ectopic expression of Shh induces expression of floor-plate marker genes in the *oep* mutant neural tube in a manner indistinguishable from wild-type embryos (Strähle et al., 1997).

Nodal signalling is also required for regional patterning of the forebrain in zebrafish (Rohr et al., 2001). Nodal mutants have several degrees of cyclopia and complete absence of *nkx2.1a*-expressing expressing cells in the hypothalamus and of *nkx2.1a* and *nkx2.1b*-expressing cells in the ventral telencephalon (Rohr et al., 2001). Interestingly, Hh signalling is both required and sufficient to specify ventral telencephalic *nkx2.1b* expression, even in Nodal mutants (Rohr et al., 2001). These results imply that Hh signalling acts downstream of nodal activity in DV patterning of the telencephalon (Rohr et al., 2001).

The up-regulation of nodal genes and nodal-responsive genes in *gli3* morphants highlights a link between Hh and Nodal signalling that had been suggested before. However, how to interpret the phenotype will need further analysis. In particular, it is equally conceivable that there is an increase in Nodal production or an increase in Nodal-signalling responsiveness, due to the fact that Sqt up-regulates its own transcription and that of *cyc* (Chen and Schier, 2002; Feldman et al., 2002). To address this question, *gli3* MO injections could be carried out in *squint*$^{-/-}$ embryos. If these embryos show a rescue of their *squint* phenotype and have control levels of *cyc* transcript, it would mean that absence of Gli3 leads to an increase in Nodal responsiveness. An easy way of scoring the *squint* phenotype would be to look at cyclopia, since *gli3* morphants do not have a cyclopean phenotype.

The fact that Nodal signalling is up-regulated in the absence of Gli3 suggests an explanation of the CE phenotype of these morphants. In frogs, it is well established that Activin or Nodals operating through a common pathway activate *Xbra* expression in an immediate-early fashion (Smith et al., 1991). The mesoderm-specific Xbra function is required for posterior mesoderm and notochord differentiation in mouse, zebrafish, and *Xenopus* embryos (Conlon et al., 1996; Herrmann et al., 1990; Schulte-Merker et al., 1994). Apart from mesoderm formation, Xbra also plays a role in morphogenetic movements (Conlon and Smith, 1999; Wilson et al., 1995). This function of Xbra became clear when it was noticed that *Xwnt11* is one of its targets and it is involved in the Wnt PCP pathway that controls CE (Heisenberg et al., 2000; Tada and Smith, 2000). The CE phenotype of *gli3* morphants could be explained as a consequence of up-regulating Nodal signalling. Indeed, over-specification of mesendoderm may result in diminished BMP signalling, which in turn produces a phenotype that closely resembles a CE phenotype.

The *gli3* morphant phenotype at 5-somites appears to be rescued when embryos are incubated in cyclopamine from shield stage until fixation (see Figure 4-22, Figure 4-23). Cyclopamine is a Hh signalling antagonist that directly inhibits Smoothened activity (Chen et al., 2002). Although the rescue of the morphant phenotype with cyclopamine is in agreement with the observation that in Shh/Gli3 and Gli3/Smo double mutant mice there is a rescue of the Shh and Smo spinal cord phenotype (Litingtung and Chiang, 2000; Persson et al., 2002; Wijgerde et al., 2002), it is difficult to interpret. The rescue is evident at 5-somites but no longer observed in embryos that remain in cyclopamine-containing buffer until 24hpf (data not shown). It seems that there is particular window in zebrafish development, between shield stage and 5-somite stage, in which cyclopamine can rescue the effects of injection of *gli3* morpholino. One possible interpretation of these results is that Gli3 during this window of development is dedicated to inhibiting Hh signalling, whereas before and/or later on in development plays a role in other Hh-independent processes.

The Gli3 protein seems to have an important function in the development of the zebrafish embryo. The possible relation to Nodal signalling is of particular interest. Hh and Nodal pathways had been postulated to cooperatively pattern the zebrafish ventral spinal cord through studies in mutants. Specifically, for specification of floor plate both pathways seem to be important: nodal mutants lack medial floor plate (Feldman et al., 1998; Hatta et al., 1991; Odenthal et al., 2000; Strähle et al., 1997); and hedgehog mutants and morphants lack lateral floor plate (Etheridge et al., 2001; Lewis and Eisen, 2001; Nasevicius and Ekker, 2000; Odenthal et al., 2000; Schauerte et al., 1998). Moreover, there is evidence that the two pathways interact. Nodal signalling has been shown to induce *shh* in ventral neural tubes of zebrafish and chick embryos (Muller et al., 2000). Conversely, ectopic expression of Shh rescues the floor plate phenotype of *oep* (Strähle et al., 1997). My work raises the possibility that interaction between these signalling pathways might occur via Gli3 acting as a common mediator.

Appendices

5 Appendices

5.1 List of zebrafish *rab* genes identified

Table 5-1 Zebrafish *rab* genes identified in this study and the corresponding closest orthologues proteins and their database accession numbers (Pereira-Leal and Seabra, 2001).

Proposed name (gene)	Accession number	Closest ortholog (protein)	Ortholog accession number (protein)
rab1a1	-	HsRab1a	NP_004152
rab1a2	BC047816	HsRab1a	NP_004152
rab1b	BC050239	HsRab1b	NP_112243
rab2a1	BC044459	HsRab2a	NP_002856
rab2a2	-	HsRab2a	NP_002856
-	-	HsRab2b	AAF00042
rab3a	-	HsRab3a	NP_002857
rab3b	-	HsRab3b	NP_002858
rab3c1	-	HsRab3c	NP_612462
rab3c2	-	HsRab3c	NP_612462
-	-	HsRab3d	NP_04274
rab4a	BX001007**	HsRab4a	NP_004569
-	-	HsRab4b	NP_057238
rab5a1	BC047803	HsRab5a	NP_004153
rab5a2	BC049057	HsRab5a	NP_004153
*rab5b**	-	HsRab5b	NP_002859
rab5c	BC045466	HsRab5c	AAF66594
rab6a1	BC044491	HsRab6a	P20340
rab6a2	-	HsRab6a	P20340
*rab6b1**	-	HsRab6b	NP_057661

*rab6b2**	AL935299**	HsRab6b	NP_057661
-	-	HsRab6c	CAB66661
*rab7a**	-	HsRab7	P51149
rab7b	-	HsRab7	P51149
-	-	HsRab8a	NP_005361
*rab8b**	-	HsRab8b	NP_057614
*rab9a**	-	HsRab9a	NP_004242
-	-	HsRab9b	NP_057454
rab10	-	HsRab10	NP_057215
rab11a1	-	HsRab11a	NP_004654
*rab11a2**	-	HsRab11a	NP_004654
rab11b1	AL929146**	HsRab11b	NP_004209
rab11b2	BC048889	HsRab11b	NP_004209
rab12	-	CfRab12	P51152
rab13	BX004983**	HsRab13	NP_002861
rab14a	BC045374	HsRab14	NP_057406
*rab14b**	-	HsRab14	NP_057406
*rab14c**	-	HsRab14	NP_057406
*rab14d**	-	HsRab14	NP_057406
rab15	BX255891**	HsRab15	P59190
-	-	HsRab17	BAB14121
rab18	-	HsRab18	NP_067075
*rab19a**	-	HsRab19	XP_294312
rab19b	AL954173**	HsRab19	XP_294312
rab20	-	HsRab20	NP_060287
*rab21**	-	HsRab21	NP_055814
*rab22a**	-	HsRab22a	AAF00047

*rab22b**	-	HsRab22b	NP_006859
-	-	HsRab22c	IGI_M!_CTG66_20
rab23	-	HsRab23	AAM21099
-	-	HsRab24	BAB13887
rab25	-	HsRab25	P57735
*rab26**	-	HsRab26	NP_055168
rab27a	-	HsRab27a	NP_004571
*rab27b**	-	HsRab27b	NP_004154
rab28	BC045389	HsRab28	AAH35054
-	-	HsRab29	NP_003920
*rab30**	-	HsRab30	NP_055303
rab32a	BC049531	HsRab32	NP_006825
*rab32b**	-	HsRab32	NP_006825
rab33a	-	HsRab33a	NP_004785
*rab33b**	AL929007**	HsRab33b	NP_112586
*rab34**	-	HsRab34	AAP36669
rab35a	AL954693**	HsRab35	NP_006852
rab35b	-	HsRab35	NP_006852
*rab35c**	AL928885**	HsRab35	NP_006852
*rab36**	-	HsRab36	NP_004905
*rab37**	-	HsRab37	Q96AX2
*rab38**	-	HsRab38	NP_071732
-	-	HsRab39a	CAA68227
rab39b1	-	HsRab39b	NP_741995
*rab39b2**	-	HsRab39b	NP_741995
rab39b3	AL954129**	HsRab39b	NP_741995
-	-	HsRab40a	CAB09136

-	-	HsRab40b	NP_006813
rab40c	BX470132**	HsRab40c	Q96S21
-	-	HsRab41	IGI_M1_CTG19178_2

*-zebrafish *rab* genes for which the sequence is not complete.

**-genomic sequence.

References

Akimaru, H., Chen, Y., Dai, P., Hou, D. X., Nonaka, M., Smolik, S. M., Armstrong, S., Goodman, R. H. and Ishii, S. (1997). Drosophila CBP is a co-activator of cubitus interruptus in hedgehog signalling. *Nature* 386, 735-8.

Akimenko, M. A., Ekker, M., Wegner, J., Lin, W. and Westerfield, M. (1994). Combinatorial expression of three zebrafish genes related to distal-less: part of a homeobox gene code for the head. *J Neurosci* 14, 3475-86.

Alcedo, J., Ayzenzon, M., Von Ohlen, T., Noll, M. and Hooper, J. E. (1996). The Drosophila smoothened gene encodes a seven-pass membrane protein, a putative receptor for the hedgehog signal. *Cell* 86, 221-32.

Allan, B. B., Moyer, B. D. and Balch, W. E. (2000). Rab1 recruitment of p115 into a cis-SNARE complex: programming budding COPII vesicles for fusion. *Science* 289, 444-8.

Alves, G., Limbourg-Bouchon, B., Tricoire, H., Brissard-Zahraoui, J., Lamour-Isnard, C. and Busson, D. (1998). Modulation of Hedgehog target gene expression by the Fused serine-threonine kinase in wing imaginal discs. *Mech Dev* 78, 17-31.

Anant, J. S., Desnoyers, L., Machius, M., Demeler, B., Hansen, J. C., Westover, K. D., Deisenhofer, J. and Seabra, M. C. (1998). Mechanism of Rab geranylgeranylation: formation of the catalytic ternary complex. *Biochemistry* 37, 12559-68.

Andrews, H. K., Zhang, Y. Q., Trotta, N. and Broadie, K. (2002). Drosophila Sec10 is Required for Hormone Secretion but not General Exocytosis or Neurotransmission. *Traffic* 3, 906-21.

Appel, B., Korzh, V., Glasgow, E., Thor, S., Edlund, T., Dawid, I. B. and Eisen, J. S. (1995). Motoneuron fate specification revealed by patterned LIM homeobox gene expression in embryonic zebrafish. *Development* 121, 4117-25.

Aza-Blanc, P. and Kornberg, T. B. (1999). Ci: a complex transducer of the hedgehog signal. *Trends Genet* 15, 458-62.

Aza-Blanc, P., Lin, H. Y., Ruiz i Altaba, A. and Kornberg, T. B. (2000). Expression of the vertebrate Gli proteins in Drosophila reveals a distribution of activator and repressor activities. *Development* 127, 4293-301.

Aza-Blanc, P., Ramirez-Weber, F. A., Laget, M. P., Schwartz, C. and Kornberg, T. B. (1997). Proteolysis that is inhibited by hedgehog targets Cubitus interruptus protein to the nucleus and converts it to a repressor. *Cell* 89, 1043-53.

Bai, C. B., Auerbach, W., Lee, J. S., Stephen, D. and Joyner, A. L. (2002). Gli2, but not Gli1, is required for initial Shh signaling and ectopic activation of the Shh pathway. *Development* 129, 4753-61.

Bakkers, J., Hild, M., Kramer, C., Furutani-Seiki, M. and Hammerschmidt, M. (2002). Zebrafish DeltaNp63 is a direct target of Bmp signaling and encodes a transcriptional repressor blocking neural specification in the ventral ectoderm. *Dev Cell* 2, 617-27.

Bao, S., Zhu, J. and Garvey, W. T. (1998). Cloning of Rab GTPases expressed in human skeletal muscle: studies in insulin-resistant subjects. *Horm Metab Res* 30, 656-62.

Barbieri, M. A., Roberts, R. L., Gumusboga, A., Highfield, H., Alvarez-Dominguez, C., Wells, A. and Stahl, P. D. (2000). Epidermal growth factor and membrane trafficking. EGF receptor activation of endocytosis requires Rab5a. *J Cell Biol* 151, 539-50.

Barth, K. A., Kishimoto, Y., Rohr, K. B., Seydler, C., Schulte-Merker, S. and Wilson, S. W. (1999). Bmp activity establishes a gradient of positional information throughout the entire neural plate. *Development* 126, 4977-87.

Barth, K. A. and Wilson, S. W. (1995). Expression of zebrafish nk2.2 is influenced by sonic hedgehog/vertebrate hedgehog-1 and demarcates a zone of neuronal differentiation in the embryonic forebrain. *Development* 121, 1755-68.

Bellaiche, Y., The, I. and Perrimon, N. (1998). Tout-velu is a Drosophila homologue of the putative tumour suppressor EXT-1 and is needed for Hh diffusion. *Nature* 394, 85-8.

Bernhardt, R. R., Chitnis, A. B., Lindamer, L. and Kuwada, J. Y. (1990). Identification of spinal neurons in the embryonic and larval zebrafish. *J Comp Neurol* 302, 603-16.

Bielli, A., Thornqvist, P. O., Hendrick, A. G., Finn, R., Fitzgerald, K. and McCaffrey, M. W. (2001). The small GTPase Rab4A interacts with the central region of cytoplasmic dynein light intermediate chain-1. *Biochem Biophys Res Commun* 281, 1141-53.

Bitgood, M. J. and McMahon, A. P. (1995). Hedgehog and Bmp genes are coexpressed at many diverse sites of cell-cell interaction in the mouse embryo. *Dev Biol* 172, 126-38.

Blanchette-Mackie, E. J. (2000). Intracellular cholesterol trafficking: role of the NPC1 protein. *Biochim Biophys Acta* 1486, 171-83.

Bock, J. B., Matern, H. T., Peden, A. A. and Scheller, R. H. (2001). A genomic perspective on membrane compartment organization. *Nature* 409, 839-41.

Bose, J., Grotewold, L. and Ruther, U. (2002). Pallister-Hall syndrome phenotype in mice mutant for Gli3. *Hum Mol Genet* 11, 1129-35.

Brand, M., Heisenberg, C. P., Warga, R. M., Pelegri, F., Karlstrom, R. O., Beuchle, D., Picker, A., Jiang, Y. J., Furutani-Seiki, M., van Eeden, F. J. et al. (1996). Mutations affecting development of the midline and general body shape during zebrafish embryogenesis. *Development* 123, 129-42.

Briscoe, J., Chen, Y., Jessell, T. M. and Struhl, G. (2001). A hedgehog-insensitive form of patched provides evidence for direct long-range morphogen activity of sonic hedgehog in the neural tube. *Mol Cell* 7, 1279-91.

Briscoe, J. and Ericson, J. (2001). Specification of neuronal fates in the ventral neural tube. *Curr Opin Neurobiol* 11, 43-9.

Briscoe, J., Pierani, A., Jessell, T. M. and Ericson, J. (2000). A homeodomain protein code specifies progenitor cell identity and neuronal fate in the ventral neural tube. *Cell* 101, 435-45.

Briscoe, J., Sussel, L., Serup, P., Hartigan-O'Connor, D., Jessell, T. M., Rubenstein, J. L. and Ericson, J. (1999). Homeobox gene Nkx2.2 and specification of neuronal identity by graded Sonic hedgehog signalling. *Nature* 398, 622-7.

Brymora, A., Valova, V. A., Larsen, M. R., Roufogalis, B. D. and Robinson, P. J. (2001). The brain exocyst complex interacts with RalA in a GTP-dependent manner: identification of a novel mammalian Sec3 gene and a second Sec15 gene. *J Biol Chem* 276, 29792-7.

Bucci, C., Lutcke, A., Dupree, P. and Zerial, M. (1995). Guidebook to the small GTPases. Oxford: Oxford University Press.

Bucci, C., Parton, R. G., Mather, I. H., Stunnenberg, H., Simons, K., Hoflack, B. and Zerial, M. (1992). The small GTPase rab5 functions as a regulatory factor in the early endocytic pathway. *Cell* 70, 715-28.

Bucci, C., Thomsen, P., Nicoziani, P., McCarthy, J. and van Deurs, B. (2000). Rab7: a key to lysosome biogenesis. *Mol Biol Cell* 11, 467-80.

Bumcrot, D. A., Takada, R. and McMahon, A. P. (1995). Proteolytic processing yields two secreted forms of sonic hedgehog. *Mol Cell Biol* 15, 2294-303.

Burke, R., Nellen, D., Bellotto, M., Hafen, E., Senti, K. A., Dickson, B. J. and Basler, K. (1999). Dispatched, a novel sterol-sensing domain protein dedicated to the release of cholesterol-modified hedgehog from signaling cells. *Cell* 99, 803-15.

Burns, M. E., Sasaki, T., Takai, Y. and Augustine, G. J. (1998). Rabphilin-3A: a multifunctional regulator of synaptic vesicle traffic. *J Gen Physiol* 111, 243-55.

Burrill, J. D., Moran, L., Goulding, M. D. and Saueressig, H. (1997). PAX2 is expressed in multiple spinal cord interneurons, including a population of EN1+ interneurons that require PAX6 for their development. *Development* 124, 4493-503.

Cantalupo, G., Alifano, P., Roberti, V., Bruni, C. B. and Bucci, C. (2001). Rab-interacting lysosomal protein (RILP): the Rab7 effector required for transport to lysosomes. *Embo J* 20, 683-93.

Capdevila, J., Pariente, F., Sampedro, J., Alonso, J. L. and Guerrero, I. (1994). Subcellular localization of the segment polarity protein patched suggests an interaction with the wingless reception complex in Drosophila embryos. *Development* 120, 987-98.

Carroll, K. S., Hanna, J., Simon, I., Krise, J., Barbero, P. and Pfeffer, S. R. (2001). Role of Rab9 GTPase in facilitating receptor recruitment by TIP47. *Science* 292, 1373-6.

Carstea, E. D., Morris, J. A., Coleman, K. G., Loftus, S. K., Zhang, D., Cummings, C., Gu, J., Rosenfeld, M. A., Pavan, W. J., Krizman, D. B. et al. (1997). Niemann-Pick C1 disease gene: homology to mediators of cholesterol homeostasis. *Science* 277, 228-31.

Casanova, J. E., Wang, X., Kumar, R., Bhartur, S. G., Navarre, J., Woodrum, J. E., Altschuler, Y., Ray, G. S. and Goldenring, J. R. (1999). Association of Rab25 and

Rab11a with the apical recycling system of polarized Madin-Darby canine kidney cells. *Mol Biol Cell* 10, 47-61.

Caspary, T., Garcia-Garcia, M. J., Huangfu, D., Eggenschwiler, J. T., Wyler, M. R., Rakeman, A. S., Alcorn, H. L. and Anderson, K. V. (2002). Mouse Dispatched homolog1 is required for long-range, but not juxtacrine, Hh signaling. *Curr Biol* 12, 1628-32.

Chamoun, Z., Mann, R. K., Nellen, D., von Kessler, D. P., Bellotto, M., Beachy, P. A. and Basler, K. (2001). Skinny hedgehog, an acyltransferase required for palmitoylation and activity of the hedgehog signal. *Science* 293, 2080-4.

Chattopadhyay, D., Langsley, G., Carson, M., Recacha, R., DeLucas, L. and Smith, C. (2000). Structure of the nucleotide-binding domain of Plasmodium falciparum rab6 in the GDP-bound form. *Acta Crystallogr D Biol Crystallogr* 56 (Pt 8), 937-44.

Chen, C. H., von Kessler, D. P., Park, W., Wang, B., Ma, Y. and Beachy, P. A. (1999). Nuclear trafficking of Cubitus interruptus in the transcriptional regulation of Hedgehog target gene expression. *Cell* 98, 305-16.

Chen, D., Guo, J., Miki, T., Tachibana, M. and Gahl, W. A. (1997). Molecular cloning and characterization of rab27a and rab27b, novel human rab proteins shared by melanocytes and platelets. *Biochem Mol Med* 60, 27-37.

Chen, J. K., Taipale, J., Cooper, M. K. and Beachy, P. A. (2002). Inhibition of Hedgehog signaling by direct binding of cyclopamine to Smoothened. *Genes Dev* 16, 2743-8.

Chen, W., Burgess, S. and Hopkins, N. (2001). Analysis of the zebrafish smoothened mutant reveals conserved and divergent functions of hedgehog activity. *Development* 128, 2385-96.

Chen, X. and Wang, Z. (2001). Regulation of intracellular trafficking of the EGF receptor by Rab5 in the absence of phosphatidylinositol 3-kinase activity. *EMBO Rep* 2, 68-74.

Chen, Y., Gallaher, N., Goodman, R. H. and Smolik, S. M. (1998). Protein kinase A directly regulates the activity and proteolysis of cubitus interruptus. *Proc Natl Acad Sci U S A* 95, 2349-54.

Chen, Y. and Schier, A. F. (2002). Lefty proteins are long-range inhibitors of squint-mediated nodal signaling. *Curr Biol* 12, 2124-8.

Chen, Y. and Struhl, G. (1996). Dual roles for patched in sequestering and transducing Hedgehog. *Cell* 87, 553-63.

Chen, Y. A. and Scheller, R. H. (2001). SNARE-mediated membrane fusion. *Nat Rev Mol Cell Biol* 2, 98-106.

Cheng, S. Y. and Bishop, J. M. (2002). Suppressor of Fused represses Gli-mediated transcription by recruiting the SAP18-mSin3 corepressor complex. *Proc Natl Acad Sci U S A* 99, 5442-7.

Chiang, C., Litingtung, Y., Lee, E., Young, K. E., Corden, J. L., Westphal, H. and Beachy, P. A. (1996). Cyclopia and defective axial patterning in mice lacking Sonic hedgehog gene function. *Nature* 383, 407-13.

Christoforidis, S., McBride, H. M., Burgoyne, R. D. and Zerial, M. (1999a). The Rab5 effector EEA1 is a core component of endosome docking. *Nature* 397, 621-5.

Christoforidis, S., Miaczynska, M., Ashman, K., Wilm, M., Zhao, L., Yip, S. C., Waterfield, M. D., Backer, J. M. and Zerial, M. (1999b). Phosphatidylinositol-3-OH kinases are Rab5 effectors. *Nat Cell Biol* 1, 249-52.

Christoforidis, S. and Zerial, M. (2000). Purification and identification of novel Rab effectors using affinity chromatography. *Methods* 20, 403-10.

Chuang, P. T. and McMahon, A. P. (1999). Vertebrate Hedgehog signalling modulated by induction of a Hedgehog-binding protein. *Nature* 397, 617-21.

Chung, S. H., Song, W. J., Kim, K., Bednarski, J. J., Chen, J., Prestwich, G. D. and Holz, R. W. (1998). The C2 domains of Rabphilin3A specifically bind phosphatidylinositol 4,5-bisphosphate containing vesicles in a Ca2+-dependent manner. In vitro characteristics and possible significance. *J Biol Chem* 273, 10240-8.

Collins, R. N. and Brennwald, P. (2000). Rab. In *GTPases*, (ed. A. Hall), pp. 137-175. Oxford: Oxford University Press.

Concordet, J. P., Lewis, K. E., Moore, J. W., Goodrich, L. V., Johnson, R. L., Scott, M. P. and Ingham, P. W. (1996). Spatial regulation of a zebrafish patched homologue

reflects the roles of sonic hedgehog and protein kinase A in neural tube and somite patterning. *Development* 122, 2835-46.

Conlon, F. L., Sedgwick, S. G., Weston, K. M. and Smith, J. C. (1996). Inhibition of Xbra transcription activation causes defects in mesodermal patterning and reveals autoregulation of Xbra in dorsal mesoderm. *Development* 122, 2427-35.

Conlon, F. L. and Smith, J. C. (1999). Interference with brachyury function inhibits convergent extension, causes apoptosis, and reveals separate requirements in the FGF and activin signalling pathways. *Dev Biol* 213, 85-100.

Cooper, M. K., Porter, J. A., Young, K. E. and Beachy, P. A. (1998). Teratogen-mediated inhibition of target tissue response to Shh signaling. *Science* 280, 1603-7.

Coppola, T., Frantz, C., Perret-Menoud, V., Gattesco, S., Hirling, H. and Regazzi, R. (2002). Pancreatic beta-cell protein granuphilin binds Rab3 and Munc-18 and controls exocytosis. *Mol Biol Cell* 13, 1906-15.

Cormont, M., Mari, M., Galmiche, A., Hofman, P. and Le Marchand-Brustel, Y. (2001). A FYVE-finger-containing protein, Rabip4, is a Rab4 effector involved in early endosomal traffic. *Proc Natl Acad Sci U S A* 98, 1637-42.

Coutinho, P. J. C. S. (2001). Molecular Characterization of *sneezy*, a Notochord Mutation, PhD Thesis, University College London.

Cremers, F. P., Armstrong, S. A., Seabra, M. C., Brown, M. S. and Goldstein, J. L. (1994). REP-2, a Rab escort protein encoded by the choroideremia-like gene. *J Biol Chem* 269, 2111-7.

Currie, P. D. and Ingham, P. W. (1996). Induction of a specific muscle cell type by a hedgehog-like protein in zebrafish. *Nature* 382, 452-5.

Dai, P., Akimaru, H. and Ishii, S. (2003). A hedgehog-responsive region in the Drosophila wing disc is defined by debra-mediated ubiquitination and lysosomal degradation of Ci. *Dev Cell* 4, 917-28.

Dai, P., Akimaru, H., Tanaka, Y., Maekawa, T., Nakafuku, M. and Ishii, S. (1999). Sonic Hedgehog-induced activation of the Gli1 promoter is mediated by GLI3. *J Biol Chem* 274, 8143-52.

Darchen, F. and Goud, B. (2000). Multiple aspects of Rab protein action in the secretory pathway: focus on Rab3 and Rab6. *Biochimie* 82, 375-84.

de Renzis, S., Sonnichsen, B. and Zerial, M. (2002). Divalent Rab effectors regulate the sub-compartmental organization and sorting of early endosomes. *Nat Cell Biol* 4, 124-33.

DeBose-Boyd, R. A., Brown, M. S., Li, W. P., Nohturfft, A., Goldstein, J. L. and Espenshade, P. J. (1999). Transport-dependent proteolysis of SREBP: relocation of site-1 protease from Golgi to ER obviates the need for SREBP transport to Golgi. *Cell* 99, 703-12.

Denef, N., Neubuser, D., Perez, L. and Cohen, S. M. (2000). Hedgehog induces opposite changes in turnover and subcellular localization of patched and smoothened. *Cell* 102, 521-31.

Deneka, M. and van der Sluijs, P. (2002). 'Rab'ing up endosomal membrane transport. *Nat Cell Biol* 4, E33-5.

Detrich, H. W., 3rd, Kieran, M. W., Chan, F. Y., Barone, L. M., Yee, K., Rundstadler, J. A., Pratt, S., Ransom, D. and Zon, L. I. (1995). Intraembryonic hematopoietic cell migration during vertebrate development. *Proc Natl Acad Sci U S A* 92, 10713-7.

Detter, J. C., Zhang, Q., Mules, E. H., Novak, E. K., Mishra, V. S., Li, W., McMurtrie, E. B., Tchernev, V. T., Wallace, M. R., Seabra, M. C. et al. (2000). Rab geranylgeranyl transferase alpha mutation in the gunmetal mouse reduces Rab prenylation and platelet synthesis. *Proc Natl Acad Sci U S A* 97, 4144-9.

Diez del Corral, R., Olivera-Martinez, I., Goriely, A., Gale, E., Maden, M. and Storey, K. (2003). Opposing FGF and retinoid pathways control ventral neural pattern, neuronal differentiation, and segmentation during body axis extension. *Neuron* 40, 65-79.

Ding, Q., Motoyama, J., Gasca, S., Mo, R., Sasaki, H., Rossant, J. and Hui, C. C. (1998). Diminished Sonic hedgehog signaling and lack of floor plate differentiation in Gli2 mutant mice. *Development* 125, 2533-43.

Drossopoulou, G., Lewis, K. E., Sanz-Ezquerro, J. J., Nikbakht, N., McMahon, A. P., Hofmann, C. and Tickle, C. (2000). A model for anteroposterior patterning of the vertebrate limb based on sequential long- and short-range Shh signalling and Bmp signalling. *Development* 127, 1337-48.

Dumas, J. J., Zhu, Z., Connolly, J. L. and Lambright, D. G. (1999). Structural basis of activation and GTP hydrolysis in Rab proteins. *Structure Fold Des* 7, 413-23.

Dunn, N. R., Winnier, G. E., Hargett, L. K., Schrick, J. J., Fogo, A. B. and Hogan, B. L. (1997). Haploinsufficient phenotypes in Bmp4 heterozygous null mice and modification by mutations in Gli3 and Alx4. *Dev Biol* 188, 235-47.

Echard, A., Jollivet, F., Martinez, O., Lacapere, J. J., Rousselet, A., Janoueix-Lerosey, I. and Goud, B. (1998). Interaction of a Golgi-associated kinesin-like protein with Rab6. *Science* 279, 580-5.

Echard, A., Opdam, F. J., de Leeuw, H. J., Jollivet, F., Savelkoul, P., Hendriks, W., Voorberg, J., Goud, B. and Fransen, J. A. (2000). Alternative splicing of the human Rab6A gene generates two close but functionally different isoforms. *Mol Biol Cell* 11, 3819-33.

Echelard, Y., Epstein, D. J., St-Jacques, B., Shen, L., Mohler, J., McMahon, J. A. and McMahon, A. P. (1993). Sonic hedgehog, a member of a family of putative signaling molecules, is implicated in the regulation of CNS polarity. *Cell* 75, 1417-30.

Eggenschwiler, J. T. and Anderson, K. V. (2000). Dorsal and lateral fates in the mouse neural tube require the cell-autonomous activity of the open brain gene. *Dev Biol* 227, 648-60.

Eggenschwiler, J. T., Espinoza, E. and Anderson, K. V. (2001). Rab23 is an essential negative regulator of the mouse Sonic hedgehog signalling pathway. *Nature* 412, 194-8.

Eisen, J. S. (1992). The role of interactions in determining cell fate of two identified motoneurons in the embryonic zebrafish. *Neuron* 8, 231-40.

Eisen, J. S., Myers, P. Z. and Westerfield, M. (1986). Pathway selection by growth cones of identified motoneurones in live zebra fish embryos. *Nature* 320, 269-71.

Eisen, J. S. and Weston, J. A. (1993). Development of the neural crest in the zebrafish. *Dev Biol* 159, 50-9.

Ekker, S. C., Ungar, A. R., Greenstein, P., von Kessler, D. P., Porter, J. A., Moon, R. T. and Beachy, P. A. (1995). Patterning activities of vertebrate hedgehog proteins in the developing eye and brain. *Curr Biol* 5, 944-55.

Entchev, E. V., Schwabedissen, A. and Gonzalez-Gaitan, M. (2000). Gradient formation of the TGF-beta homolog Dpp. *Cell* 103, 981-91.

Erdman, R. A., Shellenberger, K. E., Overmeyer, J. H. and Maltese, W. A. (2000). Rab24 is an atypical member of the Rab GTPase family. Deficient GTPase activity, GDP dissociation inhibitor interaction, and prenylation of Rab24 expressed in cultured cells. *J Biol Chem* 275, 3848-56.

Ericson, J., Morton, S., Kawakami, A., Roelink, H. and Jessell, T. M. (1996). Two critical periods of Sonic Hedgehog signaling required for the specification of motor neuron identity. *Cell* 87, 661-73.

Ericson, J., Rashbass, P., Schedl, A., Brenner-Morton, S., Kawakami, A., van Heyningen, V., Jessell, T. M. and Briscoe, J. (1997). Pax6 controls progenitor cell identity and neuronal fate in response to graded Shh signaling. *Cell* 90, 169-80.

Erter, C. E., Solnica-Krezel, L. and Wright, C. V. (1998). Zebrafish nodal-related 2 encodes an early mesendodermal inducer signaling from the extraembryonic yolk syncytial layer. *Dev Biol* 204, 361-72.

Esters, H., Alexandrov, K., Constantinescu, A. T., Goody, R. S. and Scheidig, A. J. (2000). High-resolution crystal structure of S. cerevisiae Ypt51(DeltaC15)-GppNHp, a small GTP-binding protein involved in regulation of endocytosis. *J Mol Biol* 298, 111-21.

Etheridge, L. A., Wu, T., Liang, J. O., Ekker, S. C. and Halpern, M. E. (2001). Floor plate develops upon depletion of tiggy-winkle and sonic hedgehog. *Genesis* 30, 164-9.

Feldman, B., Concha, M. L., Saude, L., Parsons, M. J., Adams, R. J., Wilson, S. W. and Stemple, D. L. (2002). Lefty antagonism of Squint is essential for normal gastrulation. *Curr Biol* 12, 2129-35.

Feldman, B., Gates, M. A., Egan, E. S., Dougan, S. T., Rennebeck, G., Sirotkin, H. I., Schier, A. F. and Talbot, W. S. (1998). Zebrafish organizer development and germ-layer formation require nodal-related signals. *Nature* 395, 181-5.

Finger, F. P., Hughes, T. E. and Novick, P. (1998). Sec3p is a spatial landmark for polarized secretion in budding yeast. *Cell* 92, 559-71.

Fjose, A., Izpisua-Belmonte, J. C., Fromental-Ramain, C. and Duboule, D. (1994). Expression of the zebrafish gene hlx-1 in the prechordal plate and during CNS development. *Development* 120, 71-81.

Forbes, A. J., Nakano, Y., Taylor, A. M. and Ingham, P. W. (1993). Genetic analysis of hedgehog signalling in the Drosophila embryo. *Dev Suppl*, 115-24.

Fukuda, M., Kuroda, T. S. and Mikoshiba, K. (2002). Slac2-a/melanophilin, the missing link between Rab27 and myosin Va: implications of a tripartite protein complex for melanosome transport. *J Biol Chem* 277, 12432-6.

Fürthauer, M., Thisse, C. and Thisse, B. (1997). A role for FGF-8 in the dorsoventral patterning of the zebrafish gastrula. *Development* 124, 4253-64.

Gallet, A., Rodriguez, R., Ruel, L. and Therond, P. P. (2003). Cholesterol modification of hedgehog is required for trafficking and movement, revealing an asymmetric cellular response to hedgehog. *Dev Cell* 4, 191-204.

Gil, G., Faust, J. R., Chin, D. J., Goldstein, J. L. and Brown, M. S. (1985). Membrane-bound domain of HMG CoA reductase is required for sterol-enhanced degradation of the enzyme. *Cell* 41, 249-58.

Goltz, J. S., Wolkoff, A. W., Novikoff, P. M., Stockert, R. J. and Satir, P. (1992). A role for microtubules in sorting endocytic vesicles in rat hepatocytes. *Proc Natl Acad Sci U S A* 89, 7026-30.

Goodrich, L. V., Johnson, R. L., Milenkovic, L., McMahon, J. A. and Scott, M. P. (1996). Conservation of the hedgehog/patched signaling pathway from flies to mice: induction of a mouse patched gene by Hedgehog. *Genes Dev* 10, 301-12.

Gorvel, J. P., Chavrier, P., Zerial, M. and Gruenberg, J. (1991). rab5 controls early endosome fusion in vitro. *Cell* 64, 915-25.

Goud, B. (2002). How Rab proteins link motors to membranes. *Nat Cell Biol* 4, E77-8.

Goud, B., Zahraoui, A., Tavitian, A. and Saraste, J. (1990). Small GTP-binding protein associated with Golgi cisternae. *Nature* 345, 553-6.

Goulding, M. and Lamar, E. (2000). Neuronal patterning: Making stripes in the spinal cord. *Curr Biol* 10, R565-8.

Goulding, M., Sterrer, S., Fleming, J., Balling, R., Nadeau, J., Moore, K. J., Brown, S. D., Steel, K. P. and Gruss, P. (1993a). Analysis of the Pax-3 gene in the mouse mutant splotch. *Genomics* 17, 355-63.

Goulding, M. D., Lumsden, A. and Gruss, P. (1993b). Signals from the notochord and floor plate regulate the region-specific expression of two Pax genes in the developing spinal cord. *Development* 117, 1001-16.

Griffin, K., Patient, R. and Holder, N. (1995). Analysis of FGF function in normal and no tail zebrafish embryos reveals separate mechanisms for formation of the trunk and the tail. *Development* 121, 2983-94.

Gritsman, K., Talbot, W. S. and Schier, A. F. (2000). Nodal signaling patterns the organizer. *Development* 127, 921-32.

Gritsman, K., Zhang, J., Cheng, S., Heckscher, E., Talbot, W. S. and Schier, A. F. (1999). The EGF-CFC protein one-eyed pinhead is essential for nodal signaling. *Cell* 97, 121-32.

Gunther, T., Struwe, M., Aguzzi, A. and Schughart, K. (1994). Open brain, a new mouse mutant with severe neural tube defects, shows altered gene expression patterns in the developing spinal cord. *Development* 120, 3119-30.

Guo, W., Grant, A. and Novick, P. (1999a). Exo84p is an exocyst protein essential for secretion. *J Biol Chem* 274, 23558-64.

Guo, W., Roth, D., Walch-Solimena, C. and Novick, P. (1999b). The exocyst is an effector for Sec4p, targeting secretory vesicles to sites of exocytosis. *Embo J* 18, 1071-80.

Guo, W., Sacher, M., Barrowman, J., Ferro-Novick, S. and Novick, P. (2000). Protein complexes in transport vesicle targeting. *Trends Cell Biol* 10, 251-5.

Hales, C. M., Griner, R., Hobdy-Henderson, K. C., Dorn, M. C., Hardy, D., Kumar, R., Navarre, J., Chan, E. K., Lapierre, L. A. and Goldenring, J. R. (2001). Identification and characterization of a family of Rab11-interacting proteins. *J Biol Chem* 276, 39067-75.

Hales, C. M., Vaerman, J. P. and Goldenring, J. R. (2002). Rab11 family interacting protein 2 associates with Myosin Vb and regulates plasma membrane recycling. *J Biol Chem* 277, 50415-21.

Hatta, K., Kimmel, C. B., Ho, R. K. and Walker, C. (1991). The cyclops mutation blocks specification of the floor plate of the zebrafish central nervous system. *Nature* 350, 339-41.

Haubruck, H., Disela, C., Wagner, P. and Gallwitz, D. (1987). The ras-related ypt protein is an ubiquitous eukaryotic protein: isolation and sequence analysis of mouse cDNA clones highly homologous to the yeast YPT1 gene. *Embo J* 6, 4049-53.

Haynes, L. P., Evans, G. J., Morgan, A. and Burgoyne, R. D. (2001). A direct inhibitory role for the Rab3-specific effector, Noc2, in Ca2+-regulated exocytosis in neuroendocrine cells. *J Biol Chem* 276, 9726-32.

Heisenberg, C. P. and Nüsslein-Volhard, C. (1997). The function of silberblick in the positioning of the eye anlage in the zebrafish embryo. *Dev Biol* 184, 85-94.

Heisenberg, C. P., Tada, M., Rauch, G. J., Saude, L., Concha, M. L., Geisler, R., Stemple, D. L., Smith, J. C. and Wilson, S. W. (2000). Silberblick/Wnt11 mediates convergent extension movements during zebrafish gastrulation. *Nature* 405, 76-81.

Herrmann, B. G., Labeit, S., Poustka, A., King, T. R. and Lehrach, H. (1990). Cloning of the T gene required in mesoderm formation in the mouse. *Nature* 343, 617-22.

Hibino, H., Pironkova, R., Onwumere, O., Vologodskaia, M., Hudspeth, A. J. and Lesage, F. (2002). RIM binding proteins (RBPs) couple Rab3-interacting molecules (RIMs) to voltage-gated Ca(2+) channels. *Neuron* 34, 411-23.

Hicke, L. (2001). A new ticket for entry into budding vesicles-ubiquitin. *Cell* 106, 527-30.

Hill, E., Clarke, M. and Barr, F. A. (2000). The Rab6-binding kinesin, Rab6-KIFL, is required for cytokinesis. *Embo J* 19, 5711-9.

Horiuchi, H., Lippe, R., McBride, H. M., Rubino, M., Woodman, P., Stenmark, H., Rybin, V., Wilm, M., Ashman, K., Mann, M. et al. (1997). A novel Rab5 GDP/GTP exchange factor complexed to Rabaptin-5 links nucleotide exchange to effector recruitment and function. *Cell* 90, 1149-59.

Hsu, S. C., Ting, A. E., Hazuka, C. D., Davanger, S., Kenny, J. W., Kee, Y. and Scheller, R. H. (1996). The mammalian brain rsec6/8 complex. *Neuron* 17, 1209-19.

Hua, X., Nohturfft, A., Goldstein, J. L. and Brown, M. S. (1996). Sterol resistance in CHO cells traced to point mutation in SREBP cleavage-activating protein. *Cell* 87, 415-26.

Hui, C. C. and Joyner, A. L. (1993). A mouse model of greig cephalopolysyndactyly syndrome: the extra-toesJ mutation contains an intragenic deletion of the Gli3 gene. *Nat Genet* 3, 241-6.

Huizing, M., Anikster, Y. and Gahl, W. A. (2000). Hermansky-Pudlak syndrome and related disorders of organelle formation. *Traffic* 1, 823-35.

Hukriede, N. A., Joly, L., Tsang, M., Miles, J., Tellis, P., Epstein, J. A., Barbazuk, W. B., Li, F. N., Paw, B., Postlethwait, J. H. et al. (1999). Radiation hybrid mapping of the zebrafish genome. *Proc Natl Acad Sci U S A* 96, 9745-50.

Hynes, M., Stone, D. M., Dowd, M., Pitts-Meek, S., Goddard, A., Gurney, A. and Rosenthal, A. (1997). Control of cell pattern in the neural tube by the zinc finger transcription factor and oncogene Gli-1. *Neuron* 19, 15-26.

Incardona, J. P., Gaffield, W., Kapur, R. P. and Roelink, H. (1998). The teratogenic Veratrum alkaloid cyclopamine inhibits sonic hedgehog signal transduction. *Development* 125, 3553-62.

Incardona, J. P., Gaffield, W., Lange, Y., Cooney, A., Pentchev, P. G., Liu, S., Watson, J. A., Kapur, R. P. and Roelink, H. (2000a). Cyclopamine inhibition of Sonic hedgehog signal transduction is not mediated through effects on cholesterol transport. *Dev Biol* 224, 440-52.

Incardona, J. P., Gruenberg, J. and Roelink, H. (2002). Sonic hedgehog induces the segregation of patched and smoothened in endosomes. *Curr Biol* 12, 983-95.

Incardona, J. P., Lee, J. H., Robertson, C. P., Enga, K., Kapur, R. P. and Roelink, H. (2000b). Receptor-mediated endocytosis of soluble and membrane-tethered Sonic hedgehog by Patched-1. *Proc Natl Acad Sci U S A* 97, 12044-9.

Ingham, P. W. (1998). Boning up on Hedgehog's movements. *Nature* 394, 16-7.

Ingham, P. W. (2001). Hedgehog signaling: a tale of two lipids. *Science* 294, 1879-81.

Ingham, P. W. and McMahon, A. P. (2001). Hedgehog signaling in animal development: paradigms and principles. *Genes Dev* 15, 3059-87.

Ingham, P. W., Taylor, A. M. and Nakano, Y. (1991). Role of the Drosophila patched gene in positional signalling. *Nature* 353, 184-7.

Inoue, A., Takahashi, M., Hatta, K., Hotta, Y. and Okamoto, H. (1994). Developmental regulation of islet-1 mRNA expression during neuronal differentiation in embryonic zebrafish. *Dev Dyn* 199, 1-11.

Jacob, J. and Briscoe, J. (2003). Gli proteins and the control of spinal-cord patterning. *EMBO Rep* 4, 761-5.

Jia, J., Amanai, K., Wang, G., Tang, J., Wang, B. and Jiang, J. (2002). Shaggy/GSK3 antagonizes Hedgehog signalling by regulating Cubitus interruptus. *Nature* 416, 548-52.

Jiang, J. and Struhl, G. (1998). Regulation of the Hedgehog and Wingless signalling pathways by the F-box/WD40-repeat protein Slimb. *Nature* 391, 493-6.

Johnson, R. L., Milenkovic, L. and Scott, M. P. (2000). In vivo functions of the patched protein: requirement of the C terminus for target gene inactivation but not Hedgehog sequestration. *Mol Cell* 6, 467-78.

Jordens, I., Fernandez-Borja, M., Marsman, M., Dusseljee, S., Janssen, L., Calafat, J., Janssen, H., Wubbolts, R. and Neefjes, J. (2001). The Rab7 effector protein RILP controls lysosomal transport by inducing the recruitment of dynein-dynactin motors. *Curr Biol* 11, 1680-5.

Kane, D. A., Hammerschmidt, M., Mullins, M. C., Maischein, H. M., Brand, M., van Eeden, F. J., Furutani-Seiki, M., Granato, M., Haffter, P., Heisenberg, C. P. et al. (1996). The zebrafish epiboly mutants. *Development* 123, 47-55.

Karlstrom, R. O., Talbot, W. S. and Schier, A. F. (1999). Comparative synteny cloning of zebrafish you-too: mutations in the Hedgehog target gli2 affect ventral forebrain patterning. *Genes Dev* 13, 388-93.

Karlstrom, R. O., Trowe, T., Klostermann, S., Baier, H., Brand, M., Crawford, A. D., Grunewald, B., Haffter, P., Hoffmann, H., Meyer, S. U. et al. (1996). Zebrafish mutations affecting retinotectal axon pathfinding. *Development* 123, 427-38.

Karlstrom, R. O., Tyurina, O. V., Kawakami, A., Nishioka, N., Talbot, W. S., Sasaki, H. and Schier, A. F. (2003). Genetic analysis of zebrafish gli1 and gli2 reveals divergent requirements for gli genes in vertebrate development. *Development* 130, 1549-64.

Kasarskis, A., Manova, K. and Anderson, K. V. (1998). A phenotype-based screen for embryonic lethal mutations in the mouse. *Proc Natl Acad Sci U S A* 95, 7485-90.

Kato, M., Sasaki, T., Ohya, T., Nakanishi, H., Nishioka, H., Imamura, M. and Takai, Y. (1996). Physical and functional interaction of rabphilin-3A with alpha-actinin. *J Biol Chem* 271, 31775-8.

Kawai, S. and Sugiura, T. (2001). Characterization of human bone morphogenetic protein (BMP)-4 and -7 gene promoters: activation of BMP promoters by Gli, a sonic hedgehog mediator. *Bone* 29, 54-61.

Kee, Y., Yoo, J. S., Hazuka, C. D., Peterson, K. E., Hsu, S. C. and Scheller, R. H. (1997). Subunit structure of the mammalian exocyst complex. *Proc Natl Acad Sci U S A* 94, 14438-43.

Keller, R. (2002). Shaping the vertebrate body plan by polarized embryonic cell movements. *Science* 298, 1950-4.

Kelsh, R. N., Schmid, B. and Eisen, J. S. (2000). Genetic analysis of melanophore development in zebrafish embryos. *Dev Biol* 225, 277-93.

Kessaris, N., Pringle, N. and Richardson, W. D. (2001). Ventral neurogenesis and the neuron-glial switch. *Neuron* 31, 677-80.

Kimmel, C. B., Ballard, W. W., Kimmel, S. R., Ullmann, B. and Schilling, T. F. (1995). Stages of embryonic development of the zebrafish. *Dev Dyn* 203, 253-310.

Kinzler, K. W. and Vogelstein, B. (1990). The GLI gene encodes a nuclear protein which binds specific sequences in the human genome. *Mol Cell Biol* 10, 634-42.

Koda, T., Zheng, J. Y. and Ishibe, M. (1999). Rab33b regulates intra-Golgi transport and utilizes a novel kinesin as an effector. *Mol Biol Cell* 10, 214a.

Koebernick, K. and Pieler, T. (2002). Gli-type zinc finger proteins as bipotential transducers of Hedgehog signaling. *Differentiation* 70, 69-76.

Kogerman, P., Grimm, T., Kogerman, L., Krause, D., Unden, A. B., Sandstedt, B., Toftgard, R. and Zaphiropoulos, P. G. (1999). Mammalian suppressor-of-fused modulates nuclear-cytoplasmic shuttling of Gli-1. *Nat Cell Biol* 1, 312-9.

Kohtz, J. D., Lee, H. Y., Gaiano, N., Segal, J., Ng, E., Larson, T., Baker, D. P., Garber, E. A., Williams, K. P. and Fishell, G. (2001). N-terminal fatty-acylation of sonic hedgehog enhances the induction of rodent ventral forebrain neurons. *Development* 128, 2351-63.

Korzh, V., Edlund, T. and Thor, S. (1993). Zebrafish primary neurons initiate expression of the LIM homeodomain protein Isl-1 at the end of gastrulation. *Development* 118, 417-25.

Kotake, K., Ozaki, N., Mizuta, M., Sekiya, S., Inagaki, N. and Seino, S. (1997). Noc2, a putative zinc finger protein involved in exocytosis in endocrine cells. *J Biol Chem* 272, 29407-10.

Koushika, S. P., Richmond, J. E., Hadwiger, G., Weimer, R. M., Jorgensen, E. M. and Nonet, M. L. (2001). A post-docking role for active zone protein Rim. *Nat Neurosci* 4, 997-1005.

Krauss, S., Concordet, J. P. and Ingham, P. W. (1993). A functionally conserved homolog of the Drosophila segment polarity gene hh is expressed in tissues with polarizing activity in zebrafish embryos. *Cell* 75, 1431-44.

Krauss, S., Johansen, T., Korzh, V. and Fjose, A. (1991a). Expression of the zebrafish paired box gene pax[zf-b] during early neurogenesis. *Development* 113, 1193-206.

Krauss, S., Johansen, T., Korzh, V., Moens, U., Ericson, J. U. and Fjose, A. (1991b). Zebrafish pax[zf-a]: a paired box-containing gene expressed in the neural tube. *Embo J* 10, 3609-19.

Kuwabara, P. E., Lee, M. H., Schedl, T. and Jefferis, G. S. (2000). A C. elegans patched gene, ptc-1, functions in germ-line cytokinesis. *Genes Dev* 14, 1933-44.

Kuwada, J. Y. and Bernhardt, R. R. (1990). Axonal outgrowth by identified neurons in the spinal cord of zebrafish embryos. *Exp Neurol* 109, 29-34.

Kuwada, J. Y., Bernhardt, R. R. and Nguyen, N. (1990). Development of spinal neurons and tracts in the zebrafish embryo. *J Comp Neurol* 302, 617-28.

Lanzetti, L., Rybin, V., Malabarba, M. G., Christoforidis, S., Scita, G., Zerial, M. and Di Fiore, P. P. (2000). The Eps8 protein coordinates EGF receptor signalling through Rac and trafficking through Rab5. *Nature* 408, 374-7.

Lapierre, L. A., Kumar, R., Hales, C. M., Navarre, J., Bhartur, S. G., Burnette, J. O., Provance, D. W., Jr., Mercer, J. A., Bahler, M. and Goldenring, J. R. (2001). Myosin vb is associated with plasma membrane recycling systems. *Mol Biol Cell* 12, 1843-57.

Lee, J., Platt, K. A., Censullo, P. and Ruiz i Altaba, A. (1997). Gli1 is a target of Sonic hedgehog that induces ventral neural tube development. *Development* 124, 2537-52.

Lee, J. D., Kraus, P., Gaiano, N., Nery, S., Kohtz, J., Fishell, G., Loomis, C. A. and Treisman, J. E. (2001). An acylatable residue of Hedgehog is differentially required in Drosophila and mouse limb development. *Dev Biol* 233, 122-36.

Lee, J. D. and Treisman, J. E. (2001). Sightless has homology to transmembrane acyltransferases and is required to generate active Hedgehog protein. *Curr Biol* 11, 1147-52.

Lee, J. J., Ekker, S. C., von Kessler, D. P., Porter, J. A., Sun, B. I. and Beachy, P. A. (1994). Autoproteolysis in hedgehog protein biogenesis. *Science* 266, 1528-37.

Lee, J. J., von Kessler, D. P., Parks, S. and Beachy, P. A. (1992). Secretion and localized transcription suggest a role in positional signaling for products of the segmentation gene hedgehog. *Cell* 71, 33-50.

Lee, K. J., Dietrich, P. and Jessell, T. M. (2000). Genetic ablation reveals that the roof plate is essential for dorsal interneuron specification. *Nature* 403, 734-40.

Lefers, M. A. and Holmgren, R. (2002). Ci proteolysis: regulation by a constellation of phosphorylation sites. *Curr Biol* 12, R422-3.

Lele, Z., Bakkers, J. and Hammerschmidt, M. (2001). Morpholino phenocopies of the swirl, snailhouse, somitabun, minifin, silberblick, and pipetail mutations. *Genesis* 30, 190-4.

Lewis, K. E. and Eisen, J. S. (2001). Hedgehog signaling is required for primary motoneuron induction in zebrafish. *Development* 128, 3485-95.

Lewis, K. E. and Eisen, J. S. (2003). From cells to circuits: development of the zebrafish spinal cord. *Prog Neurobiol* 69, 419-49.

Lewis, P. M., Dunn, M. P., McMahon, J. A., Logan, M., Martin, J. F., St-Jacques, B. and McMahon, A. P. (2001). Cholesterol modification of sonic hedgehog is required for long-range signaling activity and effective modulation of signaling by Ptc1. *Cell* 105, 599-612.

Li, C., Takei, K., Geppert, M., Daniell, L., Stenius, K., Chapman, E. R., Jahn, R., De Camilli, P. and Sudhof, T. C. (1994). Synaptic targeting of rabphilin-3A, a synaptic vesicle Ca2+/phospholipid-binding protein, depends on rab3A/3C. *Neuron* 13, 885-98.

Li, L., Omata, W., Kojima, I. and Shibata, H. (2001). Direct interaction of Rab4 with syntaxin 4. *J Biol Chem* 276, 5265-73.

Liem, K. F., Jr., Jessell, T. M. and Briscoe, J. (2000). Regulation of the neural patterning activity of sonic hedgehog by secreted BMP inhibitors expressed by notochord and somites. *Development* 127, 4855-66.

Liem, K. F., Jr., Tremml, G. and Jessell, T. M. (1997). A role for the roof plate and its resident TGFbeta-related proteins in neuronal patterning in the dorsal spinal cord. *Cell* 91, 127-38.

Liem, K. F., Jr., Tremml, G., Roelink, H. and Jessell, T. M. (1995). Dorsal differentiation of neural plate cells induced by BMP-mediated signals from epidermal ectoderm. *Cell* 82, 969-79.

Lindsay, A. J., Hendrick, A. G., Cantalupo, G., Senic-Matuglia, F., Goud, B., Bucci, C. and McCaffrey, M. W. (2002). Rab coupling protein (RCP), a novel Rab4 and Rab11 effector protein. *J Biol Chem* 277, 12190-9.

Litingtung, Y. and Chiang, C. (2000). Specification of ventral neuron types is mediated by an antagonistic interaction between Shh and Gli3. *Nat Neurosci* 3, 979-85.

Liu, F., Massague, J. and Ruiz i Altaba, A. (1998). Carboxy-terminally truncated Gli3 proteins associate with Smads. *Nat Genet* 20, 325-6.

Lloyd, T. E. and Bellen, H. J. (2001). pRIMing synaptic vesicles for fusion. *Nat Neurosci* 4, 965-6.

Loftus, S. K., Morris, J. A., Carstea, E. D., Gu, J. Z., Cummings, C., Brown, A., Ellison, J., Ohno, K., Rosenfeld, M. A., Tagle, D. A. et al. (1997). Murine model of Niemann-Pick C disease: mutation in a cholesterol homeostasis gene. *Science* 277, 232-5.

Lombardi, D., Soldati, T., Riederer, M. A., Goda, Y., Zerial, M. and Pfeffer, S. R. (1993). Rab9 functions in transport between late endosomes and the trans Golgi network. *Embo J* 12, 677-82.

Long, S., Ahmad, N. and Rebagliati, M. (2003). The zebrafish nodal-related gene southpaw is required for visceral and diencephalic left-right asymmetry. *Development* 130, 2303-16.

Lutcke, A., Parton, R. G., Murphy, C., Olkkonen, V. M., Dupree, P., Valencia, A., Simons, K. and Zerial, M. (1994). Cloning and subcellular localization of novel rab proteins reveals polarized and cell type-specific expression. *J Cell Sci* 107 (Pt 12), 3437-48.

Ma, Y., Erkner, A., Gong, R., Yao, S., Taipale, J., Basler, K. and Beachy, P. A. (2002). Hedgehog-mediated patterning of the mammalian embryo requires transporter-like function of dispatched. *Cell* 111, 63-75.

Macdonald, R., Barth, K. A., Xu, Q., Holder, N., Mikkola, I. and Wilson, S. W. (1995). Midline signalling is required for Pax gene regulation and patterning of the eyes. *Development* 121, 3267-78.

Mammoto, A., Ohtsuka, T., Hotta, I., Sasaki, T. and Takai, Y. (1999). Rab11BP/Rabphilin-11, a downstream target of rab11 small G protein implicated in vesicle recycling. *J Biol Chem* 274, 25517-24.

Maniatis, T. (1999). A ubiquitin ligase complex essential for the NF-kappaB, Wnt/Wingless, and Hedgehog signaling pathways. *Genes Dev* 13, 505-10.

Marigo, V., Davey, R. A., Zuo, Y., Cunningham, J. M. and Tabin, C. J. (1996a). Biochemical evidence that patched is the Hedgehog receptor. *Nature* 384, 176-9.

Marigo, V., Johnson, R. L., Vortkamp, A. and Tabin, C. J. (1996b). Sonic hedgehog differentially regulates expression of GLI and GLI3 during limb development. *Dev Biol* 180, 273-83.

Marti, E., Bumcrot, D. A., Takada, R. and McMahon, A. P. (1995). Requirement of 19K form of Sonic hedgehog for induction of distinct ventral cell types in CNS explants. *Nature* 375, 322-5.

Martin, V., Carrillo, G., Torroja, C. and Guerrero, I. (2001). The sterol-sensing domain of Patched protein seems to control Smoothened activity through Patched vesicular trafficking. *Curr Biol* 11, 601-7.

Martinez-Morales, J. R., Barbas, J. A., Marti, E., Bovolenta, P., Edgar, D. and Rodriguez-Tebar, A. (1997). Vitronectin is expressed in the ventral region of the neural tube and promotes the differentiation of motor neurons. *Development* 124, 5139-47.

Marzesco, A. M., Dunia, I., Pandjaitan, R., Recouvreur, M., Dauzonne, D., Benedetti, E. L., Louvard, D. and Zahraoui, A. (2002). The small GTPase Rab13 regulates assembly of functional tight junctions in epithelial cells. *Mol Biol Cell* 13, 1819-31.

Mastronardi, F. G., Dimitroulakos, J., Kamel-Reid, S. and Manoukian, A. S. (2000). Co-localization of patched and activated sonic hedgehog to lysosomes in neurons. *Neuroreport* 11, 581-5.

Masuya, H., Sagai, T., Moriwaki, K. and Shiroishi, T. (1997). Multigenic control of the localization of the zone of polarizing activity in limb morphogenesis in the mouse. *Dev Biol* 182, 42-51.

Masuya, H., Sagai, T., Wakana, S., Moriwaki, K. and Shiroishi, T. (1995). A duplicated zone of polarizing activity in polydactylous mouse mutants. *Genes Dev* 9, 1645-53.

Matanis, T., Akhmanova, A., Wulf, P., Del Nery, E., Weide, T., Stepanova, T., Galjart, N., Grosveld, F., Goud, B., De Zeeuw, C. I. et al. (2002). Bicaudal-D regulates COPI-independent Golgi-ER transport by recruiting the dynein-dynactin motor complex. *Nat Cell Biol* 4, 986-92.

Matern, H. T., Yeaman, C., Nelson, W. J. and Scheller, R. H. (2001). The Sec6/8 complex in mammalian cells: characterization of mammalian Sec3, subunit interactions, and expression of subunits in polarized cells. *Proc Natl Acad Sci U S A* 98, 9648-53.

Matesic, L. E., Yip, R., Reuss, A. E., Swing, D. A., O'Sullivan, T. N., Fletcher, C. F., Copeland, N. G. and Jenkins, N. A. (2001). Mutations in Mlph, encoding a member of

the Rab effector family, cause the melanosome transport defects observed in leaden mice. *Proc Natl Acad Sci U S A* 98, 10238-43.

Matise, M. P., Epstein, D. J., Park, H. L., Platt, K. A. and Joyner, A. L. (1998). Gli2 is required for induction of floor plate and adjacent cells, but not most ventral neurons in the mouse central nervous system. *Development* 125, 2759-70.

McBride, H. M., Rybin, V., Murphy, C., Giner, A., Teasdale, R. and Zerial, M. (1999). Oligomeric complexes link Rab5 effectors with NSF and drive membrane fusion via interactions between EEA1 and syntaxin 13. *Cell* 98, 377-86.

McCaffrey, M. W., Bielli, A., Cantalupo, G., Mora, S., Roberti, V., Santillo, M., Drummond, F. and Bucci, C. (2001). Rab4 affects both recycling and degradative endosomal trafficking. *FEBS Lett* 495, 21-30.

McCormick, C., Leduc, Y., Martindale, D., Mattison, K., Esford, L. E., Dyer, A. P. and Tufaro, F. (1998). The putative tumour suppressor EXT1 alters the expression of cell-surface heparan sulfate. *Nat Genet* 19, 158-61.

McLauchlan, H., Newell, J., Morrice, N., Osborne, A., West, M. and Smythe, E. (1998). A novel role for Rab5-GDI in ligand sequestration into clathrin-coated pits. *Curr Biol* 8, 34-45.

Mekki-Dauriac, S., Agius, E., Kan, P. and Cochard, P. (2002). Bone morphogenetic proteins negatively control oligodendrocyte precursor specification in the chick spinal cord. *Development* 129, 5117-30.

Menasche, G., Pastural, E., Feldmann, J., Certain, S., Ersoy, F., Dupuis, S., Wulffraat, N., Bianchi, D., Fischer, A., Le Deist, F. et al. (2000). Mutations in RAB27A cause Griscelli syndrome associated with haemophagocytic syndrome. *Nat Genet* 25, 173-6.

Mercer, J. A., Seperack, P. K., Strobel, M. C., Copeland, N. G. and Jenkins, N. A. (1991). Novel myosin heavy chain encoded by murine dilute coat colour locus. *Nature* 349, 709-13.

Meresse, S., Gorvel, J. P. and Chavrier, P. (1995). The rab7 GTPase resides on a vesicular compartment connected to lysosomes. *J Cell Sci* 108 (Pt 11), 3349-58.

Methot, N. and Basler, K. (2000). Suppressor of fused opposes hedgehog signal transduction by impeding nuclear accumulation of the activator form of Cubitus interruptus. *Development* 127, 4001-10.

Methot, N. and Basler, K. (2001). An absolute requirement for Cubitus interruptus in Hedgehog signaling. *Development* 128, 733-42.

Mikkola, I., Fjose, A., Kuwada, J. Y., Wilson, S., Guddal, P. H. and Krauss, S. (1992). The paired domain-containing nuclear factor pax[b] is expressed in specific commissural interneurons in zebrafish embryos. *J Neurobiol* 23, 933-46.

Milburn, M. V., Tong, L., deVos, A. M., Brunger, A., Yamaizumi, Z., Nishimura, S. and Kim, S. H. (1990). Molecular switch for signal transduction: structural differences between active and inactive forms of protooncogenic ras proteins. *Science* 247, 939-45.

Mo, R., Freer, A. M., Zinyk, D. L., Crackower, M. A., Michaud, J., Heng, H. H., Chik, K. W., Shi, X. M., Tsui, L. C., Cheng, S. H. et al. (1997). Specific and redundant functions of Gli2 and Gli3 zinc finger genes in skeletal patterning and development. *Development* 124, 113-23.

Mohler, J. and Vani, K. (1992). Molecular organization and embryonic expression of the hedgehog gene involved in cell-cell communication in segmental patterning of Drosophila. *Development* 115, 957-71.

Moon, R. T., Campbell, R. M., Christian, J. L., McGrew, L. L., Shih, J. and Fraser, S. (1993). Xwnt-5A: a maternal Wnt that affects morphogenetic movements after overexpression in embryos of Xenopus laevis. *Development* 119, 97-111.

Moore, I., Schell, J. and Palme, K. (1995). Subclass-specific sequence motifs identified in Rab GTPases. *Trends Biochem Sci* 20, 10-2.

Moskalenko, S., Henry, D. O., Rosse, C., Mirey, G., Camonis, J. H. and White, M. A. (2002). The exocyst is a Ral effector complex. *Nat Cell Biol* 4, 66-72.

Motoyama, J., Liu, J., Mo, R., Ding, Q., Post, M. and Hui, C. C. (1998a). Essential function of Gli2 and Gli3 in the formation of lung, trachea and oesophagus. *Nat Genet* 20, 54-7.

Motoyama, J., Takabatake, T., Takeshima, K. and Hui, C. (1998b). Ptch2, a second mouse Patched gene is co-expressed with Sonic hedgehog. *Nat Genet* 18, 104-6.

Moyer, B. D., Allan, B. B. and Balch, W. E. (2001). Rab1 interaction with a GM130 effector complex regulates COPII vesicle cis--Golgi tethering. *Traffic* 2, 268-76.

Mu, F. T., Callaghan, J. M., Steele-Mortimer, O., Stenmark, H., Parton, R. G., Campbell, P. L., McCluskey, J., Yeo, J. P., Tock, E. P. and Toh, B. H. (1995). EEA1, an early endosome-associated protein. EEA1 is a conserved alpha-helical peripheral membrane protein flanked by cysteine "fingers" and contains a calmodulin-binding IQ motif. *J Biol Chem* 270, 13503-11.

Muller, F., Albert, S., Blader, P., Fischer, N., Hallonet, M. and Strähle, U. (2000). Direct action of the nodal-related signal cyclops in induction of sonic hedgehog in the ventral midline of the CNS. *Development* 127, 3889-97.

Mullins, M. C., Hammerschmidt, M., Kane, D. A., Odenthal, J., Brand, M., van Eeden, F. J., Furutani-Seiki, M., Granato, M., Haffter, P., Heisenberg, C. P. et al. (1996). Genes establishing dorsoventral pattern formation in the zebrafish embryo: the ventral specifying genes. *Development* 123, 81-93.

Murone, M., Rosenthal, A. and de Sauvage, F. J. (1999). Sonic hedgehog signaling by the patched-smoothened receptor complex. *Curr Biol* 9, 76-84.

Murphy, C. and Zerial, M. (1995). Expression of Rab proteins during mouse embryonic development. *Methods Enzymol* 257, 324-32.

Murthy, M., Garza, D., Scheller, R. H. and Schwarz, T. L. (2003). Mutations in the exocyst component Sec5 disrupt neuronal membrane traffic, but neurotransmitter release persists. *Neuron* 37, 433-47.

Nagelkerken, B., van Anken, E., van Raak, M., Gerez, L., Mohrmann, K., van Uden, N., Holthuizen, J., Pelkmans, L. and van der Sluijs, P. (2000). Rabaptin4, a novel effector of the small GTPase rab4a, is recruited to perinuclear recycling vesicles. *Biochem J* 346 Pt 3, 593-601.

Nasevicius, A. and Ekker, S. C. (2000). Effective targeted gene 'knockdown' in zebrafish. *Nat Genet* 26, 216-20.

Neumann, C. J., Grandel, H., Gaffield, W., Schulte-Merker, S. and Nüsslein-Volhard, C. (1999). Transient establishment of anteroposterior polarity in the zebrafish pectoral fin bud in the absence of sonic hedgehog activity. *Development* 126, 4817-26.

Nguyen, V. H., Trout, J., Connors, S. A., Andermann, P., Weinberg, E. and Mullins, M. C. (2000). Dorsal and intermediate neuronal cell types of the spinal cord are established by a BMP signaling pathway. *Development* 127, 1209-20.

Nielsen, E., Severin, F., Backer, J. M., Hyman, A. A. and Zerial, M. (1999). Rab5 regulates motility of early endosomes on microtubules. *Nat Cell Biol* 1, 376-82.

Nishibori, M., Cham, B., McNicol, A., Shalev, A., Jain, N. and Gerrard, J. M. (1993). The protein CD63 is in platelet dense granules, is deficient in a patient with Hermansky-Pudlak syndrome, and appears identical to granulophysin. *J Clin Invest* 91, 1775-82.

Nohturfft, A., DeBose-Boyd, R. A., Scheek, S., Goldstein, J. L. and Brown, M. S. (1999). Sterols regulate cycling of SREBP cleavage-activating protein (SCAP) between endoplasmic reticulum and Golgi. *Proc Natl Acad Sci U S A* 96, 11235-40.

Novitch, B. G., Chen, A. I. and Jessell, T. M. (2001). Coordinate regulation of motor neuron subtype identity and pan-neuronal properties by the bHLH repressor Olig2. *Neuron* 31, 773-89.

Novitch, B. G., Wichterle, H., Jessell, T. M. and Sockanathan, S. (2003). A requirement for retinoic acid-mediated transcriptional activation in ventral neural patterning and motor neuron specification. *Neuron* 40, 81-95.

Oda, H., Stockert, R. J., Collins, C., Wang, H., Novikoff, P. M., Satir, P. and Wolkoff, A. W. (1995). Interaction of the microtubule cytoskeleton with endocytic vesicles and cytoplasmic dynein in cultured rat hepatocytes. *J Biol Chem* 270, 15242-9.

Odenthal, J., van Eeden, F. J., Haffter, P., Ingham, P. W. and Nüsslein-Volhard, C. (2000). Two distinct cell populations in the floor plate of the zebrafish are induced by different pathways. *Dev Biol* 219, 350-63.

Ohlmeyer, J. T. and Kalderon, D. (1998). Hedgehog stimulates maturation of Cubitus interruptus into a labile transcriptional activator. *Nature* 396, 749-53.

Ohya, T., Sasaki, T., Kato, M. and Takai, Y. (1998). Involvement of Rabphilin3 in endocytosis through interaction with Rabaptin5. *J Biol Chem* 273, 613-7.

Olkkonen, V. M. and Stenmark, H. (1997). Role of Rab GTPases in membrane traffic. *Int Rev Cytol* 176, 1-85.

Orenic, T. V., Slusarski, D. C., Kroll, K. L. and Holmgren, R. A. (1990). Cloning and characterization of the segment polarity gene cubitus interruptus Dominant of Drosophila. *Genes Dev* 4, 1053-67.

Ostermeier, C. and Brunger, A. T. (1999). Structural basis of Rab effector specificity: crystal structure of the small G protein Rab3A complexed with the effector domain of rabphilin-3A. *Cell* 96, 363-74.

Park, H. L., Bai, C., Platt, K. A., Matise, M. P., Beeghly, A., Hui, C. C., Nakashima, M. and Joyner, A. L. (2000). Mouse Gli1 mutants are viable but have defects in SHH signaling in combination with a Gli2 mutation. *Development* 127, 1593-605.

Park, Y., Rangel, C., Reynolds, M. M., Caldwell, M. C., Johns, M., Nayak, M., Welsh, C. J., McDermott, S. and Datt, S. (2003). Drosophila perlecan modulates FGF and hedgehog signals to activate neural stem cell division. *Dev Biol* 253, 247-57.

Pastural, E., Barrat, F. J., Dufourcq-Lagelouse, R., Certain, S., Sanal, O., Jabado, N., Seger, R., Griscelli, C., Fischer, A. and de Saint Basile, G. (1997). Griscelli disease maps to chromosome 15q21 and is associated with mutations in the myosin-Va gene. *Nat Genet* 16, 289-92.

Patten, I. and Placzek, M. (2002). Opponent activities of Shh and BMP signaling during floor plate induction in vivo. *Curr Biol* 12, 47-52.

Pepinsky, R. B., Zeng, C., Wen, D., Rayhorn, P., Baker, D. P., Williams, K. P., Bixler, S. A., Ambrose, C. M., Garber, E. A., Miatkowski, K. et al. (1998). Identification of a palmitic acid-modified form of human Sonic hedgehog. *J Biol Chem* 273, 14037-45.

Pereira-Leal, J. B., Hume, A. N. and Seabra, M. C. (2001). Prenylation of Rab GTPases: molecular mechanisms and involvement in genetic disease. *FEBS Lett* 498, 197-200.

Pereira-Leal, J. B. and Seabra, M. C. (2000). The mammalian Rab family of small GTPases: definition of family and subfamily sequence motifs suggests a mechanism for functional specificity in the Ras superfamily. *J Mol Biol* 301, 1077-87.

Pereira-Leal, J. B. and Seabra, M. C. (2001). Evolution of the Rab family of small GTP-binding proteins. *J Mol Biol* 313, 889-901.

Pereira-Leal, J. B., Strom, M., Godfrey, R. F. and Seabra, M. C. (2003). Structural determinants of Rab and Rab Escort Protein interaction: Rab family motifs define a conserved binding surface. *Biochem Biophys Res Commun* 301, 92-7.

Persson, M., Stamataki, D., te Welscher, P., Andersson, E., Bose, J., Ruther, U., Ericson, J. and Briscoe, J. (2002). Dorsal-ventral patterning of the spinal cord requires Gli3 transcriptional repressor activity. *Genes Dev* 16, 2865-78.

Pfeffer, S. R. (1999). Transport-vesicle targeting: tethers before SNAREs. *Nat Cell Biol* 1, E17-22.

Pham, A., Therond, P., Alves, G., Tournier, F. B., Busson, D., Lamour-Isnard, C., Bouchon, B. L., Preat, T. and Tricoire, H. (1995). The Suppressor of fused gene encodes a novel PEST protein involved in Drosophila segment polarity establishment. *Genetics* 140, 587-98.

Pierani, A., Brenner-Morton, S., Chiang, C. and Jessell, T. M. (1999). A sonic hedgehog-independent, retinoid-activated pathway of neurogenesis in the ventral spinal cord. *Cell* 97, 903-15.

Placzek, M. (1995). The role of the notochord and floor plate in inductive interactions. *Curr Opin Genet Dev* 5, 499-506.

Plutner, H., Schwaninger, R., Pind, S. and Balch, W. E. (1990). Synthetic peptides of the Rab effector domain inhibit vesicular transport through the secretory pathway. *Embo J* 9, 2375-83.

Pons, S. and Marti, E. (2000). Sonic hedgehog synergizes with the extracellular matrix protein vitronectin to induce spinal motor neuron differentiation. *Development* 127, 333-42.

Porter, J. A., von Kessler, D. P., Ekker, S. C., Young, K. E., Lee, J. J., Moses, K. and Beachy, P. A. (1995). The product of hedgehog autoproteolytic cleavage active in local and long-range signalling. *Nature* 374, 363-6.

Porter, J. A., Young, K. E. and Beachy, P. A. (1996). Cholesterol modification of hedgehog signaling proteins in animal development. *Science* 274, 255-9.

Preat, T. (1992). Characterization of Suppressor of fused, a complete suppressor of the fused segment polarity gene of Drosophila melanogaster. *Genetics* 132, 725-36.

Prekeris, R., Davies, J. M. and Scheller, R. H. (2001). Identification of a novel Rab11/25 binding domain present in Eferin and Rip proteins. *J Biol Chem* 276, 38966-70.

Prekeris, R., Klumperman, J. and Scheller, R. H. (2000). A Rab11/Rip11 protein complex regulates apical membrane trafficking via recycling endosomes. *Mol Cell* 6, 1437-48.

Price, M. A. and Kalderon, D. (2002). Proteolysis of the Hedgehog signaling effector Cubitus interruptus requires phosphorylation by Glycogen Synthase Kinase 3 and Casein Kinase 1. *Cell* 108, 823-35.

Puschel, A. W., Gruss, P. and Westerfield, M. (1992). Sequence and expression pattern of pax-6 are highly conserved between zebrafish and mice. *Development* 114, 643-51.

Rallu, M., Machold, R., Gaiano, N., Corbin, J. G., McMahon, A. P. and Fishell, G. (2002). Dorsoventral patterning is established in the telencephalon of mutants lacking both Gli3 and Hedgehog signaling. *Development* 129, 4963-74.

Rauch, G. J., Hammerschmidt, M., Blader, P., Schauerte, H. E., Strähle, U., Ingham, P. W., McMahon, A. P. and Haffter, P. (1997). Wnt5 is required for tail formation in the zebrafish embryo. *Cold Spring Harb Symp Quant Biol* 62, 227-34.

Rebagliati, M. R., Toyama, R., Fricke, C., Haffter, P. and Dawid, I. B. (1998). Zebrafish nodal-related genes are implicated in axial patterning and establishing left-right asymmetry. *Dev Biol* 199, 261-72.

Ren, M., Xu, G., Zeng, J., De Lemos-Chiarandini, C., Adesnik, M. and Sabatini, D. D. (1998). Hydrolysis of GTP on rab11 is required for the direct delivery of transferrin from

the pericentriolar recycling compartment to the cell surface but not from sorting endosomes. *Proc Natl Acad Sci U S A* 95, 6187-92.

Riddle, R. D., Johnson, R. L., Laufer, E. and Tabin, C. (1993). Sonic hedgehog mediates the polarizing activity of the ZPA. *Cell* 75, 1401-16.

Riederer, M. A., Soldati, T., Shapiro, A. D., Lin, J. and Pfeffer, S. R. (1994). Lysosome biogenesis requires Rab9 function and receptor recycling from endosomes to the trans-Golgi network. *J Cell Biol* 125, 573-82.

Rietveld, A., Neutz, S., Simons, K. and Eaton, S. (1999). Association of sterol- and glycosylphosphatidylinositol-linked proteins with Drosophila raft lipid microdomains. *J Biol Chem* 274, 12049-54.

Robbins, D. J., Nybakken, K. E., Kobayashi, R., Sisson, J. C., Bishop, J. M. and Therond, P. P. (1997). Hedgehog elicits signal transduction by means of a large complex containing the kinesin-related protein costal2. *Cell* 90, 225-34.

Roberts, M., Barry, S., Woods, A., van der Sluijs, P. and Norman, J. (2001). PDGF-regulated rab4-dependent recycling of alphavbeta3 integrin from early endosomes is necessary for cell adhesion and spreading. *Curr Biol* 11, 1392-402.

Rodionov, V. I., Hope, A. J., Svitkina, T. M. and Borisy, G. G. (1998). Functional coordination of microtubule-based and actin-based motility in melanophores. *Curr Biol* 8, 165-8.

Roelink, H., Porter, J. A., Chiang, C., Tanabe, Y., Chang, D. T., Beachy, P. A. and Jessell, T. M. (1995). Floor plate and motor neuron induction by different concentrations of the amino-terminal cleavage product of sonic hedgehog autoproteolysis. *Cell* 81, 445-55.

Rohr, K. B., Barth, K. A., Varga, Z. M. and Wilson, S. W. (2001). The nodal pathway acts upstream of hedgehog signaling to specify ventral telencephalic identity. *Neuron* 29, 341-51.

Rothman, J. E. (1994). Mechanisms of intracellular protein transport. *Nature* 372, 55-63.

Ruel, L., Rodriguez, R., Gallet, A., Lavenant-Staccini, L. and Therond, P. P. (2003). Stability and association of Smoothened, Costal2 and Fused with Cubitus interruptus are regulated by Hedgehog. *Nat Cell Biol* 5, 907-13.

Ruiz i Altaba, A. (1998). Combinatorial Gli gene function in floor plate and neuronal inductions by Sonic hedgehog. *Development* 125, 2203-12.

Sampath, K., Rubinstein, A. L., Cheng, A. M., Liang, J. O., Fekany, K., Solnica-Krezel, L., Korzh, V., Halpern, M. E. and Wright, C. V. (1998). Induction of the zebrafish ventral brain and floorplate requires cyclops/nodal signalling. *Nature* 395, 185-9.

Sasaki, H., Hui, C., Nakafuku, M. and Kondoh, H. (1997). A binding site for Gli proteins is essential for HNF-3beta floor plate enhancer activity in transgenics and can respond to Shh in vitro. *Development* 124, 1313-22.

Sasaki, H., Nishizaki, Y., Hui, C., Nakafuku, M. and Kondoh, H. (1999). Regulation of Gli2 and Gli3 activities by an amino-terminal repression domain: implication of Gli2 and Gli3 as primary mediators of Shh signaling. *Development* 126, 3915-24.

Schauerte, H. E., van Eeden, F. J., Fricke, C., Odenthal, J., Strähle, U. and Haffter, P. (1998). Sonic hedgehog is not required for the induction of medial floor plate cells in the zebrafish. *Development* 125, 2983-93.

Schlichting, I., Almo, S. C., Rapp, G., Wilson, K., Petratos, K., Lentfer, A., Wittinghofer, A., Kabsch, W., Pai, E. F., Petsko, G. A. et al. (1990). Time-resolved X-ray crystallographic study of the conformational change in Ha-Ras p21 protein on GTP hydrolysis. *Nature* 345, 309-15.

Schluter, O. M., Khvotchev, M., Jahn, R. and Sudhof, T. C. (2002). Localization versus function of Rab3 proteins. Evidence for a common regulatory role in controlling fusion. *J Biol Chem* 277, 40919-29.

Schulte-Merker, S., van Eeden, F. J., Halpern, M. E., Kimmel, C. B. and Nüsslein-Volhard, C. (1994). no tail (ntl) is the zebrafish homologue of the mouse T (Brachyury) gene. *Development* 120, 1009-15.

Seabra, M. C., Ho, Y. K. and Anant, J. S. (1995). Deficient geranylgeranylation of Ram/Rab27 in choroideremia. *J Biol Chem* 270, 24420-7.

Seabra, M. C., Mules, E. H. and Hume, A. N. (2002). Rab GTPases, intracellular traffic and disease. *Trends Mol Med* 8, 23-30.

Seachrist, J. L., Laporte, S. A., Dale, L. B., Babwah, A. V., Caron, M. G., Anborgh, P. H. and Ferguson, S. S. (2002). Rab5 association with the angiotensin II type 1A receptor promotes Rab5 GTP binding and vesicular fusion. *J Biol Chem* 277, 679-85.

Seo, H. C., Nilsen, F. and Fjose, A. (1999). Three structurally and functionally conserved Hlx genes in zebrafish. *Biochim Biophys Acta* 1489, 323-35.

Seo, H. C., Saetre, B. O., Havik, B., Ellingsen, S. and Fjose, A. (1998). The zebrafish Pax3 and Pax7 homologues are highly conserved, encode multiple isoforms and show dynamic segment-like expression in the developing brain. *Mech Dev* 70, 49-63.

Sheth, B., Fontaine, J. J., Ponza, E., McCallum, A., Page, A., Citi, S., Louvard, D., Zahraoui, A. and Fleming, T. P. (2000). Differentiation of the epithelial apical junctional complex during mouse preimplantation development: a role for rab13 in the early maturation of the tight junction. *Mech Dev* 97, 93-104.

Shin, S. H., Kogerman, P., Lindstrom, E., Toftgard, R. and Biesecker, L. G. (1999). GLI3 mutations in human disorders mimic Drosophila cubitus interruptus protein functions and localization. *Proc Natl Acad Sci U S A* 96, 2880-4.

Shirataki, H., Kaibuchi, K., Sakoda, T., Kishida, S., Yamaguchi, T., Wada, K., Miyazaki, M. and Takai, Y. (1993). Rabphilin-3A, a putative target protein for smg p25A/rab3A p25 small GTP-binding protein related to synaptotagmin. *Mol Cell Biol* 13, 2061-8.

Shirataki, H., Yamamoto, T., Hagi, S., Miura, H., Oishi, H., Jin-no, Y., Senbonmatsu, T. and Takai, Y. (1994). Rabphilin-3A is associated with synaptic vesicles through a vesicle protein in a manner independent of Rab3A. *J Biol Chem* 269, 32717-20.

Short, B., Preisinger, C., Schaletzky, J., Kopajtich, R. and Barr, F. A. (2002). The Rab6 GTPase regulates recruitment of the dynactin complex to Golgi membranes. *Curr Biol* 12, 1792-5.

Simonsen, A., Gaullier, J. M., D'Arrigo, A. and Stenmark, H. (1999). The Rab5 effector EEA1 interacts directly with syntaxin-6. *J Biol Chem* 274, 28857-60.

Simonsen, A., Lippe, R., Christoforidis, S., Gaullier, J. M., Brech, A., Callaghan, J., Toh, B. H., Murphy, C., Zerial, M. and Stenmark, H. (1998). EEA1 links PI(3)K function to Rab5 regulation of endosome fusion. *Nature* 394, 494-8.

Sisson, J. C., Ho, K. S., Suyama, K. and Scott, M. P. (1997). Costal2, a novel kinesin-related protein in the Hedgehog signaling pathway. *Cell* 90, 235-45.

Smith, J. C., Price, B. M., Green, J. B., Weigel, D. and Herrmann, B. G. (1991). Expression of a Xenopus homolog of Brachyury (T) is an immediate-early response to mesoderm induction. *Cell* 67, 79-87.

Smythe, E. (2002). Direct interactions between rab GTPases and cargo. *Mol Cell* 9, 205-6.

Solnica-Krezel, L., Stemple, D. L., Mountcastle-Shah, E., Rangini, Z., Neuhauss, S. C., Malicki, J., Schier, A. F., Stainier, D. Y., Zwartkruis, F., Abdelilah, S. et al. (1996). Mutations affecting cell fates and cellular rearrangements during gastrulation in zebrafish. *Development* 123, 67-80.

Sonnichsen, B., De Renzis, S., Nielsen, E., Rietdorf, J. and Zerial, M. (2000). Distinct membrane domains on endosomes in the recycling pathway visualized by multicolor imaging of Rab4, Rab5, and Rab11. *J Cell Biol* 149, 901-14.

Stahl, B., Chou, J. H., Li, C., Sudhof, T. C. and Jahn, R. (1996). Rab3 reversibly recruits rabphilin to synaptic vesicles by a mechanism analogous to raf recruitment by ras. *Embo J* 15, 1799-809.

Stegman, M. A., Vallance, J. E., Elangovan, G., Sosinski, J., Cheng, Y. and Robbins, D. J. (2000). Identification of a tetrameric hedgehog signaling complex. *J Biol Chem* 275, 21809-12.

Stenmark, H., Parton, R. G., Steele-Mortimer, O., Lutcke, A., Gruenberg, J. and Zerial, M. (1994). Inhibition of rab5 GTPase activity stimulates membrane fusion in endocytosis. *Embo J* 13, 1287-96.

Stenmark, H., Vitale, G., Ullrich, O. and Zerial, M. (1995). Rabaptin-5 is a direct effector of the small GTPase Rab5 in endocytic membrane fusion. *Cell* 83, 423-32.

Stinchcombe, J. C., Barral, D. C., Mules, E. H., Booth, S., Hume, A. N., Machesky, L. M., Seabra, M. C. and Griffiths, G. M. (2001). Rab27a is required for regulated secretion in cytotoxic T lymphocytes. *J Cell Biol* 152, 825-34.

Stone, D. M., Hynes, M., Armanini, M., Swanson, T. A., Gu, Q., Johnson, R. L., Scott, M. P., Pennica, D., Goddard, A., Phillips, H. et al. (1996). The tumour-suppressor gene patched encodes a candidate receptor for Sonic hedgehog. *Nature* 384, 129-34.

Strähle, U., Blader, P., Henrique, D. and Ingham, P. W. (1993). Axial, a zebrafish gene expressed along the developing body axis, shows altered expression in cyclops mutant embryos. *Genes Dev* 7, 1436-46.

Strähle, U., Blader, P. and Ingham, P. W. (1996). Expression of axial and sonic hedgehog in wildtype and midline defective zebrafish embryos. *Int J Dev Biol* 40, 929-40.

Strähle, U., Jesuthasan, S., Blader, P., Garcia-Villalba, P., Hatta, K. and Ingham, P. W. (1997). one-eyed pinhead is required for development of the ventral midline of the zebrafish (Danio rerio) neural tube. *Genes Funct* 1, 131-48.

Stroupe, C. and Brunger, A. T. (2000). Crystal structures of a Rab protein in its inactive and active conformations. *J Mol Biol* 304, 585-98.

Strutt, H., Thomas, C., Nakano, Y., Stark, D., Neave, B., Taylor, A. M. and Ingham, P. W. (2001). Mutations in the sterol-sensing domain of Patched suggest a role for vesicular trafficking in Smoothened regulation. *Curr Biol* 11, 608-13.

Swank, R. T., Novak, E. K., McGarry, M. P., Rusiniak, M. E. and Feng, L. (1998). Mouse models of Hermansky Pudlak syndrome: a review. *Pigment Cell Res* 11, 60-80.

Tabata, T., Eaton, S. and Kornberg, T. B. (1992). The Drosophila hedgehog gene is expressed specifically in posterior compartment cells and is a target of engrailed regulation. *Genes Dev* 6, 2635-45.

Tabata, T. and Kornberg, T. B. (1994). Hedgehog is a signaling protein with a key role in patterning Drosophila imaginal discs. *Cell* 76, 89-102.

Tada, M., Concha, M. L. and Heisenberg, C. P. (2002). Non-canonical Wnt signalling and regulation of gastrulation movements. *Semin Cell Dev Biol* 13, 251-60.

Tada, M. and Smith, J. C. (2000). Xwnt11 is a target of Xenopus Brachyury: regulation of gastrulation movements via Dishevelled, but not through the canonical Wnt pathway. *Development* 127, 2227-38.

Takai, Y., Sasaki, T. and Matozaki, T. (2001). Small GTP-binding proteins. *Physiol Rev* 81, 153-208.

Tan, J. T., Korzh, V. and Gong, Z. (1999). Expression of a zebrafish iroquois homeobox gene, Ziro3, in the midline axial structures and central nervous system. *Mech Dev* 87, 165-8.

Tashiro, S., Michiue, T., Higashijima, S., Zenno, S., Ishimaru, S., Takahashi, F., Orihara, M., Kojima, T. and Saigo, K. (1993). Structure and expression of hedgehog, a Drosophila segment-polarity gene required for cell-cell communication. *Gene* 124, 183-9.

Tekki-Kessaris, N., Woodruff, R., Hall, A. C., Gaffield, W., Kimura, S., Stiles, C. D., Rowitch, D. H. and Richardson, W. D. (2001). Hedgehog-dependent oligodendrocyte lineage specification in the telencephalon. *Development* 128, 2545-54.

TerBush, D. R., Maurice, T., Roth, D. and Novick, P. (1996). The Exocyst is a multiprotein complex required for exocytosis in Saccharomyces cerevisiae. *Embo J* 15, 6483-94.

TerBush, D. R. and Novick, P. (1995). Sec6, Sec8, and Sec15 are components of a multisubunit complex which localizes to small bud tips in Saccharomyces cerevisiae. *J Cell Biol* 130, 299-312.

Thaeron, C., Avaron, F., Casane, D., Borday, V., Thisse, B., Thisse, C., Boulekbache, H. and Laurenti, P. (2000). Zebrafish evx1 is dynamically expressed during embryogenesis in subsets of interneurones, posterior gut and urogenital system. *Mech Dev* 99, 167-72.

Theil, T., Alvarez-Bolado, G., Walter, A. and Ruther, U. (1999). Gli3 is required for Emx gene expression during dorsal telencephalon development. *Development* 126, 3561-71.

Thisse, C. and Thisse, B. (1998). High resolution whole-mount *in situ* hybridization. *Zebrafish Sci. Mon.*, 8-9.

Thoma, N. H., Iakovenko, A., Goody, R. S. and Alexandrov, K. (2001a). Phosphoisoprenoids modulate association of Rab geranylgeranyltransferase with REP-1. *J Biol Chem* 276, 48637-43.

Thoma, N. H., Iakovenko, A., Kalinin, A., Waldmann, H., Goody, R. S. and Alexandrov, K. (2001b). Allosteric regulation of substrate binding and product release in geranylgeranyltransferase type II. *Biochemistry* 40, 268-74.

Thompson, M. A., Ransom, D. G., Pratt, S. J., MacLennan, H., Kieran, M. W., Detrich, H. W., 3rd, Vail, B., Huber, T. L., Paw, B., Brownlie, A. J. et al. (1998). The cloche and spadetail genes differentially affect hematopoiesis and vasculogenesis. *Dev Biol* 197, 248-69.

Ting, A. E., Hazuka, C. D., Hsu, S. C., Kirk, M. D., Bean, A. J. and Scheller, R. H. (1995). rSec6 and rSec8, mammalian homologs of yeast proteins essential for secretion. *Proc Natl Acad Sci U S A* 92, 9613-7.

Tisdale, E. J., Bourne, J. R., Khosravi-Far, R., Der, C. J. and Balch, W. E. (1992). GTP-binding mutants of rab1 and rab2 are potent inhibitors of vesicular transport from the endoplasmic reticulum to the Golgi complex. *J Cell Biol* 119, 749-61.

Tokumoto, M., Gong, Z., Tsubokawa, T., Hew, C. L., Uyemura, K., Hotta, Y. and Okamoto, H. (1995). Molecular heterogeneity among primary motoneurons and within myotomes revealed by the differential mRNA expression of novel islet-1 homologs in embryonic zebrafish. *Dev Biol* 171, 578-89.

Touchot, N., Chardin, P. and Tavitian, A. (1987). Four additional members of the ras gene superfamily isolated by an oligonucleotide strategy: molecular cloning of YPT-related cDNAs from a rat brain library. *Proc Natl Acad Sci U S A* 84, 8210-4.

Tseng, T. T., Gratwick, K. S., Kollman, J., Park, D., Nies, D. H., Goffeau, A. and Saier, M. H., Jr. (1999). The RND permease superfamily: an ancient, ubiquitous and diverse family that includes human disease and development proteins. *J Mol Microbiol Biotechnol* 1, 107-25.

Ullrich, O., Reinsch, S., Urbe, S., Zerial, M. and Parton, R. G. (1996). Rab11 regulates recycling through the pericentriolar recycling endosome. *J Cell Biol* 135, 913-24.

Valencia, A., Chardin, P., Wittinghofer, A. and Sander, C. (1991). The ras protein family: evolutionary tree and role of conserved amino acids. *Biochemistry* 30, 4637-48.

Vallstedt, A., Muhr, J., Pattyn, A., Pierani, A., Mendelsohn, M., Sander, M., Jessell, T. M. and Ericson, J. (2001). Different levels of repressor activity assign redundant and specific roles to Nkx6 genes in motor neuron and interneuron specification. *Neuron* 31, 743-55.

Valsdottir, R., Hashimoto, H., Ashman, K., Koda, T., Storrie, B. and Nilsson, T. (2001). Identification of rabaptin-5, rabex-5, and GM130 as putative effectors of rab33b, a regulator of retrograde traffic between the Golgi apparatus and ER. *FEBS Lett* 508, 201-9.

van den Heuvel, M. and Ingham, P. W. (1996). smoothened encodes a receptor-like serpentine protein required for hedgehog signalling. *Nature* 382, 547-51.

van den Hurk, J. A., Schwartz, M., van Bokhoven, H., van de Pol, T. J., Bogerd, L., Pinckers, A. J., Bleeker-Wagemakers, E. M., Pawlowitzki, I. H., Ruther, K., Ropers, H. H. et al. (1997). Molecular basis of choroideremia (CHM): mutations involving the Rab escort protein-1 (REP-1) gene. *Hum Mutat* 9, 110-7.

van der Sluijs, P., Hull, M., Webster, P., Male, P., Goud, B. and Mellman, I. (1992). The small GTP-binding protein rab4 controls an early sorting event on the endocytic pathway. *Cell* 70, 729-40.

van der Sluijs, P., Hull, M., Zahraoui, A., Tavitian, A., Goud, B. and Mellman, I. (1991). The small GTP-binding protein rab4 is associated with early endosomes. *Proc Natl Acad Sci U S A* 88, 6313-7.

van Eeden, F. J., Granato, M., Schach, U., Brand, M., Furutani-Seiki, M., Haffter, P., Hammerschmidt, M., Heisenberg, C. P., Jiang, Y. J., Kane, D. A. et al. (1996). Mutations affecting somite formation and patterning in the zebrafish, Danio rerio. *Development* 123, 153-64.

van IJzendoorn. S. C., Tuvim, M. J., Weimbs, T., Dickey, B. F. and Mostov, K. E. (2002). Direct interaction between Rab3b and the polymeric immunoglobulin receptor controls ligand-stimulated transcytosis in epithelial cells. *Dev Cell* 2, 219-28.

Varga, Z. M., Amores, A., Lewis, K. E., Yan, Y. L., Postlethwait, J. H., Eisen, J. S. and Westerfield, M. (2001). Zebrafish smoothened functions in ventral neural tube specification and axon tract formation. *Development* 128, 3497-509.

Vincent, J. P. (2003). Membranes, trafficking, and signaling during animal development. *Cell* 112, 745-9.

Vitale, G., Rybin, V., Christoforidis, S., Thornqvist, P., McCaffrey, M., Stenmark, H. and Zerial, M. (1998). Distinct Rab-binding domains mediate the interaction of Rabaptin-5 with GTP-bound Rab4 and Rab5. *Embo J* 17, 1941-51.

Vitelli, R., Santillo, M., Lattero, D., Chiariello, M., Bifulco, M., Bruni, C. B. and Bucci, C. (1997). Role of the small GTPase Rab7 in the late endocytic pathway. *J Biol Chem* 272, 4391-7.

Vogel, A. M. and Gerster, T. (1999). Promoter activity of the zebrafish bhikhari retroelement requires an intact activin signaling pathway. *Mech Dev* 85, 133-46.

von Mering, C. and Basler, K. (1999). Distinct and regulated activities of human Gli proteins in Drosophila. *Curr Biol* 9, 1319-22.

Walther, C. and Gruss, P. (1991). Pax-6, a murine paired box gene, is expressed in the developing CNS. *Development* 113, 1435-49.

Wang, B., Fallon, J. F. and Beachy, P. A. (2000a). Hedgehog-regulated processing of Gli3 produces an anterior/posterior repressor gradient in the developing vertebrate limb. *Cell* 100, 423-34.

Wang, G., Amanai, K., Wang, B. and Jiang, J. (2000b). Interactions with Costal2 and suppressor of fused regulate nuclear translocation and activity of cubitus interruptus. *Genes Dev* 14, 2893-905.

Wang, X., Emelyanov, A., Sleptsova-Friedrich, I., Korzh, V. and Gong, Z. (2001). Expression of two novel zebrafish iroquois homologues (ziro1 and ziro5) during early development of axial structures and central nervous system. *Mech Dev* 105, 191-5.

Wang, Y., Okamoto, M., Schmitz, F., Hofmann, K. and Sudhof, T. C. (1997). Rim is a putative Rab3 effector in regulating synaptic-vesicle fusion. *Nature* 388, 593-8.

Watari, H., Blanchette-Mackie, E. J., Dwyer, N. K., Watari, M., Neufeld, E. B., Patel, S., Pentchev, P. G. and Strauss, J. F., 3rd. (1999). Mutations in the leucine zipper motif and sterol-sensing domain inactivate the Niemann-Pick C1 glycoprotein. *J Biol Chem* 274, 21861-6.

Waters, M. G. and Pfeffer, S. R. (1999). Membrane tethering in intracellular transport. *Curr Opin Cell Biol* 11, 453-9.

Weide, T., Bayer, M., Koster, M., Siebrasse, J. P., Peters, R. and Barnekow, A. (2001). The Golgi matrix protein GM130: a specific interacting partner of the small GTPase rab1b. *EMBO Rep* 2, 336-41.

White, J., Johannes, L., Mallard, F., Girod, A., Grill, S., Reinsch, S., Keller, P., Tzschaschel, B., Echard, A., Goud, B. et al. (1999). Rab6 coordinates a novel Golgi to ER retrograde transport pathway in live cells. *J Cell Biol* 147, 743-60.

Whyte, J. R. and Munro, S. (2002). Vesicle tethering complexes in membrane traffic. *J Cell Sci* 115, 2627-37.

Wijgerde, M., McMahon, J. A., Rule, M. and McMahon, A. P. (2002). A direct requirement for Hedgehog signaling for normal specification of all ventral progenitor domains in the presumptive mammalian spinal cord. *Genes Dev* 16, 2849-64.

Wilson, S. M., Yip, R., Swing, D. A., O'Sullivan, T. N., Zhang, Y., Novak, E. K., Swank, R. T., Russell, L. B., Copeland, N. G. and Jenkins, N. A. (2000). A mutation in Rab27a causes the vesicle transport defects observed in ashen mice. *Proc Natl Acad Sci U S A* 97, 7933-8.

Wilson, V., Manson, L., Skarnes, W. C. and Beddington, R. S. (1995). The T gene is necessary for normal mesodermal morphogenetic cell movements during gastrulation. *Development* 121, 877-86.

Wu, X., Bowers, B., Rao, K., Wei, Q. and Hammer, J. A. r. (1998). Visualization of melanosome dynamics within wild-type and dilute melanocytes suggests a paradigm for myosin V function In vivo. *J Cell Biol* 143, 1899-918.

Wu, X. S., Rao, K., Zhang, H., Wang, F., Sellers, J. R., Matesic, L. E., Copeland, N. G., Jenkins, N. A. and Hammer, J. A., 3rd. (2002). Identification of an organelle receptor for myosin-Va. *Nat Cell Biol* 4, 271-8.

Zahraoui, A., Joberty, G., Arpin, M., Fontaine, J. J., Hellio, R., Tavitian, A. and Louvard, D. (1994). A small rab GTPase is distributed in cytoplasmic vesicles in non polarized cells but colocalizes with the tight junction marker ZO-1 in polarized epithelial cells. *J Cell Biol* 124, 101-15.

Zeng, J., Ren, M., Gravotta, D., De Lemos-Chiarandini, C., Lui, M., Erdjument-Bromage, H., Tempst, P., Xu, G., Shen, T. H., Morimoto, T. et al. (1999). Identification of a putative effector protein for rab11 that participates in transferrin recycling. *Proc Natl Acad Sci U S A* 96, 2840-5.

Zerial, M. (1995). Guidebook to the small GTPases. Oxford: Oxford University Press.

Zerial, M. and McBride, H. (2001). Rab proteins as membrane organizers. *Nat Rev Mol Cell Biol* 2, 107-17.

Zhang, X. M., Ramalho-Santos, M. and McMahon, A. P. (2001). Smoothened mutants reveal redundant roles for Shh and Ihh signaling including regulation of L/R symmetry by the mouse node. *Cell* 106, 781-92.

Zheng, J. Y., Koda, T., Fujiwara, T., Kishi, M., Ikehara, Y. and Kakinuma, M. (1998). A novel Rab GTPase, Rab33B, is ubiquitously expressed and localized to the medial Golgi cisternae. *J Cell Sci* 111 (Pt 8), 1061-9.

Zhou, Y., Yamamoto, M. and Engel, J. D. (2000). GATA2 is required for the generation of V2 interneurons. *Development* 127, 3829-38.

Zhu, A. J., Zheng, L., Suyama, K. and Scott, M. P. (2003). Altered localization of Drosophila Smoothened protein activates Hedgehog signal transduction. *Genes Dev* 17, 1240-52.